DOCTOR OF PHILOSOPHY

Function of two closely related fibroblast growth factors in early mesoderm development of Drosophila melanogaster

Klingseisen, Anna

Award date:
2009

DOCTOR OF PHILOSOPHY

Function of two closely related fibroblast growth factors in early mesoderm development of Drosophila melanogaster

Anna Klingseisen

2009

University of Dundee

University of Dundee

College of Life Sciences

Function of two closely related fibroblast growth factors in early mesoderm development of *Drosophila melanogaster*

by Anna Klingseisen

A thesis submitted for the degree of Doctor of Philosophy

University of Dundee

December 2009

Table of contents

Index of tables

Index of figures

Abbreviations

A	Alanine
aa	Amino acids
AP	alkaline phosphatase
β-Gal	β-galactosidase
BCIP	5-Bromo-4-chloro-3-indolyl phosphate
bp	base pairs
C	Cysteine
C-terminal	Carboxy-terminal
cDNA	coding DNA
Chr	chromosome
Δ	delta (“deleted”)
Df	deficiency
DIG	Digoxygenine
dH2O	demineralised water
DAPI	4',6-diamidino-2-phenylindole
DNA	Desoxyribonucleic acid
dNTP	Desoxyribonucleotide triphosphate
E.coli	Escherichia coli
e.g.	for example (“exempli gratia”)
ERK	extracellular signal-related kinase
dpERK	diphosphorylated ERK (activated ERK)
F	Phenylalanine
FGF	fibroblast growth factor
FGFR	fibroblast growth factor receptor
Fig	Figure
ftz	*fushi tarazu*
GEF	guanine nucleotide exchange factor
GDP	guanosine diphosphate
GTP	guanosine triphosphate
HA	Hemagglutinin-epitope
HRP	Horse raddish preoxidase
HSPG	Heparan sulfate proteoglycan

k…	kilo…(10^3)
kDa	kilo Dalton
LB medium	Luria Bertani broth medium
m…	milli...(10^{-3})
M	Molarity (mol/l)
MAPK	Mitogen-activated-protein-kinase
min	minutes
mRNA	messenger RNA
n…	nano (10^{-9})
NBT	Nitro blue tetrazolium
PCR	Polymerase-chain reaction
PI3K	Phosphoinositide 3-kinase
PKA / PKC	protein kinase A / protein kinase C
R	Arginine
Rpm	revolutions per minute
RT	room temperature
RT-PCR	reverse transcription from mRNA followed by PCR
S	Serine
UAS	Upstream Activating Sequence
V	Valine
V	Volt
Q	Glutamine

The work described in this thesis has been published in part in the following article

Anna Klingseisen, Ivan B. N. Clark, Tanja Gryzik and H.-Arno J. Müller

Differential and overlapping functions of two closely related Drosophila FGF8-like growth factors in mesoderm development (2009) *Development* **136**, 2393-2402

Declaration

I declare that the following thesis is based on the results of investigations conducted by myself, and that this thesis is of my own composition. Work other than my own is clearly indicated in the text by reference to the relevant researchers or to their publications. This dissertation has not in whole, or in part, been previously submitted for a higher degree.

Anna Klingseisen

I certify that Anna Klingseisen has fulfilled the conditions of the relevant Ordinance and Regulations of the University of Dundee and is qualified to submit the accompanying thesis in application for the degree of Doctor of Philosophy.

Dr. H.–Arno J. Müller

Summary

Thisbe (Ths) and Pyramus (Pyr) are the ligands for the Fibroblast-Growth-Factor (FGF) receptor Heartless (Htl), which is expressed in all mesodermal cells during gastrulation. To understand how these two FGFs orchestrate mesoderm spreading in gastrulation and mesoderm differentiation during organogenesis, loss and gain of function studies were performed. In an approach of functional analysis, a single mutant allele of *ths* was generated, ths^{759}, for comparison of the single mutant conditions of *ths* and the null allele pyr^{18}. Mesoderm migration and differentiation was analysed in embryos homozygous mutant for either *ths* or *pyr*; for both *ths* and *pyr*; and in the hemizygous condition, where only one copy of either FGF gene is present in absence of the other, respectively. The aspects investigated therein include the dispersal of mesoderm cells over the ectoderm, the formation of protrusions in mesoderm cells and the activation of MAPK.

ths^{759} mutant embryos show slight defects in mesoderm migration, and Ths function appears to promote adhesion of mesoderm cells to the ectoderm. *pyr* loss of function causes defects in migration, specification and differentiation of mesodermal cells. Pyr is required for activation of MAPK signalling in the mesoderm and polarisation of mesoderm cells during migration in dorsal direction. Both *ths* and *pyr* single mutants are semi-lethal with <2% sterile homozygous flies hatching, but neither of them exhibits as strong defects as *htl,* or *pyr, ths* double mutant embryos. In embryos lacking *htl* or both Htl ligands Ths and Pyr, cellular protrusions of mesoderm cells are strongly reduced during gastrulation and mesoderm spreading is blocked. Pyr-mediated Htl signalling was identified to be essential for the formation of dorsal protrusions, whereas Ths is involved in extension of radial filopodia.

To investigate differentiation events, embryos were analysed for the formation of Eve positive pericardial cell precursors, and muscle progenitors as well as muscle fibres expressing Mef-2 and Myosin heavy chain (Mhc), respectively. Both overlapping and differential functions of Pyr and Ths were identified during mesoderm differentiation. While Pyr is absolutely required for specification of pericardial cells, Ths is dispensable for this process. In contrast, both FGF ligands are required to ensure differentiation of cardioblasts in each segment. In addition, Ths and Pyr are required for the dorsal alignment of heart precursors and the formation of specific subtypes of somatic muscles in later stages of embryogenesis.

To gain further insight in FGF mediated regulation and to address the functional ability of Ths and Pyr FGF signals, overexpression studies were performed. Utilising different sites of expression to investigate the influence of ectopic signalling, Pyr/Htl mediated MAPK signalling was identified to induce differential cellular responses dependent on the site of expression and the developmental time point during mesoderm development. Ectopic MAPK activation by Pyr/Htl signalling interferes with mesoderm migration and differentiation. Forced MAPK signalling during later phases of mesoderm development only interferes with signalling pathways involved in specific differentiation of mesoderm derivatives. These results indicate that the regulation of ligand expression is pivotal for Htl dependent mesoderm development.

In conclusion, both FGF ligands create an environment that provides specific signals for mesodermal cells to migrate and differentiate in a precise pattern.

I. Introduction

The fruit fly *Drosophila melanogaster* is a particularly well-characterized model organism. Genetic analysis over many years have led to the functional characterisation of approximately one fourth of the estimated 13,500 genes present in the genome. All major signalling pathways involved in cell-cell interactions during development of higher animals are conserved in the fruit fly, and the *Drosophila* mesoderm provides an excellent system for studying signalling networks as multiple signalling pathways are involved in mesoderm development, and *Drosophila* can be subjected to complex genetic manipulations.

It was known for 16 years that mesoderm development in *Drosophila melanogaster* involves fibroblast growth factor (FGF) signalling (Shishido et al., 1993), but the mechanism of mesodermal cell movements still is not fully understood. Many other components involved in mesoderm migration and required for mesoderm specific FGF signalling have been identified, and the analysis of their function has contributed to gain insight into a number of regulatory mechanisms of mesodermal cell behaviour. The activating ligand for the FGF receptor expressed in the mesoderm however was unknown for over 10 years, and the eventual identification of two closely related FGF ligands raised additional questions of whether and how FGF signals might be differentially regulated and transmitted into particular cellular behaviours. The present study aims to contribute to answering these questions using a genetic approach of loss-of-function and gain-of-function analyses of the two FGF receptor ligands during gastrula mesoderm movements and differentiation.

I. 1 Cell movement is fundamental in embryonic development

Cells move during morphogenesis of the developing embryo. From gastrulation to organogenesis, the migration of cell collectives or single cells plays a key role in these processes. Many developmental processes start with a uniform pool of multipotent progenitor cells. In order to achieve distinct positions within the embryo, the initially unstructured formation of multipotent cells has to be patterned into fate specific territories and fundamentally rearranged (Leptin, 1999; Heisenberg and Solnica-Krezel, 2008). Only if these rearrangements and specific migratory processes progress in a spatiotemporally concerted fashion will the cells acquire distinct identities of differentiated cells and are able to generate structures of unique functions. Thus, cell movements are a prerequisite for differentiation during embryonic development.

I. 1. 1 General mechanism of cell migration

The movement of cells is influenced by many factors, and the responses to locally provided signals or gradients of signalling molecules show a variety of consequences in cellular behaviour. First, the direction of migration can be guided by the instructive signal in an attractive or repulsive fashion. Second, adhesion properties of the substrate can direct migration by subdividing the area of migration into migratory zones of high or low adhesiveness, thereby creating 'routes' for the moving cell collectives (Boucaut et al., 1990). Both the actin cytoskeleton and the microtubular network have to be reorganised extensively in a migrating cell, ultimately contributing to the forward movement and to the temporal stability of the cell shape (Lauffenberger and Horwitz, 1996; Ribeiro et al., 2003).

The most common response of a cell to a migration promoting agent is to polarise and to extent protrusions in the direction of migration. These protrusions can be broad

lamellipodia or thin filopodia of varying length. The formation of cellular protrusions usually is driven by actin polymerisation and disassembly of the cortical myosin thick filament network, and the protrusion is stabilised by adhering to the extracellular matrix or adjacent cells via transmembrane receptors linked to the actin cytoskeleton (Webb et al., 2002; Affolter and Weijer, 2005)

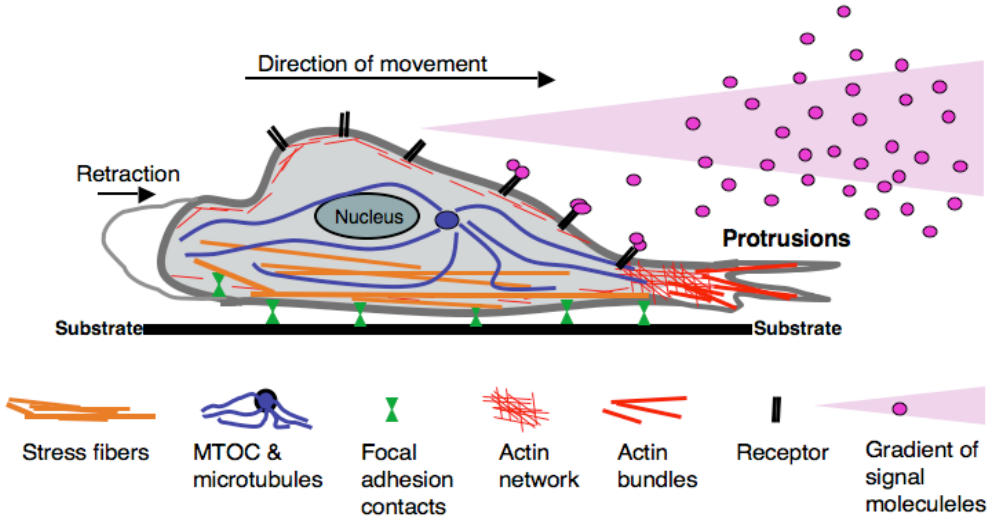

Fig. 1. Polarisation and directed cell movement upon instructive signalling.
Upon polarisation, the cell forms protrusions at the tip in the direction of migration. Polarisation is also manifested in the localization of the MTOC in front of the nucleus The branched actin cytoskeleton becomes focused into filopodia, consisting of parallel actin bundles held together by actin bundling proteins. In order for the cell to move, it must be anchored to the substrate, which is achieved through transmembrane receptors. Protrusions are stabilized by the formation of adhesions (focal complexes which mature to focal adhesions) and transmit the generated force of actin-myosin contraction to the substrate via transmembrane receptors. At the rear end of the cell, adhesions are disassembled also by the delivery of components by microtubules. This leads to retraction of the cell's rear end. Cell movement thus is achieved by a cycle of formation and disassembly of adhesion contacts. (adapted from Bailly et al., 2000; Petit et al., 2002; Affolter and Weijer, 2005)

Dynamic cell movement and chemotaxis involves both extension and retraction of cell protrusions into the surrounding environment (Lauffenberger and Horwitz, 1996). If sufficiently strong adhesion develops between the protrusion and the substratum, then retraction is prevented, stabilizing certain extensions while less-adherent protrusions disappear. The translocation of the cell body ultimately requires also the release of the back of the cell, either through loosening of adhesive contacts or an active contraction or combination of both (Montell, 1999). Thus, the cell remodels its cytoskeleton in response to induction by migratory signals.

The mechanisms that lead to cytoskeletal rearrangements to enable migration into a given direction have been investigated more in the context of single cells. A very dynamic model of attractive chemotaxis represents the movement of the single motile cells of the social amoeba *Dictyostelium discoideum*. These individually moving cells sense gradients of the signalling molecules cyclic AMP and polarise dependent on the cAMP gradient to move in direction of the highest source of cAMP (van Haastert and Devreotes, 2004). The ellipsoid shaped cells can deform very fast and repeatedly extend and retract lamellipodia and filopodia at the leading edge of the cell (van Haastert and Devreotes, 2004; Dormann and Weijer 2006). This chemotactic behaviour enables the single amoeboid cells to enter a multicellular developmental cycle in response to starvation, as they utilise this mechanism of mediating directionality for their movement towards a centre of aggregation (Weijer, 2004; Weijer, 2009).

I. 1. 2 Different kinds of movement and instruction - examples from *Drosophila*

The cell's responses to instructive migrational signals have been studied in detail *in vitro* (Iijima et al., 2002) and have shown how the use of molecular, cellular, and genetic approaches can lead to a deeper understanding of guided cell migration. However, many of these seminal studies utilise deprivation of stimuli prior to controlled application of signals and two-dimensional substrates, excluding other interfering progresses such as morphogenetic events as epiboly or germband extension (Lauffenburger and Horwitz, 1996, Bailly et al., 1998; van Haastert and Devreotes, 2004; Dormann and Weijer, 2006). Movement of cells *in vivo* involving dynamic and three-dimensional conditions can differ substantially from observations of cell migration *in vitro* (Horwitz and Webb, 2003, Prasad and Montell, 2007). Cells are in

contact with a number of different tissues and as mentioned above and exposed to extrinsic factors such as guidance cues or repellent agents.

In the environment of a multicellular organism, cells are faced additionally with a number of additional constraints. During embryonic development, cells first have to detach from surrounding cells or the tissue of origin to invade other territories. Cell migration has to be initiated and terminated at precise developmental stages. Cells can move as single cells or in a collective, and within such not all cells perform the same role in migratory processes (Fig. 2). In particular cases, for example tracheal development in *Drosophila*, cell migration sculpts the three dimensional appearance of entire organ systems. When reaching their destination of migration, cells have to stop their movement and differentiate into non-motile cells of distinct functions.

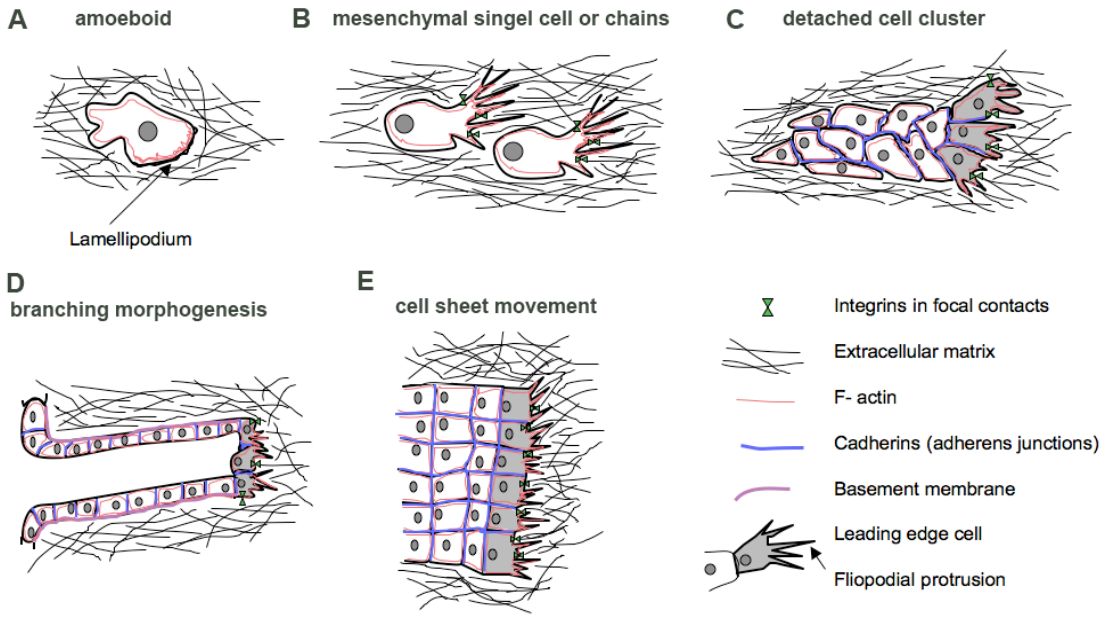

Fig. 2. Different types of cell migration.
(A),(B) individual- vs. collective cell migration **(C)-(E). (A)** Amoeboid migrating cells develop a dynamic lamellipodial leading edge, rich in small pseudopodia, and an ellipsoid cell body. **(B)** Mesenchymal cells show a tissue-dependent elongation, form focal contacts and require proteases in order to degrade the extracellular matrix (ECM). Chains of cells often move in proteolytic migration tracks as also seen for neural crest cells. **(C)** Clusters of cells display one or several leading cells, which provide the migratory traction and pull the following group forward via cell-cell junctions. **(D)** Branching morphogenesis is established via leading edge cells, which proteolytically alter the ECM. The matrix defects are filled up by following cells, which generate a basement membrane at the interface to the ECM and an internal lumen. **(E)** Multicellular sheets can migrate with a small number of leading cells and are connected to the proliferating origin via cell-cell junctions. (adapted from Friedl, 2004).

The coordination of movement and different microenvironments requires a regulation of motility by events that control cell adhesion, either between similar and/or different cells and the extracellular matrix (Fig. 2) (Ribeiro et al., 2003; Weijer, 2009).

In vivo, each process of cell migration has its own particularity with regard to coordination of movement, adhesion, and interference with morphogenetic events or different signalling pathways providing specific guidance cues. Therefore, it is important to study cell movements in their natural setting. The next chapters will outline different types of regulation of cell migration during development of *Drosophila melanogaster*, with regard to the utilisation of the fruit fly as a model organism for the present study of cell movement and differentiation. The different modes of cell movement are demonstrated using the example of migratory processes of amoeboid single cell migration of the primordial germ cells, the clustered border cell migration during oogenesis, and the migration of cells as an epithelial sheet during dorsal closure of the embryo.

I. 1. 2. 1 Single cell movements of primordial germ cells: polarisation in response to chemoattractants triggers directed transepithelial migration

The migration of single cells occurs during migration of mesenchymal cells and in amoeboid movements (Fig. 2A, B). Examples are leukocyte immigration, fibroblast and vascular endothelial cell migration in wound healing or tumor cell invasion in disease (Friedl, 2004; Friedl and Gilmour, 2009). Single cell migration is also required in developmental processes. In higher organisms, examples are migrating primordial germ cells, neural crest cells or ingressing mesoderm cell during embryogenesis (Santos and Lehmann, 2004; Weijer, 2009).

In *Drosophila*, a well-characterised example of single cell movement is the translocation of the primordial germ cells (PGCs). As in many vertebrate organisms, the

PGCs arise far from the region where their somatic gonadal tissues are specified. To reach the somatic component of the gonad during terminal stages of embryogenesis, PGCs have to migrate through and along various somatic tissues soon after their specification prior to gastrulation (Fig. 3). In the gonad, specific interactions between germ cells and soma regulate sex-specific development and differentiation into egg and sperm.

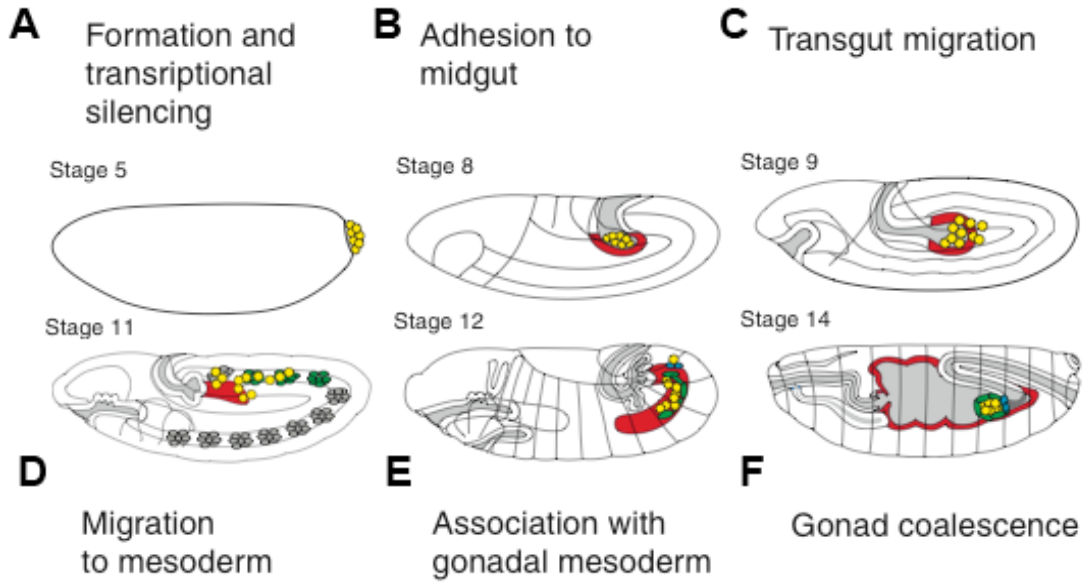

Fig. 3. Stages of PGC migration in *Drosophila*.
Schematic drawings of embryos after Hartenstein et al., 1995; anterior is to the left and dorsal to the top. Yellow, germ cells; red, midgut; green, mesodermally derived somatic gonadal precursor clusters; blue, male specific somatic gonadal precursors, drawn as in male gonad morphogenesis. (A-F) Stage-related phases of PGC migration are indicated and described in the text. (A) PGCs are formed at the posterior pole of the embryo containing the pole plasm. (B) The PGC are invaginated together in a pocket through the hindgut invagination. (C) Transepithelial migration of the PGC through the midgut primordium (D) The PGCs are attracted to the mesoderm and associate with the somatic gonad (E). The PGC are enclosed by somatic gonadal cells in formation of a cyst (adapted from Santos and Lehmann, 2004)

The early embryo is a syncytium and the germ cells are the first cells to form at the posterior pole of the embryo. They contain the germ plasm, which provides determinants sequestered during oogenesis (Fig. 3A) (Santos and Lehman, 2004). The germ plasm determines both fate decision and fate maintenance as well as migration of the germ cells (Starz-Gaiano et al., 2001; Blackwell, 2004). The first phase of PGC migration is a passive movement, as the PGCs are carried inside the embryo in close

association with the midgut primordium (Fig. 3B). Subsequent to the posterior midgut invagination, the germ cells actively migrate across the posterior midgut epithelium and then dorsally (Fig. 3C). Finally, the PGCs migrate away from the midgut towards the adjacent mesoderm where they associate with the somatic gonadal precursor cells (Fig. 3D, E). The germ cells and associated gonadal precursors then migrate anteriorly during germ band retraction, until they coalesce into the embryonic gonad (Fig. 3F) (Santos and Lehmann, 2004).

The different steps of movement of the PGCs are regulated by changes in adhesive behaviour and both attractive and repulsive signals. The crossing of the midgut epithelium is regulated by the G-protein coupled receptor (GPCR) trapped in endoderm 1 (Tre-1) in three essential aspects: polarisation of the germ cells, dispersal into individual cells, and transepithelial migration (Kunwar et al., 2008). Live imaging studies have shown that the cells first become polarised, orienting their leading edges towards the midgut epithelium. Next, their mutual adhesion dissolves, the cells start to protrude towards the epithelium and the germ cells subsequently disperse as they migrate through the epithelial layer. During this transmigration, the cells display an amoeboid behaviour of polarised cell shape with an actin-rich leading edge. The polarisation of the cells in response to GPCR signalling results in redistribution of signalling molecules such as Rho1 and cell adhesion molecules such as E-cadherin. Thus, the dispersal and directional migration of the germ cells through the midgut primordium might be triggered by polarisation in response to high concentrations of chemoattractants (Kunwar and Lehman, 2003; Kunwar et al., 2008).

Both an attractive and repulsive signalling pathway regulates the further movement of the PGCs towards the bilaterally forming mesodermally derived gonadal precursors (Fig. 4). The lateral mesoderm expresses an enzymatic protein directly providing the germ cells with an attractive cue (3-Hydroxy 3-Methylglutaryl Coenzyme A

(HMGCoAR)), suggesting that a lipid-modified attractant guides the germ cells towards the mesoderm (Santos and Lehmann, 2004).

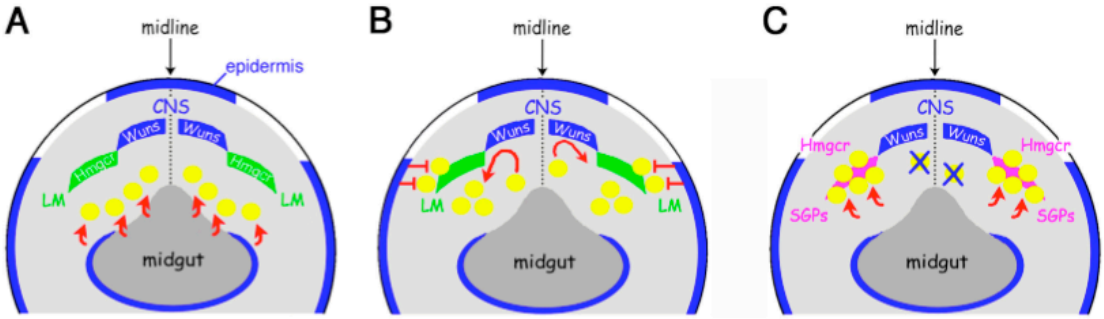

Fig. 4. Model for the guidance of primordial germ cells (PGCs) to the somatic gonadal precursors (SGPs).
The dorsal half of the embryo is shown (**A**) At stage 10, PGCs (yellow) move in response to Wun and Wun-2 (blue) expressed in the ventral side of the posterior midgut (PMG) to the dorsal surface of the PMG. Hmgcr and other unknown factors expressed in the lateral mesoderm (LM; green) attract PGCs from the PMG. (**B**) CNS-expressed Wun and Wun-2 repel PGCs and promote lateral migration. Wun and Wun-2 also prevent PGCs from migrating into the epidermis. (**C**) Eventually, PGCs are close to the SGPs (pink) and can be more easily captured by SGPs. PGCs that fail to migrate and remain in the middle of the embryo are eliminated by the high amounts of Wun and Wun-2 expressed in the CNS. (adapted from Sano et al., 2005).

In addition to the attractive signal towards the mesoderm gonadal precursors, the migration of PGCs is controlled by the repulsive signals of the functional redundant lipid phosphate phosphatases (LPPs) Wunen and Wunen-2 (Wun/Wun-2) (Zhang et al., 1997; Starz-Gaiano et al., 2001). *wun* and *wun-2* are expressed ventrally by the posterior midgut, the epidermis and in the CNS at the dorsal midline of the embryo (Fig. 4). The primordial germ cells migrate away from the sites of wun/wun-2 expression, and are therefore forced to move bilaterally towards the regions *wun/wun-2* are not expressed. LPPs represent membrane-localised ectoenzymes with catalytic domains facing the outside of the cell to dephosphorylate extracellular phospholipid substrates. Thus, the current model hypotheses that the LPPs Wun and Wun-2 create a gradient of a phospholipids through their restricted expression pattern and that PGCs migrate toward the region with the highest phospholipids levels (Sano et al., 2005).

I. 1. 2. 2 Collective cell movements: border cell migration and dorsal closure

Collective cell migration in development is a process by which specified groups of cells are transported to new locations where they are required to perform specific functions (Weijer, 2009). Precise guidance signals orchestrate the movement of a cell collective. Such instruction can be provided by intracellular signalling induced by transcriptional regulation, short- or long- range dynamic gradients of extracellular signalling molecules, and also importantly by adhesive regulation mediated by the substrate of migration. Cells can migrate as epithelial or endothelial sheets or in cohorts of closely interacting cells (Fig. 2 B-E) (Friedl, 2004). The movement of cell collectives is further characterized by the number of cells migrating in a collective, whether leader cells exist that mediate the primary signal, and the distance of their movement (Weijer, 2009). However, the mechanisms of cells to respond to instructive signals are diverse and dependent on the state of differentiation and fate of the cells.

I. 1. 2. 2. 1 Movement of follicle border cell clusters: different levels of MAPK signalling generate a motive force towards the source of chemoattractants

A mechanism of cell movement guided by chemoattractants and involving a collective of cells is demonstrated by migration of a specific set of follicle cells, forming the so-called border cell cluster during *Drosophila* oogenesis. A cluster of up to ten cells is specified from the follicular epithelium at the anterior pole of the egg chamber and, after undergoing a partial epithelial-to-mesenchymal transition (EMT), migrates initially towards the oocyte and then dorsally to form the microphyle, a structure important for sperm entry (Montell, 2003; Weijer, 2009). The small cluster of six to eight border cells surrounding two central cells moves between the nurse cells and towards the developing oocyte (Fig. 5). The cells migrate in response to a gradient of the epidermal growth factor (EGF) and PVF (PDGF- and PDGF/VEGF-related factor)

secreted by the oocyte. During migration, the cells are polarised and extend protrusions in direction of migration, and the tip of the moving collective is characterised by obvious leader cells (Bianco et al., 2007; Prasad and Montell, 2007).

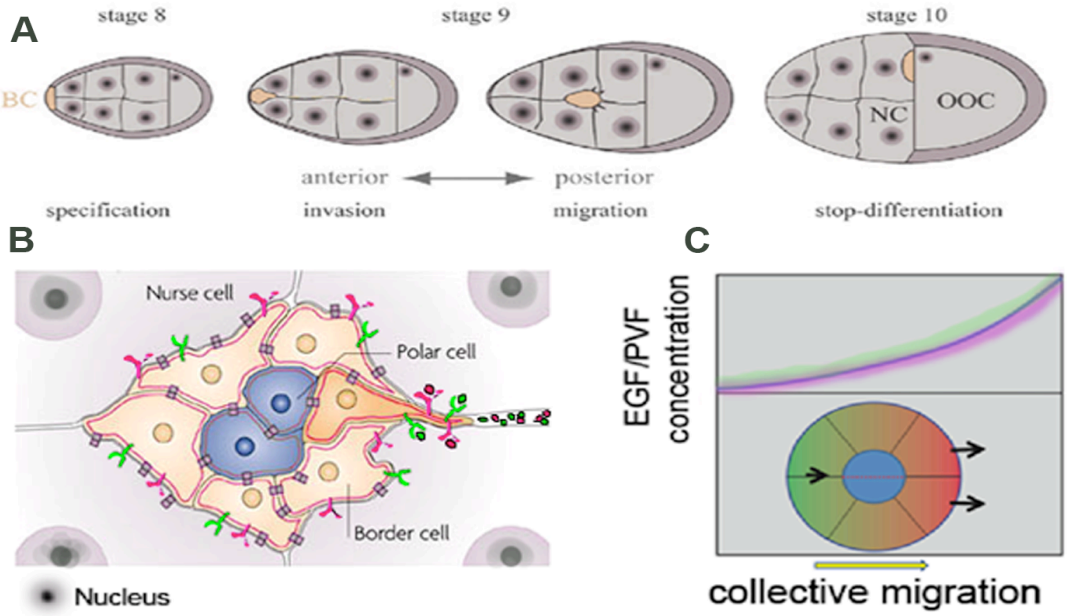

Fig. 5. Border cell migration in *Drosophila* oogenesis
(A) Schematic drawing of *Drosophila* egg chambers, with stages indicated above. Border cells (BC) migrate between the nurse cells (NC) towards the oocyte (OOC). **(B)** BC form a cluster of eight to ten cells. Shown are the two central polar cells (blue), surrounded by six peripheral cells, which form a quasi-epithelial structure in which the cells are connected through adherens junctions (dark purple). The BC cluster moves in direction of the highest concentration of EGF/PVF (light green/pink) expressed by the oocyte (OOC) (as depicted in the graph in (C)) **(C)** Detection of the PVF and EGF signal gradients results in MAP kinase activation: cells at the front of the cluster show the highest level of activation (red), and cells at the back show lower levels of activation (green). This difference translates to a motive force that results in movement of the tightly connected cell cluster towards the source of the signal, without the need for specialised permanent leader cells in the cluster. (adapted and modified from Friedl, 2004 Schober, 2005 and Weijer, 2009)

Interestingly, the cells in leader positions of the cluster are exchangeable. The question of how the cell cluster maintains directionality of movement if leader cell function is only temporary was answered by analysis of mitogen-activated protein kinase (MAPK) activation within the border cell cluster. The cells in leader positions exhibit high levels of activated MAPK, whereas cell at the back show only low levels of phosphorylation (Fig. 5C) (Bianco et al., 2007). Thus, a gradient of signalling is established across the cell cluster, and the difference in signal response translates into a motive force.

The proposed model favours the ability of the border cell cluster as a whole to sense the signal gradient so that the specification of explicit leader cells is not required. Rather, the cells in front positions closer to the source of the signal might exhibit a motile force of higher strength than the cells at the rear of the cluster, and determine the direction of migration (Rorth, 2007). In addition to the requirement of a directional instruction of movement, the migration is highly dependent on modulation of cell-cell contacts, which regulate the general motility of the moving cells (Prasad and Montell, 2007). The detachment of the border cells of the epithelium of origin is dependent on Notch signalling and also on modulation of directional EGF/PVF signalling.

Remarkably, inhibition of EGF/PVF signalling severely inhibits border cell migration and leads to undirectional protrusive activity, whereas constitutive activation of EGF or PVF receptor in all cells of the cluster inhibits cell motility by inhibition of protrusive activity and a block of the detachment from the epithelium. Thus, collective cell movements can be governed by both directional and adhesive regulation that can simultaneously be influenced by the same signalling pathway.

I. 1. 2. 2. 2 Movement of cell sheets during dorsal closure: leading edge cells utilise filopodia to sense signals in their environment

The movement of cellular sheets displaying stable cell-cell interactions is another key process involved in both morphogenetic events during embryonic development and adult tissue responses. Migration of cell sheets and the fusion of epithelia occur in development during tracheal branching or the formation of the vasculature and are well studied in tissue repair processes during wound healing (Hou et al., 1997; Kiehart et al., 2000; Leptin, 2005; Martin and Parkhurst, 2004; Matsubayashi et al., 2004; Redd et al., 2004; Vitorino and Meyer, 2008). At present, dorsal closure in later development of the

Drosophila embryo is the best-characterized example of epithelial sheet movement (Harden, 2002).

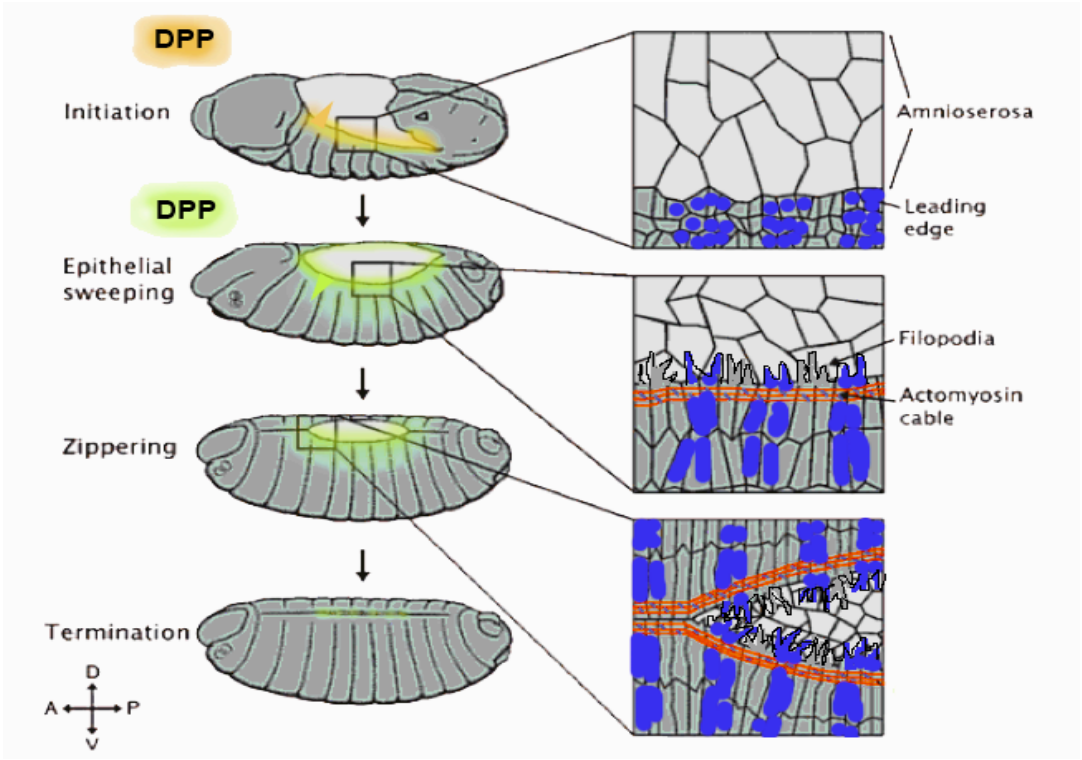

Fig. 6. Epithelial sheet movement during dorsal closure.
Four phases of epithelial sheet migration during dorsal closure are shown with the ectoderm (dark grey) and the amnio serosa (light grey). Boxed regions show the epithelial leading edge. Early Dpp signalling (orange) presumably initiates the contraction of the large amnio serosa cells. A second round of Dpp signals (green) is essential for epidermal morphogenesis and is contributing to the adhesion between leading edge and amnio serosa cells. The epithelial cells of the leading edge assemble an actinmyosin cable (red) and extend filopodia to fuse with the opposing leading edge by a 'purse-string' and 'zippering' mechanism. The closure occurs with high accuracy, such that segmental patterning (blue) is perfectly maintained across the fusion seam at single-cell resolution. Each cell at the leading edge is able to identify, and specially fuses with, its matching cell in the opposing epithelial sheet. The filopodia contribute to this matching in sensory and motile function. (adapted and modified from Fernández et al., 2007 and Millard and Martin, 2008)

During the final stages of embryogenesis, the *Drosophila* embryo exhibits a dorsal hole in consequence to germ band retraction, covered by a simple extra-embryonic epithelium of large cells termed the amnio serosa (AS) (Fernández et al., 2007; Fig. 6). Dorsal closure involves migration and connection of the two lateral opposing epithelial sheets of the epidermis, and requires the coordination of cellular activities within both the amnioserosa and the epidermis (Harden, 2002; Millard and Martin, 2008).

It is thought that dorsal closure is initiated by the dorso-ventral elongation of the dorsal most epidermal cells (leading edge cells), followed by a progressive reduction of the amnioserosa surface and the elongation of the more lateral epidermal cells (Fernández et al., 2007). Only the leading cells then accumulate an actomyosin cable in their dorsal leading edge, and the synchronised contraction of these cables generates a 'purse-string' like force around the amnioserosa (Mizuno et al., 2002). The closure of the initially elliptical hole progresses from the most anterior and posterior ends, zipping closed toward the centre (Jacinto et al., 2002). This zipping process is associated with actin protrusions (lamellipodia and filopodia) extending from the leading edge cells which appear to stitch the two edges together (Jacinto et al., 2000), and also requires microtubules in the epidermal cells (Jankovics and Brunner, 2006).

Detailed genetic studies have revealed a network of interacting signalling molecules regulating this process. At the centre of this network is a Jun N-terminal kinase (JNK) cascade, acting at the leading edge of the migrating epidermis. JNK signalling in the dorsal-most epidermal cells activates the expression of *decapentaplegic* (*dpp)*, a member of the superfamily of bone morphogenetic proteins (BMP) and transforming growth factor-β (TGF-β). Dpp seems to be acting as a coordinator of dorsal closure to ensure that the cell shape changes in the epidermis and in the AS result in the desired final pattern (Fernández et al., 2007). In a first phase of transcriptional activation, Dpp is proposed to control the initiation of cellular activities of the amnioserosa cells that are required for the later contraction of the amnioserosa, which also leads to elongation of lateral epidermis cells. During the closing process, a second round of JNK driven *dpp* expression in the leading edge is necessary for epidermal morphogenesis and appears to contribute to the adhesive integrity of the interface between cells of the leading edge and the amnioserosa.

The signalling modules involved in this process also regulate the cytoskeletal reorganization and cell shape changes including signals from the amnioserosa and input from a variety of proteins at cell junctions. The regulation of the dynamic filopodial and lamellar protrusions at the leading edge has a key function during accurate alignment of the two cellular sheets across the fusion seam (Millard and Martin, 2008). Since the lateral epithelia are molecularly patterned along the anterior-posterior axis, the precise alignment of matching opposing domains is essential. This accurate fusion is dependent on interdigitating leading edge cells through their filopodia to prime correct formation of adhesions between matching segments. In a specific recognition event, filopodia facilitate one cell to search for its match and also pull laterally misaligned sheets into alignment by the formation of tethers between cells. Thus, the leading edge cells utilise filopodia to sense their environment and depending on the specific intracellular signalling components present, respond to the signals in individual fashion.

The movement of cell sheets involves obvious restriction of migrational freedom by strong interaction of neighbour cells and a network of directional regulation by specified leading edge cells (Zallen and Blankenship, 2008; Weijer, 2009). Nevertheless, cell sheet migration represents a dynamic mode of movement driven by regulators of directionality and adhesive properties, and clear differences in cell type specific behaviour with regard to leading edge versus following cells or previously specified cell fates.

The processes described thus far show that different types and mechanisms of cell movements are characteristic for particular cell types and stages of embryonic development. Genetic analysis of cell migration in *Drosophila* has led to the identification of a number of signal molecules and their receptor systems, and revealed the importance of coordination of diverse, mutually dependent signalling networks and mechanisms of cell behaviour regulation. Particularly during gastrulation, the

orchestration of versatile signals regulating specification and movement is obvious for normal development. The following chapter aims to emphasise this relationship of cell fate and migration.

I. 2 Cell movement is intricated with cell fate decisions

The processes of cell movements described above demonstrate an intricate relation of the regulation of cell migration, cell fate specification and subsequent differentiation during the development of a multicellular organism. Morphogenesis of the embryo thus requires a precise coordination of inductive events and cell movements. This interrelation becomes already obvious during gastrulation in both vertebrate and invertebrate embryos.

Gastrulation represents a series of extensive cell rearrangements that result in the formation of the three germ layers of ectoderm, endoderm and mesoderm. In *Drosophila*, the territories of the different primordia are defined by anterior-posterior and dorso-ventral positional information, through a network of transcriptional regulation and cell signalling (Leptin, 2005). The primordia of the future internal tissues endoderm and mesoderm segregate into the interior of the embryo by major cell and tissue movements. These movements of cell sheets, collectives or single motile cells have to be coordinated and require the regulation of changes in cell shape and cell adhesion. This complex network of coordinated regulation of cellular processes is strongly influenced by signalling pathways instructing and influencing both cell fate decisions and cell movements (Ciruna and Rossant, 2001; Branford and Yost, 2002; Myers et al., 1999; Wilson et al., 2005; Johnson et al., 2007; Franzdottir et al., 2009).

Different models were proposed for how this complex functional coordination is achieved from studies on vertebrate models (Heisenberg and Solnica-Krezel, 2008). One possibility proposes a linear pathway where a signal establishing positional

information in the embryo also specifies cell fates and subsequently determines specific cell behaviours. Such a program would contain not only the information of future fate and function of a specific cell type, but also a unique program of cell movements during gastrulation. Another model suggests that a signal pathway specifying positional information would trigger parallel programs of cell fate specification and cell movement behaviours depending on position within the embryo. Parallel programs would not necessarily have to be independent, because signals that regulate cell movements indirectly influence specification of cell fates by positioning the cells relative to inductive tissues for further differentiation.

The fibroblast growth factor (FGF) signal transduction pathway serves as one of the key regulators of early metazoan development and regulates both specification and movement of mesendodermal precursors (Wilson et al., 2005; Matus et al., 2007; Heisenberg and Solnic-Krezel, 2008; Röttinger et al., 2008). FGF signalling regulates many different aspects of development including proliferation and survival of cells (Kunath et al., 2007; Grieshammer et al., 2008), migration and differentiation (Sato and Kornberg, 2002; Dubrulle J, Pourquié, 2004; Nechiporuk and Raible, 2008; Shi et al., 2009), and also patterning and body axis establishment (Fischer et al., 2002; Fürthauer et al., 2004; Neugebauer et al., 2009).

The central role of FGF signalling in mesoderm development intersects with other key regulatory signal pathways such as PDGF and VEGF (Chuai and Weijer, 2009), BMP and Hh signalling (Pera et al., 2003; Verheyen, 2007; von der Hardt et al., 2007), Notch, Wnt and retionoid acid (RA) signalling (Akai et al., 2005; Olivera-Martinez and Storey, 2007). The regulation via FGF signals is further proposed not only to act in parallel but to control the influence of other key regulators such as Notch and Wnt (Wahl et al., 2007).

In *Drosophila,* migration, lineage commitment and differentiation of mesoderm cells similarly to the vertebrate models depends on FGF signalling (Beimann et al., 1996; Shishido et al., 1997; Gryzik and Müller, 2004; Leptin, 2005; Dutta et al., 2005; Wilson et al., 2005; Kadam et al., 2009; Klingseisen et al., 2009). With regard to the analysis of FGF signalling during mesoderm development being subjective to this study, FGF characteristics, signalling mechanisms and functions during morphogenesis are elaborated further in the following chapters.

I. 3 The family of fibroblast growth factors and the components involved in their pathway of signalling

I. 3. 1 FGF families and protein structure

Fibroblast growth factors make up a large family of polypeptide growth factors that are found in organisms ranging from nematodes to humans (Ornitz and Itoh, 2001). In vertebrates, 22 FGFs and four FGF receptors have been identified, and FGF signalling involves different combinations of FGF and receptor interactions (Ornitz and Itoh, 2001; Itoh and Ornitz, 2004). By contrast, only two or three FGF genes were found in *Caenorhabditis elegans* and *Drosophila melanogaster*, respectively, indicating that the FGF gene family greatly expanded during evolution. Two phases of gene diversification led to the emergence of several subfamilies by gene duplications of two or three to six FGF genes during early metazoan evolution, and via two large-scale genome duplications during early vertebrate evolution (Itoh and Ornitz, 2004 and 2008). Further diversity of FGF proteins and as well as of their receptors is acquired through alternative splicing (Thisse and Thisse, 2005; Guo and Li, 2007; Itoh and Ornitz, 2008). Vertebrate FGFs range in molecular mass from 17 to 34 kDa sharing 13-71% amino acid identity and are highly conserved between vertebrate species (Ornitz and Itoh,

2001). The FGF family can be classified into several subfamilies according to structure, biochemical properties, and expression (Böttcher and Niehrs, 2005). For example, members of the FGF 8 subfamily (FGF 8/17/18) share 70-80% amino acid sequence identity and similar receptor-binding properties, and also show overlapping expression patterns. The other subfamilies compromise receptor-binding signal proteins and are characterised as hormon-like (FGF 15/21/23), and canonical (FGF 1/2/5, FGF 3/4/6, Fgf 7/10/22, FGF 8/17/18 and FGF 9/16/29). The subgroup of FGFs 11-14 represents an exceptional group of intracellular growth factors, which act in a FGF receptor independent manner (Goldfarb, 2005). Most of the receptor-binding FGFs (FGFs 3-10, 15, 17-19, and 21-23) contain amino-terminal signal peptides or a hydrophobic sequence (in case of FGF 9) for secretion. Common to all FGFs is a high affinity for heparin and an internal core of high-sequence homology of 120 amino acids, which interacts with the FGF receptor (Fig. 7A) (Plotnikov et al., 1999; Ornitz and Itoh, 2001; Böttcher and Niehrs, 2005).

Most FGFs act through binding and activation of FGF receptors, which are cell surface receptor tyrosine kinases (RTKs). FGF receptors are single spanning transmembrane proteins with an extracellular ligand-binding regions and an intracellular domain harbouring the kinase activity (Fig. 7B). The extracellular region is composed of immunoglobulin-like (Ig-like) domains that are required for growth factor binding and also regulate the binding affinity and ligand specificity. Expression of different isoforms of the receptor proteins, through alternative splicing of the FGFR genes, determines the specificity for different FGFs (Powers et al., 2000). Receptor proteins can contain one to three Ig-like domains. The Ig-like domain III is most important with regard to the specificity of ligand binding. Alternative splicing may result in three different Ig-like III variants and is regulated in a tissue-specific manner, thus facilitating a high diversity of FGF ligand-receptor combinations and corresponding signalling.

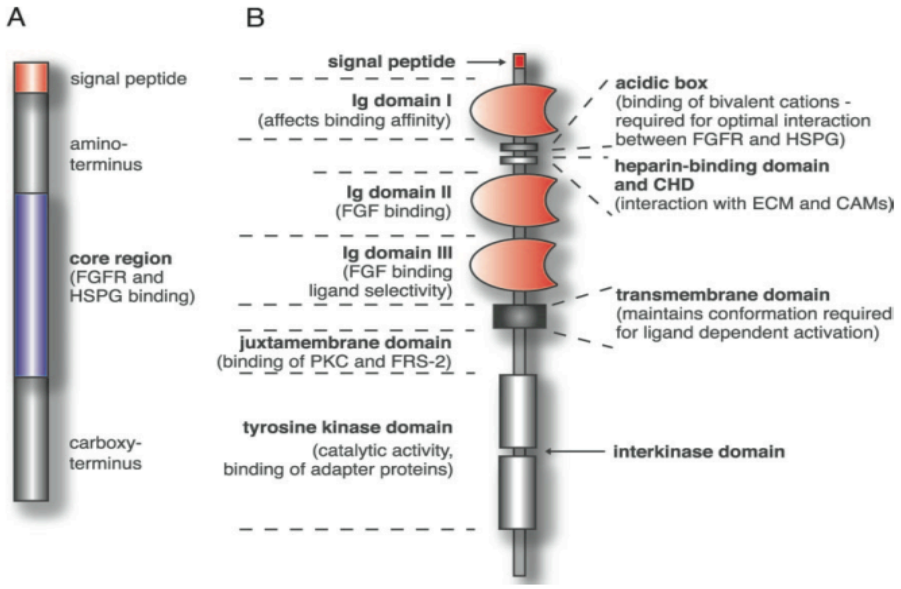

Fig. 7. Domain structure of generic FGF and FGFR proteins.
(A) Generic FGF protein with depicted daomains containing a signal sequence and the conserved core region that contains receptor- and HSPG-binding sites. **(B)** The main structural features of the FGF receptor are illustrated with respective functions. These include Ig domains, acidic box, heparin-binding domain, CAM-homology domain (CHD), transmembrane domain, and tyrosine kinase domain. CAM, Cell adhesion molecule; ECM, extracellular matrix; PKC, protein kinase C. (adapted from Böttcher and Niehrs, 2005)

I. 3. 2 FGF signal transduction

RTKs control a wide variety of processes in multicellular organisms, including proliferation, differentiation, migration and survival. Their activity is tightly controlled through the coordinated action of both positive and negative regulators that function at multiple levels of the signal transduction cascade, and at different time points within the growth-factor-induced response (Mason et al., 2006).

Like other RTKs, FGF receptors transmit extracellular signals after ligand binding through tyrosine phosphorylation to various cytoplasmic signal transduction pathways.

Upon ligand binding, monomeric FGF receptors dimerise which results in tyrosine kinase activation and auto-phosphorylation of the intracellular domain (Schlessinger et al., 2000). The phosphorylated tyrosines function as binding sites for signalling proteins containing Src homology (SH2) or phosphotyrosine binding domains, which upon binding leads to their phosphorylation and activation. SH2 containing proteins can

mediate the signal acting as adaptors or propagate the signal via intrinsic catalytic activities. FGF signalling is transduced by three main pathways, via the phospholipase Cγ (PLCγ), the phosphatidylinositol-3 (PI3) kinase and most commonly, the Ras/MAPK pathway (Fig.8).

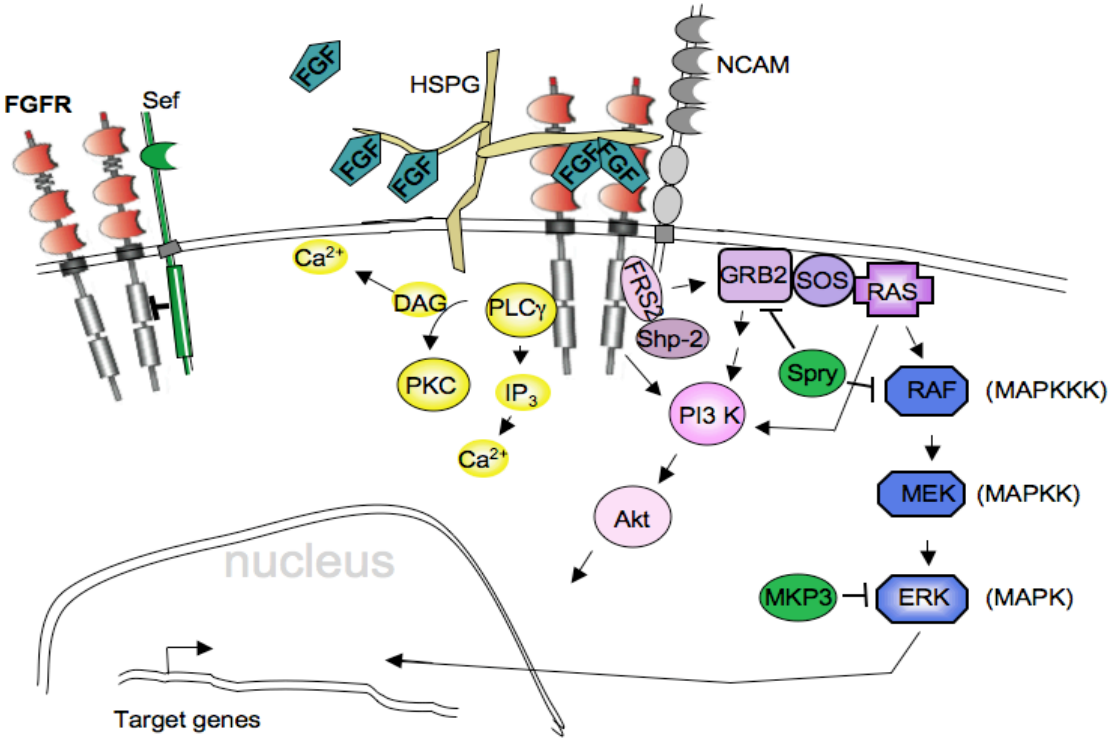

Fig. 8. Intracellular signalling pathways activated through FGFRs in vertebrates.
For simplicity, only those proteins are indicated that are discussed in the main text. The formation of a ternary FGF-heparin-FGFR complex leads to auto-phosphorylation of the receptor and activation of intracellular signaling cascades, including the Ras/MAPK pathway (shown in blue), PI3 kinase/Akt pathway (shown in pink), and the PLC□/Ca_2□ pathway (shown in yellow). Proteins connected with two pathways are shown in purple. Members of the FGF synexpression group of inhibitory function are illustrated in green. The Ras/MAPK cascade is activated by binding of Grb2 to phosphorylated FRS2. The subsequent formation of a Grb2/SOS complex leads to the activation of Ras. The PI3 kinase/Akt pathway can be activated via three routes as indicated. First, via FRS2 and Grb2; second, by binding to a phosphorylated tyrosine residue of the FGFR; third, activated Ras can induce membrane localization and activation of PI3 kinase. DAG, diacylglycerol; IP3, inositol-1,4,5-triphosphate. (adapted from Böttcher and Niehrs, 2005).

In contrast to most other RTKs, FGF receptors lack a binding site for Grb2/Sos (Son of sevenless) and need to recruit a docking protein, FRS2, to activate the MAPK pathway (Kouhara et al., 1997). It was shown for FGFR1 that FRS2 constitutively binds to the receptor even without activation (Xu et al., 1998). FRS2 binds to Grb2 upon

phosphorylation of the receptor, which leads to translocation of the Grb2/Sos complex to the plasma membrane. The close proximity thus attained allows the guanine nucleotide exchange factor (GEF) Sos to activate the membrane-bound GTPase Ras by GTP exchange. Activation of Ras then induces the activation of several effector proteins, including Raf leading to a cascade of MAPK signalling, which ultimately activates target transcriptions factors.

PLCγ contains a SH2 domain and binds directly to the phosphoylated tyrosine residues of the activated receptor. PLCγ cleaves phosphatidylinositol-4,5-diphosphate into diacylglycerol, activating protein kinase C (PKC), and inositol-1,4,5-trisphosphate (IP3) which stimulates the release of intracellular Ca^{2+}. This signalling cascade is not essential for mitogenesis and differentiation and also is not directly involved in cell motility. However, it has been implicated in neuronal development of vertebrates and oocyte maturation of *C.elegans* (Powers et al, 2000; Böttcher and Niehrs, 2005; Bui and Sternberg, 2002).

The PI3 kinase pathway can be directly activated, through Grb2 activation or via Ras signalling after FGF receptor activation, triggering target proteins such as Akt or protein kinase B (PKB). Activation of the PI3 kinase pathway is essential for differentiaion during embryogenesis (Chen et al., 2000) and is involved in regulation of cell proliferation and survival (Eswarakumar et al., 2005; Hyashi et al., 2008; Ninov et al., 2009). PI3 kinase signalling often is acting in parallel to the Ras/MAPK pathway, as shown for the induction of the mesoderm in *Xenopus* embryogenesis (Carballada et al., 2001; Keenan et al., 2006). FGF induced Ras/ERK activation and PI3 kinase activity thereby attenuate the respectively induced cellular responses and act antagonistically during differentiation (Sasson and Stern, 2004; Hyashi et al., 2008).

Through involvement of PI3 kinase/Akt signalling in the TOR (target of rapamycin) signalling pathway, FGF signals are linked to growth and developmental timing,

fertility and lifespan (Wilson et al., 2007). PI3 kinase activation and subsequent TOR involvement was also found to be required as essential modulators for epithelial remodelling such as during tubule formation (Walid et al., 2008). Activation of Ras, PI3kinase and TOR pathways are therefore in focus of cancer research, as their concerted functions can thus modulate a range of aspects in tumor growth (Shaw and Cantley 2006; Engelmann, 2009).

I. 3. 3 Regulation of FGF signalling

FGFs appear to be diffusible and are able to act in a dose-dependent fashion suggesting that these signal molecules might act as morphogens (Leptin and Affolter, 2004; Cayoso and Marti, 2005; Böttcher and Niehrs, 2005). Several mechanisms have been revealed to regulate FGF signals during development.

Heparan sulfate proteoglycans (HSPGs) play an important role in regulating FGF concentrations and in mediating receptor binding of FGFs (Ornitz, 2000; Böttcher and Niehrs, 2005; Thisse and Thisse, 2005). HSPGs are cell surface and extracellular matrix macromolecules compromised of sulfated glycosaminoglycan chains covalently bound to a core protein (Bernfield et al., 1999). HSPGs are required for FGFs to effectively activate the receptor, by either facilitating the interaction or stabilising the ligand-receptor complex. Furthermore, they determine the interaction between individual FGF family members with certain FGFRs. Structure analysis of ternary FGF-heparin-FGFR complexes has revealed that heparin bridges two receptor molecules to form a dimer that binds two ligands (Schlessinger et al., 2000). It is shown that each ligand-receptor pair has distinct requirements for both complex formation and signalling. Changes in heparan sulfate (HS) synthesis depending on glycosyltransferases and sugar sulfotransferases are spatiotemporally regulated during embryonic development. Thus, changes in HS are suggested to act as critical temporal regulators of growth factor

signalling (Allen and Rapreaeger, 2003). The binding to HSPGs also protects FGFs from thermal denaturation and proteolysis and also limits FGF diffusion, thereby regulating FGF activity within a tissue (Flaumenhaft et al., 1990; Park et al., 2000).

In addition to HSPGs, transmembrane cell adhesion molecules (CAMs) can modulate FGF signalling and activate the receptor even in absence of a FGF ligand (Kiselyov, 2008; Murakami et al., 2008). N-CAM, N-Cadherin and L1 (lumbar spinal nerve1) can interact with FGF receptors via their extracellular domains and induce the formation of multiprotein signalling complexes. Such complexes may mediate neurite outgrowth and cell-matrix adhesion (Niethammer et al., 2002; Williams et al., 2002).

A negative regulator of FGF signalling is the transmembrane protein Sef (Similar to FGF). It is synexpressed with and under control of FGF signalling in zebrafish and mouse, recapitulating the characteristic pattern of FGF8 (Lin et al., 2002; Fürthauer et al., 2002). Sef inhibits FGF signalling as an antagonist of FGF mediated Ras/MAPK signalling, but two controversial models propose either interaction with the receptor or inhibition of ERK nuclear translocation as molecular mechanism of Sef action (Fürthauer et al., 2002; Tsang et al., 2004). Intracellular inhibitory ERK regulation is also mediated by MAPK phosphatase 3 (MKP3), the expression of which is also regulated by FGF signalling in negative feedback regulation (Eblaghie et al., 2003; Kawakami et al., 2003; Li et al., 2007; Ekerot et al., 2008).

A third group of well-known negative regulators of FGF signalling are the proteins of the Sprouty (Spry) family, compromised of four members in vertebrates (Minowanda et al., 1999; Mason et al., 2006). Sprys mediate different protein-protein interactions that result in events antagonizing and mediating cross-talk between RTK signalling including FGF signalling (Kim and Bar-Sagi, 2004; Kim et al., 2007; Ding et al., 2007), whereby investigation of Sprys function led to controversy. Many studies have identified Sprys as negative regulators of the MAP kinase ERK, others however

determine Spry inhibition upstream of Ras or at the level of Raf. However, most of the studies performed show that Sprys associate with Grb2, resulting in repression of the signal by blocking Grb2 interaction with FRS2. It was also shown that Spry proteins are in vivo targets of the tyrosine phospohatase Csw/Shp-2 (Jarvis et al., 2006). Spry proteins regulate FGF signalling in a feedback-induced antagonism during essential developmental processes such as stem cell maintenance and differentaiation, axis specification and morphogenesis (Fürthauer et al, 2001; Klein et al., 2006, 2008).

I. 4 FGF signalling in *Drosophila*

Invertebrate model organisms such as *Drosophila* or the nematode *Caenorhabditis elegans* are particularly amenable for functional analysis, as their repertoire of FGFs and their receptors is less complex compared to vertebrates. Only two FGFs signal through a single FGF receptor in development and differentiation of *C. elegans*, and two FGF signalling pathways regulate different developmental processes *Drosophila*. The *Drosophila* genome contains two FGFR encoding genes, *breathless* (*btl*) and *heartless* (*htl*), and three genes coding for their respective ligands, *branchless* (*bnl*), *thisbe* (*ths; FGF8-like1*) and *pyramus* (*pyr; FGF8-like2*) (Shishido et al., 1993; Itoh and Ornitz, 2004).

The FGF receptor Btl and its ligand Bnl are required for border cell migration during oogenesis and are essential during branching morphogenesis of the respiratory (tracheal) system in embryogenesis and pupal development of *Drosophila* (Murphy et al., 1995; Lee et al., 1996; Sato and Kornberg, 2002). Htl is activated by its two ligands Ths and Pyr, and Htl mediated FGF signalling is essential for migration and differentiation of mesoderm cells and their derivatives (Michelson et al., 1998; Schumacher et al., 2004; Gryzik and Müller, 2004; Stathopuolos et al., 2004).

I. 4. 1 The FGF8-like Htl ligands Ths and Pyr

Ths (FGF8-like1) and Pyr (FGF8-like2) were both identified to be ligands for the mesodermally expressed FGF receptor Htl (Gryzik and Müller, 2004; Stathopoulos et al., 2004). Similar to the third known FGF protein in *Drosophila*, Bnl, Ths and Pyr represent larger FGF proteins (84 kDa and 86 kDa) compared to the vertebrate FGFs (17 – 34 kDa) (Fig. 9).

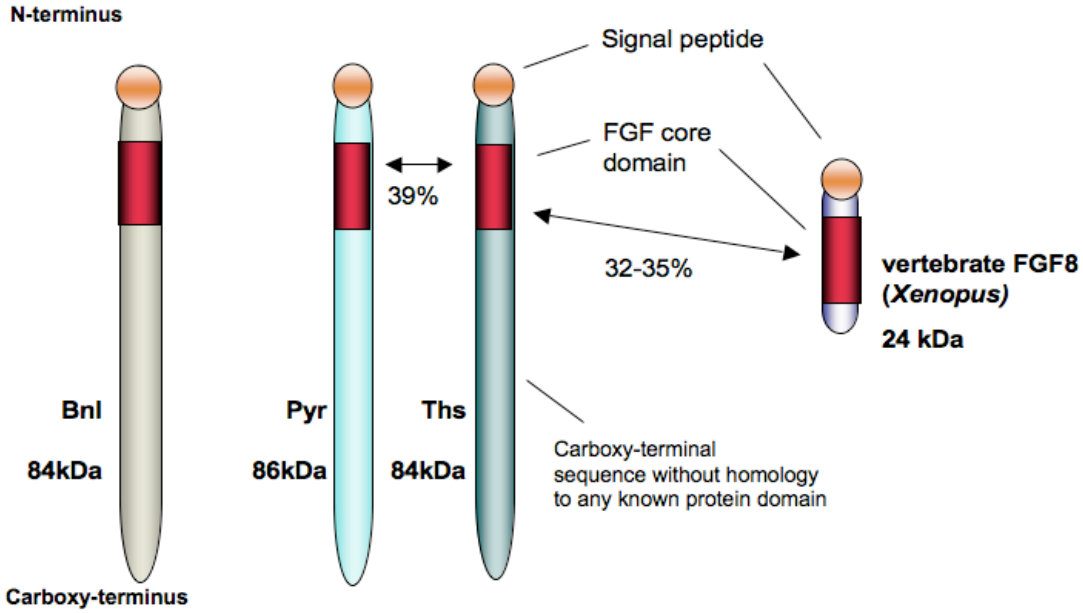

Fig. 9. Structural comparison of the *Drosophila* FGFs Branchless (Bnl), the FGF8-like Htl ligands Pyramus (Pyr) and Thisbe (Ths), and a vertebrate FGF8 family member (*Xenopus* FGF8).
FGF molecules and domains are not shown in actual scale but to illustrate structural differences. All FGF proteins in *Drosophila* are large in comparison to vertebrate molecules (as indicated). The FGF core domains of Ths and Pyr show identity of 39% of the peptide sequence. Ths and Pyr FGF core domains are conserved to the vertebrate FGF8 FGF core domain sequence in 32-35% of all residues with Pyr being slightly more related than Ths. As Ths shows higher conservation with the ancestor FGF gene in the genome of *Anopheles gambiae*, Ths may represent the ortholog of the original FGF gene that upon a duplication event gave rise to the two closely related *ths* and *pyr* genes (Gryzik and Müller, 2004; Stathopoulos et al., 2004).

The polypeptide sequence of both Ths and Pyr contain a signal peptide at the N-terminus suggesting that the proteins are secreted. In addition to the conserved FGF core domain Pyr and Ths contain a carboxy-terminal tail, which is not conserved and unrelated to any known protein domains.

FGFs Bnl and the *C.elegans* FGF genes LET-756 are related to viral FGF-like molecules, and Bnl shows a 40% identity of its FGF domain with vertebrate FGFs 1, 2 and 9 (Sutherland et al., 1996; Stathopoulos et al., 2004). In contrast, sequence comparison with vertebrate FGF subfamilies classifies Ths and Pyr as members of the FGF 8/17/18 group (Gryzik and Müller, 2004). The FGF core domains of Ths and Pyr exhibit 39% identical amino acid residues, and a similar high identity of 32% to 35% amino acids to the FGF core domain of members compromising the vertebrate FGF8/17/18 subfamily.

However, the classification of Ths and Pyr, and also Htl, to a particular subfamily of FGF or FGFR is not undisputed, as they are also thought to be ancestral FGF genes that have been lost during metazoan development in vertebrates (Itoh and Ornitz, 2004; Itoh, 2007). The same is suggested for LET-756 from the *C.elegans* genome. Interestingly, LET-756 also contains an untypical long carboxy-terminus, which has been shown to contain several domains that serve for intracellular functions (Popovici et al., 2006a and 2006b). Whether Ths and Pyr similarly contain such additional function remains to be investigated.

Within their FGF core domain, all FGFs exhibit 28 highly conserved amino acids, six of which are identical (Ornitz and Itoh, 2001). Ths and Pyr FGF core domains contain nine amino acids identical within the FGF8 subfamily, four of which are identical in all FGFs (Gryzik and Müller, 2004). Both *ths* and *pyr* are conserved in the *Drosophila pseudoobscura* genome, but there is only a single gene in the mosquito, *Anopheles gambiae* (Stathopoulos et al., 2004). The *A. gambiae* FGF gene is more closely related to *ths* than *pyr* suggesting that ancestral dipterans contained a single copy of an FGF gene that underwent duplication after the divergence of mosquito but prior to the divergence of *Drosophila melanogaster* and *Drosophila pseudoobscura*. The equal relation of two genes chromosomally closely linked to *ths* and *pyr* are hold as evidence

that an ~50-kb interval containing the ancestral FGF gene, along with its neighbour, underwent a tandem duplication event. The sequence of *ths* shows greater conservation than *pyr* between their respective orthologs in *Drosophila pseudoobscura* suggesting that selection may be acting on *ths* to maintain some ancestral function, whereas *pyr* has been released from constraint and is rapidly evolving in the Drosophilids (Stathopoulos et al., 2004).

Their roles in development of *Drosophila melanogaster* and their signalling properties mediated by Htl are not fully understood. Analysis of Ths and Pyr function in development of the mesoderm is subject to this study.

I. 4. 2 Components of the FGF signal transduction in *Drosophila*

The *Drosophila* genome contains two FGF receptors, namely Btl and Htl (Shishido et al., 1993). In contrast to Btl containing five extracellular Ig-like domains, two Ig-like domains are characteristic for the Htl FGFR (Fig. 10A) (Shishido et al., 1993). The intracellular tyrosine kinase domains of Htl however shows a high identity of 79% with Btl kinase domains, and 60% identity to vertebrate FGFRs with all tyrosine kinase subdomains conserved. As in vertebrates, the formation of an active FGF-FGFR complex in *Drosophila* involves the function of HSPGs as co-receptors on the cell surface (Lin et al., 1999; Kamimura et al., 2001). Recent studies also show evidence that HSPG function is necessary for FGF signalling through Btl or Htl, as HSPG components and enzymes synthesising the glycoproteins were identified to be required for Btl signalling (Kamimura et al, 2006; Tian and ten Hagen, 2007a and b; Yan and Lin, 2007). The requirement for CAMs such as the homolog to vertebrate L1, Neuroglian (Nrg), and FasciclinII (FasII) has been shown to be essential for Htl dependent guidance of neurite outgrowth (Garcia-Alonso, 2000; Forni et al., 2004).

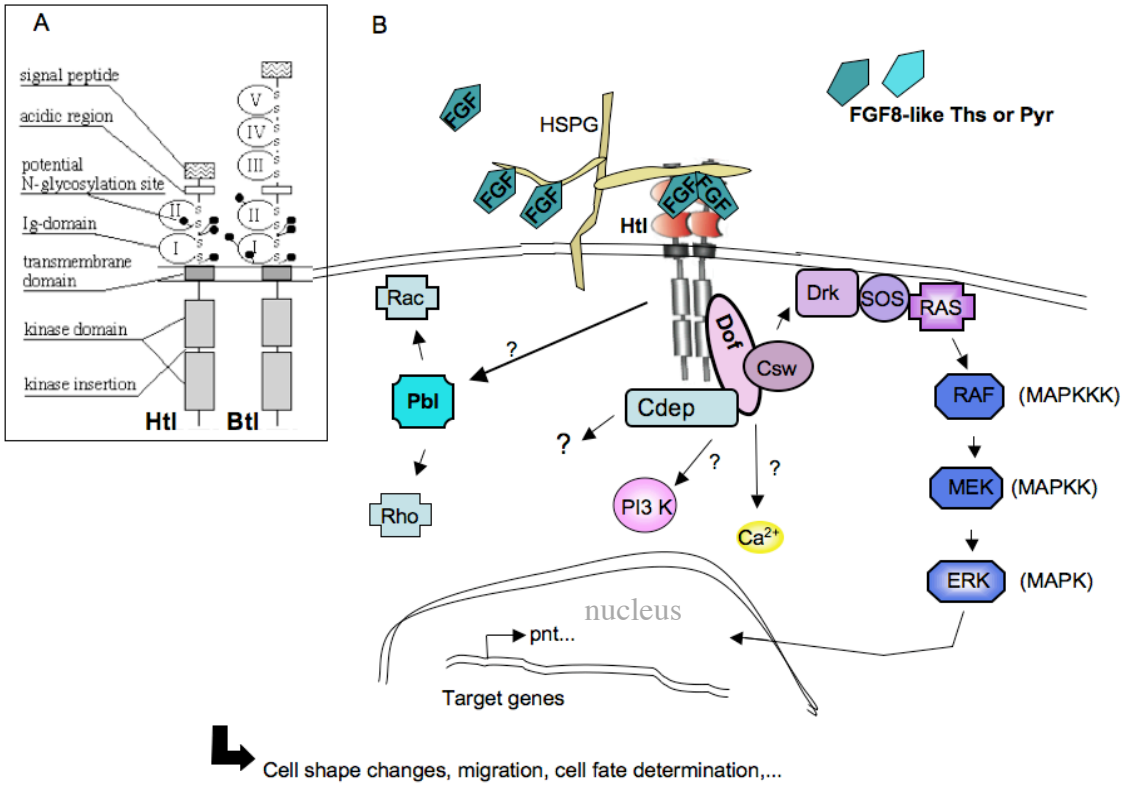

Fig. 10. Intracellular signalling pathways activated through FGFR Htl in *Drosophila*.
For simplicity, only those proteins are indicated that are discussed in the main text. **(A)** Structure of the two FGFRs present in *Drosophila*, Htl and Btl. **(B)** Formation of a ternary FGF-heparin-FGFR complex leads to receptor autophosphorylation and activation of the Ras/MAPK pathway (shown in dark blue). PI3 kinase/Akt pathway (pink) and Ca2+ (yellow) may be activated by Dof, as well as the FERM-GEF Cdep, the function of which is not known. Proteins connected with two pathways are purple. Dof binds to phosphorylation sites of Htl upon activation by Ths or Pyr, and recruits Csw. Whether Drk(Grb2) activation to activate the Ras/MAPK cascade involves complex formation with Dof or Csw is not known. The Rho GEF Pbl acts downstream or in parallel to FGFR signalling. Upon Htl activation, the substrate specificity of Pbl might be changed to promote Rac activation. (after Battersby et al., 2003, Petit et al., 2004; Sandmann et al., 2006; adapted and modified from Shishido et al., 1993; Böttcher and Niehrs, 2005)

Intracellularly, two components were identified which link FGF receptor activation to the Ras/MAPK pathway (Fig. 10B). These components are the adaptor protein Downstream-of-FGF (Dof, also known as Stumps (Sms) or Heartbroken (Hbr)) and the tyrosine phosphatase Corkscrew (Csw) (Vincent et al., 1998; Michelson et al, 1998b; Imam et a., 1999; Johnson Hamlet and Perkins, 2001; Petit et al., 2004). Dof is a specific adaptor for FGF signal transduction upstream of Ras in *Drosophila* exclusively expressed in Btl or Htl expressing tissues (Dossenbach et al., 2001). Dof is a founding member of a small family of proteins including BCAP and BANK that have been

identified to regulate B-cell-receptor-specific PI3 kinase activation and Ca^{2+} mobilisation (reviewed in Petit et al., 2004).

Csw encodes a non-receptor protein tyrosine phosphatase containing two SH2 domains, structurally related to the vertebrate tyrosine phosphatase Shp2. Shp2 is known as a positive regulator of RTK signalling that is bound by activated FRS2 and recruits Grb2, which leads to activation of the cell survival pathway via PI3K (Perkins et al., 1996; Ong et al., 2001).

In *Drosophila*, the only gene most related to vertebrate FRS2 (Flybase no. *CG13398*) shows a high degree of divergence to its vertebrate counterpart and is not required for Btl or Htl regulated processes, and the FGFR binding sites for FRS proteins are not conserved in FGFRs Btl and Htl (Battersby, 2003; Wilson et al., 2004). The family of Dof proteins conclusively are thought to have evolved in parallel to vertebrate FRS adaptor proteins in FGF signal transduction, linking the activated receptor with Csw to recruit the Grb2 homolog Drk (Downstream of receptor kinases) in order to activate the Ras/MAPK signalling cascade (Petit et al., 2004). In a yeast-two-hybrid screen, several putative binding partners of Dof have been identified (Battersby et al., 2003). Very interesting is its reported binding to spectrin, which could link cytoskeletal organisation to a response upon FGF receptor activation. A second interesting protein binding *in vitro* is Cdep, a FERM domain containing protein, which also comprises a RhoGEF activity (Koyano et al., 1997, 2001). Additionally, *in vitro* analysis of Dof suggests that Dof is sumoylated, and constructs of *dof* lacking the putative sumoylation sites affect receptor binding and intracellular localisation of Dof (Battersby, 2001). The mediation of FGF signalling via Dof thus contains high potential to direct different cellular responses, however particular regulation other than activation of Ras remains to be established in *vivo*.

In contrast to Dof that acts exclusively downstream of the FGF receptors Btl and Htl (Dossenbach et al., 2001), Csw also acts downstream of other RTKs such as the EGF receptor and RTKs Sevenless and Torso (Perkins et al., 1996; Firth et al., 2000; Johnson Hamlet and Perkins, 2001; Zhang et al., 2004). Csw is involved in nuclear localisation of phosphorylated ERK in response to integrin activation (Lorenzen et al., 2001; James et al., 2007). The functions as adaptor protein mediating activation of Ras upon growth factor signalling and nuclear localisation of activated ERK make Csw an important component mediating cellular response to parallel RTK signals.

First identified as an inhibitor of EGFR mediated MAPK signalling, the *Drosophila* Sprouty (Sty) is shown to inhibit FGF signal transduction to the MAPK signalling cascade upstream of Ras (Casci et al., 1999). Both Btl and Htl mediated signalling pathways were shown to respond to the inhibitory effect on MAPK activation of Sty by *sty* overexpression (Reich et al., 1999). Regulation of/by Htl mediated FGF signalling in mesoderm development however has not been demonstrated so far. *sty* expression is induced by Btl signalling and consequently absent in *bnl* or *btl* mutants (Hacohen et al., 1998). Interference of Sty inhibition of Htl mediated MAPK signalling is proposed to be regulated by simultaneous transcriptional activation of both *htl* and *sty* by Twist (Twi) (Dutta et al., 2005), or by both Htl signalling and other factors (Franzdottir et al., 2009). However, the function of Sty proteins as antagonists of RTK mediated MAPK activation is discussed controversy, and different studies indicate specific roles of the *sty* genes in development and multiple modes of action of the Sty proteins in regulation of the RTK-induced response (Mason et al., 2006).

Another mechanism to regulate FGFR activity was shown for Btl signalling during tracheal cell migration (Dammai et al., 2003). Abnormal wind disc (Awd) is involved in attenuation of Btl activity by vesicle-transport-mediated turnover through a dynamine-mediated pathway. In embryos mutant for *awd* or *shibire (shi)* (the gene encoding

dynamin in *Drosophila*), a phenotype in tracheal development was observed classified as ectopic tubule formation and aberrant migration of embryonic tracheal cells (Dammai et al., 2003). Reducing the amount of Btl in tracheal cells could rescue this phenotype. Thus, Awd controls the levels of active Btl receptor complexes at the cell surface, restricting the signalling events transduced to influence the migrational behaviour of tracheal cells.

Like other RTK signalling cascades involving MAPK activation, inhibitors of nuclear translocation of phosphorylated MAPK also regulate the FGF pathway. Phosphorylated MAPK initiates the transcription of target genes, or proteins facilitating MAPK function (Schlessinger, 2000; Tsang and Dawid, 2004).

In *Drosophila*, several proteins regulating MAPK signalling were found for processes dependent specifically on signalling via RTKs EGFR or Sevenless. These include the invertebrate MKP homolog Mkp3, the transcriptional repressor Yan/Anterior open (Yan/Aop) and transcriptional activator Pointed (Pnt), ETS-family proteins both regulated by Mae (modulator of the activity of Ets), or MASK, the inhibitive mechanism of which is still unknown (Smith et al., 2002; Cela and Limargas, 2006; Qiao et al., 2006). Pnt and Yan/Aop were also found to regulate MAPK signalling mediated by activation of Btl in a negative feedback mechanism (Sutherland et al., 1996; Cabernard and Affolter, 2005; Myat et al., 2005). A specific MAPK regulator has not been identified to be specific for MAPK signalling upon activation via Htl/FGF signalling. However, *pnt* also shows expression in the mesoderm during stages of mesoderm migration, and recent functional analysis of Htl mediated FGF signalling in glia differentiation and screening for RTK target genes suggest Htl dependent MAPK signalling is also able to regulate *pnt* expression (Klämbt, 1993; Franzdottir et al., 2009; Leatherbarrow and Halfon, 2009).

The importance of a general RTK signal for FGFR function equally to Htl and Btl signals was demonstrated by analysis of hybrid receptor molecules of Htl and Btl extracellular domains fused to kinase domains of the EGFR, another RTK, Torso, and Btl as well as Htl intracellular kinase domains, respectively (Dossenbach et al., 2001). Both Htl and Btl-dependent cell migration processes could be rescued by these hybrid receptors in absence of either Htl or Btl, indicating that cell migration occurred in response to a general RTK signal, however during a specific time window.

In conclusion, FGF signalling in *Drosophila* acts through classic RTK signalling pathways, and response as well as regulation of either Btl or Htl mediated FGF signalling seems to be dependent on the cell type specific composition of regulatory proteins.

I. 4. 3 FGF signalling to Rho proteins

The requirement of both the Btl and Htl signalling pathways in cell migratory processes during development is well known and will be described in the following. How signalling from the FGF receptor is transduced to control cell behaviour is still an issue unsolved. The family of Rho (Ras homologous) GTPases proteins seems to play a pivotal role in this signal transduction and is most relevant to cell migration (Raftopoulou and Hall, 2004).

A large body of evidence suggests that in the same way as RTK mediated activation of PI 3-kinase, PLCγ, and the MAPK pathway, RTK signalling to Rho proteins is a common signal transduction mechanism (Schiller, 2006). Members of the Rho family are major regulators of the cell cytoskeleton and respond to external stimuli (Petit et al., 2002). Similar to Ras, Rho GTPases act as molecular switches that cycle between inactive GDP-bound and active GTP-bound forms. This cycling is regulated by Guanine nucleotide exchange factors (GEFs), which exchange GDP for GTP, and GTPase-

activating proteins (GAPs), which induce the hydrolysis of bound GTP to GDP. Their best-characterised function is in the regulation of actin dynamics (Raftopoulou and Hall, 2004). Classic tissue culture studies classically carried out in fibroblasts, have shown that Rho regulates the assembly of contractile, actin-myosin filaments, while two other family members, Rac and Cdc42, regulate the polymerisation of actin to form peripheral lamellipodial and filopodial protrusions, respectively (Fig. 11). In addition, all three GTPases promote the assembly of integrin-based, matrix adhesion complexes.

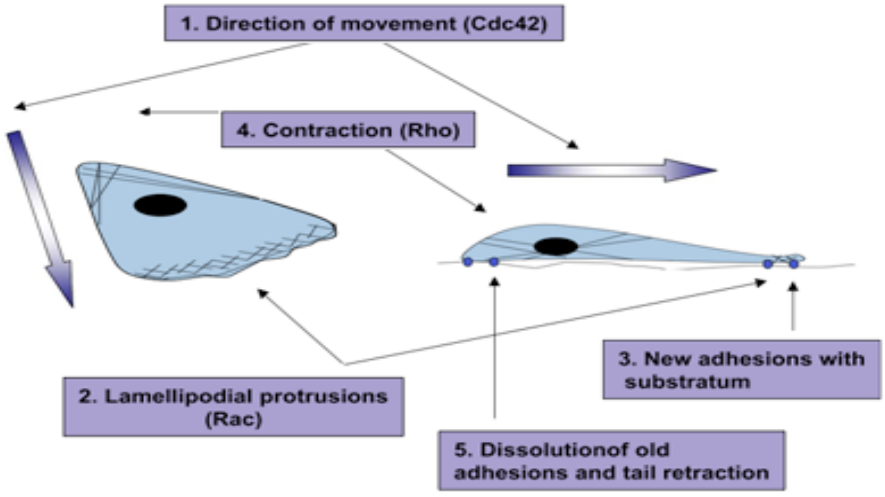

Fig. 11. Roles of Rho GTPases in migrating cells.
A migrating cell (seen from the top and side; the broad arrows indicate direction of movement) needs to perform a coordinated series of steps to move. Cdc42 regulates the direction of migration. Rac induces membrane protrusions at the front of the cell through stimulation of actin polymerization and integrin adhesion complexes. Rho promotes actin-myosin contraction in the cell body and at the rear (after Raftopoulou and Hall, 2004).

The small GTPase Rac has been suggested to play a major role in controlling actin dynamics and cell adhesion induced by chemoattractants such as growth factors (Etienne-Manneville and Hall, 2002). Interestingly, a recent study shows evidence for a proposed role of the RhoGEF Pebble (Pbl) required during mesoderm migration, to activate Rac at the cell membrane at the expense of Rho1 activation in response to Htl activation during migration (van Impel et al., 2009). Thus, initiating cell migration, the activation of the FGF receptor is thought to stimulate actin polymerisation and

protrusive activity, whereas activation of particular target genes is involved in the process of cell fate decision and differentiation.

I. 4. 4 Bnl/Btl signalling regulates cell migration of tracheal cells

The tracheal system of *Drosophila* consists of hundreds of interconnected tracheal tubes that transport oxygen and other gases throughout the body (Cabernard et al., 2004). Tracheal branches are simple tubes consisting of an epithelia monolayer wrapped into a tube around a central lumen. The development of the tracheal system is initiated in the embryonic ectoderm by formation of ten bilaterally symmetrical placodes of ~20 tracheal precursor cells. After invagination of the tracheal placodes and two additional cell divisions, each of the tracheal sacs undergoes a similar sequence of morphogenetic events to generate one segment of the network (Fig. 12).

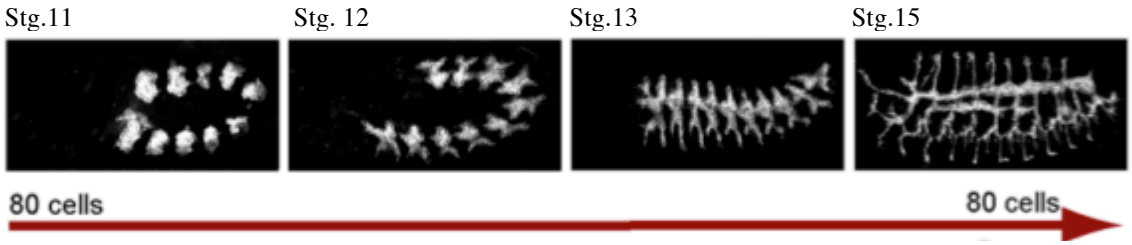

Fig. 12. Tracheal development in the *Drosophila* embryo.
The tracheal system arises from 10 placodes on each side of the embryo that bud in from the epidermis. On invagination of the tracheal cells and after 2 rounds of cell divisions, the individual tracheal metameres consist of 80 cells. From each placode, 6 branches grow out into different directions. Subsequently, some of these branches fuse to form a continuous network that will be used for oxygen supply in the hatching larva (adapted from Cabernard et al., 2004)

The determination of tracheal identity within the tracheal placode is achieved by expression of the transcriptions factors Trachealess (Trh) and Drifter/Ventral veinless (Drf/Vvl) (Petit et al., 2002). Activity of Trh/Vvl transcription initiation results in expression of genes crucial for tracheal development, such as *btl*, *dof* and the gene *tkv* coding for the Dpp receptor Thick veins (Tkv). The Dpp signalling pathway specifies the fate of the tracheal cells that will form the bud from the dorsal and ventral part from

the tracheal placode (Fig.13). In addition, Dpp signalling is required for directional guidance during subsequent tracheal cell migration.

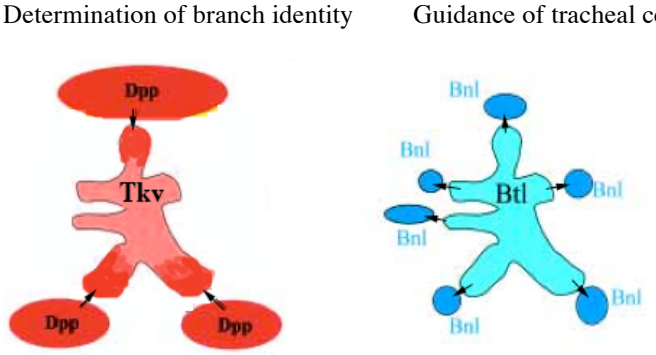

Fig. 13. Illustration of a tracheal placode and two signalling pathways involved in branch fate determination and guidance of tracheal cells.
The six primary branches are represented: The dorsal branch and the lateral anterior and posterior trunk branches depend on Dpp signaling to express identity genes, represented in dark red. Tracheal cell migration in the proper direction is guided by chemotaxis through Bnl (adapted and modified from Petit et al., 2002).

The spatial control of tracheal branch formation is exerted by Bnl/Btl signalling (Klämbt et al., 1992; Reichman-Fried et al., 1994; Sutherland et al., 1996). The FGFR Btl is expressed in the tracheal cells, whereas its ligand Bnl is expressed in distinct, developmentally defined groups of ectoderm and mesoderm cells surrounding the invaginating tracheal placode (Fig. 13).

Tracheal cells initially form sac-like, polarised epithelial sheets with a well-developed apical side toward the lumen (Affolter and Weijer, 2005). As a response to the local secretion of Bnl, the basal membranes of the tracheal cells form dynamic filopodial and lamellipodial extensions that explore the environment. Bnl signalling is essential for these protrusions to form and for the ultimate movement of the cells towards the source of the signal. However, only a subset of cells responds to the signal, presumably the ones in closest proximity to the source. The tight linkage of the tracheal epithelium results in a deformation of the entire structure upon the local cell movement and ultimately in the formation of bud-like extensions. Further cell rearrangements and cell

intercalation extend these bud-like structures and thus establish a highly regular tubular network (Ribeiro et al., 2002). Bnl acts as a chemo attractant for the tracheal cells to migrate, but recent studies discovered the necessity of both Bnl/Btl and Dpp signals for regulation of target gene expression (Myat et al., 2005).

Further insight in FGF signalling mediated control of tracheal cell migration was achieved in studies of the outgrowth of the air sac of the dorsal thorax (Sato and Kornberg, 2002). During larval development, air sac precursor cells form buds from a particular tracheal branch in response to the FGF ligand Bnl, proliferate and migrate to the adepithelial layer of the wing imaginal disc, an epithelial tissue that will give rise to part of the dorsal thorax and the wing of the adult fly (Fig. 14).

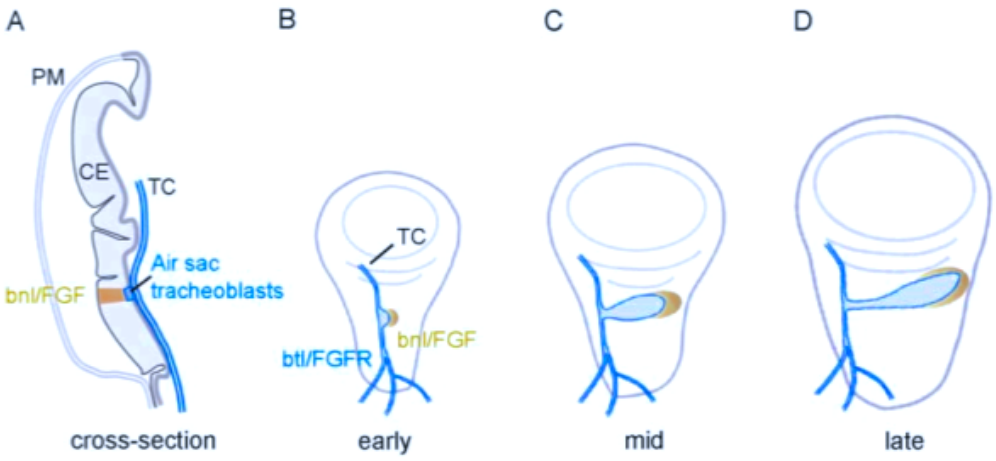

Fig. 14. Air sac development in the third instar larva of *Drosophila*.
(A) Cross section through a wing imaginal disc of a *Drosophila* third instar larva. The transverse connective branch (TC) attaches to the columnar epithelium (CE) of the wing imaginal disc. A group of CE cells, which lie underneath of the airsac, secrete the Btl ligand Bnl (yellow). PM, peripodial membrane. **(B-D)** Schematic drawings of three stages of air sac development corresponding to early, mid, and late third instar larval stages. Cells from CE express Bnl/FGF (yellow). The tracheal cells of the TC as well as the air sac tracheoblast cells express the Bnl/FGF receptor Btl/ FGFR (blue). The air sac tracheoblast cells migrate following the Bnl/FGF-secreting CE cells. Cell proliferation contributes to increase of size of the air sac (adapted from Cabernard et al., 2004)

In this system, FGF signalling is proposed to act as a mitogen, a chemoattractant, and an instructive determinant, reprogramming the cells in the tracheal branch to become air sac tracheoblasts (Cabernard and Affolter, 2005). Live imaging studies have shown that

Bnl signalling induces rearrangements of the cytoskeleton resulting in formation of filopodia (Ribeiro et al., 2002; Sato and Kornberg, 2002). This induction of dynamic protrusive activity was interpreted as induction of cell motility and thus a conditional necessity for migration (Cabernard and Affolter, 2005).

The outgrowth of the air sac thereby is delineated as an equivalent to the directed enlargement of an epithelial sheet by random cell division and directional migration. The luminal space is generated by the directional migration of a few cells at the tip of the epithelial structure away from the cuticle of the existing tracheal branch and is controlled by FGF signalling. Increasing cell numbers in the sac-like epithelium by cell divisions then lead to expansion of the epithelial structure, and cell division and cell survival both depend on EGFR signalling in these cells. The tracheal cells do not undergo EMT, but remain within the epithelium; even the protruding cells at the tip of the air sac remain embedded within the epithelial cell collective and maintain adherens junctions with their neighbours. Live imaging confirmed that the tip cells actively migrate and use the filopodial extensions to sense the chemoattractant gradient of Bnl in their environment (Cabernard and Affolter, 2005). Furthermore, Btl mutant clones of cells were excluded from the tip during migration, indicating a role of clear leader cells that respond to the signal and generate the movement of the structure through epithelial connection to the cells behind.

In contrast to the epithelial cell movements of tracheal cell migration in embryonic tracheal morphogenesis or larval air sac outgrowth, the migration of mesoderm cells during gastrulation is a movement of a mesenchymal cell collective. The spreading of mesoderm cells after invagination of the mesodermal cell sheet is regulated and dependent on FGF signalling via Ths and Pyr through the second *Drosophila* FGFR,

Htl. The process of mesoderm development and its involvement of FGF signals will be further explained in the following chapters completing the introduction.

I. 5 FGF signalling in vertebrate mesoderm development

FGFs are implicated in multiple processes during embryonic development such as patterning, morphogenesis, differentiation, and regulation of cell proliferation and migration (for review see Goldfarb, 1996; Powers et al., 2000; Coumoul and Deng, 2003; Böttcher and Niehrs, 2005; Thisse and Thisse, 2005). Prominent examples of FGF function are the induction, initiation and maintenance of limb development and limb regeneration after injury (Xu et al., 1999; Yokoyama et al., 2001). However, induction and patterning of the mesoderm during gastrulation is one of the earliest events in which FGF signalling was revealed to be essential (Thisse and Thisse, 2005; Böttcher and Niehrs, 2005).

In chick, zebrafish, the amphibian (*Xenopus laevis)* and mammals (mouse, rabbit), FGF signalling acts in concert with BMP, retinoic acid (RA) and canonical Wnt signalling in dorsal-ventral patterning (Nutt et al., 2001; Fürthauer et al., 2004; Olivera-Martinez and Storey, 2007). Similar requirements have been demonstrated in the control of left-right asymmetry, where FGF signalling interacts with Nodal and Pitx2 homeobox gene function (Wright, 2001; Fischer et al., 2002). In vertebrates, FGF signalling during mesoderm formation was interpreted as a competence factor, facilitating and regulating the response to signalling of the cells to other pathways such as BMP, Nodal, RA and Wnt. However, during differentiation FGF signalling is often attenuated by these signals to modulate regional specific responses.

During vertebrate gastrulation, the mesendoderm cells move into the embryo to take up their characteristic positions, and cells move extensively in a collective manner (Weijer,

2009). The epithelial precursors of the mesendoderm undergo a partial (*Xenopus*, fish) or complete (chick, mouse) EMT as they ingress through the blastopore or primitive streak, respectively. This morphogenic cell movement is achieved by different modes of mesodermal cell ingression during amphibian, avian and mammalian gastrulation (Fig. 15), but follows comparable signalling patterns.

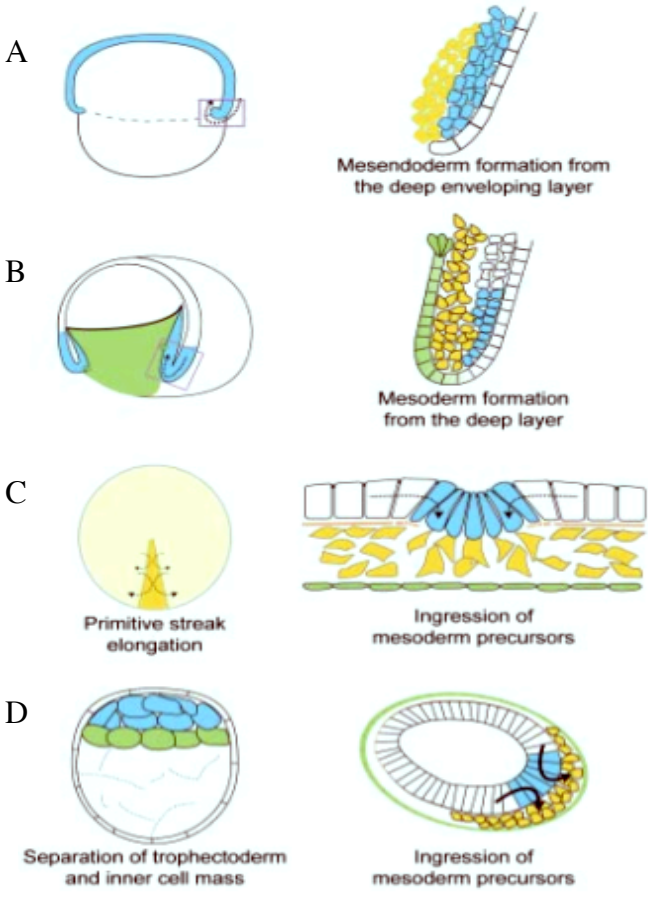

Fig. 15. Processes of mesoderm formation in several triploblastic animals.
Blue, mesoderm precursors located in the ectoderm; yellow, mesoderm; green, endoderm. **(A)** zebrafish; During the involution movement at the blastoderm margin, the deep enveloping layer flattens due to radial cell intercalation. Differential cell adhesion mediated by cadherins and differential tensile force in cells of different germ layers have been shown to contribute to germ layer segregation. **(B)** Xenopus;, the deep layer cells intercalate radially prior to the involution. They adopt an epithelioid morphology with a single-cell layer and a thin basement membrane, but without tight junctions. These cells involute and form the majority of the mesoderm lineage. EMT occurs incompletely. **(C)** chick; Most of the mesoderm cells are formed by the convergence of epithelial-shaped epiblast cells towards the forming primitive streak, which subsequently undergo EMT and ingress to adopt a mesenchymal morphology. **(D)** mouse; Similar to chick, the mesoderm and definitive endoderm cells in mammals are derived from the epithelial-shaped epiblast cells through the EMT process. Adapted from Nakaya and Sheng, 2008.

Common to all these examples, the migration of mesoderm cells and formation of mesodermal structures are largely dependent on FGF signals (Böttcher and Niehrs, 2005; Solnica-Krezel, 2005; Dormann and Weijer, 2006).

During gastrulation of the chick embryo, mesoderm migration is regulated by FGF signalling in a chemo-attractive as well as -repulsive manner (Yang et al., 2002; Chuai and Weijer, 2009). Epiblast cells ingress through the primitive streak and migrate away to form the endodermal, mesodermal and extraembryonic structures (Fig. 15C). Cells emerging at different anterior-posterior positions from the streak show characteristic cell migration patterns in response to guidance signals from neighbouring tissues (Fig. 16). The mesoderm cells move away from the streak repelled by FGF 8 mediated signalling in the posterior moving streak region, and are attracted by the source of FGF 4 in the region of the head forming anterior (Chuai and Weijer, 2009). In later differentiation of the extending body axis, FGF 8 antagonizes RA signalling to control differentiation of the presomitic mesoderm, which in addition is regulated by an intermediate function of Wnt signalling (Olivera-Martinez and Storey, 2007).

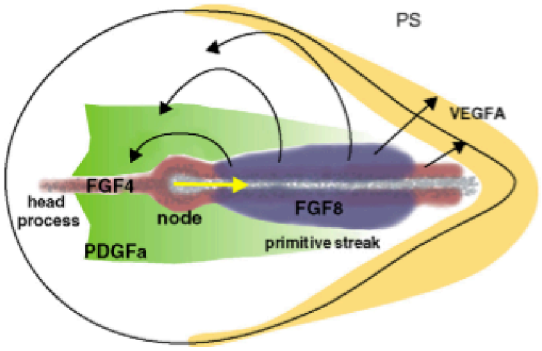

Fig. 16. Signals controlling cell movement in the fully extended streak stage.
Black arrows indicate movement from cells out of the streak in various anterior to posterior positions. Cells move out of the streak under the influences of FGF8. Anterior cells move back in response to FGF4 produced in the forming head process, cells in the posterior streak move in response to VEGF. PDGF signalling in the epiblast controls N-cadherin expression of migrating mesoderm cells and lays out a migration domain. Adapted from Chuai and Weijer, 2009).

In *Xenopus* and zebrafish embryos, FGF signalling in combination with Nodal signalling is required for mesoderm induction and mesodermal cell fate maintenance. FGFs also regulate mesoderm migration and later posterior mesoderm development and disruption of FGF signalling results in the loss of most trunk and tail mesoderm (Nutt et

al., 2001; Draper et al., 2003). In the mouse embryo, cells ingress through the streak in absence of FGF signalling, but fail to migrate away from the site of ingression subsequently, resulting in severe reduction of paraxial mesoderm structures (Ciruna and Rossant, 2001).

In summary, FGF signalling plays simultaneous roles during gastrulation to induce mesodermal cell fate and morphogenetic movements in positive interference with other signalling pathways.

I. 6 FGF8-like function in *Drosophila* mesoderm development

Mesoderm development in *Drosophila* is also controlled by FGF signalling, and in agreement with the predominant role of FGF 8 in vertebrate models, the Htl ligands Ths and Pyr show highest similarity to the vertebrate FGF 8/17/18 subfamily.

I. 6. 1 Dorso-ventral axis patterning

The specification of the mesoderm in the *Drosophila* embryo is regulated via a transcriptional network and signalling of the Toll receptor (Schneider et al., 1991; Stathopoulos and Levine, 2002; Hong et al., 2008). The patterning of the dorso-ventral axis of the embryo is controlled by the transcription factor Dorsal (Dl), which is related to the mammalian NF-κB. Differential activation of the Toll receptor leads to the formation of a nuclear Dl gradient with highest levels in ventral regions and progressively lower levels in dorsal regions (Fig. 17). The Dl gradient initiates dorsal-ventral patterning by regulating 60-70 target genes in a concentration-dependent manner (Hong et al., 2008). At the ventral side of the embryo, Dl activates the expression of the transcription factors Twi and Snail (Sna), and the Dl/Twi/Sna network activates and

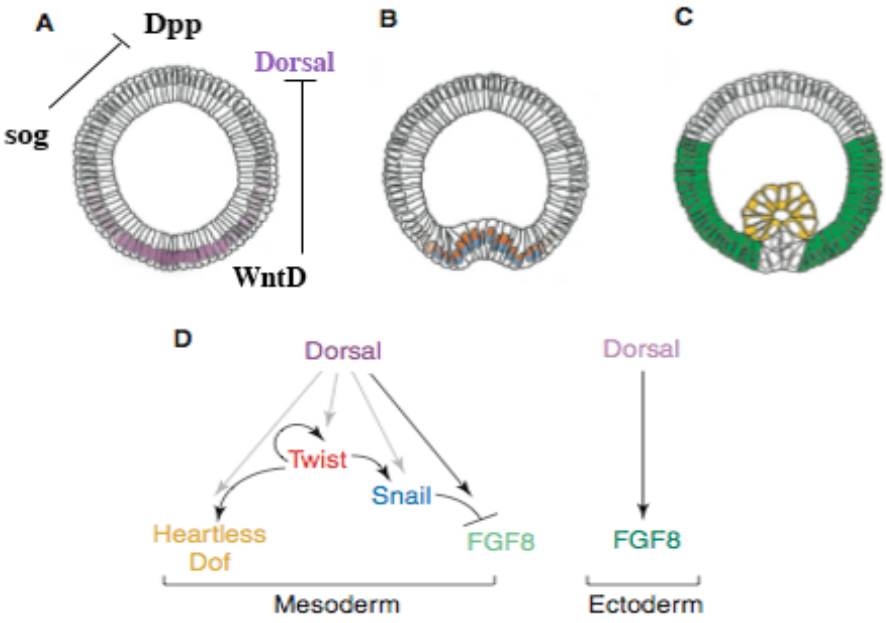

Fig. 17. Expression patterns and hierarchy of genes involved in FGF-dependent morphogenesis of the mesoderm.
The expression patterns are shown on cross-sections of embryos in successive stages of gastrulation. The drawings reflect the logical succession of the hierarchy of gene activities. The ventral side of the embryo is at the bottom. **(A)** The amount of Dorsal (Dl) protein in the nuclei forms gradient with highest levels at the ventral side. Dl activity prevents expression of *dpp* but promotes expression of *wntD*. Moderate amounts of Dl activate Sog expression, which restricts the Dpp domain laterally **(B)** high amounts of Dl activate Twist (Twi) (red) and Snail (Sna) (blue). **(C)** The FGF receptor Heartless and its signal transduction substrate Dof (both yellow) are expressed in the central portion of the invaginated mesoderm. The ligand for the receptor, Fgf8 (green), is expressed in the ectoderm. **(D)** Genetic hierarchy of genes shown in A–C. *htl* also can respond directly to Dorsal, but critically depends on Twist, which acts as an activator promoting its own transcription as well as that of *snail, htl* and *dof*. Snail is predicted to block the expression of the Fgf8 genes in the mesoderm. Right: low levels of Dl, activate FGF expression but not mesodermal identity genes (adapted from Leptin and Affolter, 2004)

represses other zygotic genes to form the correct expression patterns along the dorso-ventral axis (Stathopoulos and Levine, 2002; Ganguly et al., 2005). Twi activates genes characteristic for mesodermal cell fates such as *htl* and *dof*. The lateral neuroectoderm is specified by expression of *short gastrulation* (*sog*) -the invertebrate homolog of *chordin* – and refined by inhibition of lateral extension through dorsal Dpp expression. Dorsal and Sna binding sites were also identified within the sequence of the FGF8-like genes *ths* and *pyr* as well as *wntD*, a Wnt family member, which results in lateral expression domains in the neuroectoderm and avoiding the ventral mesodermal domain (Stathopuolos et al., 2004; Hong et al., 2008). It was shown that WntD in turn negatively regulates Dl function, probably at a step upstream of Dl nuclear localisation,

and thus maintaining the Dl gradient and the dorsal expression of Dpp (Ganguly et al., 2005).

I. 6. 2 Invagination and EMT

Following specification of the mesoderm domain, mesoderm cells are internalized by invagination as an epithelial sheet through a ventral furrow (Fig. 18) (Leptin and Grunewald, 1990). Cells at the most ventral medial positions flatten on their apical (outer) sides while their nuclei begin to migrate basally.

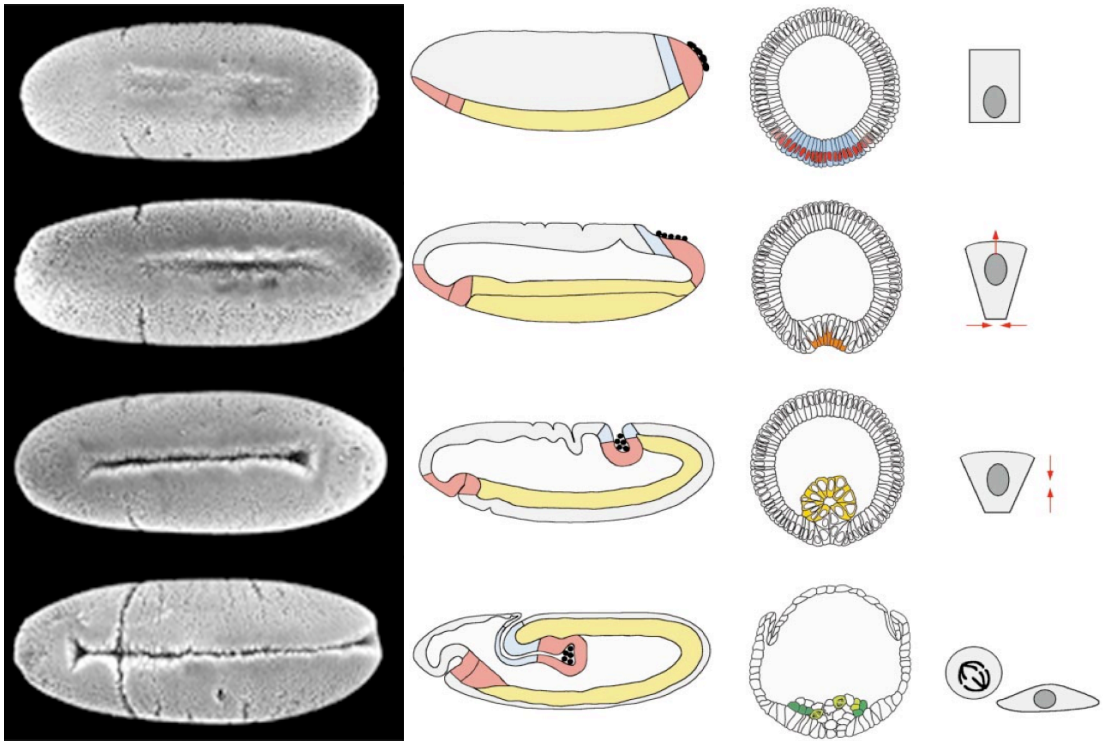

Fig. 18. Ventral invagination of the mesoderm in *Drosophila* and collapse of the invaginated epithelium.
The right panel shows scanning electron microscope photographs of embryos during mesoderm invagination from ventral view (www.sdbonline.org/fly/aimain/turner). The mesoderm invaginates as an epithelial sheet. The middle panel shows cartoons of the corresponding stages during germband extension from a lateral view; yellow: mesoderm. The right panel shows drawings from cross sections of the respective phases and characteristic mesodermal cell shapes. Colors correspond to transcripts and proteins as described in Fig.16. Fog and Cta are active during apical constriction. As the mesoderm starts to invaginate, the nucleus moves basally and the apical side constricts. The invaginated mesoderm forms a tube and the cells divide and undergo a transition to acquire mesenchymal characterists. Dof and Htl are required for the subsequent steps. The cells disperse onto the ectoderm and cells at the margin activate MAPK/ERK. Red: Twi; blue: sna; orange: Fog, Cta; yellow: Htl, Dof; green: phosphorylated ERK (adapted from Leptin, 1999 and Wilson and Leptin, 2000).

The cells progressively constrict their apical domains until they are wedge shaped, and finally shorten along their apical-basal axis, which leads to the formation of a furrow along the ventral midline and the eventual invagination of the mesoderm (Leptin, 1999; Kölsch et al., 2007). The known regulators of this process are Concertina (Cta), the α - subunit of the heterotrimeric G protein, a secreted peptide coded by *folded gastrulation* (Fog) and the transmembrane protein T48. The two Twist targets Fog and T48 appear to act in separate pathways to converge on RhoGEF2, resulting in activation of the Rho1 kinase (DROK) by activated Rho, which integrates the signal consequently at the apical side to activate the contractility of myosin and modify the actin cytoskeleton (Dawes-Hoang et al., 2005; Kölsch et al., 2007). The mesodermal cell sheet such is internalised and forms an epithelial tube along the ventral midline.

Following invagination, the mesoderm cells undergo an epithelial to mesenchymal transition (EMT), when their epithelial characteristics such as apical adherens junctions and apico-basal polarity, are lost (Oda et al., 1998; Schumacher et al., 2004; Kölsch et al., 2007; Nakaya and Sheng, 2008). As observed so far, the transition from epithelial-shaped mesoderm precursors to mesenchymal-shaped mesoderm cells is rapid and appears to take place simultaneously for all precursors (Wilson and Leptin, 2000).

The current understanding of EMT involves a switch from E-Cadherin to N-Cadherin expression, resulting in different adhesive properties of the cells and dissociation from the epithelial cohesion, and generation of motility (Oda et al., 1998; Hay, 2005; Lee et al., 2006; Acloque et al., 2008; Nakaya et al., 2008). Although cell divisions in the mesoderm occur concurrently, cell shape changes associated with these are not responsible for disintegration of the mesodermal epithelial tube, as it occurs also in embryos mutant for Cdc25 (String), in which mitotic division in the embryo are blocked (Leptin and Grunewald, 1990).

FGF signalling as well was shown not to be involved in mesoderm invagination or to be essential for the mesenchymal transition process. Embryos lacking the FGF receptor show loss of all epithelial characteristics from mesoderm cells after invagination, but then again fail to dissociate properly (Gisselbrecht et al., 1996; Schumacher et al., 2004). The Rho GEF Pbl was identified as an important regulator for EMT, and studies suggest initial mesodermal-ectodermal contacts mediated by Htl signalling and Pbl to be key events for initiation of the flattening and subsequent disintegration of the mesodermal tube (Schumacher et al., 2004; Smallhorn et al., 2004; Wilson et al., 2005). The importance of these initial contacts for mesoderm migration will be addressed in the following.

I. 6. 3 Mesoderm spreading

Mesoderm development subsequent to specification, invagination and acquirement of mesenchymal characteristics depends on FGF signalling (Beimann et al., 1996; Gisselbrecht et al., 1996; Michelson et al., 1998a and 1998b; Gryzik and Müller, 2004; Stathopoulos et al., 2004). Following the release of the epithelial cohesion of mesoderm precursors, the mesoderm cells attach to the underlying ectodermal cell surfaces and align symmetrically along the ventral midline (Fig. 19A). In a lateral-dorsal movement, the mesoderm migrates as a mesenchymal cell collective over the ectodermal cell layer away from the site of invagination until the entire surface is covered (Fig. 19B,C). After completion of mesoderm spreading, the mesoderm has formed a monolayer that spans the entire dorso-ventral axis on either side of the extended germband (Michelson et al., 1998).

The mesoderm cells expressing the FGF receptor Htl respond to the ectodermally expressed FGF8-like ligands Ths and Pyr (Gryzik and Müller, 2004; Stathopoulos et al., 2004). Shortly after invagination, the cells closest to the ectoderm are observed to

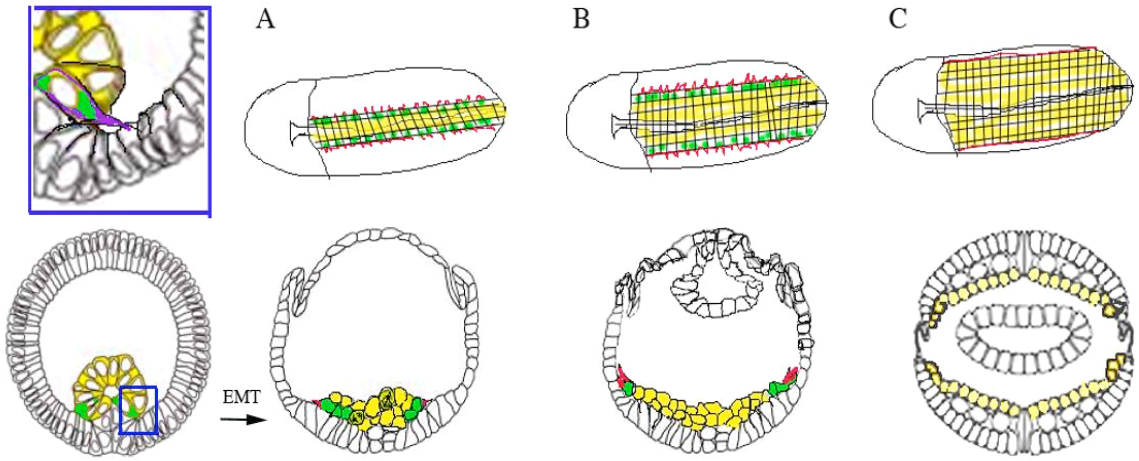

Fig. 19. Phases of mesoderm spreading.
The upper row shows mesoderm (yellow) spreading in embryos from ventral view; the lower panel shows drawing from cross sections of the corresponding phases. **(A)** Initial contacts via cytoplasmic extensions (purple) are formed by mesoderm cells closest to the ectoderm; the site of contact is highlighted by a blue box. These cells show activation of MAPK (green) depending on FGF signalling. After acquiring mesenchymal motility, the cells attach symmetrically to the ectoderm and activate MAPK at the leading edge, where cells can be observed to protrude in direction of migration (red). **(B)** During early phase of migration, the mesoderm cells spread out over the ectoderm evenly as a cohesive cell collective in dorsal direction. Leading edge cells exhibit dynamic filopodia (red) and show activated MAPK. **(C)** Completed mesoderm movement results in coverage of the entire ectodermal cell layer in a perfect monolayer. Activated MAPK has diminished (adapted and modified from and Knust and Müller, 1998, Wilson and Leptin, 2000, Wilson et al., 2005.)

extend cytoplasmic extensions towards the inner surfaces of the ectoderm (Wilson et al., 2005). The epithelial tube then flattens symmetrically against the ectoderm, and the cells make intimate contact with the ectoderm cells and activate MAPK (Fig. 19A).

It was shown that Htl signalling as well as function of the Rho GEF Pbl is essential for these initial cell shape changes, ectodermal contacts and for MAPK to be activated at this point (Schumacher et al., 2004; Wilson et al., 2005). During dorsal migration, a subset of mesoderm cells at the leading edge of the migrating collective activates MAPK signalling, and during this early phase of migration, MAPK activation is exclusively dependent on FGFR Htl activation (Gabay et al., 1997; Gryzik and Müller, 2004; Smallhorn et al., 2004). As yet, the role as well as the mechanism of this localised MAPK activation in mesoderm migration is not understood. However, the cells at the leading edge of the cell collective exhibit a dynamic protrusive activity during migration, which is dependent on FGF signalling, and as well on Pbl function in early

phases (Schumacher et al., 2004; Gryzik and Müller, 2004). In later stages of embryogenesis, activity of mesodermal cells independent of FGF signalling as well as Pbl function can be observed, as mesoderm cells exhibit protrusions in embryos mutant for either *htl* or *pbl*.

Thus, mesoderm migration depends on FGF signalling, but appears to involve other yet unknown regulation as well. The involvement of integrins and cadherins in adhesion - signalling is likely but difficult to investigate. These components of cell-cell adhesion and contacts to extracellular matrix are essential throughout development and thus not easy to manipulate for analysis of a specific requirement during mesoderm migration. So far, specific involvement of integrins and cadherins in the dispersal of mesoderm cells could not be demonstrated (Leptin et al., 1989; Oda et al., 1998).

I. 6. 4 Mitotic activity of mesoderm cells during migration

Mesoderm migration coincides with germband extension of the embryo in stages 7-10 of embryogenesis (Fig. 18). Within this developmental phase, all mesoderm cells perform three consecutive, concurrent mitoses. The cells divide within a very short time after invagination, in early stage 8, and again approximately 30 minutes later in early stage 9 after the primary, fast phase of their migration; another third wave of mitosis occurs at stage 10 when mesoderm spreading is almost completed (Nabel-Rosen et al. 2005; Murray and Saint, 2007). The exact timing of this mitotic activity in the mesoderm is essential for proper mesoderm invagination and migration, as cell division is incompatible with these types of morphogenic cell behaviour (Seher and Leptin, 2000). In *Drosophila*, the mitotic activity of mesoderm cells is controlled by inhibition of String (Stg)/Cdc25 activity (Großhans and Wieschaus, 2000; Seher and Leptin, 2000; Nabel-Rosen et al, 2005; Toledano-Katchalski et al., 2007). The repressor isoform of the RNA binding protein Held Out Wing (HOW(L)) is required to inhibit *stg* mRNA,

and a putative serine/threonine kinase, Tribbles (Trbl) was identified to inhibit Stg/Cdc25 protein function (Großhans and Wieschaus, 2000; Seher and Leptin, 2000). Embryos mutant for *stg* show absence of cell divisions, but mesoderm migration is largely unaffected (Wilson et al., 2005). By contrast *how* or *trbl* mutant embryos exhibit premature cell divisions in the mesoderm. These cell divisions interfere with normal invagination and, in case of *how*, also severely with mesoderm migration and differentiation. Thus, the inhibition of uncontrolled mesoderm proliferation but not the cell divisions per se are important for mesoderm spreading to occur normally.

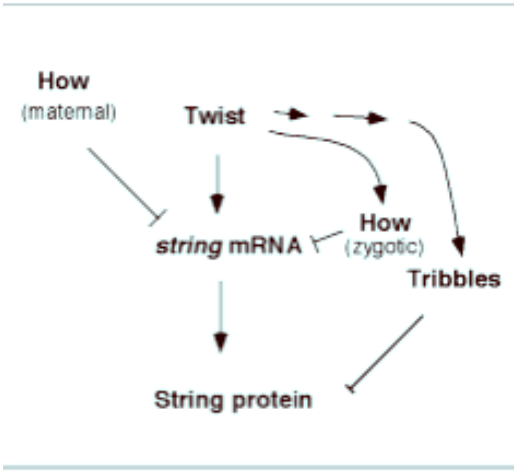

Fig. 20. Scheme of *string* (*stg)* Regulation in the Mesoderm at embryonic stages 5 and 6
Twist induces transcription of *stg* mRNA and zygotic *how(L)*. However, transcript levels of *stg* in the mesoderm are reduced by maternally provided HOW(L), and zygotic HOW(L). Twist (and Snail) additionally regulate zygotic Tribbles activity, which reduces String protein levels. Both HOW(L)'s and Tribbles's activities eliminate String levels. The combination of regulation on transcript and protein level of Stg leads to a complete inhibition of cell divisions during mesoderm invagination. (adapted from Nabel-Rosen et al., 2005)

The transcription factor Twi activates expression *stg, trbl* and zygotic expression of *how* in the mesoderm, thus providing a mechanism that silences Stg/Cdc25 activity (Fig. 20). The model for this fine tuned control proposes that activity of both HOW and Trbl should enable an eventual accumulation of Stg/Cdc25 protein at defined time points of mesoderm development to allow cell-cycle progression. FGF signalling as yet was not identified to contribute to the regulation of mesodermal cell divisions. However, HOW was also shown as a necessary repressor of *miple* transcripts. The heparin-binding motif of the midkine and pleiotrophin homolog Miple is suggested to affect the affinity of the Htl ligands to the FGFR Htl, thereby modulating the strength of Htl-dependent FGF signalling (Toledano-Katchalski et al., 2007). How thus appears to influence mesoderm spreading on other levels as well apart from control of mitotic activity. The concomitant

regulation of levels of active Stg/Cdc25 and FGFR Htl provide a fine tuned balance of instructive signals for mesodermal cell behaviour.

I. 6. 5 Cellular behaviour of mesoderm cells during migration

Recently live imaging studies utilized GFP-tagged nuclear or cytoskeletal markers suggested models of mesoderm spreading that support the function of FGF signalling as regulator of orchestrated mesoderm-ectoderm attachment rather than providing directional guidance during migration (Fig. 21) (Murray and Saint, 2007; McMahon et al., 2008).

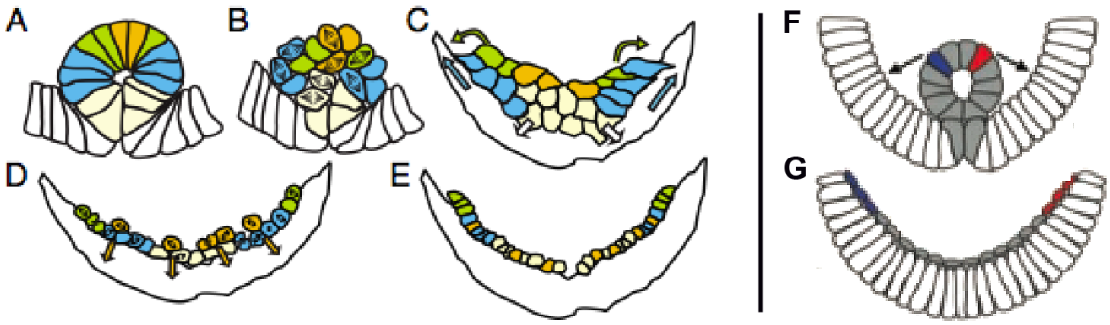

Fig. 21. Model for mesodermal spreading in *Drosophila* embryos.
(A-E) Model from live imaging using cell surface markers. (F-G) Similar findings from nuclear mesoderm markers utilised for analysis of migration. **(A)** The invaginated epithelial tube before the EMT. **(B)** The mesodermal cells disperse onto the ectoderm as EMT and mitosis occur. **(C)** Outer cells polarise and migrate dorso-laterally as a group (blue). As they move away, other cells take up their positions on the ectoderm (white arrows). Inner lateral cells (green) move over the outer cells to establish ectodermal contact. **(D)** During the second mitosis, inner medial cells (orange) intercalate into the outer cell layer to establish ectodermal contact. **(E)** The monolayer is formed with cells in most dorsal positions that started out in dorsal-lateral position of the epithelial tube. **(F)** Mesoderm tube before ectodermal attachment. **(G)** Analysis of tracked cell movements show that cells previously in dorso-lateral positions within the tube take up most dorsal positions within the mesodermal monolayer. (adapted from Murray and Saint, 2007; McMahon et al., 2008)

The live imaging data showed that upon the formation of initial contacts, the mesoderm cells spread down on the ectoderm as EMT and the first wave of cell divisions occur. Conditional on their previous position in the epithelium, 'outer' cells in most lateral positions polarise and proceed to migrate dorso-laterally as a group. Other more medial cells take up their positions and make contact to the ectoderm in more ventral positions. A third movement is performed by cells that, previously in lateral-dorsal position within the mesoderm tube, are now in lateral positions but not in contact to the ectoderm.

These cells move over the outer, temporal leading edge cells to take up the most dorsal positions in response to the attractive FGF signal from the ectodermal source. During the second mitosis, cells in medial, inner positions that have failed to contact the ectoderm then intercalate into the outer cell layer, to form eventually the monolayer covering the ectoderm (Murray and Saint, 2007). In the absence of a FGF signal the spreading defects were explained by disruption of the collapse of the epithelial mesoderm and subsequently the lack of signals for the cells to attach to their substrate of migration (Fig. 22)

Fig. 22. Furrow collapse and spreading of mesoderm cells are disrupted in htl mutants. The collapse of the epithelial tube in *htl* mutants is impaired which results in asymmetric and random distribution of cells to one side of the embryo. Cells laterally or dorsally positioned within the tube that reach the ectoderm (light blue) undergo normal spreading, whereas cells that remain not attached to the ectoderm spread abnormally and adhere only to mother mesoderm cells (dark blue). Red cells indicate cells from ventral positions within the tube. (adapted from McMahon et al., 2008).

I. 6. 6 Differentiation of mesodermal derivatives

After migration is complete, the mesoderm is partitioned into visceral, somatic and cardiac subdomains. Subpopulations of uncommitted mesoderm cells then receive differentiation signals from specific regions of the ectoderm and develop into precursors of heart, muscle, fat body, somatic gonad, glia cells and other tissues. Autonomous and non-autonomous signals control segmental pattern of the mesoderm and allocates regions from which progenitors of the different mesodermal tissues will arise.

With regard to the present study, mesoderm differentiation will be outlined with focus on cardiac and somatic muscle progenitors, as they are known to depend on proper mesoderm migration as well as Htl mediated FGF signalling (Gisselbrecht et al., 1996; Michelson et al., 1998a and 199b, Carmena et al., 1998, 2002, 2006).

A network of signalling pathways regulates the establishment of complex spatiotemporal patterns of gene expression that govern the specification and subsequent differentiation of mesoderm cells. FGFR Htl-dependent activation of the Ras/MAPK pathway contributes to the signalling network controlling mesodermal cell identity (Sandmann et al. 2006). Gradients of Dpp and Wnt family proteins secreted from the ectoderm determine mesoderm cell fates according to the position of the mesoderm cell related to the anterior-posterior and dorso-ventral axes of the embryo. The consequent specific composition of active transcription factors then leads to the spatially regulated differentiation into pericardial cells, cardioblasts and muscle progenitor cells (Gajewski et al. 1997; Reim and Frasch, 2005; Tao and Schulz, 2007).

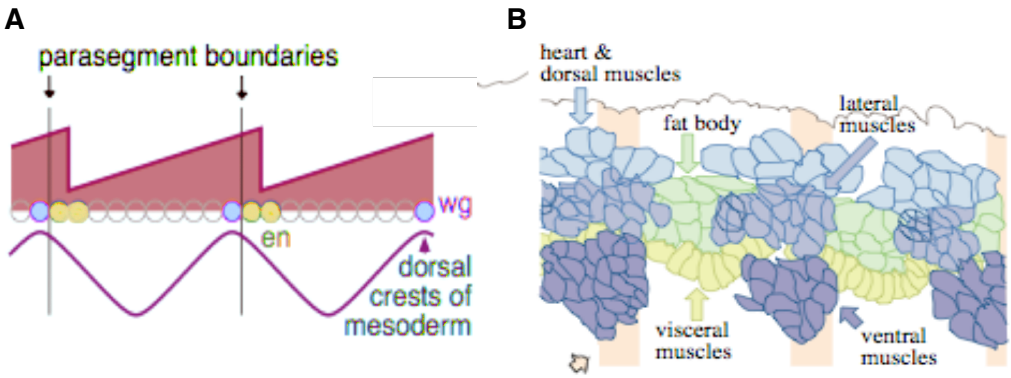

Fig. 23. Modulated expression pattern of Twist (red) along the anterior-posterior axis subdivides the mesoderm in each segment into two groups.
(A) Summary diagram to show relative positions of parasegment borders, sharp A/P boundary for Twist expression and mesodermal crests. At the crests of twist expression, e*ngrailed* (*en*) and *wg* expression define the boundaries of the hemisegments and patterns the mesoderm in each segment. **(B)** The location of the different progenitor cell populations is indicated with reference to ectodermal *en* expression (light orange). Different shades of blue indicate more external cells and those indicated in different shades of green represent internal cells (adapted from Dunin Borkowski et al., 1995.)

When the mesoderm becomes segmentally structured after completion of dorsal migration, two layers of mesodermal cells are formed. The anterior part of each segment expresses low levels of Twi and gives rise to an inner (more internal) layer of mesodermal cells the progenitors of the visceral musculature will derive from. An outer (peripheral) layer of mesodermal cells neighbouring ectodermal cells is defined by high

levels of Twi and provides the progenitor cells of the somatic musculature and the heart (Fig. 23) (Azpiazu and Frasch, 1993; Taylor et al., 1995; Borkowski et al., 1995).

I. 6. 6. 1 The determination of pericardial cell fates

The pericardial cells are specified at the dorsal margin of the mesoderm after completed dorsal movement. A cluster of 2-5 pericardial cells becomes specified by Eve expression from stage 10 of embryogenesis in each abdominal segment on both sides of the embryo (Fig. 24).

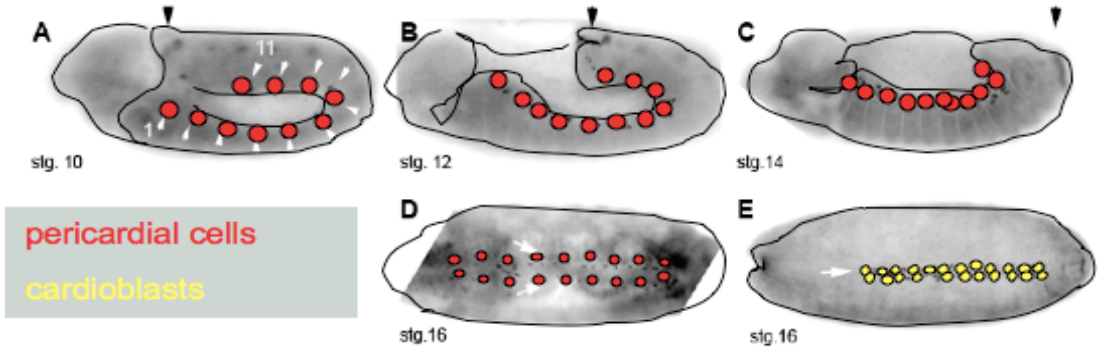

Fig. 24. Illustration of Even skipped (Eve) positive pericardia cells specified in 11 clusters in a segmental pattern.
Developmental stages are indicated; the arrowhead marks the posterior of the embryo during germband retraction **(A-C).** The pericardial cells (red), arise from mesoderm alcells ventral from the dorsal most heart precursors. Once differentiated, the pericardial cells do not proliferate and remain in dorsal positions until they reside next to the tubular arranged cardioblasts (yellow) **(D, E)**.

Pericardial cells reside next to the cardiac tissue and they differentiate into 20-25 excretory cells surrounding the tubular heart after dorsal closure at the end of embryogenesis (Mills and King, 1965). The formation of the pericardial cells is a well-studied example of mesoderm differentiation by combinatorial signalling of several pathways. FGF 8-like signalling is essential for pericardial cell fates (Carmena et al., 1998; Tao and Schulz 2007). In each segment, a progenitor is singled out of a cluster of mesoderm cells pre-specified by Dpp and Wg signalling and subsequent expression of the neurogenic gene *lethal of scute* (*l'sc*) (Fig. 25).

Htl-dependent Ras/MAPK signalling results in specific expression of the transcription factor Eve, which indicates the induced differentiation of the pericardial cell. Surrounding cells are repressed from progenitor cell fates by lateral inhibition through Notch (N) signalling (Carmena et al., 2002). The level of activated Ras/MAPK thus is determinant for the cell within this cluster, to express and maintain *eve* expression and differentiate into a pericardial cell progenitor (Fig. 26A, B).

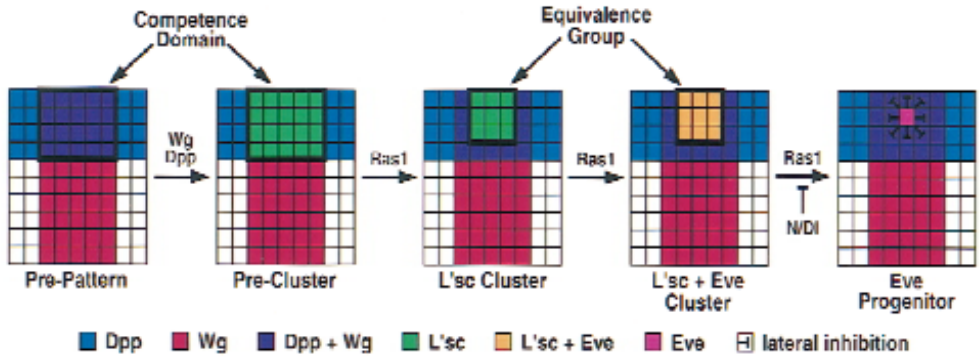

Fig. 25. Model for the combinatorial effects of Wg, Dpp, Ras1, and neurogenic signals in embryonic mesoderm development.
Pre-clusters in the dorsal mesoderm (purple) are patterned by intersection of Wg (red) and Dpp (blue) expression domains. Within these, Lethal of scute (L'sc) is initially expressed (green). All cell of this pre-cluster are competent to respond to a subsequent RTK/ Ras1 signal. Localised activation of Htl and DER restricts L'sc to a subset of cells from the precluster that represent an equivalence group. Further RTK/ Ras1 signalling activates Eve expression in all cells of the L'sc cluster (orange). The influence of neurogenic genes signles out a progenitor cell (pink) by lateral inhibitory regulation.(adapted from Carmena et al., 1998).

The current model of signal regulation moreover links Wg, N and Ras/MAPK signals through interaction with the PDZ protein Canoe (Cno) (Fig. 26C). Canoe interacts with N and active Ras mediated by Dishevelled (Dsh), an effector of Wg signalling. The binding of Dsh to Cno facilitates the release of Ras inhibition and reciprocally, the inhibition of N and the inactivation of the canonical pathway of Wg signalling. Thus, the pathways leading to progenitor differentiation from uncommitted mesoderm cells are carefully modulated by regulation of their signalling thresholds. In addition to pericardial cell specification, the muscle founder cell of the dorsal muscle achute 1(DA1) is also specified from the same mesodermal cell cluster, but requires EGFR

(DER) signalling in addition to FGF mediated Ras/MAPK activation (Frasch et al., 1987; Baylies et al. 1998; Buff et al., 1998).

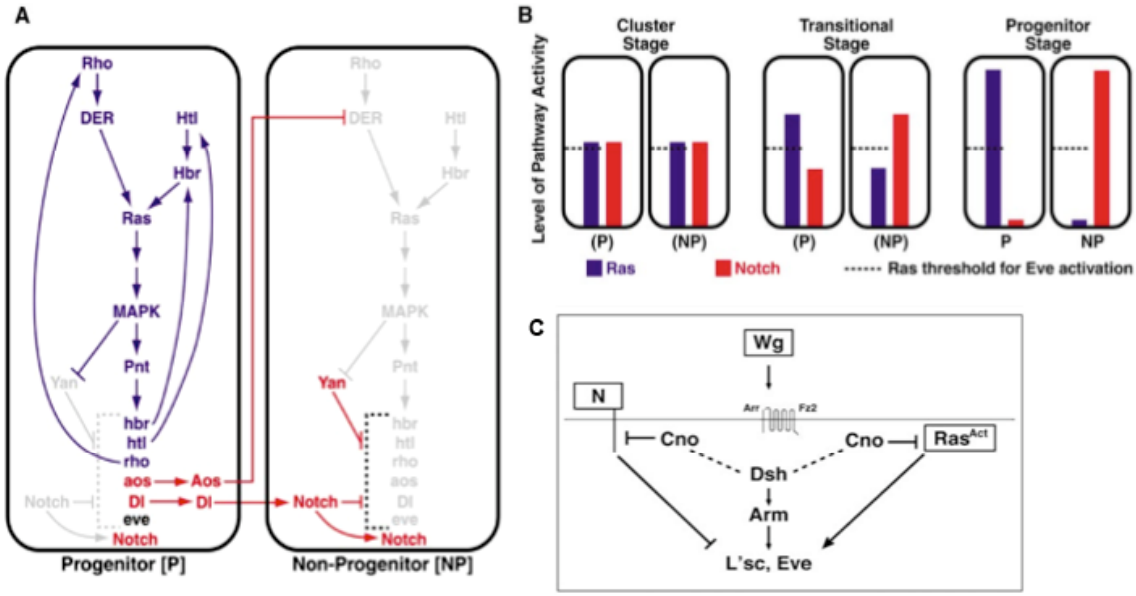

Fig. 26. Model for feedback and cross-talk in the Ras and N signaling pathways during muscle and heart progenitor specification.
(A) A singled out progenitor (P) and neighbouring non-progenitor (NP) from the same equivalence group are shown after fate acquisition. In the P cell, EGF and FGF receptor signalling via the Ras/MAPK induce target gene expression, whereas N signaling suppresses this pathway in NP cells. A positive feedback loop of RTK signalling results in expression of the muscle identity gene *eve* that is inhibited in NP cells. **(B)** Diagram of the temporal changes of Ras and N levels during progenitor specification. Ras activity predominates in P and N activity predominates in NP cells. **(C)** Model of signal regulation by Wg and Cno. Cno interacts with Wg, N and Ras- MAPK pathways, negatively regulating the induction of transcription of the key progenitor targets, L'sc and Eve. Cno/Dsh interaction facilitates the release of Cno repression on Ras^{Act} signaling and the inhibition of N signaling by Cno. Dsh recruitment by Cno leads to canonical Wg signal inhibition. Fz2, Frizzled2. (Adapted from Carmena et al., 2002; Carmena et al., 2006.)

I. 6. 6. 2 The differentiation of cardiac and somatic muscle progenitors

Progenitor specification of somatic muscles is regulated similarly by interaction of signalling and transcriptional networks. Each somatic myofibre of the ~30 body wall muscles per hemisegment of the larva derives from a specific mono-nucleated cell that possesses the information for its unique identity (Fig. 27A) (Bate and Rushton, 1993). These founder cells fuse with neighbouring undifferentiated, fusion-competent myoblasts to form a syncytial muscle fibre.

The most dorsal mesoderm cells become specified as heart precursors and are distinguishable from the somatic muscle progenitors in each segment by their beaded arrangement. The somatic muscle progenitor cells form in three groups according to their position, namely the dorsal, pleural (lateral) and ventral group (Fig. 23B) (Hartenstein, 1993). The transcription factor Myocyte enhancing-binding factor 2 (Mef-2) is essential for terminal differentiation of these three major muscle cell types (Lilly et al., 1994; Bour et al., 1995; Taylor et al., 1995; Gajewski et al., 1997). Following an early phase of broad mesodermal expression, *mef-2* expression becomes restricted to the dorsal mesoderm in later stages and is expressed specifically by all precursors of visceral and somatic muscles, including the heart progenitors (Bour et al., 1995; Nguyen and Xu, 1998).

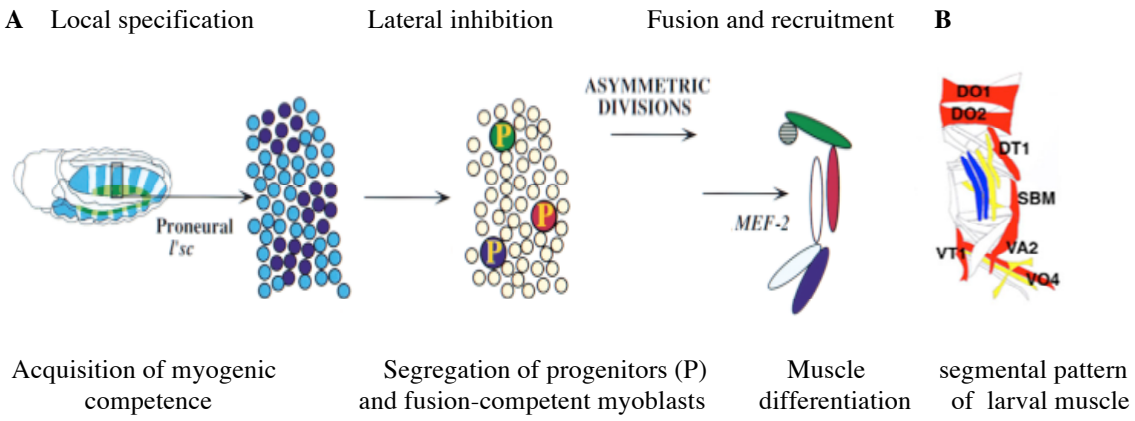

Fig. 27. Successive steps in the formation of the *Drosophila* muscle pattern.
(**A**) Cartoon of a stage 10 embryo. The shades of blue stripes indicate the modulated pattern of *twi* expression. The somatic muscles derive from domains of high twi expression (medium blue). Within the domain expressing high levels of twi, clusters of cells are specified by expression of the proneural gene, lethal of scute (*l'sc*), (dark blue circles) that have the potential to become muscle progenitors. Via lateral inhibition, l'sc expression is restricted to single cells that become the muscle progenitors (P). Cells not specified as progenitors of the myogenic clusters will give rise to fusion-competent myoblasts. Asymmetric division of the progenitors gives rise to pairs of founder cell or to a founder and an adult muscle precursor cell. Each muscle is formed specifically by a progenitor **(B)** by fusion with fusion-competent myoblasts (adapted from Baylies et al, 1998).

Transcriptional activation by Mef-2 in turn represents a key regulator of a large number of other transcription factors, many of which are involved in early aspects of myogenesis (Sandmann et al., 2006 and 2007).

It was shown that loss of Htl function leads to strongly reduced numbers of Mef-2 expressing mesoderm cells, causing severe defects in muscle progenitor formation and further muscle development (Gisselbrecht et al., 1996; Michelson et al., 1998a and 1998b). FGF signalling also is suggested not only to be required for the formation of muscle progenitors but also in regulation of muscle syncytia formation and further maintenance of sarcomeric stability of the muscle fibre. Recently, the putative E3 ubiquitin ligase Mind bomb 2 (Mib2), was found to be specifically required in myoblasts for fusion and later muscle stability (Carrasco-Rando and Ruiz-Gómez, 2008). Interestingly, a recent screen identified *mib2* as a positively regulated target gene of Htl mediated FGF signalling, (Leatherbarrow and Halfon, 2009). Thus, through transcriptional regulation of components required for muscle integrity, FGF signalling contributes to later muscle development.

I. 7 Aim of study

Based on the dynamic and partially overlapping expression domains of the Htl ligands *ths* and *pyr*, redundant as well as individual functions were suggested during mesoderm development. It is shown that upon loss of both *ths* and *pyr* function, Htl activation does not occur and activation of ERK no longer is detectable in mesoderm cells. Embryos lacking both *ths* and *pyr* show severe defects in mesoderm spreading and differentiation in resemblance to the *htl* mutant condition, as spreading is severely impaired and mesoderm cells fail to exhibit cellular protrusions. Eve positive pericardial progenitors are not specified and the pattern of Mef-2 expressing muscle precursors is disrupted. Utilising RNAi to silence transcript translation showed that expression of the differentiation marker Eve depends on *pyr* function and is not affected in *ths* depleted embryos (Gryzik and Müller, 2004). Analysis of the *pyr* null allele *FGF8-like2*^{18} (*pyr*^{18}) confirmed this result (Gryzik, 2005). But surprisingly, overexpression of *ths* was shown

to have the ability of rescuing the pericardial cell fate in embryos lacking both *ths* and *pyr* genes, and also of uniform activation of the MAPK signalling cascade in the mesoderm (Stathopoulos et al., 2004). This raises the question how Ths and Pyr might induce different cellular responses, or if similar signalling properties are required for robust mesoderm spreading and differentiation.

As outlined above many factors involved in FGF signalling and regulation of mesoderm movement have been identified so far, and live imaging of migrating mesoderm cells has contributed valuable insights in this process. However, the mechanisms by which FGF signalling leads to dispersal of mesodermal cells over the ectoderm are not known, and the role of FGF signalling to prevent an instructive or a permissive signal for mesoderm migration is discussed controversial.

The present study aims to elucidate whether *ths* and *pyr* play individual roles in mesoderm development, to identify what these functions are and how they can act in distinct ways. A single mutant of *ths* was generated to distinguish between effects upon loss of function individual for Pyr or Ths. The effects upon individual loss of function on mesoderm spreading and differentiation were investigated in detailed comparison of *ths* and *pyr* single mutant phenotypes. The contrast to deletion of both genes will show if Ths and Pyr exhibit redundancy in their functions. Conclusively, such analysis will provide further criteria and insight to dissect which processes depend on Ths or Pyr function in particular or may require both. In addition, analysis of the hemizygous conditions where only one copy of either *ths* or *pyr* is present should reveal whether Htl signalling is dependent of Ths or Pyr dosage, and if altered ratio of Ths and Pyr results in different response of Htl signalling. Finally, further aim of this work is to investigate how ectopic over-expression of Ths or Pyr influence mesoderm development in order to characterise individual cellular response to Ths/Htl or Pyr/Htl mediated FGF signalling.

II Experimental Procedures

II. 1 Materials

II. 1. 1 Chemicals

All chemicals were obtained from the following companies in pro analysis quality:
Acros (Geel, Belgium), Baker (Deventer, Netherland), Biomol (Hamburg, Germany), Bio-Rad (München, Germany), Difco (Detroit, USA), Fluka (Buchs, Switzerland), Gibco/BRL LifeTechnologies (Karlsruhe, Germany), Macherey-Nagel (Düren, Germany), Merck (Darmstadt, Germany), Roth (Karlsruhe,Germany), Serva (Heidelberg, Germany), Sigma- Aldrich (Steinheim, Germany), Qiagen (Hilden, Germany).

Enzymes for molecular work were purchased from:

MBI Fermentas (St. Leon-Rot, Germany), Boehringer/Roche Diagnostics (Mannheim, Germany), Stratagene (La Jolla, USA) and Promega (Madison, USA).

Used Kit products

For plasmid DNA preparation and for DNA extraction from agarose gels, kits from Qiagen (Hilden, Germany), Macherey-Nagel (Düren, Germany) or Promega (Madison, USA) were used.

polyA+ RNA was isolated using the μMACS mRNA Isolation Kit from Miltenyi Biotec, Bergisch Gladbach.

RT-PCR was performed using the OneStep RT-PCR Kit, Qiagen, Hilden

In situ hybridisations were performed using the DIG RNA labelling MIX from, Mannheim, Germany, and the TSA™ Detection Kit for fluorescent in situ hybridisation from Invitrogen, Groningen, Netherlands.

General solutions:

PBS (10x): 1,3M NaCl; 70mM NaHPO4; 30mM NaH2PO4 (adjust pH to 7.4)

PBT: 1x PBS with 0.1% Tween20

LB medium: 1% bactotrypton, 0.5% bactoyeast, 1% NaCl

LB-agar: 6.3g agar for 300ml LB

All solutions used for molecular biology were based on dH2O from Millipore or were autoclaved.

Media for immunohistochemistry and embedding of embryos for microscopy:

Fixative for embryos 4% FA: 1.82ml 1xPBS

1.92ml n-heptane

0.26ml 37% formaldehyde

Solutions for staining procedures:

For detection of horseradish peroxidase (HRP), the Vectastain ABC Kit (Vector labs) was used.

DAB-staining solution for HRP detection using the Vectastain Kit:

800 l 1xPBT + 200 l DAB-stock (activate previously with 1-2 µl 3% H_2O_2)

DAB-Stock: 1mg/ml DAB (3,3´-Diaminobenzidin-Tetrahydrochlorid, Aldrich, Steinheim) in 1xPBS, store at -20°C

AP Buffer: 100mM Tris pH 9,5; 50m $MgCl_2$; 100mM NaCl; 0,1% Tween 20

AP staining solution: 1ml AP-Buffer + 4,5 l NBT + 3,5 l BCIP

Embedding media:

Mowiol: Mix 2.4g mowiol with 6ml glycerin and 6ml H2O. Incubate for 2h at RT, add 12ml 200mM Tris pH8.5 and incubate at 50°C for 3h. Centrifuge at 4000rpm for 10min and aliquot supernatant.

Araldite (50 g): 27,175 g Durcupan component A/M; 23,705 g Durcupan component B. Shake for 1 h to mix the components well. To the mixture add: 1,75 g Durcupan component C and 1,00 g Durcupan component D. Again shake for 1h to mix thoroughly.

II. 1. 2 Bacterial strains

The E.coli host strains XL1-blue (electrocompetent) and DH5-α (chemocompetent) were used for plasmid DNA amplification.

II. 1. 3 Microscopy, image acquisition and employed software

Microscopy was performed on a Zeiss Axiophot, an Olympus BX61 as well as on Zeiss 510 Meta and Leica-SP2 confocal microscopes (Zeiss, Jena, Germany; Olympus, Watford, UK; Leica, Heidelberg Germany).

Images were processed using Adobe Photoshop (Adobe Systems, San Jose, USA), Volocity (Improvision, a PerkinElmer Company, Coventry, UK), the LSM software (Zeiss, Jena, Germany) and Canvas 8 (Deneba Systems, Miami, USA).

For sequence analysis DNA-Star Lasergene V6 (DNASTAR Inc., Madison, USA) was used on a Macintosh system (Apple, Ismaning, Germany).

II. 2 Molecular biology

Standard techniques in molecular biology such as: measurement of DNA or RNA concentration, DNA cleavage by restriction enzymes, 5` dephosphorylation of linear DNA using alkaline phosphatase (calf intestine phosphatase "CIP", *Boehringer*, Mannheim, Germany), Phenol/Chloroform purification of plasmids, ligation using T4 DNA ligase and electrophoresis of DNA fragments are described in Molecular cloning: A laboratory manual (2nd edition, Shambrook, Fritsch and Maniatis, Cold Spring

harbour Laboratory Press) and will therefore not be described in detail.

Whenever kit systems were used, protocols were followed according to manufacturer's instructions. Elution of DNA fragments from agarose gels was performed using the NucleoSpin Extract Kit from Macherey-Nagel (Düren, Germany).

To verify the accuracy of cloned plasmids or to determine to sequence in RT-PCR products, sequencing reactions were performed either by *SEQLAB* (Göttingen, Germany) or by the Sequencing Service of the University of Dundee (Dundee, UK).

II. 2. 1 Transformation of electro- or chemo-competent bacteria

In *E.coli* cells, particular DNA fragments can be amplified for further cloning or sequenceing. After ligation of the DNA fragment into a linearised vector molecule (see II .2.3.1) giving rise to a ring-like plasmid molecule, the plasmid DNA is transformed into suitable E. coli cells where it is replicated together with the bacterial DNA.

The concentration of the plasmid DNA was adjusted to 100-300ng/μl by dilution in H2O. 50μl aliquots of XL1-blue cells were thawed on ice. 1-2μl of plasmid DNA was added to the cells. The mixture was incubated for 5min on ice before transferring it to an electroporation cuvette (Bio-Rad). Electroporation was performed as recommended by manufacturer's instructions. After electroporation, the bacteria were resuspended in 1ml LB-medium, transferred to an Eppendorf tube and incubated for 1h at 37°C. Eventually, the bacteria were plated on LB-plates containing the recommended concentration of the appropriate antibiotic and incubated overnight at 37°C.

If chemo-competent *E. coli* cells were transformed, an aliquot of the cells is thawed on ice and mixed with the appropriate amount plasmid DNA (see above). The mix is incubated for 30 min on ice before the cells are heat-shocked for 30-40 seconds in a

42°C waterbath. Afterwards the cells are put back on ice for a few seconds before 1 ml of pre-warmed LB medium is added. After an one hour incubation at 37°C on a bacteria shaker, the cells are spun down (2 min at 5000rpm) and re-suspended in approximately 100μl of the supernatant. The cells are plated on agar-plates selective for ampicillin resistance (100μg/ml ampicillin) and grown over night at 37°C.

II. 2. 2 Plasmids used for cloning, probe generation for in situ hybridisations and transgenesis

Name	**Description**	**Origin/Reference**
pBS KS II (+/-)	Vector for subcloning	Stratagene
pUAST *w+*	*Drosophila* germline transformation vector, marked with *white* gene	*{Perrin, 2003 #278}*
pCRII-TOPO	Vector for subcloning	From TOPO TA Cloning Kit, Invitrogen, Groningen, Netherlands
pBSKSII - *ths*	pBS vector containting the cDNA of *ths*; used for generation of in situ hybridisation probes	T.Gryzik, 2005
pBSKSII - *pyr*	pBS vector containting the cDNA of *pyr* used for generation of in situ hybridisation probes	T.Gryzik, 2005
pUAST- *ths** -HA	pUAST vector containing ths* tagged with HA(hemagglutinin); sequenceing revealed 4 point mutations within the FGF core domain encoding sequence (see Results, Fig.X)	T.Gryzik, 2005
pUAST –	pUAST vector containing *pyr* cDNA tagged	Cloning facility,

pyr -HA	with HA(hemagglutinin)	university of Dundee

Table 1. Plasmids used for cloning, probe generation for in situ hybridisations and transgenesis

II. 2. 3 Isolation of DNA molecules

II. 2. 3. 1 Small-scale plasmid DNA amplification and isolation (Minis)

Single bacterial colonies were selected with a tip and used to inoculate 2ml of LB media with the recommended concentration of the appropriate antibiotic. The cultures were grown overnight in a shaking incubator at 37°C. The bacteria from one colony were transferred to a 1.5ml Eppendorf tube, harvested by centrifugation for 1min at 13.000rpm and resuspended in 300μl of buffer P1 (Qiagen). The resuspended bacteria were lysed in buffer P2 (Qiagen). The suspension was neutralised after 5min by the addition of 300μl buffer P3. The suspension was incubated for 5min on ice and centrifuged for 15min at 13.000rpm. The supernatant was transferred to a new Eppendorf tube and the DNA was precipitated by the addition of 500-700μl of 2-propanol and centrifugation for 30min at 13.000rpm at 4°C. The supernatant was discarded and the pellet was washed with 700μl ice cold 70% ethanol by centrifugation for 10min at 13.000rpm at 4°C. The supernatant was discarded and the pellet was dried on air before resuspension in 30μl H2O.

II. 2. 3. 2 Medium-scale plasmid DNA amplification and isolation (Midis)

For amplification and isolation of highly concentrated plasmid DNA, single bacterial colonies were inoculated in 40ml LB media with the recommended concentration of the appropriate antibiotic. The cultures were grown overnight in a shaking incubator at 37°C. The DNA was isolated using the Midi Kits from Quiagen (Hilden, Germany) or Macherey-Nagel (Düren, Germany) and following the instructions in the user manual.

II. 2. 3. 3 Isolation of genomic DNA from adult flies

The following protocol was generated by E.J. Rehm from the Berkely Drosophila Genome project (BDGP) and was modified for specific requirements:

About 30 adult flies were frozen in liquid nitrogen and homogenised in 400μl Buffer A (see below) using a biovortexer (Biospec products). The homogenised mixture was incubated at 65°C for 30min. 800μl of LiCl/KAc solution were added to exclude the protein fraction and the mixture was vortexed and incubated for 10min on ice before centrifugation for 15 min at 13.000rpm at room temperature. 1ml of the supernatant was transferred into a new Eppendorf tube and 600 μl Isopropanol were added to precipitate the DNA. Subsequent centrifugation for 15 min at 13000 rpm (room temperature) allows to discard the supernatant. The DNA is pelletized and can be dried after washing with 70% EtOH. To resolve the DNA, 150 μl TE were added.

Solutions:

Buffer A : 100 mM Tris-HCl, pH 7.5; 100 mM EDTA; 100 mM NaCl; 0,5% SDS

LiCl/KAc-Lsg.: 1 Teil 5 M KAc: 2,5 Teile 6 M LiCl

TE: 10 mM Tris-HCl, pH 8,0; 1 mM EDTA, pH 8.0

II. 2. 3. 4 Isolation of genomic DNA from sorted embryos using Chelex

Chelex is a specific resin which posseses high affinity for polyvalent metal ions, which can be used to protect DNA from degradation at high temperatures and in addition facilitates the denaturation of enzymes. Chelex exists in small beads and is not soluble in water. It is used in sterile water in a 5% weight/volume ratio. Chelex-extraction was used for the isolation of genomic DNA from fixed and stained embryos (Walsh et al., 1991).

5 embryos of the required phenotype were sorted out according to the phenotype and frozen in a clean Eppendorf tube in liquid nitrogen. After mixing with 50 μl Chelex and

mechanical homogenisation using sterile pipette tips, the embryos were incubated for 10 min at 95°C or in boiling water, cooled at RT and centrifuged for 1 min at 13000 rpm. 1-10μl of the supernatant was directly used for PCR or was transferred into a new Eppendorf tube, which was then stored at –20°C .

II. 2. 3. 5 Isolation of genomic DNA from single flies

For qualitative PCR tests, genomic DNA can be isolated in a quick procedure from single flies of a desired phenotype to test for chromosomal deletion for instance. However, the DNA isolated is not very stable and can only be stored for approximately 2 weeks at -20°C until the sample is degraded.

A single fly from the line to test was frozen within an Eppendorf tube in liquid nitrogen and pounded with a pipette tip after adding 50μl SB solution (see below) containing proteinaseK to degrade most protein fractions. The tube was sealed with tape or parafilm and incubated at RT for 15 minutes. To inactivate the proteinaseK activity the tube was incubated subsequently for 5 minutes at 100°C between two heating blocks. The tube was cooled down slowly at RT to avoid evaporation.

5 μl of the supernatant solution was used for PCR analysis.

II. 2. 4 Isolation of polyA+ RNA

PolyA+ RNA was isolated from embryos using the μMACS Kit from Miltenyi Biotec, Bergisch Gladbach, Germany. The mechanism by which mRNA is isolated involves the binding of polyA+ to the magnetic MACS Oligo (dT) micro beads. RNA fractions not containinf a polyA+ tail such as rRNA und tRNA therefore are eliminated by purification steps. Following the protocol proposed by the providing company, polyA+ RNA was isolated and used as template for RT-PCR (see II. 2. 5. 2).

II. 2. 5 Amplification of DNA molecules

II. 2. 5. 1 Polymerase-chain-reaction (PCR) (standard)

The Polymerase-chain-reaction (PCR) is a possibility to generate multiple copies of a certain DNA fragment in vitro. Initially, double stranded DNA containing the sequence of interest isdenatured at 94°C. Using sequence specific oligonucleotides, the region of the DNA that should be subsequently amplified is flanked by these primer molecules. The binding of the primers to the template DNA (annealing) occurs after every denaturing step. In the following step, the elongation, the primers are used as starting points for the synthesis of the complementary DNA strand. This cycle is repeated several times and leads to an exponential increase in the number of copies of the amplified DNA sequence. The DNA synthesis is performed by temperature stable DNA polymerases that are not inactivated by the high temperature during the denaturing step. Beside the standard polymerase Taq performing at 72°C best, another polymerase, Pfu, was used. The Pfu polymerase possesses a proofreading activity and therefore generates fewer errors when synthesising the complementary DNA strand. Pfu polymerase is used especially when PCR products subsequently are used for cloning of expression constructs. The Pfu polymerase performs best at 75°C.

An example for a PCR reaction mix with 50μl total volume is shown below:

Xμl DNA (~ 50 - 100ng)
1μl forward primer (50μM)
1μl reverse primer (50μM)
1μl dNTP mix (10mM)
5μl 10x Pfu-polymerase-buffer (+$MgCl_2$)
+ 0.5μl Pfu-polymerase
add dH2O to a total volume of 50μl

PCRs were performed in a Thermocycler PTC-200 (MJ Research, Watertown, USA) using the standard program indicated below. The elongation time depends on the length of the amplified DNA molecule (the Pfu polymerase amplifies a 1kb DNA fragment in approximately one minute). The annealing temperature depends on the G/C proportion of the used primer molecules.

Duration	**Temperature**	**Reaction**	
5min	94°C	initial denaturation	35x
30sec	94°C	denaturation	
1min	primer-dependent	primer annealing	
Amplicon size dependent	72°C/ 75°C	DNA synthesis	
7min	72°C / 75°C	final DNA synthesis	
∞	4°C	end	

Table 2. Standard PCR program

Following oligonucleotides were used for standard PCR:

Name	**Sequence (5' → 3')**	**Used for**
FW2	GGATATCGAGGTTGGGTACGAACTAAAGTG	Sequencing of *ths*^{141} and *ths*^{759} RT-PCR products
C	CAACACGCGCTCAACGACTTAGAT	Test for excision of *EP(2)G18816*
UP	GACGGGACCACCTTATGTTATTTCATCATG	Test for excision of *EP(2)G18816*
D	CCCTTGCGCTTGCTGCTCA	Test for excision of *EP(2)G18816* and sequencing of *ths*^{141}

		and *ths*^{759} RT-PCR products
E4fw	GTTCAAAATGCGGACTACTAATG	Test for deletion of termial sequence of exon 4 of *ths*
E4rw	CTACGCAACTGTCAAAAGAGCA	Test for deletion of termial sequence of exon 4 of *ths*
A	CCACCCATCACTGACGACATT	Test for deletion of exon 3 of *ths*
B	TGCACCATAGCGCCATAAACT	Test for deletion of exon 3 of *ths*
Tango3Efw	GGCGCCATTATGACCACAC	Test for deletion of the gene *tango* upstream of *ths*
Tango3Erv	CACGGATAGGCAGTACAATGACA	Test for deletion of the gene *tango* upstream of *ths*
PP1for	TGTCGGGTTCACGCACCGAGGTAA	Tests primers to determine the extent of the lesion in *ths*^{759} generated by imprecise P-element excision of *EP(2)G18816*
PP1rev	GTCGCAGCAGCAGCGATGGATCAT	
PP2rev	CGCCGTTGCCGCTATTGTTGATGTTA	
PP5for	CGGCGAAGAAAGGCCAAGGTC	
PP5rev	CCGCATTGCGCACATAGGTC	
PP6for	TCGCCTCGGCTTATGAAATATGAG	
PP6rev	AGATAATCCGGGAAGCCGACTATC	
PP7for	ACACCGCTCCACTTGACCACTGGT	
PP7rev	TTGGGCCCCACAGGCTTACCTC	
PP8for	AGCGGGGCTGAACCCAGTCAC	
PP8rev	CTTCCCGAGAAAAGCCAGCTAAGG	
PP9rev	AGCGCGTGTTGCTGCCAGTTG	
PP10for	CGGCGGCCAAAGGTGTGAA	
PP10rev	GTGCATCTGCCCCTCTGCTCAGTA	
PP11for	CGCCCACCGATCTTTCGGATCT	

PP11rev	AATTTCGGGCGGGGCTGGTT	
PP12for	TGCTCCACTCGGGGTTTGT	
PP12rev	TGTCGTCAGTGATGGGTGGTTGTC	
PP13for	CCCGCGCAACAACAAAAACAATC	
PP14for	AGGCAGCAACAGCAGCAACATCAGGT	
PP14rev	CTGCCGTGGCAAGTAGCTGCAACTG	
PP15for	AGAAGCGGCGCAAGCAACAGAAG	
PP15rev	GCCCGCTAGCAACATGTCGGAATT	
SeqF1for	CGCATGTCGAATCAGTTAGAG	Sequencing of the region encoding the FGF core domain of Ths
SeqF1rev	GCGGCCTCGATCTTGTTGAA	Sequencing of the region encoding the FGF core domain of Ths
UAS13194for	AAGGAAAAAAG**CGGCCG**C-CTCGGACACCAAACTCAGC The bold red bases represent the NotI restriction site for cloning into pUAST-HA	Generation of the UAS-*pyr*-HA construct for transgenesis *
UAS13194rev	CCG**CTCGAG**CGG-GCTAACAAAATACTTACCACAGTG The bold red bases represent the XhoI restriction site for cloning into pUAST-HA	Generation of the UAS-*pyr*-HA construct for transgenesis *

Table 3. Oligonucleotides used for standard PCR
The PCR test primers for P-element excision that generated significant products to estimate the extent of the lesion are indicated in Fig. 35 of III. Results; * the primers for generation of the UAS-*pyr* construct were modified by the cloning facility, university of Dundee, only very long primers comprising 40-45bp resulted in insertion of the PCR product obtained into the pUAST vector. The final sequence of the primers used was not revealed but were based on the primers indicated here.

II. 2. 5. 2 RT-PCR (reverse transcription and following PCR)

RT-PCR involves the previous reverse transcription (RT) of a RNA template (for isolation of polyA+ RNA see II. 2. 4). From polyA+ RNA, a single stranded DNA molecule is transcribed which serves as further template for following DNA polymerase activity. The reverse transcriptases also posess a RNAse H activity to degrade the RNA/DNA hybrids generated. To obtain a specific DNA fragment from pooled polyA+

RNAs, specific oligonucleotides (primer) were used to amplify only the mRNA product of *ths*. A standard PCR was performed using the products obtained from RT-PCR as templates ('nested' PCR), because the amount of RT-PCR product obtained was to low for sequencing For RT-PCR, the One-step RT-PCR Kit from Quiagen, Hilden, Germany was used which combines the reverse transcription with subsequent PCR.

The RT-PCR mix and PCR program was composed after recommendation of the manufacturer.

Following oligonucleotides were used for RT-PCR:

Name	**Sequence (5' → 3')**	**Used for**
CG12443 RT5.1*	TAGAAACGTGCCCCCAATAAAGTA	RT-PCR on polyA+-RNA templates of *ths*
CG12443 RT3.1*	AAATGTTGTTGCCTGTGAAAGTGG	RT-PCR on polyA+-RNA templates of *ths*
CG12443 RT5.2	ACGCCGAAACTGCCCAATGT	PCR on templates from RT-PCR products ('nested' PCR) of *ths*
CG12443 RT3.2	CTAATAGCCAAAATGCGTCAATCC	PCR on templates from RT-PCR products ('nested' PCR) of *ths*

Table 4. Oligonucleotides used for RT-PCR
taken from T.Gryzik, 2005 in pursuing the project

II. 2. 6 Generation of the plasmids used for transgenesis

The plasmid for transgenesis pUAST-*ths**-HA was cloned by T.Gryzik (2005).

The cloning of the construct for transgenesis of the full length *pyr* cDNA was difficult and not successful despite utilisation of different ligation techniques and protocols. The

sequence successfully cloned never was accurate and contained inversions and lesions of the sequence.

The vector pUAST-HA together with *pyr* cDNA and oligonucleotides for amplification therefore were submitted to the cloning facility of the university of Dundee. Using different approaches and extra-long oligonucleotides of over 40 bp, the cloning was eventually successful and the construct was injected into embryos for germline transgenesis.

II. 3 Germline Transformation of *Drosophila melanogaster*

Transgenic flies were generated according to standard procedures by Dejardin and Cavalli (2004) and are described in detail by Bachmann and Knust (2008), and therefore are not further elucidated here. The first injection of the construct pUAST-pyr-HA did not produce a stable transgenic line and only few lines were obtained that were putatively transgenic for UAS-*pyr*-HA.

For this reason the construct was injected again by *Rainbow Transgenic Flies, Inc.* (Newbury Park, USA). Only 70 larvae were obtained from two rounds of injections, which otherwise produce approximately 200 larvae according to *Rainbow Transgenic Flies, Inc.*

One transgenic line could eventually be established on the third chromosome, which was used for the experiments described in this study and in Klingseisen et al., 2009. The transgene insertion is homozygous viable and causes no side effects.

II. 4 Genetic methods

II. 4. 1 *Drosophila* stocks

Fly stocks were raised on standard medium and kept at 18°C and 25°C. For collection of embryos, flies were kept in cups on apple juice plates with fresh yeast to stimulate egg laying.

Standard food medium: 356g mays coarse meal, 47.5g soy flour, 84g dry yeast, 225g malt extract, 75ml 10% Nipagine, 22.5ml propionic acid, 28g agar, 200g sugar beet syrup with 4.9l dH2O

II. 4. 2 Fly stocks, chromosomes and alleles

The following tabs summarize all used fly stocks, including balancer chromosomes, recombinant lines and mutant stocks.

Affected chromosome	**Symbol**	**Marker/ Genotype**
2	CyO	Cy[1] dp[lvI] pr[1] cn[2]
2	CyO, P [ftz::lacZ]	P [ftz-lacZ], Cy[1], cn [2]
2	CyO, P[twi::GFP]	P[twi-GFP], Cy[1], cn [2]
3	MKRS	M(3)76A1 kar[1] ry[2] Sb[1]
3	TM3, P[ftz::lacZ]	P[ftz-lacZ.ry+] Sb[1] ry
3	TM6b	Antp[Hu] e[1]
Transposon	**insertion line used for imprecise**	**P-element excision**
EP(2)G18816	Transposable element inserted into the fourth exon of the *ths* locus	

Table 5. Used Balancer chromosomes and transposable element insertion line

Used Gal4 driver lines

Name	**Genotype; chromosome**	**Reference; expression pattern**
twiG4, CD2	*twi::Gal4, twi::CD2;* II	Bloomington stock centre; expression in all mesoderm cells
eveS3-G4	*eve(stripe3)::Gal4* ; II	Bloomington stock centre; Expression in one stripe (3) of the early *even-skipped (eve)* expression pattern
enG4	*en::Gal4*; II	Bloomington stock centre; expression in stripes of trhe *engrailed (en)* expression pattern
69BG4	*69B::Gal4*; III	Bloomington stock centre; expression from stage 9 in the lateral ectoderm

Table 6. Used Gal4 driver lines
The expression pattern of each line are described.

Generated mutant fly stocks

Affected chromosome	**Stock name**	**Description**
2	ths^{141}	Single mutation in *ths* created by imprecise P-element excision. chromosomal deletion within ths gene, removing 330bp whitin the *ths* gene locus, relating to a deletion of 11 amino acids of 107amino acids of the FGF core domain; homozygous viable and fertiale; 30% reduced fertility in females
2	ths ^{759}	Single mutation in *ths* created by imprecise P-element excision. chromosomal deletion within *ths* gene locus, removing 2,4 kb of gene sequence relating to a deletion of 84amino acids out of 107amino acids of the FGF core domain; homozygous lethal to 98%, escapers are sterile
2	pyr ^{18}	Single mutation of *pyr* created by imprecise P-element excision.

		chromosomal deletion taking out pyr gene sequence; homozygous lethal to 99%, escapers are sterile Generated by T. Gryzik, 2005

Table 7. Generated mutant fly stocks by imprecise P-element excision
Generated mutant fly stocks by imprecise P-element excision of the inserted transposons *EP(2)G18816* in case of *ths* and *P(2)5-SZ-3066* in case of *pyr*.

Generated recombinant lines

For generation of recombinant lines, the mechanism of female meiotic recombination was utilised. Random crossing-over events were singled out by genetic markers in proximity to the allele of interest and by subsequent test for complementation of the deficiency *Df(2R)ED2238* or the allele *pyr* ^{18}. For overview, see Greenspan, 2004.

Name	Genotype	Event
Df2238, CD2, twiGal4	*Df(2R)ED2238, twi::CD2, twi::Gal4*	Recombination of Df(2R)ED2238, twiCD2 with twi::Gal4 on chromosome II
Df2238,CD2, UAS-ths*	*Df(2R)ED2238, twi::CD2, UAS::ths*-HA*	Recombination of Df(2R)ED2238, twiCD2 with UAS::ths*-HA on chromosome II
pyr^{18}, UAS-ths*	*pyr^{18}, UAS::ths*-HA*	Recombination of pyr^{18} with UAS::ths*-HA on chromosome II
ths^{759}, CD2	*ths^{759}, twi::CD2*	Recombination of ths^{759} and twi::CD2 on chromosome II
pyr^{18}, CD2	*pyr^{18}, twi::CD2*	Recombination of pyr^{18} and twi::CD2 on chromosome II

Table 8. Stocks generated by meiotic recombination of alleles on the second chromosome

II. 4. 3 The UAS/Gal4-system

The UAS-Gal4 system is a genetic tool that allows ectopic expression of any gene of interest (Brand et al., 1993). It is a bipartite technique, in which one transgenic line, the activator- or driver line, expresses the yeast transcription factor Gal4 in a known temporal and/or spatial pattern. A second transgenic line, the responder- or effector line, contains a gene of interest under the control of upstream activating sequences (UAS), which are targeted by Gal4 (Fig. XX). To activate gene expression, activator-lines are crossed to effector-lines. The resulting progeny carries both transgenes, thus expressing the gene of interest under the control of the desired regulatory sequence.

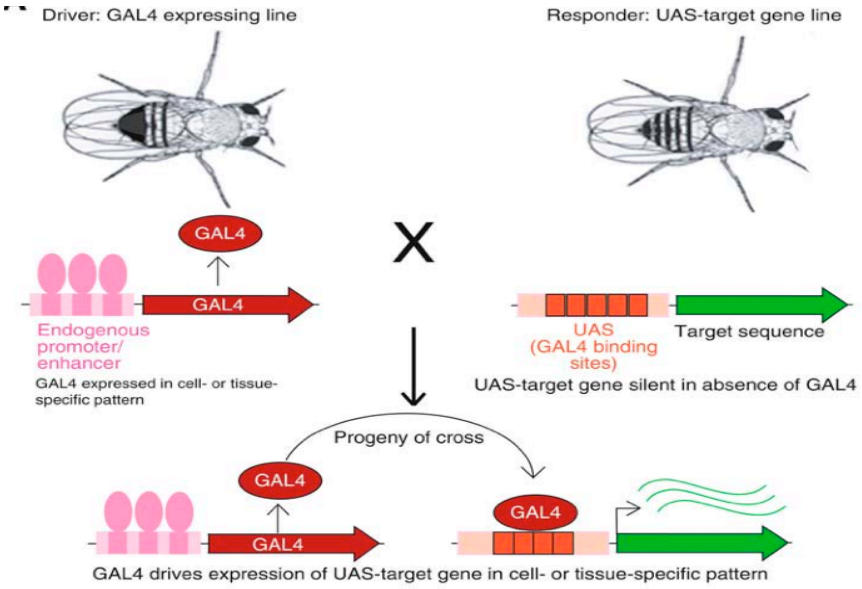

Fig. 28. The UAS/Gal4-system
Schematic diagram of the UAS/Gal4-system. The system is comprised of activator- or driver lines, in which the yeast transcription factor Gal4 is expressed in a known temporal and/or spatial pattern, and responder- or effector lines, which carry UAS-dependent transgenes. To activate gene expression, driver lines are crossed to effector lines. The resulting progeny carries both transgenes, thus expressing the gene of interest in the desired temporal and/or spatial expression pattern. (adapted from Elliott and Brand, 2008).

II. 4. 4 Imprecise P element excision

P-elements are transposable elements that have entered the *Drosophila* population less than 100 years ago and have since become a common tool to study gene function in the fly (Ryder and Russell, 2003). P-elements that are used to create mutations or deletions in a particular genomic region are non-autonomous transposable elements, which lack transposase activity. They need an external source of Transposase in order to move.

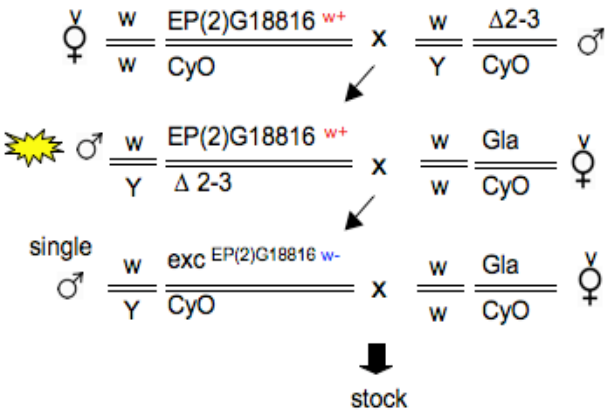

Fig. 29. Crossing scheme for mobilisation of a transposable element.
The insertion containing flies are crossed to flies carrying the gene for the transposase Δ 2-3. If both the transposase and the transposon are present in the genome of the F1 generation, excision events can occur. If the P-element containing the w+ mini-gene is removed, the excision event is discernible in the progeny by a white eye colour, e.g. lost red eye colour. All crosses are performed in w- background, thus the mini-w+ gene is a suitable marker for the successful excision of the transposon. Males containing white- eyes further were used to establish stocks, which were tested by PCR for the extent of a possible lesion generated by imprecice excision (Fig. 30)

The sites of action of the Transposase are terminal inverted repeats (IR) consisting of 42bp at each side of the element. Depending on the site of insertion in the genome, the P-element insertion itself can already lead to a mutation or disruption of the gene function.

The Transposition of P-elements is restricted to the germline by the inhibition of correct splicing in somatic cells by a splicing repressor protein (Amarasinghe et al., 2001).

By crossing flies containing the P element in their genome to flies carrying a transgene encoding Transposase, in the germline of the offspring (F1), the P-element can be

moved. The event of a successful P element excision can be followed in the resulting progeny (F2) by loss of the eye colour: the P-element contains a sequence of the white gene, a "mini-white" gene, which is responsible for the pigmentation of the eye; all crosses are performed in endogenously *white-* genetic background. Partial or complete excision of the P element results in a loss of function of the "mini-white" gene (see crossing scheme Fig. 29).

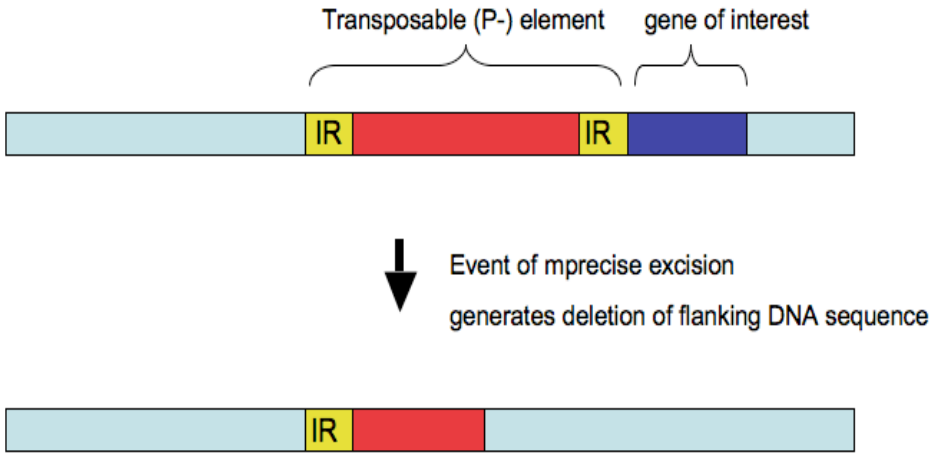

Fig. 30. Exemplified event of an imprecise P-element excision.
By PCR tests, the presence if the IR element can be tested using the universal primer (UP) and a second oligonucleotide binding in the flanking genomic region of interest.

The excision of a P-element from a chromosome creates double-strand breaks in the DNA (Engels et al., 1990; Ryder and Russell, 2003) and can result in a partial or complete removal of the transposon. If the ends of the double strand breaks are degraded before repair, a deletion of the genetic material will occur, an event known as imprecise excision (Fig. 30) The frequency of imprecise excision is approximately 1% of excision events and deletion sizes range from a few base pairs to several kilo bases (Daniels et al., 1985; Ryder and Russell, 2003).

II. 5 Histological Methods

II. 5. 1 Used antibodies

Antibody	Dilution	Source
rabbit α ß-Gal	1:1000	Cappel
mouse α ß-Gal	1:100	DSHB
mouse α CD2	1:500	Serotec
mouse α HA	1:1000	Roche
mouse α Eve	1:50 - 1:100	DSHB
mouse α Dig	1:800	Roche Dig labelling Kit
mouse α Lbe	1: 1000	Jagla et al., 1997
rabbit α dpERK	1:250	Sigma
rabbit α Mef-2	1:500	Gift from K. Jagla, Clermont-Ferrand, France
rabbit α Mhc	1:500	Gift from B. Patterson, Bethesda, USA
rabbit α Twist	1:1000	Müller lab
rat α DN-Cadherin	1:50	DSHB

Table 9. Primary antibodies used

Antibody	Dilution	Source
donkey α rabbit Alexa488	1:200	Molecular Probes
donkey α mouse Cy3	1:200	Jackson ImmunoResearch
goat α rabbit Cy3	1:200	Jackson ImmunoResearch
goat α mouse Alexa488	1:200	Molecular Probes

goat α rat Alexa488	1:200	Molecular Probes
goat α rat Alexa647	1:200	Molecular Probes
donkey α rat Cy3	1:200	Jackson ImmunoResearch
goat α rabbit Biotin	1:200	Vector Laboratories
goat α mouse Biotin	1:200	Vector Laboratories
goat α rabbit-AP	1:800	Dianova
goat α mouse-AP	1:800	Dianova
	fluorescent dye	
DAPI	1:1000 (stock:1mg/ml)	Sigma-Aldrich

Table 10. Secondary antibodies used

II. 5. 2. Immunocytochemistry

Embryos were obtained, fixed, stained and sectioned as described in here and in (Müller, 2008).

II. 5. 2. 1 Fixation of embryos

To obtain embryos, flies were kept on egg collection cages with apple juice plates. Embryos at the desired stage were dechorionated for 5min in a 3% sodium-hypochlorite solution. Dechorionated embryos were transferred to a wire mesh basket and rinsed with tap water. Embryos were fixed for 20-25 min in 4% formaldehyde on an overhead mixer. Therefore, embryos were transferred to a glass scintillation vial, containing 4ml 4% formaldehyde in 1xPBS pH 7.4 and 4ml n-heptane, which ensures that the embryos float between the two phases.

After fixation, the lower formaldehyde layer was replaced by 100% methanol. Subsequently, embryos were devitellinised by vortexing the vial for 20sec. Devitellinised embryos were collected from the methanol phase with a Pasteur pipette and transferred to an Eppendorf tube with 100% methanol. Embryos were washed three times with 100% methanol to remove all n-heptane and formaldehyde.

Eventually, embryos were either used directly for immunohistochemistry, or stored at -20°C (protocol adapted from Müller, 2008)

II. 5. 2. 2 Antibody staining of embryos

Embryos were permeabilised by washing three times for 20min in PBT/Tween20 pH7.4. Permeabilised embryos were blocked by washing three times 20min in PBT/Tween20 with 5% NHS, before incubation with the primary antibody in PBT/Tween20 with 5% NHS overnight at 4°C. The primary antibody was removed and the embryos washed three times for 20min in PBT/Tween20 before incubation with the secondary antibody in PBT/Tween20 with 5% NHS for 2h at RT. The secondary antibody was removed and the embryos washed for three times 20min in PBT/Tween20. Eventually, embryos were mounted in mowiol/DABCO.

In case HRP stainings should be performed, an aliquot of the avidin-biotin- enhancer system (Vectastain ABC kit from *Vector Laboratories*, Burlingame, USA) is prepared after the first of the previously mentioned three to four washing steps. Therefore, 500μl of PBT are mixed with 5μl of solution A and afterwards 5μl of solution B are added and the solution is mixed again followed by a 30 min incubation at RT. After the last washing step, the AB solution is added to the embryos and left on a shaker for 45min (RT). After three 15 min washing steps with PBT, the staining solution is prepared: 500μl of a 1mg/ml DAB stock (3,3- Diaminobenzidine-tetrachloride, *Sigma-Aldrich,* Steinheim, Germany) are added to 500μl PBS. After addition of 2μl 10% H2O2, the

staining solution is added to the embryos and the staining reaction is controlled under a dissecting microscope. To stop the reaction, the embryos are briefly washed twice with PBT.

In case an (additional) AP staining should be performed, the embryos are washed twice for 5 min in PBT and then two times in AP-buffer for 10 min (see II. 1. Materials; 0.1% Tween 20 is added only prior to use). The AP-staining solution is prepared by mixing 500μl AP-buffer with 1.7μl BCIP and 1.5μl NBT and it is added to the embryos. The staining reaction is controlled by eye under the dissecting microscope and stopped by addition of PBT.

After the HRP or AP staining embryos are washed 3x 10min with PBT and then incubated in 30%, 50%, 70%, 95% and 100% ethanol (5min each) followed by an incubation in 100% acetone for 5-10 min. Afterwards, a 1:1 solution of araldite and acetone is added to the embryos and the closed reaction tube is left o/n at 4°C. The following day the embryos are transferred onto a slide with as little araldite/acetone as possible and oriented using an eyelash. The slide is incubated o/n at 65°C. After this step, the embryos are mounted in 100% araldite, which is hardened at 65°C o/n.

II. 5. 2. 3 In situ hybridisations on embryos

For in situ hybridizations, the Dig labelling Kit from Roche was used to produce Dig labelled RNA probes. Quantity and quality of the probes were analyzed in a denaturating Formaldehyde gel prepared as follows:

add to 3μl probe and 3 μl of RNA ladder:
5μl deionized Formamid
2 μl Formaldehyde
1,5 μl 10X MOPS
1μl Ethidium Bromide (0,4mg/ml)
denaturate probe for 5 minutes at 65°C and store on ice before applying
Formaldehyde gel:

51,8 ml H_2O
6 ml 10X MOPS
0,9 g Agarose
3,2 ml Formaldehyde
(add after agarose solution cooled down to 70°C and immediately pour the gel)
Electrophoresis at 80V under the hood

In situ hybridization:

50-100 fixed embryos or embryos stored at -20°C in 100% Ethanol (EtOH) after previous fixation were incubated for 30 minutes in a mixed solution of 500μl Ethanol and 500μl Xylol. After 5 washing steps with 100% EtOH and two washing steps with methanol (MeOH), the embryos are washed in three steps with PBT. All washing steps involve 5 minutes incubation. The embryos were then fixed again for 25 minutes in 4% Formaldehyde solution, which is removed by 5 washing steps with PBT (5 minutes each time). Next, the embryos were incubated with Proteinase K (4μg/ml in PBT)for exactly 8 minutes, which is important as otherwise the protein fraction of the tissue is too much degraded for subsequent staining. To stop the enzymatic reaction, the embryos were washed 4 times with PBT(5 minutes each)and fixed again for 25 minutes in 4% Formaldehyde solution. After subsequent washing steps with PBT (5 minutes each), the embryos were rocked for 10 minutes in a 1:1 PBT/ hybridisation solution (see below). The hybridisation solution was removed and added freshly for three times. To prepare the embryos for the actual hybridisation step, the embryos were incubated with hybridisation solution for 1 hour at 55-65°C (temperature depends on the probe) in a waterbath.

For hybridisation, the probe was denaturated for 5 minutes at 65°C (heat block) (1-2 μl probe added to 100μl of hybridization solution). This hybridisation mix is added to the embryos after the pre-hybridisation solution is removed, and embryos were incubated with the antisense-probe over night (>12 hours) at 55-65°C (waterbath).

After washing four times with PBT within 1 hour at RT, the hybridised embryos were incubated with anti Dig antibody (1:800) in PBT for 1 hour. Four washing steps with PBT followed to remove the antibody (15 minutes each).

Then the embryos were equilibrated for 3x 5 minutes in AP buffer (AP buffer as used for normal immunohistochemistry) and the staining was performed after the nirmal staining procedure described above.

The embryos were embedded in araldite as described for antibody stainings above.

Hybridization solution:

50% Formamid

5X SSC

100μg/ml denaturated salmon sperm DNA

50μg Heparin

0.1% Tween20

For fluorescent RNA hybridisation, the TSA labelling Kit was used from TSA™ Detection Kit for fluorescent in situ hybridisation from Invitrogen, Groningen, Netherlands. The staining procedure is similar to the protocol described above and was performed after the recommendations of the user manual.

The RNA hybridisation on ovaries was performed in similar procedure to embryo in situ hybridisation. Following differences are to be noted compared to in situ hybridisations on embryos:

The fixation of ovaries was performed on ice in 5% paraformaldehyde and after the staining process, an additional fixation step is recommended. The ovaries are to fragile for araldite embedding and therefore were embedded for imaging in 100% glycerol.

II. 6 Measurement of mesodermal protrusions using *Volocity* software of fixed and stained *Drosophila* embryos

Fixed and stained embryos were mounted in mowiol/DABCO using spacers between the slide and coverslip to ensure the natural round shape of the embryos.

Using the Leica confocal software (see II.1), multiple scans in z-direction of up to 300 optical sections were performed.

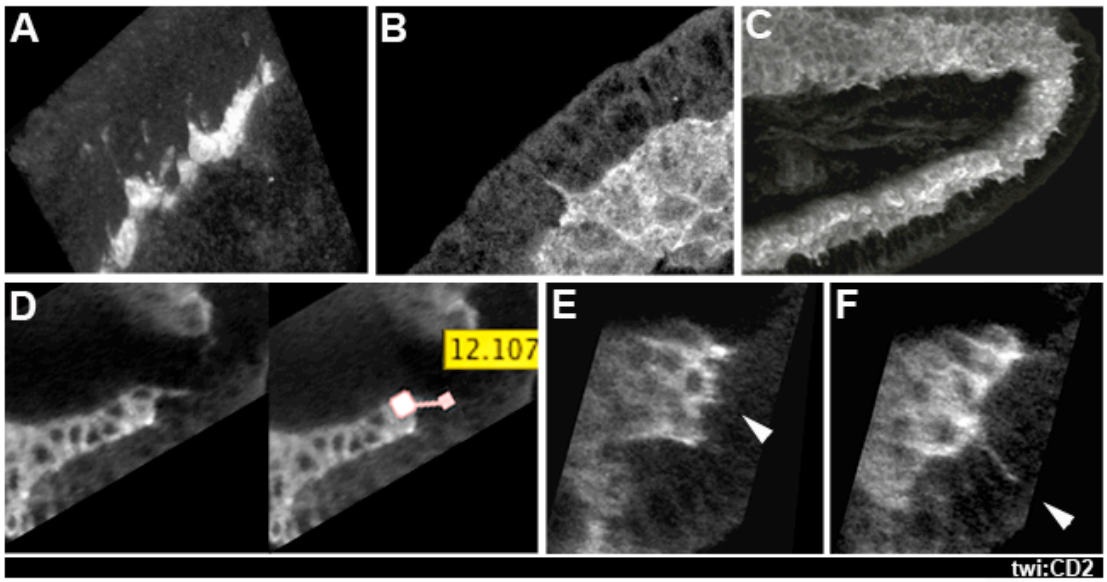

Fig. 31: 3D models of mesodermal protrusions and measurement.
(A) Leading edge protrusions into dorsal direction (dorsal is up left). **(B)** Example for radial filopodium **(C)** 3D model of one half of the embryo. Anterior is to the left, dorsal is up. Multiple radial protrusions are discernible. **(D)** Measurement of a leading edge filopodium, here 12 μm were measured. **(E)** Example for a protrusive extension counted as minimal length of filopodia, in contrast to the maximal length of radial protrusions **(F).**

The distance between each z-section was adjusted to 0.15μm for imaging of leading edge protrusions (Fig. 31 A), in this case, only 30 to 50 scans in z-direction were obtained.

For radial protrusion measurements, the distance was adjusted to 0.5μm-1.5μm, depending on the sample and orientation of the embryo. Using velocity software, the z-

stacks were composed to a 3D model (Fig. 31 C-F). The software allows measuring the distance between two set points within the created model.

The measurements are dependent on the points set for the measurement by the software and therefore can differ with regard to the person that sets the point of start and end of the protrusion of each cell. The first point for distance measurement therefore was always set in the middle of the cell as accurately as possible and discernible (Fig. 31 D). The 'end-point' of the cellular protrusion was set to the last bright pixel discernible of the computerised picture. For this reason, all measurements were done on black and white models to ensure a high level of contrast.

The measurement of the protrusion length thus does not reflect the actual length of the protrusion, which emerges at the leading edge of the cell and not from the centre of the cell. But as all protrusions were measured using this method, a comparison is possible between all analysed embryos, which allows comparing different genotypes.

To further exclude mistakes in the measurements, always the same region and length of 20μm along the anterior-posterior axis were analysed, from mesoderm posterior and anterior of the curve created by the extended germband. Thus, the counted numbers of protrusions always relate to a similar size of mesoderm area and can be compared. Moreover, the obtained lengths were always rated only in full μms, e.g. protrusions measured at 12.5μm to 13.5μm for example were all counted to the group of protrusions of 12 μm length. Examples for the shortest and longest radial protrusions counted and included in the measurements are shown in Fig. 31 E and F.

III Results

III. 1 Generation of *ths* and *pyr* single mutants by chromosomal deletion

Mesoderm migration during embryogenesis of *Drosophila melanogaster* is dependent on FGF signalling. The FGF receptor Htl is expressed in all mesodermal cells and two FGF8-like growth factors, Ths and Pyr, were identified as its ligands. The two genes originated from a common ancestor and share a high structural similarity. *ths* (*FGF8-like1)* and *pyr* (*FGF8-like2*) were identified in a screen using synthetic deficiencies (Gryzik and Müller, 2004) and expression profiling of Dorsal (Dl) target genes (Stathopoulos 2004; Stathopoulos and Levine, 2004).

A chromosome affecting both FGF genes is difficult to create because of the two genes being apart only 64kb. Because of this genetic proximity, the usual method of choice, a recombination of two single mutations, would have a predicted efficiency of recombination events of 0, 01 %. With an efficiency this low, at least 10.000 flies would have to be screened in order to obtain 1 recombinant carrying a chromosome containing both ths^{759} and pyr^{18} single mutations. As a substitute for a clean double mutant of *ths* and *pyr*, the small deficiency *Df(2R)ED2238 (Df* ^{2238}*)* was used to represent a *ths*, *pyr* double mutant background. To distinguish from a clean double mutant, *Df* ^{2238} homozygous mutant embryos are referred to as *ths*, *pyr* deficient embryos. *Df* ^{2238} deletes ~440kb on the second chromosome, including the chromosomal loci of *ths* and *pyr* (Gryzik and Müller 2004) (Fig. 32A). Of all genes deleted, *ths* and *pyr* were identified as the genes uncovered in *Df* ^{2238} that account for the defects in mesoderm development of *Df* ^{2238} homozygous embryos (Gryzik and Müller, 2004; Gryzik, 2005).

To characterize the individual function of *ths* and *pyr* during mesoderm development in embryogenesis, chromosomes affecting only a single FGF gene were generated.

As Ths and Pyr are ligands for the same receptor, functional regulation of signalling by heterodimeric or homodimeric receptor activation is possible, which would be altered in change of ligand ratio. Also, gradient formation of secreted Htl ligands was proposed to be involved to control localised Htl activation (Gabay et al., 1997), and the regulation of ligand concentration and signalling by binding to HSPGs (Lin et al., 1999, Lin, 2004). HSPG binding affinities were shown to favour FGF homodimers and that FGF dimer formation is crucial for receptor formation (Kwan et al., 2001; Harada et al., 2009). Thus, not only the presence but also the levels of available ligand proteins have importance in signalling properties. To investigate possible effects upon gene dosage reduction on Ths and Pyr mediated Htl signalling, the hemizygous conditions ths^{759} in trans to *Df(2R)ED2238* (ths^{759}, Df^{2238}) and pyr^{18} in trans to *Df(2R)ED2238* (pyr^{18}, Df^{2238}) were analyzed in addition to single mutant conditions. In hemizygous embryos, only one copy of either FGF gene is present in absence of the other FGF ligand. In absence of possible substitutive function of one ligand, effects upon dosage reduction of the other then would be detectable.

III. 1. 1 pyr^{18} represents a null allele of *pyr*

A null mutation of *pyr*, *FGF8-like2*^{18} (pyr^{18}), was created by imprecise P-element excision and is described in Gryzik (2005). The P-element *P(2)5-SZ-3066* is inserted 1kb proximal to the transcription start site of *pyr*. Imprecise excision of the P-element resulted in deletion of the chromosomal region distal of the P-element insertion site, deleting the entire gene locus of *pyr*. The extent of the chromosomal lesion was tested by PCR analysis of flanking genomic sequences, which confirmed that *pyr* was absent, but neighbouring genes were not affected. In situ hybridisations on pyr^{18} single mutants

utilising *pyr* antisense probes confirmed that *pyr* no longer is expressed in pyr^{18} homozygotes (data not shown).

A comparable single mutant analysis has not yet been done for the *ths* gene and will be described in the following.

III. 1. 2 Two alleles of *ths* were obtained by imprecise P-element excision, ths^{141} and ths^{759}

The use of P-elements (transposable elements, transposons) in *Drosophila* to create chromosomal deletions is described in Experimental Procedures, II. 4. 4. The excision of a P-element from a chromosome creates double-strand breaks in the DNA (Engels et al., 1990; Ryder and Russell, 2003) and can result in a partial or complete removal of the transposon. If the ends of the double strand breaks are degraded before repair, a deletion of the genetic material will occur, an event known as imprecise excision. The frequency of imprecise excision is approximately 1% of excision events and deletion sizes range from a few base pairs to several kilo bases (Daniels et al., 1985; Ryder and Russell, 2003). The mobilisation of a P-element transposon insertion leads to a precise excision in 99% of all events. In about 1% of P-elements being excised cause a deletion of flanking genomic DNA sequence (Daniels et al., 1985; Ryder and Russell 2003). The sizes of the chromosomal deletions created this way range from a few base pairs to several kilo bases.

To obtain a deletion of *ths*, 800 excision events of the P-element *EP(2)G18816* were tested by PCR analysis of sequence flanking the P-element insertion site. *EP(2)G18816* was inserted 113bp downstream of the sequence coding for the FGF core domain within the forth exon of the gene (Fig. 32B, C).

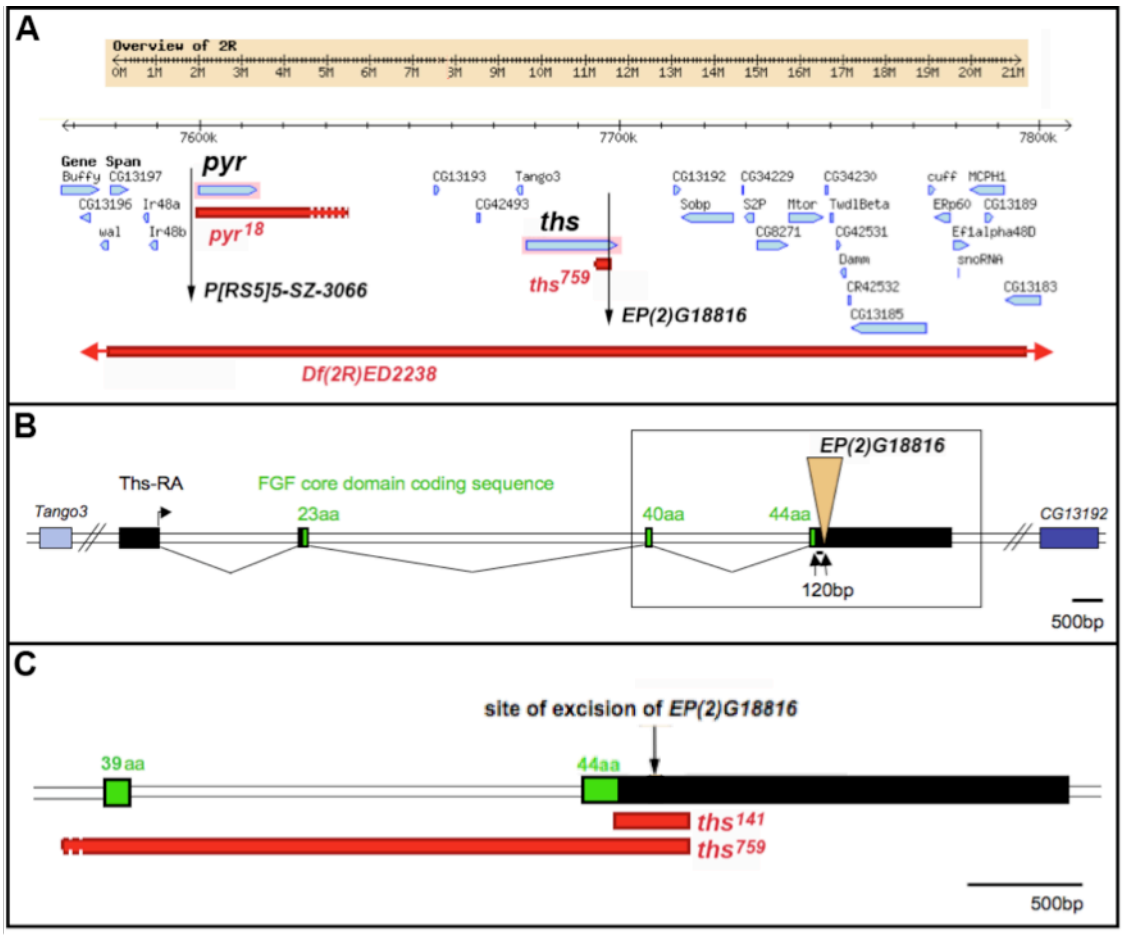

Fig. 32. Genomic characterisation of single mutant alleles for *ths* and *pyr*.
(A) Drosophila Genomic region of chromosome 2R corresponding to the cytological position 48C1-48C2. Red bars indicate the extent of the deletions in *Df(2R)ED2238*, pyr^{18} and ths^{759}, as determined by PCR and RT-PCR mapping (striped bars mark region containing break points that have not been confirmed by sequencing; arrows indicate the full extension of *Df(2R)ED2238* proximal and distal from 47F13-48D1). The pyr18 deletion extends to the insertion site of *P[RS5]5-SZ-3066* proximally and excludes *CG13193* distally. **(B)** Genomic region of *ths*. The P element *EP(2)G18816* is inserted into the forth exon 120bp distally from the sequence of exon 4 encoding amino acids of the FGF core domain (regions encoding amino acids of the core domain are indicated in green). **(C)** Magnification of the boxed region in (B). ths^{141} deletes a part of exon 4 including the coding sequence for 11 amino acids of the FGF core domain. ths^{759} deletes exon 3, the third intron and part of exon 4 of *ths*. The deletion includes the coding sequence for 84 amino acids of the FGF core domain. Both ths^{141} and ths^{759} extend proximal and distal 178bp and 180bp, respectively, from the insertion site of *EP(2)G18816*. Shown is only the translated coding region of exon 4.

Only lines carrying a deletion affecting the sequence encoding the FGF core domain of *Ths* proximal of the insertion site were kept for further analysis, for three reasons.

(1) The P-element line *EP(2)G18816* itself is homozygous viable despite an inserted element of 8kb size within RNA coding sequence of *ths*. Most likely, the transcription of *ths* is disrupted at the insertion site of the transposon, leading to a shorter mRNA providing the template for translation of the N-terminal signal peptide and the FGF core

domain only. Because the P-element insertion line was viable and fertile and showed no defects in mesoderm migration, a deletion of the C-terminus distal of *EP(2)G18816* therefore was not considered to result in a non-functional protein.

(2) The C-terminal amino acid sequence downstream of the FGF core domain is not conserved and does not contain any predicted known protein domains. Hence, the probability of creating a loss-of- function allele by deleting gene sequence downstream of the insertion site seemed very low.

(3) Being a ligand of the FGF receptor Htl, which is essential for embryogenesis and viability, a loss-of-function mutation of *ths* was suspected as well to cause severe defects or to be lethal similar to flies mutant for *htl*. Since *EP(2)G18816* is homozygous viable and the FGF domain is the only predicted protein domain besides the N-terminal signal peptide, a deletion of the sequence encoding the FGF core domain was considered to lead to a loss of function mutation.

Of all 800 candidate lines, only two of the candidate showed an upstream deletion of more than 120bp, only one of which was homozygous lethal. A deletion of more than 120bp was crucial as this was the distance of the P-element insertion site from the sequence encoding the FGF core domain (Fig. 32). The two candidate lines, the homozygous viable allele, ths^{141} and the homozygous allele ths^{759}, were analyzed further.

III. 1. 2. 1 The allele *ths* ^{141}

In ths^{141}, the imprecise excision of the complete sequence of the P-element resulted in a small deletion of 324bp of the forth exon (Fig. 32C). The deleted region includes the coding sequence for 11amino acids of the FGF core domain and 97 amino acids of the C-terminus (appendix 2). The lesion, however, does not cause a shift of the open reading frame. The ths^{141} allele still shows expression, but the transcript is shorter than

wild-type *ths* mRNA (Fig. 33A). Most certainly, the translation of *ths*^{141} mRNA leads to an internal deletion of 108 amino acids of in total 748 amino acids the protein compromises. The expression of such a slightly smaller protein could not be tested on a Western Blot, because there is currently no reliable antibody against Ths.

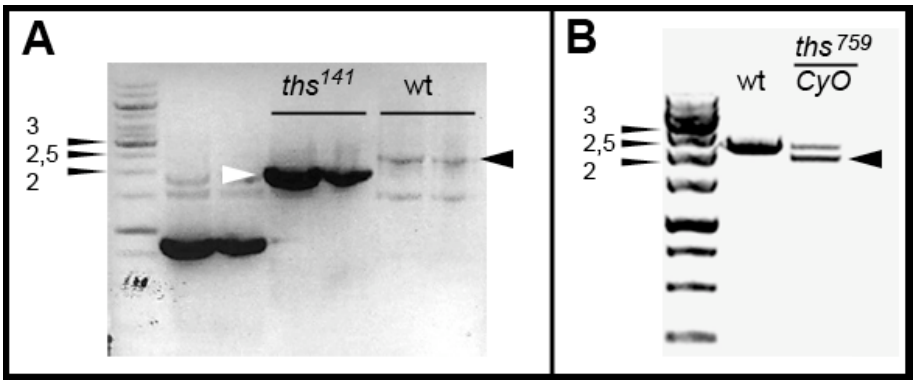

Fig. 33. RT-PCR on polyA+ RNA from wild-type (wt), *ths*^{141} homozygous and *ths*^{759} heterozygous embryos.
(**A**) RT-PCR from wild-type and *ths*^{141} homozygous embryos showing a 2.4 kb band corresponding to the wild-type ths mRNA and a 2 kb band in *ths*^{141} homozygotes. The 2 kb band was sequenced and corresponds to the deletion depicted in Fig. 1C. (**B**) RT-PCR from wt and *ths*^{759} heterozygous embryos showing a 2.4 kb band corresponding to the wild-type *ths* mRNA and an additional 1.9 kb band in *ths*^{759} heterozygotes. The 1.9 kb band was sequenced and corresponds to the deletion depicted in Fig. 1C

ths ^{141} shows normal mesoderm development but reduced fertility

The lesion in *ths*^{141} did not translate into defects in mesoderm development. Mesoderm invagination and migration was normal (Fig. 34D, E). Nevertheless, a slight defect on the migrational balance of the cells moving away from the ventral midline was observed (Fig. 34B, E). *ths*^{141} homozygotes showed no defect in the differentiation of mesodermal derivatives. For example, all 11 Eve expressing clusters of pericardial cells within each hemisegment are being specified as in wild-type (Fig. 34C, F).

In addition, *ths*^{141} complemented the deficiency *Df* ^{2238} genetically. Flies hemizygous for *ths*^{141} in trans to *Df* ^{2238} were viable and fertile as well as *ths*^{141} homozygous mutant flies. The only notable difference compared to wild-type was a significantly lower number of progeny. *ths*^{141} homozygotes produced 30% less progeny (hatching adult flies) compared to wild-type under the same conditions (Table 11).

	laid eggs		hatched flies	
day	wt	*ths*^{141}	wt	*ths*^{141}
1	407	287	243	174
2	525	348	361	228
3	498	331	340	171
4	472	328	293	190
5	397	278	247	281
total	2299	1572	1484	1044
		68.6% of wt		70.3% of wt

Table 11. Quantification of laid eggs and hatched adult flies from wild-type and *ths*^{141} homozygous crosses of the same number of parental flies.
ths^{141} homozygotes produced progeny 30% less than wild-type. The difference is equal in numbers of laid eggs and hatched flies, indicating that the reason for the reduced fertility is caused by defects during oogenesis.

To investigate further which period in development led to decreased numbers of progeny, the same number of parental flies was used to collect all laid eggs, larvae and pupae. The experiment revealed that the difference was based upon a 31,4% reduction in egg laying compared to wild-type (Table 11). These data suggested that *ths*^{141} homozygotes exhibit a defect during oogenesis as the cause of a 30% reduced fertility. To reveal possible defects during oogenesis, egg chambers of *ths*^{141} homozygous flies were examined for morphological abnormalities.

In *Drosophila*, the ovaries are paired and are composed of 12 to 16 ovarioles each. The most proximal structure of the ovariole is the germarium, which contains somatic and germline stem cells. The germarium is followed by successive stages of developing egg chambers that are arranged in a linear fashion with the most mature egg chamber at the most distal end (Kirilly and Xie, 2007). In wild-type, the stage 10 egg chamber is composed of the oocyte, 15 polyploid nurse cells and a surrounding monolayer of somatic follicle cells (Fig. 34G, I). Nuclear morphology represents an easy marker for the various cell types present during oogenesis in *Drosophila*. Wild-type ovarioles show an orderly progression of increasingly more mature stages that can be visualised by stainings with DAPI for DNA (Cooley et al., 1994).

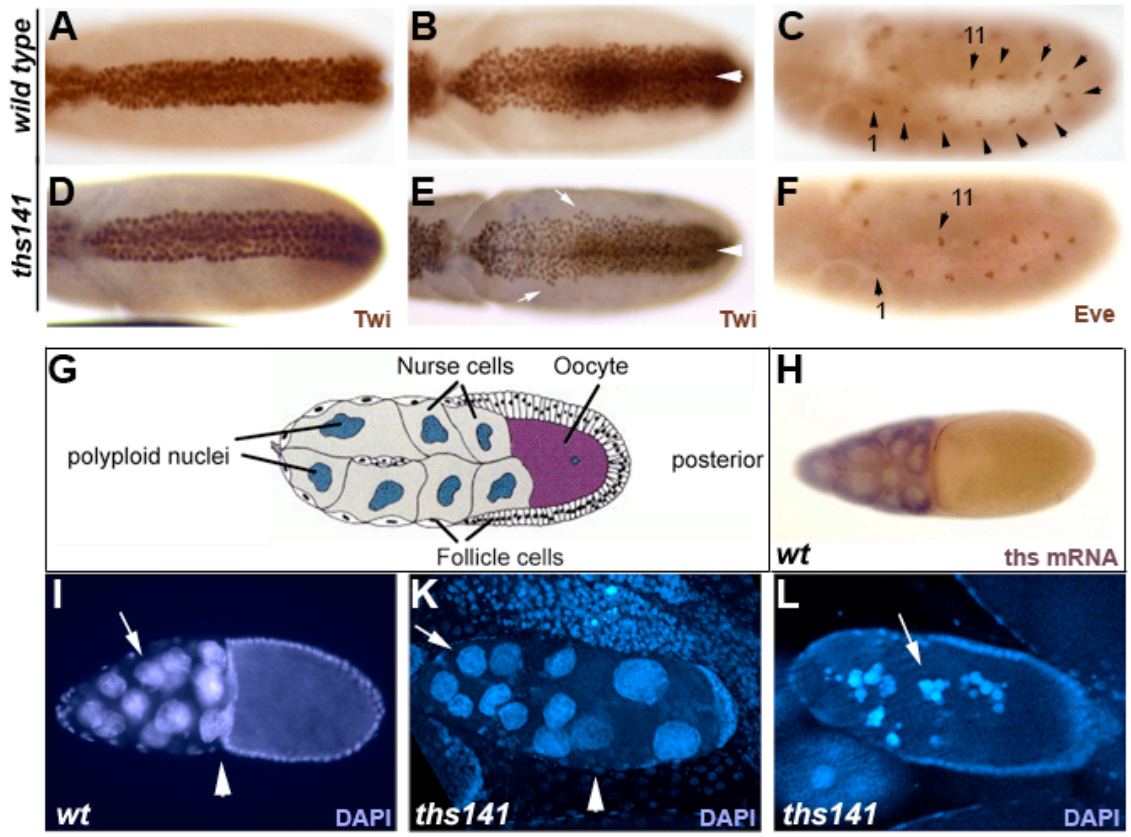

Fig. 34. Mesoderm spreading and defects in oogenesis of *ths*^{141} homozygous embryos and adults.
(**A-F**) *Drosophila* embryos of the indicated phenotypes stained with anti-Twi from ventral view (A, B (stage 7) and D,E (stage 8); arrowheads in B,E indicate the ventral midline) and with anti-Eve from lateral view (C, F (stage10)). Anterior is to the left. In *ths*^{141} homozygotes the ectodermal attachment is normal, but uneven spreading can be observed at stage 8 (arrows). The differentiation of pericardial cells is normal in *ths*^{141} mutants, all 11 cell cluster show expression of the differentiation marker Eve. (**G-L**) stage 10 egg chambers. The cartoon in (G) shows the structure of the egg chamber with polyploid nurse cells in the anterior part of the egg chamber which express ths mRNA (H). (I-L) wild type (I) and *ths*^{141} egg chambers (K,L) stained for DAPI to visualize the polyploid nuclei of the nurse cells (arrow in I, K). The arrowhead marks the position of the anterior pole of the oocyte, which is no longer pertained in *ths*^{141} homozygous mutants (K). Other *ths*^{141} homozygous mutant egg chambers only show degenerated, presumably apoptotic structures (L).

ths^{141} mutant ovaries were analyzed by a DAPI staining to visualise the general morphology during oogenesis. Stage 10 egg chambers exhibited severe defects in structure. In wild-type (Fig. 34G, I), the stage 10 egg chamber is composed of the oocyte, 15 polyploid nurse cells and a surrounding monolayer of somatic follicle cells (labelled in Fig. 34G).

In *ths*^{141} ovaries in contrast, about 30% of stage 10 egg chambers showed abnormalities compared to wild-type follicles (Fig. 34K, L). These abnormalities were manifested in two phenotypes. A third of all abnormal egg chambers showed polyploid nurse cell

nuclei in posterior positions normally obtained by the oocyte (Fig. 34K). Most of the abnormal egg chambers, however, showed neither nurse cells or the oocyte, nor their related nuclei. Inside these abnormal *ths*^{141} egg chambers, only clumps of DNA were detectable (Fig. 34L). The surrounding layer of follicle cells showed no degeneration and appeared normal. This phenotype is described for the degeneration of egg chambers during mid-oogenesis (McCall, 2004). In order to develop further, the egg chamber has to progress past a mid-oogenesis checkpoint. Thus, in *ths*^{141} homozygous females, 20% of stage 10 egg chambers obviously degenerate due to developmental abnormalities.

Before stage 9, the morphology of *ths*^{141} egg chambers appeared normal, suggesting that *Ths* function is not required in early oogenesis. During oogenesis, *ths* is strongly expressed in nurse cells of wild-type egg chambers from stage 9/10 (Fig. 34H). These findings both point to an important role of Ths during late stages of oogenesis. The phenotype of the allel *ths*^{141} is very severe since it leads to degradation of the whole follicle, but it affects only a third of all egg chambers.

In summary, in *ths*^{141} an internal deletion removes the coding sequence for 11 C-terminal amino acids of the 107 amino acids FGF core domain of Ths. *ths*^{141} adult females exhibit a markedly reduced fertility, caused by a -presumed apoptotic- degeneration of stage 10 egg chambers. Despite of this phenotype, the allele *ths*^{141} complemented the deficiency *Df* ^{2238} removing both ligands of the FGF receptor, although *ths*^{141},*Df*^{2238} hemizygous females showed a similar reduced fertility. First analysis of mesoderm development during embryogenesis of the surviving homozygous progeny showed no obvious defects compared to wild-type. Thus, the allele *ths*^{141} was not considered a functional null allele of *ths*, or to involve a second site mutation causing the weak phenotypes detected in *ths*^{141} homozygous embryos. Because the aim of the project was to characterise the function of the ligand during embryonic mesoderm

development, a functional null allel of the gene had to be established, and *ths*^{141} was not investigated any further.

III. 1. 2. 2 The allele *ths* ^{759}

In case of *ths*^{759}, 547 bp of the *ths* coding sequence were deleted by imprecise excision of the P-element *EP(2)G18816*. The deletion removes the coding sequence for 84 amino acids of the FGF core domain and 98 amino acids of the C-terminus (appendix 2). Despite of the internal lesion, the allel *ths*^{759} is still expressed, at RNA level. The deletion did not result in a frame shift of the open reading frame (ORF) that would lead to a stop codon or non-sense mutations within the sequence. Thus, the deleted region in *ths*^{759} results in transcription of a shorter mRNA compared to wild-type (Fig. 33B).

The break points of the deletion locate in the second intron and within the last exon of the *ths*^{759} allele. The precise distal breakpoint of the deletion within exon 4 was confirmed by sequencing of the reverse transcribed mRNA (Fig. 32C). To ascertain the proximal breakpoint, PCR tests were performed on genomic DNA isolated from *ths*^{759} homozygotes (Fig. 35). The tests showed that both the distal and the proximal end of the P-element have been excised. PCR fragments were obtained upstream of exon 3 and downstream of the P-element insertion site in exon 4, indicating a deletion of the sequence within. Exon 3 is removed completely, but exon 4 is only partially deleted (Fig. 35B, E).

Using primer pairs producing overlapping fragments, the region of the proximal breakpoint site could be narrowed down to 200 bp directly upstream of the coding sequence of exon 3 (Fig. 35A). Primer combinations binding to sequence flanking the breakpoint regions were used to produce DNA fragments covering the deleted area (Fig. 35B, D, F, G). Strikingly, the obtained PCR products were longer from genomic DNA of *ths*^{759} homozygotes than of wild-type embryos. The extent of the deleted region in

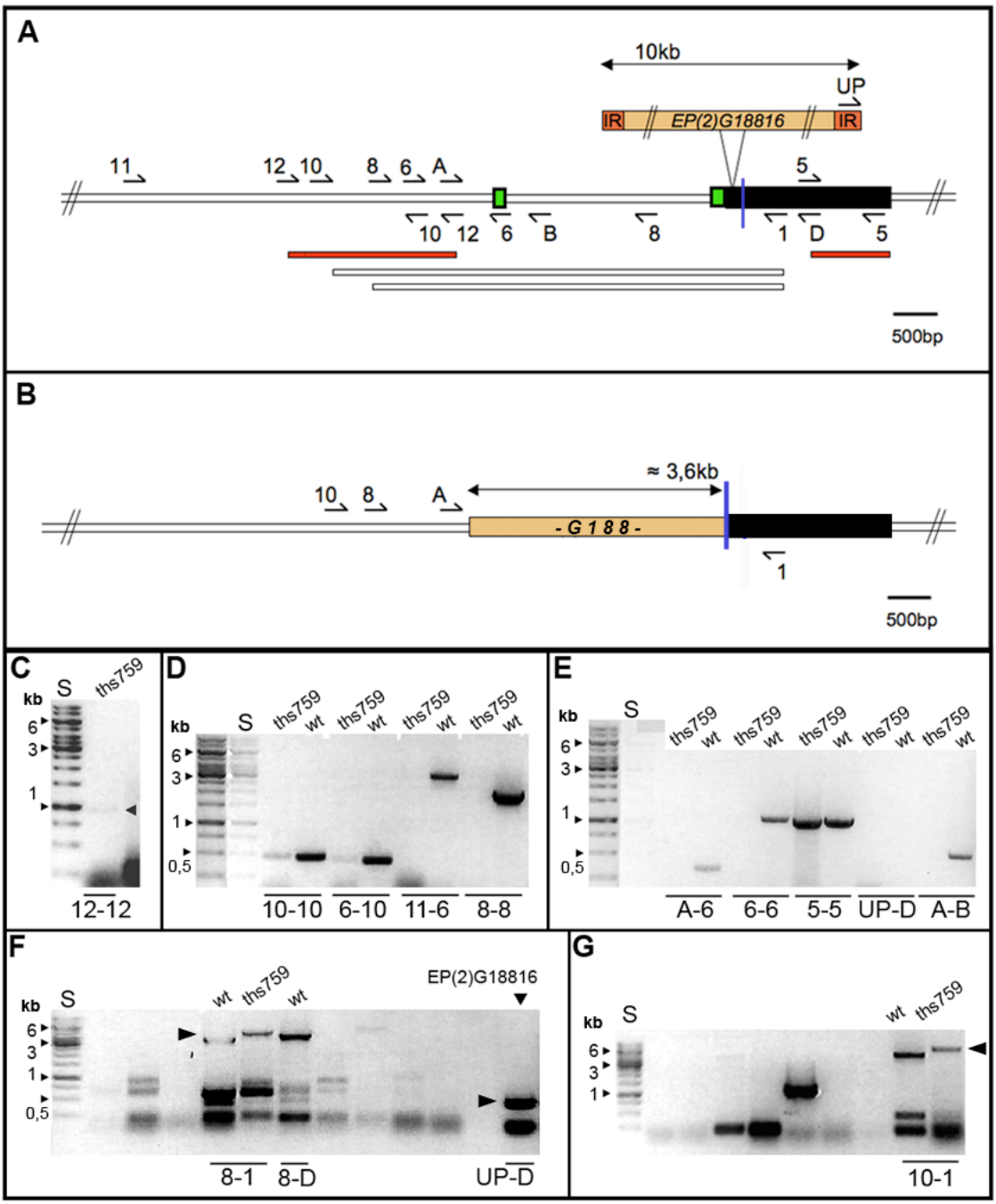

Fig. 35. Determination of the extent of the lesion in *ths*^{759}.
(A) Region of ths corresponding to the lesion in *ths*^{759}. Prior to the imprecise excision, the P-element *EP(2)G18816* is inserted in exon 4 as indicated. DNA primers of indicated locations and direction of PCR synthesis were applied to determine the extent of the region deleted proximal *EP(2)G18816*. The UP primer binds to the inverted repeats of the P element (F) and showed that the proximal and distal end of *EP(2)G18816* was excised (not shown; (E)). Red bars mark the regions that produced DNA fragments of size as in wild type (C-E). The open bars mark the region that produced DNA fragments of larger size than in wild type (F, G). Sequences encoding amino acids of the FGF core domain are indicated in green; the blue bar indicates the position of the distal extent of the lesion in (B). **(B)** Presumed structure of ths759 in the region corresponding to the lesion. The breakpoint of the deletion in the forth exon is indicated (blue bar) and was confirmed by sequencing. The forward primers 11, 10 and A produced fragments ~1.5 kb longer than the wild type extent of this genomic region of 3.8 kb. A ~3.6 kb fragment of *EP(2)G18816* is therefore assumed to be still inserted. **(C)-(G)** PCR products obtained from indicated primers 1, 5, 6, 8, 10, 11, 12, A, B, D, and UP. Reward primers 6, B and 8 did not generate PCR products in *ths*^{759} homozygotes ((D), (E)), indicating that exon 3 and the region distal of which are removed. The primer combinations of 10-1 and 8-1 generated bands of ~5.5 kb in contrast to 3.8 kb in wild-type ((F), (G)).

ths^{759} so far was determined to 2,4kb - 2,6kb. The expected length of the PCR product therefore was at 1,3kb in contrast to 3,8kb in wild-type. The obtained DNA fragment however, was about 1,5kb longer from *ths*^{759} genomic DNA compared to wild-type. The difference in fragment length suggests that the P-element *EP(2)G18816* was not removed completely. Since PCR tests showed, that 5' and 3' regions of the P-element were excised in *ths*^{759} (data not shown and Fig. 35E), a middle part of *EP(2)G18816* sequence presumably is still present (Fig. 35B). Considered the previously determined deletion in *ths*^{759} of 2,5kb and the obtained fragment length of ≈5kb (Fig. 35F, G), about 3kb -4kb of P-element sequence most probably are still inserted. Sequencing of the long PCR products covering the particular area in *ths*^{759} were not successful due to low DNA concentrations of the respective samples.

Despite the deletion and residual P-element sequence, the allele *ths*^{759} is being transcribed and the open reading frame is intact. *ths*^{759} cDNA does not include DNA fragments from the P-element, as confirmed by sequencing of *ths*^{759} cDNA. Thus, the remaining sequence of *EP(2)G18816* obviously is not being transcribed or is being spliced along with intronic sequence.

In summary, *ths*^{759} cDNA sequence and PCR analysis of *ths*^{759} genomic DNA indicate a genetic deletion of about 2,5kb of coding and non-coding sequence of *ths*. The deletion results in a mRNA 547bp shorter than in wild-type, lacking the coding sequence for 84 amino acids of the 107 amino acids comprising FGF core domain. As mentioned above, there is currently no reliable antibody against Ths to test for the presence of a smaller protein Ths^{759}. With regard to the ≈80% deletion of sequence coding for the FGF core domain however, the allele *ths*^{759} is considered a functional null allele of the FGF ligand Ths. Its effect on mesoderm development is described in the following in context with the analysis of *pyr*^{18} single mutants and the *ths*, *pyr* double mutant condition of *Df*^{2238}.

III. 1. 3 *ths*^{759} and *pyr*^{18} single mutants are semi-lethal and infertile

Both *ths*^{759} and *pyr*^{18} single mutants are semi-lethal, but viable homozygous mutant flies are low in numbers. From a heterozygous cross, viable *ths*^{759} homozygous adults were hatching at a rate of 3,4% (total offspring n= 4148) and viable *pyr*^{18} homozygotes at a rate of 0.71% (total offspring n= 565) (S 3A in appendix 1). However, crosses of *ths*^{759} and *pyr*^{18} homozygous adults, respectively, did not produce any progeny. To determine if the infertility of homozygous single mutants results from defects prior to onset of zygotic offspring development or after, both *ths*^{759} and *pyr*^{18} homozygous adults were crossed to wild-type flies.

pyr^{18} homozygous mutant adults both male and female were able to produce heterozygous progeny, therefore the lack of progeny was to be explained by zygotic defects during embryonal, larval or pupal development of the next generation.

ths^{759} male and female homozygous single mutants in contrast could not produce any progeny, even if crossed to wild-type flies each. *ths*^{759} females did not lay any eggs at all (monitored were n=54 females after mating with wild-type males). Dissection of the abdomen revealed that the ovaries are not developed in *ths*^{759} homozygous females. wild-type female flies crossed to *ths*^{759} homozygous males were laying eggs, but these all turned out to be unfertilized. Thus, *ths*^{759} homozygous females and males are equally infertile. These findings, in line with the effect on oogenesis in *ths*^{141} homozygous females as described above, suggest a possible role of *ths* during oocyte growth or in germline development.

The initial motivation to characterize the two Htl ligands in their function, however, was to better understand the process of mesoderm migration itself during *Drosophila* gastrulation and later embryogenesis. Therefore, the main focus was riveted on the behaviour of mesodermal cells during this process, and which aspects of their migration are regulated by FGF signalling. Analysis of mesodermal derivatives then

predominantly concentrated on testing for the presence of differentiated cell lineages or their precursors as a means to obtain information about whether, or how accurate, the spreading of the mesoderm progressed.

III. 2 Analysis of *ths* and *pyr* loss-of-function in mesoderm development

III. 2. 1 *ths* and *pyr* expression patterns indicate overlapping and individual functions

It was shown before that elimination of both FGF genes resembles the null mutation phenotype of their receptor Heartless, and that the FGF signalling pathway is not activated in embryos lacking both *ths* and *pyr* (Gryzik and Müller 2004). Having the same origin, the two Htl ligands were expected to partly fulfil analogical functions during mesoderm development. In this study, *ths* and *pyr* were analyzed with regard to redundant or individual functions in mesoderm development. The expression patterns of the ligands show striking similarities as well as clear differences (S4 in appendix 1). In early stages, both *ths* and *pyr* are expressed broadly in the lateral ectoderm (S4 stage 5, appendix 1). With the beginning of gastrulation, the expression domain of *pyr* is confined to the dorsal area of the ectoderm, while *ths* is expressed in ventral and lateral ectodermal cells (Fig. 39O; S4 stage 8, appendix 1). This divergence is very crucial as its timing correlates with active mesoderm migration towards dorso-lateral positions (Fig. 36A2-A4, B2-B4). At later stages of embryogenesis, *ths* and *pyr* are progressively expressed in differential patterns. There are overlapping domains of expression, such as a striped segmental expression pattern at stage 10 and expression in ectodermal muscle attachment sites from stage 12 onwards. But only *ths* is expressed strongly in the visceral mesoderm, and *ths* and *pyr* are expressed in different subsets of neuroblasts (S4 in appendix 1; Stathopoulos, 2004). In general, the two genes exhibit dynamic and

partially overlapping patterns of expression in tissues that induce the development of different mesoderm lineages, including the neurogenic ectoderm, muscle precursors, the hindgut and neuroblasts.

In situ hybridizations on homozygous *pyr*^{18} mutants using a probe against *ths* mRNA, and using a probe against *pyr* mRNA on *ths*^{759} homozygous mutant embryos, confirmed that the elimination of one FGF did not affect the expression of the other FGF at all (S1 in appendix 1). Heterozygous embryos showed the same expression pattern as embryos homozygous mutant for *ths* or *pyr*. Evidently, there is no positive or negative influence on a level of transcriptional regulation from both Htl ligands to one another.

III. 2. 2 Mesoderm spreading

The mesoderm is internalized as an epithelial tube through the ventral furrow. In wild-type embryos, the tube breaks down in a highly regular fashion after EMT and the mesenchymal cells arrange evenly at the ventral midline along the anterior-posterior axis (Fig. 36B1-2, C1- 2). During germband extension, mesoderm cells then migrate equably to both sides of the embryo in dorso-lateral direction (Fig. 36A3, B3, C3). During migration, the cells at the dorsal edge of the mesoderm maintain equidistant positions related to the dorso- ventral axis and synchronously reach the dorsal-most positions of the ectodermal margin (Fig. 36A4, B4, C4). After mesoderm spreading is complete, mesodermal cells coat the underlying ectoderm with a cellular monolayer (Fig. 36A5, B5, C5). The exact staging of fixed embryos allows the comparison of these key events in mesoderm spreading, referred to as symmetric tube collapse, even dispersal and synchronous, dorsal positioning of the cells, and monolayer formation. Following gastrulation, dpERK is detected in the mesoderm dependent Htl dependent FGF signalling (Gabay et al., 1997; Michelson, et al. 1998b). As early as stage 7, MAPK activation is restricted to 1-2 cells on each lateral side of the tube (Fig. 36D1;

Wilson et al., 2005). With the onset of migration at stage 8, dpERK is detected in 1-4 bilateral anterior-posterior cell rows (Fig. 36D2). As spreading advances, only the dorsal-most 1-2 rows of cells show activation of MAP kinase until it diminishes in stage 9 (Fig. 36D3-5).

Embryos mutant for the FGF receptor Htl exhibit severe defects in mesoderm spreading after normal mesoderm specification and invagination (Beiman et al., 1996; Gisselbrecht et al., 1996). The cells undergo EMT after invagination, but fail to make

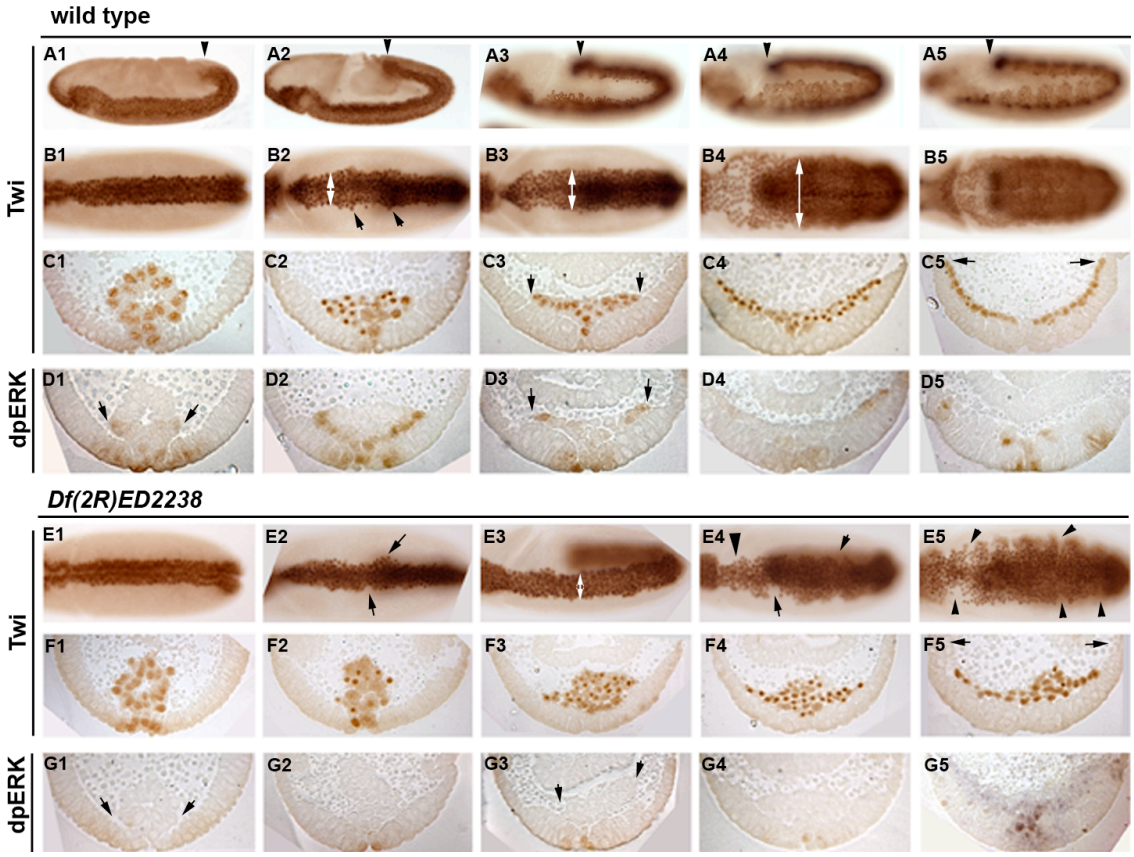

Fig. 36. Normal mesoderm spreading in wild-type and defects in *ths, pyr* deficient embryos.
Embryos of the indicated phenotypes stained with anti-Twi (A-C and E,vF 1-5, respectively) and anti-dpERK (D1-5 and G1-5; detects activated MAPK) shown as whole mount (A1-5 lateral view; B1-5, E1-5 ventral view; anterior is to the left) or cross section (between 40% and 60% egg length). Stages 7, 8 early, 8 late, 9 and 10 are shown in panels 1-5 each, respectively. **(A1-5, B1-5, C1-5)** Wild type. The arrowheads in A1-5 mark the stage of germband extension as indicator of developmental stage. White double arrows in B2-4 show the even extension of the mesoderm domain during spreading, also shown by arrows in (C3). Mesoderm cells acquire dorsalmost positions relative to the ectodermal margin (arrows in (C5)). **(D1-5)** Note activation of MAPK at mesoderm-ectoderm contacts and at the leading edge (arrows). **(E1-5, F1-5)** In embryos lacking both *ths* and *pyr* function, mesoderm cells fail to establish initial contacts, ectodermal attachment is uneven (arrows, (E2)), and spreading is unequal and asymmetric (E4, E5, arrows). Lateral spreading is delayed (double arrow in E3) and the anterior mesoderm domain fails to expand (E4, arrowhead). A monolayer is not achieved and the dorsal-most positions are not covered (F5). **(G1-5)** MAPK is not activated at any stage (arrows).

contacts to the ectoderm and do not form cellular protrusions (Schumacher 2004; Wilson et al., 2005). Mesoderm migration is impaired and incomplete, and mesodermal cells consequently do not acquire positions at the dorsal edge relative to the inductive ectoderm (Shishido et al. 1997); Michelson et al., 1998a). MAPK activation in the mesoderm is lost from *htl* mutant embryos (Michelson et al., 1998b).

III. 2. 2. 1 The combined function of both *ths* and *pyr* is required for mesoderm migration

The phenotypes shown in the following represent phenotypes occurring in >50% of all embryos examined. They were thus rated as the representative phenotype of the particular genotype, respectively. Other occurring phenotypes were weaker than shown here or similar to wild-type.

Deletion of both *ths* and *pyr* impairs mesodermal cell migration

Closely resembling the *htl* mutant phenotype, Df^{2238} mutant embryos lacking both *ths* and *pyr* exhibit severe defects in mesoderm spreading after normal mesoderm specification and internalisation (Gryzik and Müller, 2004) (Fig. 36E1-5, F1-5, G1-5). Prior to onset of migration, a mutant phenotype is less obvious. With ongoing mesodermal development, the defects upon deletion of both *ths* and *pyr* then become more visible and distinct.

In *ths, pyr* deficient embryos, the mesodermal tube did not collapse upon EMT as in wild-type and the cells failed to dissociate properly in order to adhere to the underlying ectoderm (Fig. 36F1-2). The lateral distribution of cells onto the ectoderm thus was irregular and the mesoderm was not aligned symmetrically along the ventral midline (Fig. 36E2).

Lateral mesoderm spreading was delayed in embryos lacking both *ths* and *pyr* compared to wild-type embryos. In relation to germ band extension and thus to stage of development, lateral spreading hardly progressed until stage 9 (Fig. 36E2-4, F2-4). The phases of mesoderm development in *ths*, *pyr* deficient embryos at stages 8-10 can rather be associated to the respective previous stages in wild-type (Fig. 36B2-4, C2-4, 6E3-5, F3-5).

Mesoderm spreading in absence of *ths* and *pyr* progressed in an asymmetric and uneven fashion, and the cells formed an irregular margin of a 'snake-like' shape along the anterior-posterior axis (Fig. 36E4, F4). The spreading process remained incomplete and the mesoderm cells failed to acquire dorsal-most positions at the edge of the ectodermal cell layer (Fig. 36E5, F5). A monolayer was not achieved in *ths, pyr* deficient embryos, and a fraction of cells still remained unevenly distributed in ventral-lateral regions (Fig. 36F5). According to the defects of stage related spreading, the precise timing of mitoses in the mesoderm at stages 8, 9 and 10 was entirely disturbed in these embryos. Instead of a timed, stage specific mitotic activity at certain intervals, cross sections of *ths, pyr* deficient embryos revealed a fraction of mesodermal cells being in mitosis continuously from early stage 8 onwards to stage 10 (Fig. 36F1-3).

MAPK is not activated in mesoderm cells in absence of both *ths* and *pyr* (Gryzik and Müller, 2004) (Fig. 36G1-5) as expected, since Htl activation is necessary for Ras/MAPK signalling in the mesoderm (Gabay et al., 1997; Michelson et al., 1998b; Carmena et al., 1998). MAPK activation within the ectoderm dependent on EGF signalling is not affected (Fig. 36G1-5) (Gryzik and Müller, 2004).

ths^{759} and pyr^{18} single mutants showed defects in mesoderm migration much less severe than those observed in embryos lacking both FGFs. Mesoderm spreading progressed with rather minor disturbances, but the process was not as robust as in wild-type (Fig. 37A1-5, D1-5).

ths function is required during early phases of dorso-lateral migration

The mesodermal tube collapse was normally onto the ectoderm, but the lateral attachment to the ectoderm was uneven along the anterior-posterior axis (Fig. 37E1-2, D1-2). Cells attached to the ectoderm however established normal contacts, and mesoderm-ectoderm interaction after tube collapse even seemed to be slightly enhanced in *ths*^{759} single mutants in comparison to wild-type (Fig. 37C2, Fig. 36D2, Fig. 9L).

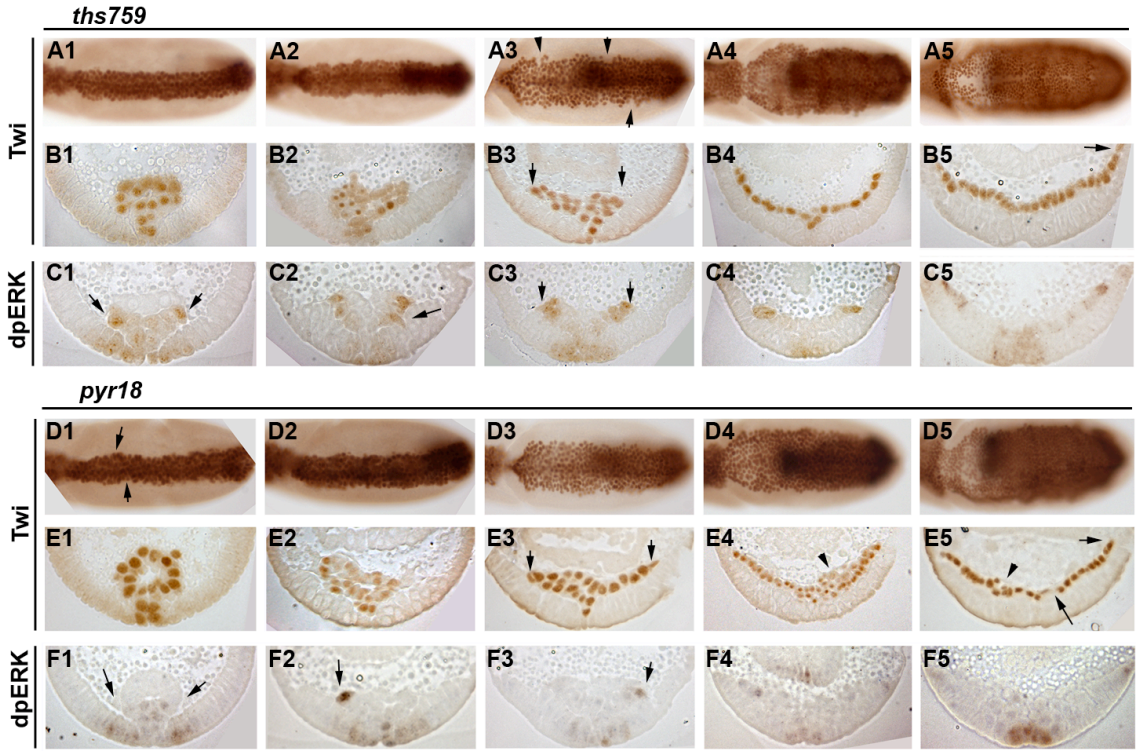

Fig. 37. Mesoderm spreading defects in *ths*^{759} and *pyr*^{18} single mutants.
Embryos of the indicated phenotypes stained with anti-Twi (A, B and D, E 1-5, respectively) and anti-dpERK (C1-5 and F1-5; detects activated MAPK) shown as whole mount (A1-5 , D1-5 from ventral view; anterior is to the left) or cross section (between 40% and 60% egg length). Stages 7, 8 early, 8 late, 9 and 10 are shown in panels 1-5 each, respectively. **(A1-5, B1-5)** In *ths*^{759} homozygotes, initial contact is normal, but early spreading is uneven (arrows in A3,B3). **(C1-5)** MAPK is activated as normal (arrows). Early ectodermal contacts are prominent in *ths*^{759} (arrow in C2). **(D1-5, E1-5)** *pyr*^{18} homozygous embryos show defects in even early ectodermal attachment (arrows in D1) and spreading (arrows E3). Monolayer formation is impaired (arrows in E4,5). **(F1-5)** MAPK activation is strongly reduced and restricted to stage 8 (arrows in F2, 3).

The analysis of fixed samples, however, does not allow an unequivocal prediction of this difference. During early migration, mesoderm cells were unequally distributed in relation to the ventral midline (Fig. 37B3), and consequently, the dorso-lateral migration was not regular (Fig. 37A3). However, when large numbers of *ths*^{759} embryos

were compared to wild-type embryos of respective stages, these differences were rather subtle.

Nevertheless, the uneven distribution of mesoderm cells during early migration phases is obvious in cross sections (Fig. 37B3), and was displayed in over 50% of all examined samples. These early irregularities are compensated in later stages of mesoderm migration (Fig. 37A4- 5). Loss of *ths* function further had no effect on monolayer formation and consistent positioning of mesoderm cells relative to the dorsal margin of the ectoderm (Fig. 37B4-5).

ths^{759}, Df^{2238} hemizygous mutant embryos showed similar defects in even ectoderm attachment and early regular spreading of the mesoderm (Fig. 38A2-3, B2-3) as ths^{759} single mutants. The consequent positional irregularities of dorsal edge cells, however, were balanced only later if only one copy of *pyr* was present in absence of *ths* (Fig. 38A4-5, B4-5). Nevertheless, a single copy of *pyr* is sufficient for the formation of a continuous monolayer that covers the ectoderm including the dorsal-most positions in absence of *ths* function (Fig. 38B5).

Remarkably, MAPK activation was not affected in ths^{759} single mutants and dpERK was detected as in wild-type, from stage 7 onwards in the most dorsal rows of migrating cells (Fig. 37C1-5). ths^{759}, Df^{2238} hemizygous embryos showed a MAPK activation pattern not as robust as ths^{759} single mutants (Fig. 38C1-5). During early stages, regular MAPK activation was disturbed along the anterior-posterior axis. MAPK was activated only unilateral, or cells in medial positions showed higher levels of dpERK than cells at the dorsal edge of the mesoderm (Fig. 38C2, C3). The initial activation of MAPK prior to tube collapse, however, was not affected (Fig. 38C1), and MAPK activation was normal as well in dorsal edge cells during later migration (Fig. 38C5). Thus, one copy of *pyr* is not sufficient for robust MAPK activation in stages where defects in mesoderm spreading occur in absence of *ths* function.

pyr^{18} single mutant embryos show spreading defects not only in early but also in later stages of mesoderm migration

Similar to *ths* loss of function mesoderm cells in pyr^{18} single mutants were not attached symmetrically to the ectoderm along the ventral midline after tube collapse (Fig. 37D2, E2). During dorso-lateral movement in absence of *pyr*, the distribution of mesoderm cells was transversely uneven and the dorsal front of migrating cells was not as continuously regular as in wild-type (Fig. 37E3, D3). As in ths^{759} mutants, the defects in regular lateral migration were compensated when spreading progressed (Fig. 37D4). In contrast to ths^{759} single mutants however, embryos lacking *pyr* also exhibited defects in later mesoderm spreading (Fig. 37E4, E5). Mesoderm cells acquired dorsal-most positions relative to the ectodermal margin, but a continuous coating of the ectoderm was not established (Fig. 37E5).

The spreading phenotype of embryos lacking *pyr* function suggests a delay in onset of migration compared to wild-type embryos. The interval between tube collapse and first lateral movements of stage 7 and early stage 8 appeared to be slightly longer, in contrast to later normal progression of migration. The timing of both mitotic waves appeared unimpaired (Fig. 36C2, Fig. 37E2). However, comparison of live imaging data from GFP tagged mesoderm cells will be required to substantiate this idea.

pyr^{18}, Df^{2238} hemizygous embryos showed an enhancement of the spreading defects in ths^{759} and pyr^{18} single mutants. In absence of *pyr*, a single copy of *ths* is not sufficient to ensure a symmetric ventral alignment of the mesoderm collective (Fig. 38D1-2) and even dorso-lateral spreading (Fig. 38D3-4, E3-4). Defects occurred not only in early but also in later stages and were more penetrant and expressive in pyr^{18}, Df^{2238} hemizygotes (Fig. 38D2-4, E3). Similar to pyr^{18} single mutants, mesoderm cells reached the dorsal edge of the ectoderm but failed to form a continuous monolayer (Fig. 38E4-5).

In contrast to *ths* function, *pyr* is required for normal MAPK activation during mesoderm migration. dpERK was occasionally detected only in stages 7 and 8, with onset of migration (Fig. 37F1-5). In absence of *pyr*, MAPK was activated asymmetrically and only in a subset of cells at the dorso-lateral edge of the mesoderm (Fig. 37F2-3). pyr^{18}, Df^{2238} hemizygous embryos showed no alteration of the pyr^{18} single mutant phenotype. dpERK was detected only during early phases in stages 6-8 and the MAPK activation pattern was asymmetric and restricted to a subset of mesoderm cells (Fig. 38F1-5).

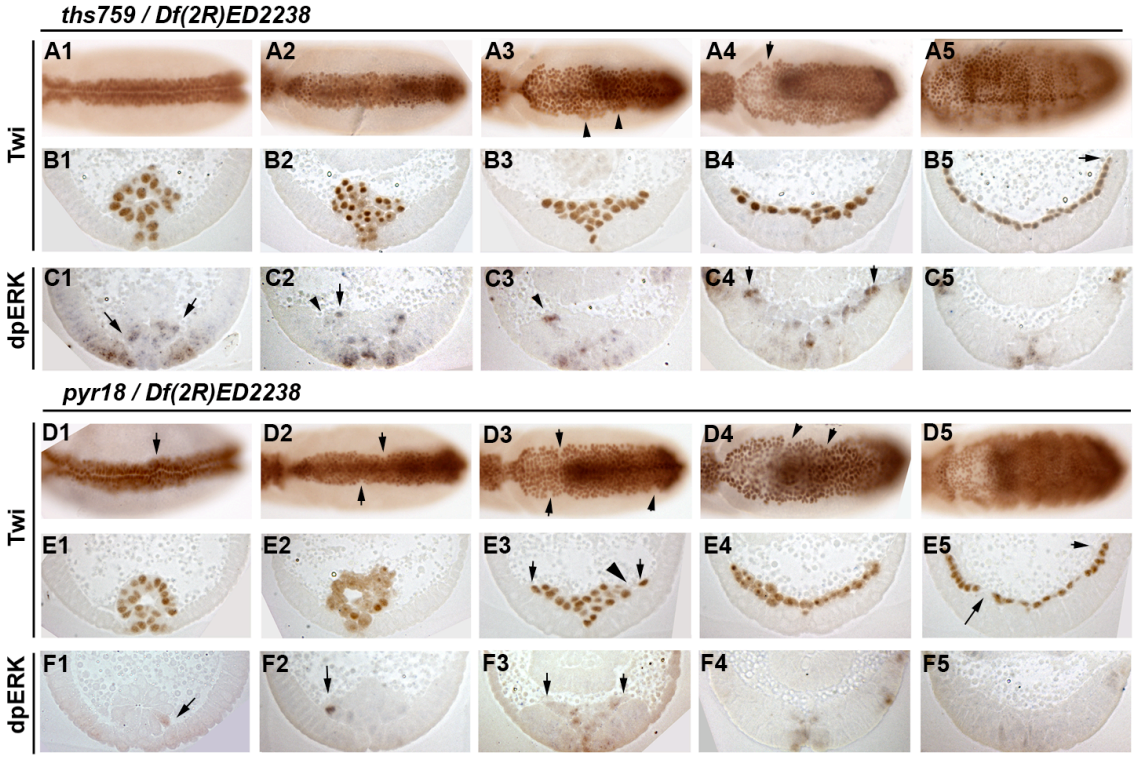

Fig. 38. Mesoderm spreading defects in ths^{759}, Df^{2238} and pyr^{18}, Df^{2238} hemizygous embryos. Embryos of the indicated phenotypes stained with anti-Twi (A,B and D,E 1-5, respectively) and anti-dpERK (C1-5 and F1-5; detects activated MAPK) shown as whole mount (A1-5 , D1-5 from ventral view; anterior is to the left) or cross section (between 40% and 60% egg length). Stages 7, 8 early, 8 late, 9 and 10 are shown in panels 1-5 each, respectively. (**A1-5, B1-5**) Embryos lacking *ths* function and one copy of *pyr* (ths^{759}/ Df^{2238}) exhibit defects in even spreading (arrows, A3) similar to ths^{759} single mutant embryos. Later positioning of mesoderm cells at the dorsal ectoderm is normal (arrow, B5). (**C1-5**) MAPK activation in ths^{759}, Df^{2238} hemizygotes is normal during initial ectoderm attachment and late phse of migration (arrows, C1 and C5), but is disturbed at the dorsal edge of the mesoderm during early migration in stage 8 (C2, C3, arrowheads mark normal activation sites) in response to reduced *pyr* dosage. (**D1-5, E1-5**) Embryos lacking *pyr* function and one copy of *ths* (pyr^{18}/ Df^{2238}) show defects in early symmetric migration (arrows in D1-4; arrows in E3 indicate dorsal edge cells, the arrowhead marks dorso-ventral discontinuity of migration) and monolayer formation (E4, arrow in E5) similar to the pyr^{18} single mutant phenotype. (F1-5) MAPK activation in pyr^{18}, Df^{2238} hemizygotes is strongly reduced at the dorsal front (F3) and irregularly asymmetric (arrows F1, F2).

In summary, both *ths*^{759} and *pyr*^{18} single mutants show defects in even spreading during early stages of migration, but normal mesoderm migration with respect to monolayer formation and Htl dependent MAPK activation, is only achieved in presence of *pyr*.

Early migration and MAPK activation is normal when at least one copy of each *ths* and *pyr* is present, as observed in *ths*^{759} or *pyr*^{18} heterozygous, *Df* ^{2238} heterozygous embryos, and *ths*^{759}, *pyr*^{18} hemizygous embryos (Fig. 39H and data not shown).

Consequently, the results indicate that both *ths* and *pyr* are required for regular, even attachment to the ectoderm as a condition for normal Pyr dependent MAPK activation during early stages of mesoderm spreading, because a single copy of *pyr* is sufficient for normal MAPK activation if *ths* function is present. Thus, the combined function of both *ths* and *pyr* is required for robust mesoderm migration.

III. 2. 2. 2 Initial MAPK activation occurs only in cells that form ectodermal contact

It is shown that ectodermal attachment and MAPK activation is disturbed in absence of FGF signalling (Beiman et al., 1996; Gisselbrecht et al. 1996; Gabay et al., 1997; Shishido et al., 1997; Michelson et al., 1998a; Vincent et al., 1998; Imam et al., 1999; Gryzik and Müller, 2004). The formation of initial contacts of mesoderm cells to the adjacent ectoderm is a crucial event in mesoderm migration and reflects the initiation of mesoderm movement. A correlation between early ectodermal attachment and FGF dependent MAPK activation is evident from mutant analysis of *htl,* and the RhoGEF *pbl*, which acts downstream and in parallel to the FGF signalling pathway (Schumacher et al., 2004; Smallhorn et al., 2004; van Impel et al., 2009). Overexpression experiments of Htl and other RTKs as Btl, EGFR, and PVR also showed a specificity of these events for FGF receptor activity.

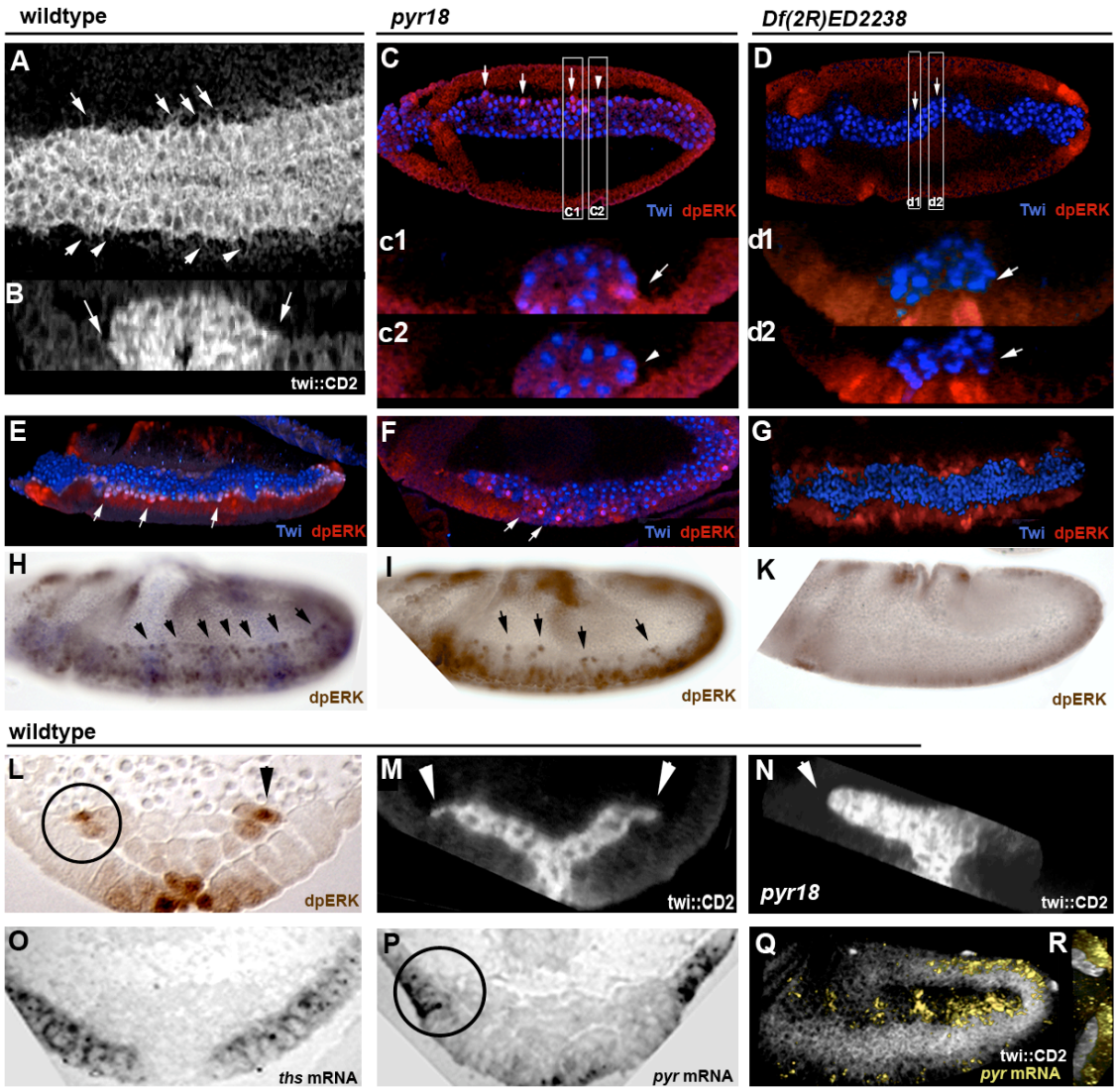

Fig. 39 Pyr is involved in initial contact establishment of mesoderm and ectoderm.
Embryos are oriented anterior to the left; dorsal is up. Proteins or transcripts analysed are indicated. **(A, B)** wild-type mesoderm tube after invagination, in optical longitudinal section (A) and cross section (B). The mesoderm cells exhibit protrusions (arrows) towards the ectoderm as they are still in formation of the invaginated tube. **(C)** *pyr*^{18} single mutant embryo from ventral; only a subset of mesoderm cells shows phosphorylated ERK (arrows); cells displaying dpERK are in contact to the ectoderm **(c1)** whereas cells lacking ERK activation are not in contact with the ectoderm **(c2). (D)** *Df(2R)ED2238* mutant embryo from ventral. ERK is not activated in the mesoderm and cells do not attach properly to the ectoderm **(d1, d2)**. **(E-G)** 3D reconstruction of wild-type, *pyr*^{18} single mutant and *Df(2R)ED2238* mutant embryos. In wild-type, mesoderm cells attach evenly to the ectoderm and MAPK is activate at the forming leading edge (arrows). *pyr*^{18} single mutants show uneven mesoderm attachment and only some cells display dpERK. In *Df(2R)ED2238* mutants lacking both *ths* and *pyr* the mesoderm does not adhere properly to the ectoderm and MAPK is not activated. **(H-K)** wild-type, *pyr*^{18} and *Df(2R)ED2238* mutants from lateral at stage 8. MAPK activation at the leading edge of the mesoderm is continuous in wild-type, but reduced in *pyr*^{18} and absent in *ths, pyr* deficient embryos. (L-P) cross sections. **(L)** Leading edge cells in wild-type show high levels of MAPk activation (arrow) and ectodermal contact (circle). **(M)** Cells at the leading edge exhibit protrusions towards the ectoderm (arrows) that are lost in absence of *pyr* **(N). (O)** *ths* is expressed in all lateral ectoderm cells. **(P, Q, R)** *pyr* is expressed in dorsal ectoderm cells according to the position of the mesoderm leading edge (circle in (P)) in early (P) as well as late (Q, R) phases of mesoderm migration.

The flattening of the mesodermal tube against the ectodermal cell layer, and MAPK activation during the initial phase at stages 6-7 are similarly induced only by the other *Drosophila* FGF receptor Btl, and are particularly dependent on Htl activation (Wilson et al., 2005). Analyses of *pyr* expression and phenotypes of pyr^{18} single mutants indicated a possible role of Pyr in this event of contact establishment and according MAPK activation. pyr^{18} single mutants thus were further analyzed to investigate whether missing MAPK activation was associated with lack of ectodermal contact.

In wild-type, protrusions indicating initial contact formation to ectoderm cells are seen prior to the disintegration of the epithelial tube (Fig. 39A, B). Similarly, at this stage and slightly after, MAPK is activated in mesodermal cells closest to the ectodermal surface (Fig. 36D1, Fig. 39E, L). Subsequently, mesoderm cells are attached to the ectoderm and show robust MAPK activation in dorsal edge cells that form protrusions towards the ectoderm as they disperse symmetrically (Fig. 39H, L, M). Both *ths* and *pyr* are expressed in the adjacent ectoderm in the phase of initial contact formation and MAPK activation (Fig. 39O, P), but only *pyr* expression is restricted to the exact region where MAPK is activated in the mesoderm during migration (Fig. 39L, P-R).

Mesoderm cells in *ths, pyr* deficient embryos never show activated MAPK and exhibit a 'snake'-like pattern indicating severely disturbed adhesion to the ectoderm (Fig. 39D, d1-2, G). The same mutant phenotype is observed in *htl* mutant embryos, and it was shown that Htl function is required for early attachment to the ectoderm (Schumacher et al., 2004). The phenotype of pyr^{18} single mutants thus represents an intermediate state between wild-type and absence of Htl signalling. dpERK is not completely absent in the mesoderm but MAPK is activated only in a subset of cells close to the ectoderm (Fig. 39 C, D, H-K).

Comparative analysis of mesodermal cells, which showed MAPK activation and those that showed a lack of staining for dpERK, revealed that the cell displaying activated

MAPK was in contact to the adjacent ectoderm (Fig. 39c1). Cells that showed no activation of MAPK in contrast were separate from the underlying ectoderm (Fig. 39c2). To establish further contact during subsequent lateral migration, dorsal edge cells of the mesoderm exhibit protrusions towards the ectoderm (Fig. 39N). These protrusions were lost in absence of *pyr* (Fig. 39N, M).

Consequently, the data show that *pyr* is involved in initial contact formation and according MAPK activation. Whether *pyr* function is rather necessary for the establishment of ectodermal contacts, or responsible for Htl dependent MAPK activation, remains to be discussed and investigated further.

III. 2. 2. 3 Cellular protrusive activity during mesoderm migration

During migration, the mesoderm cells exhibit cellular protrusions towards the ectoderm (Schumacher et al., 2004; Smallhorn et al., 2004; Murray and Saint, 2007). Cells at the dorsal front exhibit filopodia in direction of migration, and cells in rather ventral-lateral positions extend protrusions in radial direction towards the underlying ectodermal cell layer (Fig. 40, Fig. 41).

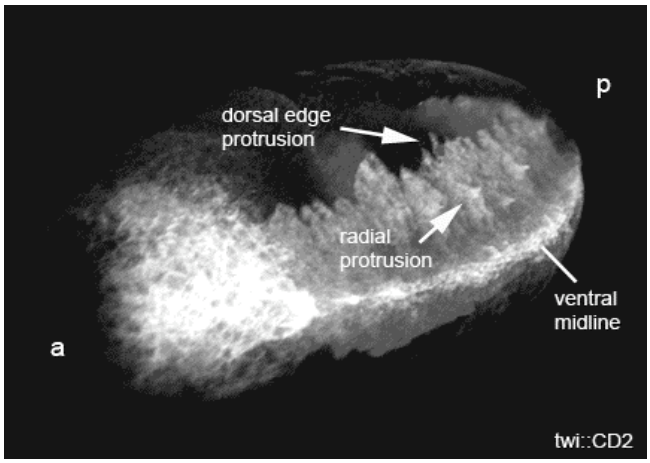

Fig. 40. Mesodermal protrusions at the dorsal edge and in radial direction.
During spreading, mesoderm cells form protrusions into direction of migration (dorsal edge protrusion) and in radial directiontowards the ectodermal substrate (radial protrusion. (a, anterior; p, posterior; ventral is to the right. Cell surfaces are visualized by antibody staining for the mesodermal membrane marker twi::CD2).

Both *ths* and *pyr* are expressed in the ectoderm during mesoderm migration and *pyr* shows dynamic expression in the dorsal region the mesodermal cells migrate towards. To investigate whether the formation of protrusions is affected by loss of *ths* or *pyr* function, mesodermal cell surfaces of mutant embryos were visualized by the transgenic marker CD2 (Dunin-Borkowski and Brown, 1995). Cells at the dorsal edge of the mesoderm were examined for cell shape changes and the formation of filopodia and lamellipodia during phases of first lateral movements (initial phase), dorso-lateral migration (early phase) and terminal dorsal positioning at the ectodermal margin (late phase) at stages 7, 8 and 9 of embryogenesis (Fig. 41A-C).

To compare the protrusion quantity and average length of mesoderm cells, protrusions were counted and measured in length using *Volocity* software (Experimental Procedures II. 4. 4, Fig. 31; Fig. 42). However, statistical tests turned out to be inappropriate to these data sets, because values vary too much between different stages of normal mesoderm spreading. To factor in stage related differences, values would have to be compared not only for each genotypic condition but also separately for the same phases of migration. Additionally, protrusion formation is a process very dynamic and the measurements were performed using fixed samples. Live imaging of GFP tagged actin filaments of a statistically reasonable number of mutant embryos could be utilised to investigate dynamic aspects of protrusion formation. Thus, the obtained data do not represent an actual quantification of mesoderm protrusions or absolute length measurements. Also, protrusion lengths here represent the distance from cell centre to protrusion tip and thus are not representing the actual length of the cellular extension as such. For this reason, 'counting' instead of 'quantification' is used as the referring term and 'extent' substitutes for 'length' in the following. Nevertheless, the data show characteristic differences in protrusion formation upon *ths* or *pyr* loss of function that are conformal with results from other mutant analysis.

The formation of dorsal edge protrusions requires *pyr* function

In wild-type embryos, the mesoderm cells exhibit dynamic filopodia during initial and early phase of migration towards lateral and dorsal directions (Fig. 41D, E). In later phase, also lamellipodia are observed, coinciding with a stretched cell shape (Fig. 41F). In embryos lacking both FGFs, no protrusions were formed during the initial phase (Fig. 41G) consistent with previous findings that ectoderm attachment was severely disturbed. At early and late phases in stages 8-10 of embryogenesis, mesoderm cells in *ths, pyr* deficient embryos only exhibited very few and short, hairy protrusions (Fig. 41H, I). The cells also did not contain any lamellipodia, and remained rounded rather than to stretch towards dorsal regions. When measured, these rudimental protrusions in *ths, pyr* deficient mutant embryos were of drastically shorter length on average as wild-type filopodia (Fig. 42 A, L). The counting of protrusions confirmed as well that the number of mesodermal protrusions was highly reduced in absence of both *ths* and *pyr*.

ths^{759} single mutants showed no differences in formation of dorsal edge protrusions compared to wild-type embryos. The mesoderm cells contained filopodia towards the ectoderm during the initial phase of lateral movement (Fig. 41K) and long filopodia during dorsal migration in early phase (Fig. 41L). According to progressive spreading, the cells were stretched in dorsal direction and showed lamellipodia and filopodia formation during the terminal, late phase of migration (Fig. 41M).

The counting of dorsal protrusions showed a normal profile of extent and amount of protrusions (Fig. 42C, L). Protrusions in direction of migration were also normal in ths^{759}, Df^{2238} hemizygous mutant embryos (Fig. 41Q-S). Thus, one copy of *pyr* is sufficient to ensure protrusive activity at the dorsal edge of the mesoderm in absence of *ths*, indicating that *ths* function is not essential for this process. Nevertheless, the counting of dorsal edge protrusions showed that the average extent of dorsal protrusions

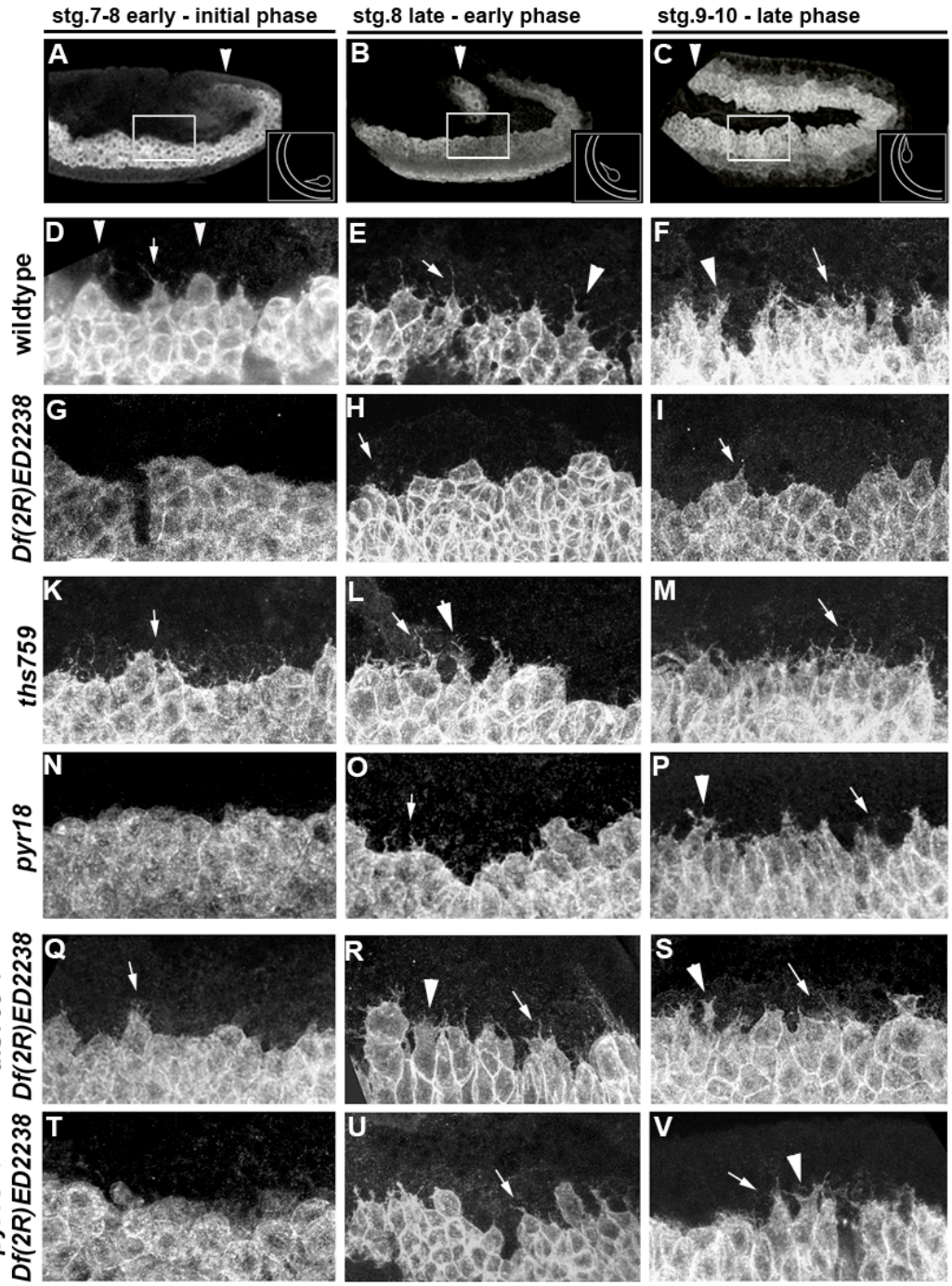

Fig. 41. Protrusive activity and shape of dorsal edge cells during initial, early and late phase of mesoderm migration in *ths*^{759} and *pyr*^{18} single mutants.

Phases of mesoderm migration and genotypes are indicated. (D-V) show magnifications of the boxed areas in A, B, and C, respectively. Arrows indicate filopodial protrusions, arrowheads indicate lamellipodial structures. **(A-C)** Initial, early and late mesoderm migration in wild-type embryos. The stage of embryogenesis is indicated by the phase of germband elongation (arrow). Cartoons at the right bottom illustrate the phase of mesoderm migration with regard to the leading edge cell. **(D-F)** Cellular protrusions of mesoderm leading edge cells in wild-type. During initial ectoderm attachment, the cells exhibit hairy filopodia and are of round shape (D). During early lateral migration, many long filopodia are discernible and the cells appear active (E). In late phase of mesoderm spreading, mesoderm leading edge cells show a dorsally stretched shape and more lamellipodia are formed (F). **(G-I)** mesoderm cells in absence of both *ths* and *pyr* exhibit only very few, thin and short filopodia and the cell shapes remain rounded. **(K-M)** *ths*^{759} single mutants show normal formation of protrusions at the leading edge in each phase of mesoderm migration. **(N-P)** In *pyr*^{18} single mutants, protrusions of leading cells are strongly reduced. Only in later phase normal protrusions are exhibited and the cells stretch in dorsal direction. **(Q-S)** *ths, Df*^{2238} hemizygous embryos show normal protrusive activity, whereas *pyr, Df2238* hemizygotes show reduced activity in formation of protrusions **(T-V)** as *pyr*^{18} homozygotes.

is reduced in *ths*^{759}, *Df*^{2238} hemizygotes (Fig. 42L). Despite the reduction in average length, protrusions were found to reach as well normal maximal extents (Fig. 42G). Thus, although one copy of *pyr* is sufficient for protrusion formation per se, the average protrusive extent is reduced at the dorsal edge of *ths*^{759}, *Df*^{2238} hemizygous embryos in comparison to wild-type. In contrast to *ths* loss of function, the deletion of *pyr* resulted in clear defects in protrusion formation at the dorsal edge. In *pyr*^{18} single mutants, mesodermal protrusions were absent during the initial phase of mesoderm spreading, and the cells maintained a rounded shape (Fig. 41N). Compared to the dorsal filopodia-rich mesoderm cells of wild-type embryos, mesoderm cells in *pyr*^{18} mutants showed only few and short protrusions towards dorsal directions during early phase of migration, and are rather comparable to *ths, pyr* deficient embryos (Fig. 41O). At this stage, the defects in protrusion formation upon *pyr* loss of function were most expressive. In absence of *pyr*, filopodia and lamellipodia were observed only during the terminal, late phase of mesoderm migration, and cells then showed a stretched shape towards the ectodermal dorsal margin (Fig. 41P). These findings show a coincidence with defects in MAPK activation and ectodermal attachment during initial and early phases that were observed previously. Thus, they substantiate the hypothesis of a connection between ectodermal contact formation and MAPK signalling events, and the requirement of *pyr* function of this pathway.

The counting of dorsal protrusions in *pyr*^{18} single mutants showed filopodia of normal extent, but a reduction of average extent of protrusions (Fig. 42E, L). This profile of *pyr*^{18} single mutants however does not clearly reflect the characteristic, phase specific defects upon loss of *pyr* function as described above. Because mesoderm cells in late phase of migration contained filopodia as wild-type mesodermal cells, the early defects are not as prominent in averaged numbers. Therefore, a separate comparison of average

values from each phase for each genotypic condition would be necessary to make statements more representative.

Similar to the phenotype of pyr^{18} single mutants, pyr^{18}, Df^{2238} hemizygotes showed defects in protrusion formation during initial and early phases of mesoderm migration (Fig. 41T, U). During late phase of mesoderm spreading, normal filopodia and lamellipodia were observed, and the cells were stretched in dorsal direction (Fig. 41V). Filopodia were present of each normal length, but short filopodia were more frequent than long filopodia, and less protrusions were formed in general compared to wild-type (Fig. 42I). Values from averaged measurements, however, are obscuring the clear defects in protrusion formation during initial and early mesoderm spreading of pyr^{18}, Df^{2238} hemizygotes, as explained for pyr^{18} single mutants.

The general formation of dorsal edge protrusions consequently is not dependent on individual *ths* or *pyr* function, because one copy of either *ths* or *pyr* is sufficient to ensure normal protrusive activity during late phase of mesoderm migration. Filopodia formation in late phase of migration is only disturbed in absence of both *ths* and *pyr*. Importantly however, *pyr* is required for normal formation of dorsal edge protrusions in initial and early phases of mesoderm spreading.

The formation of radial protrusions involves *ths* function

Radial filopodia are formed in ventral-lateral positions by cells of no defined specific position within the cell collective. Thus, radial filopodia are more difficult to characteristically image for each ths^{759} and pyr^{18} mutants. To compare radial protrusion formation in wild-type and in absence of either *ths* or *pyr*, radial protrusions were counted and measured in the same way as dorsal edge protrusions (Experimental procedures, II. 4. 4, Fig. 31). Possible stage-specific divergences within the same genotype are not regarded here as well.

A

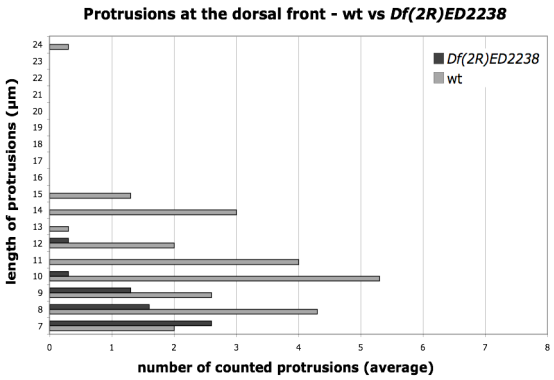
Protrusions at the dorsal front - wt vs Df(2R)ED2238
Df(2R)ED2238
wt
length of protrusions (µm)
number of counted protrusions (average)

B

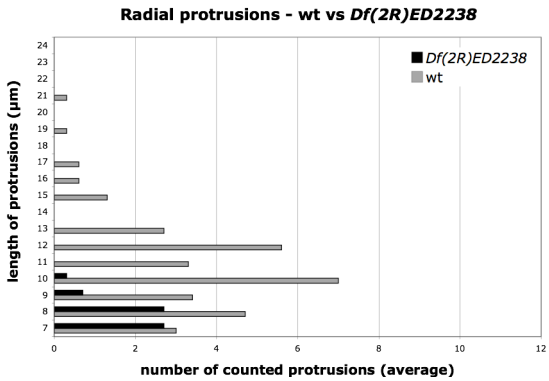
Radial protrusions - wt vs Df(2R)ED2238
Df(2R)ED2238
wt
length of protrusions (µm)
number of counted protrusions (average)

C

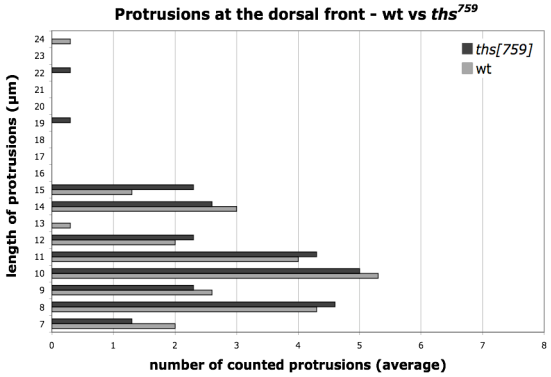
Protrusions at the dorsal front - wt vs ths759
ths[759]
wt
length of protrusions (µm)
number of counted protrusions (average)

D

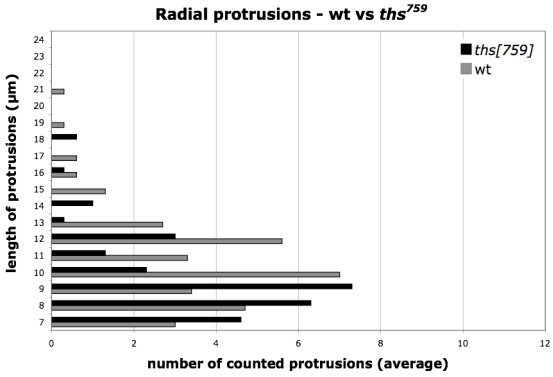
Radial protrusions - wt vs ths759
ths[759]
wt
length of protrusions (µm)
number of counted protrusions (average)

E

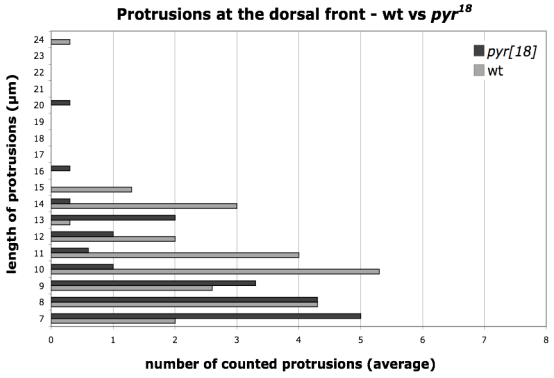
Protrusions at the dorsal front - wt vs pyr18
pyr[18]
wt
length of protrusions (µm)
number of counted protrusions (average)

F

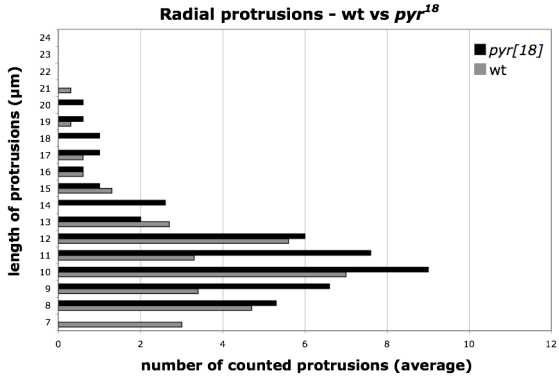
Radial protrusions - wt vs pyr18
pyr[18]
wt
length of protrusions (µm)
number of counted protrusions (average)

G

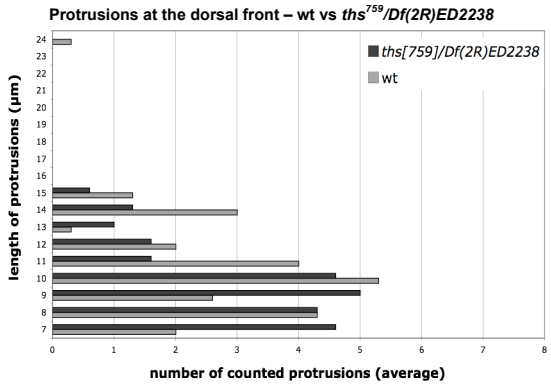
Protrusions at the dorsal front – wt vs ths759/Df(2R)ED2238
ths[759]/Df(2R)ED2238
wt
length of protrusions (µm)
number of counted protrusions (average)

H

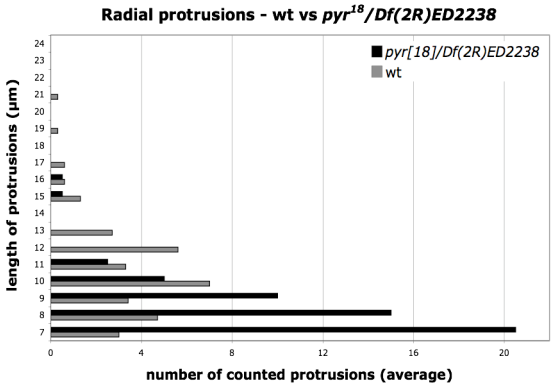
Radial protrusions - wt vs pyr18/Df(2R)ED2238
pyr[18]/Df(2R)ED2238
wt
length of protrusions (µm)
number of counted protrusions (average)

I

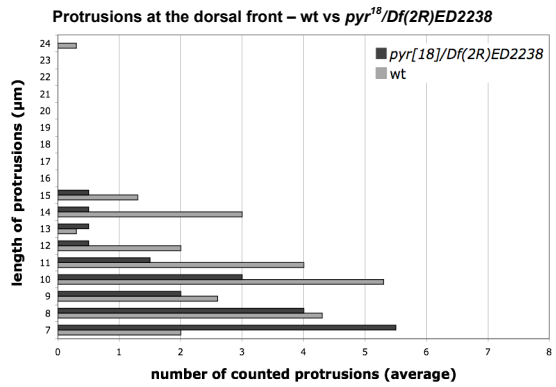

K

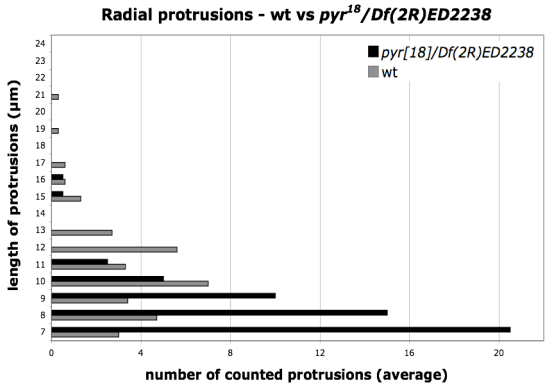

L

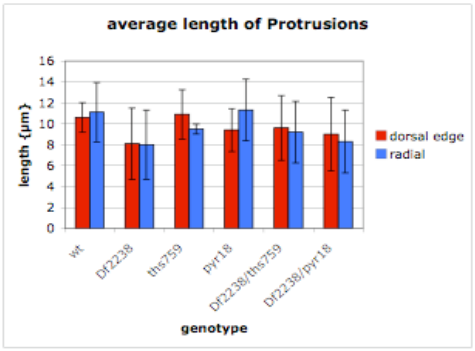

Fig. 42. Counting and length measurement of protrusions at the dorsal edge and in radial direction towards the ectoderm.
(A-K) Diagrams show the measurements of protrusions at the leading edge (dorsal front) of the mesodermal cell collective or in radial direction as indicated for each genotype in comparison to wild-type values. The diagrams display how many protrusions (x/category axis) were present at each length (y/value axis). The criteria for measurement are described in II. 6 of Experimental Procedures. **(A, B)** *ths, pyr* deficient embryos contain significantly less and shorter protrusions in dorsal as well as radial direction than wild-type embryos. **(C, D)** In ths^{759} homozygotes, leading edge protrusions are normal but in radial direction, the number of short protrusions is higher than in wild-type and long protrusions are less. **(E, F)** pyr^{18} homozygotes contain less protrusions of greater length but only protrusions of short lengths compared to wild-type; protrusions in radial direction are similar to wild-type. **(G, H)** In *ths,* Df^{2238} hemizygous embryos, the number of long protrusions at the leading edge is reduced in favour of more short protrusions in addition to the effect on radial protrusion number and length observed in absence of ths alone. **(I, K)** In *pyr,* Df^{2238} hemizygotes, the number of long protrusions at the leading edge is reduced as in pyr^{18} single mutants, but in addition the number of long radial protrusions is reduced. **(L)** Diagram displaying average values of protrusion length at the leading edge and in radial direction for each genotype. Loss of ths function shows impact on the presence of long radial protrusions, whereas loss of pyr function affects number and length of dorsal leading edge protrusions. Hemizygous embryos show combinatorial effects indicating that Ths and Pyr act non-redundant. One copy of either *ths* or *pyr* is sufficient for the formation of normal radial or leading edge protrusions, respectively. The average length however is reduced if the gene dosage is reduced in absence of the other Htl ligand.

In wild-type embryos, the counting of radial protrusion showed a similar profile of filopodia amount and extent as the protrusion counting of the dorsal edge (Fig. 42B), and also a similar average extent of filopodia (Fig. 42L). In embryos lacking both *ths*

and *pyr*, radial protrusions were drastically reduced in numbers and length (Fig. 42B). In contrast to wild-type, the average extent of filopodia was significantly shorter in *ths, pyr* deficient embryos (Fig. 42L). The protrusion counting in ths^{759} single mutant embryos showed radial filopodia of normal lengths, but more filopodia of short length were formed in contrast to reduced numbers of long filopodia (Fig. 42D). Thus, the average extent of radial protrusions is reduced in absence of *ths* (Fig. 42L).

In contrast to the defects in formation of dorsal edge protrusions, the formation of radial protrusions was not disturbed in pyr^{18} single mutants. Filopodia towards the ectoderm were neither reduced in extent nor in numbers, and the average filopodia extension in radial direction was similar to wild-type (Fig. 42F, L).

ths^{759}, Df^{2238} hemizygous embryos showed a reduced filopodia extent in radial direction (Fig. 42 I) as observed in ths^{759} single mutants. In contrast to pyr^{18} single mutants, radial filopodia were also reduced in extent in pyr^{18}, Df^{2238} hemizygous embryos (Fig. 42 K). Thus, the extent of filopodia towards the ectoderm in radial direction is disturbed only in absence of *ths* function. The measurements show that both *ths* and *pyr* are required for normal formation of radial protrusions, as only embryos lacking both *ths* and *pyr* show severe defects in this process, resulting in only few, very short protrusions. However, the formation of long filopodia requires *ths* function to be robust.

In summary, the formation of mesoderm cell protrusions in general, requires function of both Ths and Pyr (Fig. 42 L). Only embryos lacking both FGF ligands show a loss of mesodermal protrusive extension towards the ectoderm with regard to both amount and extent of protrusions. Formation of dorsal edge protrusions is dependent on Pyr function during early mesoderm spreading, whereas radial protrusion extension involves the activity of *ths*. Accordingly, ths^{759}, Df^{2238} and pyr^{18}, Df^{2238} hemizygous embryos show defects in protrusion formation in both dorsal and radial direction, as the combined

function of Ths and Pyr is required for normal protrusive activity of mesoderm cells during migration.

III. 2. 2. 4 Differentiation of mesodermal derivatives

Proper and robust mesoderm migration is the prerequisite for the formation of cardioblasts and pericardial cells, somatic and visceral muscles, and fat body (Beiman et al., 1996). The crucial parameters of this process, pertaining to the differentiation of mesodermal derivatives are the positions of the mesoderm cells relative to the inductive ectoderm, and the related time points these particular positions are populated. To investigate the impact of *ths* and *pyr* loss of function on later mesoderm development, ths^{759} and pyr^{18} single mutant embryos and *ths, pyr* deficient mutant embryos were analyzed for the expression of certain markers featuring the differentiation into particular cell types. Mesodermal derivatives including pericardial cells, cardioblasts and somatic muscles were examined for their presence and development.

The differentiation of pericardial cells requires Pyr function

The formation of the pericardial cells requires FGF signalling in mesodermal cell clusters pre- patterned by Dpp and Wg signalling from the dorsal ectoderm (Carmena et al., 1998; Tao and Schulz, 2007). In consequence of inefficient or incomplete mesoderm migration and lineage specification, pericardial cell fates and according mesodermal Eve expression are lost in *htl* mutant embryos (Buff et al., 1998; Carmena et al., 1998; Michelson et al., 1998a).

In resemblance to the *htl* mutant phenotype, mesodermal Eve expression is lost in *ths, pyr* deficient embryos and pericardial cells do not differentiate (Gryzik and Müller, 2004; Stathopoulos, 2004) (Fig. 43D).

Deletion of *ths* function has no effect on pericardial cell specification. In ths^{759} homozygous embryos, expression of the differentiation marker Eve was observed as in wild-type in all 11 cell clusters (Fig. 43A, B). In contrast, pericardial cells invariably were lost in absence of *pyr* (Fig. 43E, F). Moreover, only one copy of *pyr* was sufficient to properly ensure the formation of all pericardial cells in ths^{759}, Df^{2238} hemizygous embryos (Fig. 43C). These data indicate that differentiation of a mesodermal subset of cells to obtain pericardial cell fate is dependent on *pyr*. The expression pattern of *pyr* shows transcripts in segmental patches of ectodermal dorsal domains close to the site of pericardial progenitor specification.

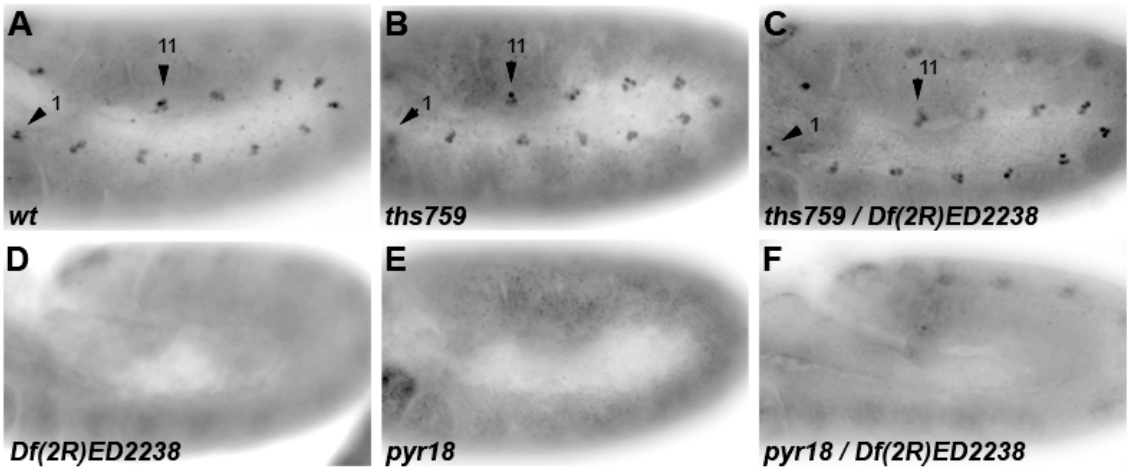

Fig. 43. *pyr* function is essential for differentiation of pericardial cell differentiation marked by the expression of Even-skipped (Eve).
Embryos at stage 10 were stained for the transcription factor Eve indicating pericardial cell fates. Anterior is to the left. **(A)** wild-type expression of Eve in 11 hemisegmental cell clusters of pericardial cell precursors (arrowheads). **(B, C)** ths^{759} homozygous (B) or hemizygous (C) embryos show normal Eve expression. (D) In *Df(2R)2238* homozygotes lacking both *ths* and *pyr*, Eve expression is absent. (E, F) pyr^{18} homozygous (E) and hemizygous (F) embryos, dorsal mesodermal precursors and correlating Eve expression are absent.

Ths is unable to substitute Pyr function in activation of Htl signalling in prospective pericardial cells, indicating that Htl signalling differentiates in Htl activation upon Ths opposed to Pyr essentially in this process.

Prior to, and accordantly with, Eve expression, dpERK is detected in the prospective pericardial cells (Carmena et al. 1998) (Fig. 44A, C). Input of both the mesodermal (i.e.

Htl) and the epidermal growth factor receptor (DER/Egfr) is required for proper differentiation of the muscle founder cell emerging from the same segmental cluster as the pericardial cells. Different to activation of MAPK in pericardial cell progenitors is dependent on Htl signalling but not on DER activation (Frasch et al., 1987; Buff et al., 1998; Carmena et al., 1998).

During mesoderm spreading, as shown above, normal MAPK activation in the mesoderm was significantly disturbed in *pyr*^{18} homozygous mutant embryos, however not completely absent (Fig. 37 D-F, Fig. 39). After mesoderm spreading is complete, MAPK normally is activated in clusters of prospective pericardial cells at the dorsal margin of the mesoderm (Fig. 44A, C). The specific segmental MAPK activation was lost in *pyr*^{18} mutants (Fig. 44B) and instead, dpERK was displayed in cell clusters of irregular shape and size (Fig. 44D).

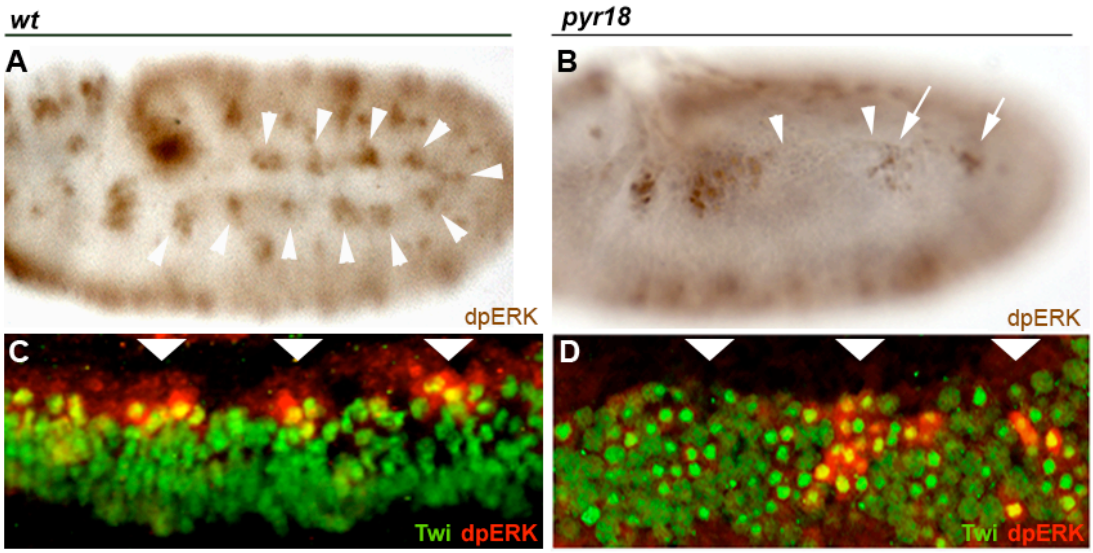

Fig. 44. Htl dependent MAPK activation in dorsal mesodermal cell clusters of prospective pericardial cell precursors requires *pyr* function.
Embryos at stage 10 were stained for dpERK (A, B) and dpERK and Twi (C, D). Anterior is left, dorsal is up; lateral view; C, D show magnifications of the dorsal edge, arrowheads mark the same positions, respectively. **(A, C)** In wild-type, dpERK is displayed in cell clusters of prospective pericardial cells in a segmental pattern. Only a subset of cells of the very dorsal mesoderm show activated MAPK. **(B, D)** In absence of pyr, the pattern of dpERK is disturbed and segmental cell clusters displaying dpERK are not present. Instead, cells randomly in larger clusters that extend beyond the dorsal edge display dpERK. The remaining MAPK activity is likely in response to Efgr signalling, which normally specifies dorsal muscle progenitors.

These clusters of cells displaying high levels of dpERK, occurred in dorsal regions of the mesoderm but were not restricted to the dorsal margin as in wild-type. Cells in more ventral positions that were included or separate from these clusters, also showed activation of MAPK. In these clusters, MAPK activation might occur in response to DER signalling in muscle progenitors, because pericardial cell fates that require Htl mediated MAPK signalling are lost in pyr^{18} mutants completely,.

These results indicate that the observed defects upon *pyr* deletion are related to impaired Htl signalling concerning the subsequent activation of the Ras/MAPK signalling cascade. The other Htl ligand *Ths* has no effect on MAPK activation in mesoderm cells and cannot substitute for loss of Pyr mediated Htl signalling. Thus, during migration and differentiation of pericardial cell progenitors, Htl dependent MAPK activation in the mesoderm depends on *pyr* function.

Both *ths* and *pyr* are individually involved in progenitor differentiation of heart and somatic muscles

A subset of mesoderm cells in each segment provides the progenitor cells of the somatic musculature and the heart (Azpiazu and Frasch, 1993; Taylor et al., 1995; Azpiazu et al. 1996; Dunin-Borkowski et al., 1995). The transcription factor Myocyte enhancing-binding factor 2 (Mef-2) is essential for terminal differentiation of these muscle cell types and is specifically expressed in all muscle progenitors, including the heart precursers (Bour et al., 1995; Nguyen and Xu, 1998) (Fig. 45A-D). Mef-2 also represents a key regulator of a large number of transcription factors, many of which are involved in early aspects of myogenesis (Sandmann et al., 2006 and 2007).

It was shown that loss of Htl function leads to strongly reduced numbers of Mef-2 expressing mesodermal cells, causing loss of heart precursors and severe defects in

muscle progenitor formation and further muscle development (Gisselbrecht et al., 1996; Michelson et al., 1998a and 1998b).

To investigate the effects of and loss of function mutations on muscle development, mutant embryos were stained for Mef-2 at stages 12, 13 and 15 to follow the formation of muscle progenitors and cardioblast precursors (Fig. 45). The resulting effects on later differentiation of the somatic musculature and dorsal vessel were examined by antibody stainings against the muscle specific protein Myosin heavy chain (Mhc) at stage 16/17 of embryogenesis (Fig. 46).

Deletion of both *ths* and *pyr* results in loss of progenitors

ths, pyr deficient embryos showed severe defects in formation of muscle progenitors, and showed a similar phenotype as *htl* mutant embryos. Similar defects were also observed in embryos mutant for the larger deficiency *Df(2R)BSC25* removing 200kb including both FGF genes (Stathopoulos, 2004).

In absence of both *ths* and *pyr,* the formation of the characteristic pattern of heart and muscle precursors was evidently disturbed (Fig. 45E, F). Heart precursors were probably formed initially (Fig. 45F) but lost during further development, so that the tubular alignment of cardioblasts was never achieved in *ths, pyr* deficient embryos (Fig. 45G). Stainings against Tin, which highlights mesodermal heart precursors showed a similar phenotype of highly disorganized mesodermal cells at stage 12 (Fig. 45F, small window) and loss of dorsal mesodermal structures in later embryogenesis (Beiman et al., 1996; Gisselbrecht et al., 1996; Shishido et al., 1997). Ventral regions in *ths, pyr* deficient mutants contained Mef-2 expressing mesoderm cells, but the stereotypic pattern of muscle progenitors was lost like in the dorsal domains (Fig. 45H). The developing muscles in mutant embryos lacking both *ths* and *pyr* were misshaped in consequence to the severe disruptions of cell fate commitment to muscle and heart

progenitors and general morphogenesis (Fig. 46B, B'). The loss of all specific mesodermal structures in dorsal and ventral regions consequently makes the formation of the dorsal vessel or the ventral oblique muscles impossible and all dorsal structures were absent in these embryos (Fig. 46H).

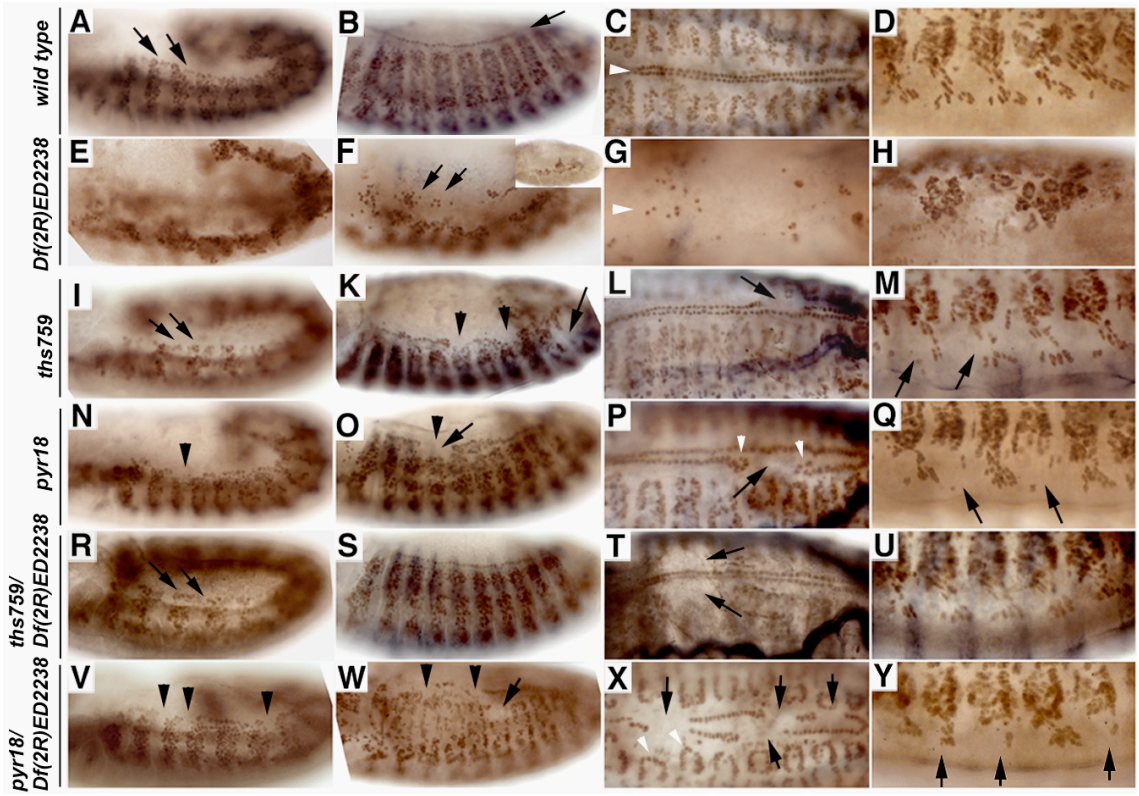

Fig. 45. Defects in somatic and cardiac muscle progenitor formation in *ths*^{759} and *pyr*^{18} mutant embryos and in absence of both *ths* and *pyr*.
Embryos at stage 12 (left column), stage 13/14 (left middle column) and stage 16 (right columns) were stained for the transcription factor Mef-2 highlighting specified heart and somatic muscle progenitors. Left columns show lateral views, the right columns show dorsal and ventral sections. Genotypes are indicated. **(A-D)** Wild-type pattern of cardiac and somatic muscle cell nuclei. The cardioblasts align at the dorsal midline in two parallel rows (C). Stereotypical pattern of ventral muscle progenitors (D). **(E-H)** in absence of both *ths* and *pyr*, the formation of somatic muscle progenitors is disrupted. Cardioblsts are probably specified (F, arrows) but the prospective heart is not formed (G). Ventral structures are absent (H). **(I-M)** *ths*^{759} homozygotes show normal pattern in early stages (I, arrows) but lack of Mef-2 positive nuclei in later stages (arrowheads and arrow in K). Some segments failed to specify heart precursors (arrow in L). Ventral progenitors are missing from segments (arrows in M). **(N-Q)** *pyr*^{18} single mutants show early defects (arrowhead in N) and lack Mef-2 positive nuclei in single segments (arrowhead and arrow in O). (P) The alignment of cardioblasts is disrupted, heart precursors are missing (arrow), or displaced (white arrowheads). (Q) Muscle progenitors are missing ventrally. **(R-U)** In *ths, Df* ^{2238} hemizygotes, most Mef-2 positive mesoderm cells are present as in wild-type. Some segments however show missing dorsal muscle progenitors (arrows in T). **(V-Y)** *pyr*^{18}*, Df* ^{2238} hemizygous embryos show missing Mef-2 positive nuclei in highest penetrance compared to the other genotypes. Cardioblast specification fails in early stages (arrowheads in V). Mef-2 positive progenitors are missing in dorsal, lateral and ventral positions (arrows in W-Y). Cardioblasts fail to align (X) but dorsal muscle progenitors are present (white arrows in X).

Both *ths*^{759} and *pyr*^{18} single mutants show defects in progenitor differentiation

To be expected from previous analyses described above, *pyr* loss of function caused defects of higher penetrance and expressivity in differentiation of mesodermal derivates. *ths*^{759} single mutants showed differentiation defects of heart and muscle formation from stage 13 of embryogenesis. Heart precursors failed to differentiate in some segments (Fig. 45K), resulting in defects of the tubular arrangement of cardioblasts (Fig. 45L). Strikingly, the incidence of failed precursor differentiation during stages 12-15 did not translate into defects of heart development in later stages 16/17 (Fig. 46I).

Progenitors of the segment border muscle (SBM) were duplicated but never missing in *ths*^{759} single mutants (Fig. 47F), and resulted in formation of two SBM fibers in later stages (Fig. 47 and Table1 in appendix 1). The lateral and ventral muscle progenitors of the lateral transverse muscles LT1 and 2 and ventral oblique muscles VO4-6 occasionally were missing in *ths*^{759} homozygous embryos (Fig. 45K, M), and loss of respective muscle formation was observed in later stages (Fig. 46C, C' and data not shown; Table 1, appendix 1). The defects in progenitor formation, however, could not be defined to occur in a particular region or pattern within the arrangement mesodermal progenitor cells or the derivative muscles.

First analysis of *ths*^{759}, *Df*^{2238} hemizygous mutant embryos showed, surprisingly, a very low penetrance of defects in differentiation of muscle progenitors. Cardioblast specification and heart development was normal in all examined embryos (Fig. 45T, Fig. 46L). Occasionally, progenitors of dorsal muscle groups were not developed in singular segments in *ths*^{759}, *Df*^{2238} hemizygotes (Fig. 45T), but defects were observed at higher penetrance in development of the SBM (Fig. 47G) and ventral oblique muscles VO4-6 (Table 1, appendix 1). Nevertheless, the reduced expressivity of defects in progenitor formation compared to *ths*^{759} single mutants is surprising

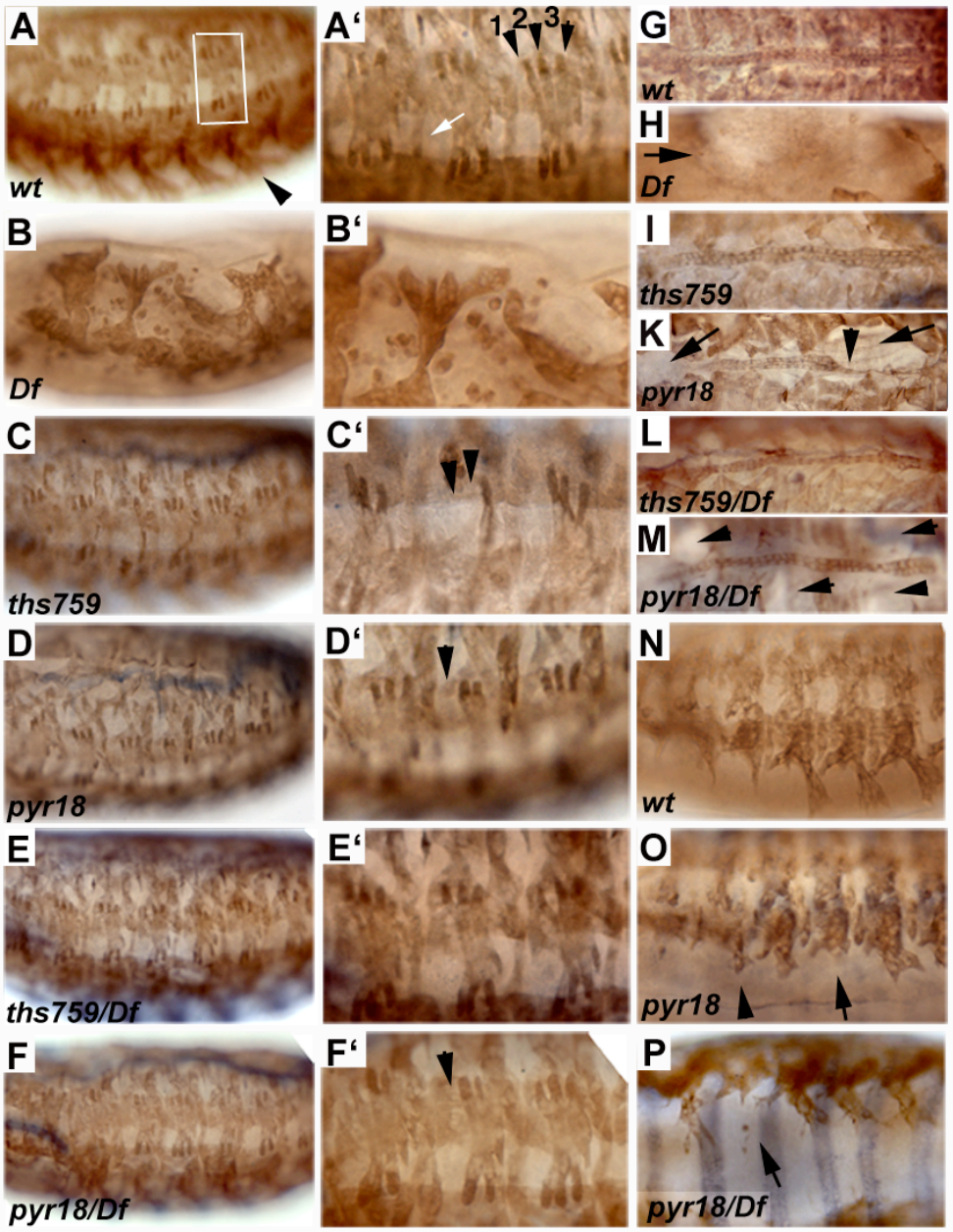

Fig. 46. Requirement of FGF ligands Ths and Pyr for the differentiation of the dorsal vessel and specific subgroups of somatic muscles.

Myosin heavy chain (Mhc) staining showing somatic muscles in stage 17 embryos. Genotypes are indicated. Lateral views in left and middle column, the middle column shows magnifications of three consecutive segments, respectively. Highlighted are the lateral transverse muscles LT1-3. (G-M) dorsal sections showing the dorsal vessel (heart). (N-P) ventral sections showing defects in ventral oblique muscles VO4-6. **(A, A')** pattern of somatic muscles in wild-type embryos. In each segment, LT1-3 are prominent (arrows). **(B, B')** In absence of both *ths* and *pyr*, the somatic muscles are without structure. **(C, C')** ths^{759} single mutants show missing LT1 and 2 muscles (arrowheads). **(D, D')** pyr^{18} single mutants fail to form LT1 (arrowhead). **(E, E')** ths^{759}, Df^{2238} hemizygotes show lower penetrance of defects in somatic muscle formation. **(F, F')** pyr^{18}, Df^{2238} hemizygotes show similar phenotypes as pyr^{18} single mutants. LT1 is missing from some segments. **(G)** wild-type dorsal vessel. The dorsal muscles show stable attachment in each segment. **(H)** the vessel is absent in *ths, pyr* deficient embryos. **(I)** ths^{759} homozygotes show normal formation of the dorsal vessel. **(K)** in pyr^{18} single mutants, the vessel shows defects (arrowhead) and dorsal muscles fail to develop in some segments (arrows). **(L)** ths^{759}, Df^{2238} hemizygotes show normal formation of the dorsal vessel. **(M)** one copy of *ths* is sufficient for formation of the dorsal vessel, but dorsal muscles fail to form or detach (arrows). **(N)** wild-type ventral muscles. Ventral VO4-6 form only from segment t1-t9. pyr^{18} homozygous embryos show defects in ventral muscle formation **(O)** the expressivity and penetrance of which is increased in pyr^{18}, Df^{2238} hemizygous embryos **(P).**

Previous experiments never showed a rescue from defects that occur upon deletion of *ths* function by the chromosome of Df^{2238}. ths^{759}, Df^{2238} hemizygotes rather exhibited defects similar to ths^{759} homozygotes but of higher penetrance and defects in response to reduction of *pyr* copies (as described above for mesoderm spreading, protrusion formation and MAPK activation). Hence, these findings indicate a possible involvement of Pyr levels in absence of *ths*. Alternatively, the data could suggest a second mutation on the chromosome of ths^{759} outside of the deleted region of *Df(2R)ED2238*. In case of a second mutation, the affected allele but not ths^{759} would be responsible for the observed defects in the ths^{759} homozygous condition, however only with regard to differentiation of specific muscle cell fates.

In absence of *pyr*, embryos exhibited a higher penetrance of defects during muscle development than upon *ths* loss of function. Compared to 22% of ths^{759} homozygotes, 38% of all examined embryos mutant for pyr^{18} showed missing progenitor cells, over 50% of which were heart precursors. These failed to differentiate at earlier stages than in ths^{759} homozygotes (Fig. 45I, N), and pyr^{18} single mutants showed defects in formation of cardioblasts (Fig. 45P) and the dorsal vessel in later stages (Fig. 46K).

Progenitors from dorsal and ventral positions were occasionally lost (Fig. 45O, Q) and consequently, defects were observed in respective muscle development of the dorsal muscles DO1-2 and DA1-2 and ventral muscles VO4-6 in individual segments (Fig. 46K, O). Similar to *ths* homozygotes, lateral muscles LT1 were not developed in some segments (Fig. 46D, D'), however only LT1 (contrary to LT1 and 2) was missing in pyr^{18} homozygotes. In conlusion, deletion of *pyr* function causes occasional defects in differentiation of heart and somatic muscles of all groups of progenitors, but the defects occur in no specific pattern of affected segments or progenitor groups.

pyr^{18}, Df^{2238} hemizygous embryos exhibited a similar mutant phenotype in muscle development as described for pyr^{18} homozygotes, but defects were more penetrant and

did affect more segments within a single embryo (Fig. 45V-Y, Fig. 46M). 42% of all examined hemizygotes showed severe defects during cardioblast formation (Fig. 45X). These defects might lead to an arrest in embryonic development, because the analysis of embryos at later stages did not reveal undeveloped or misshaped dorsal vessels (Fig. 46M).

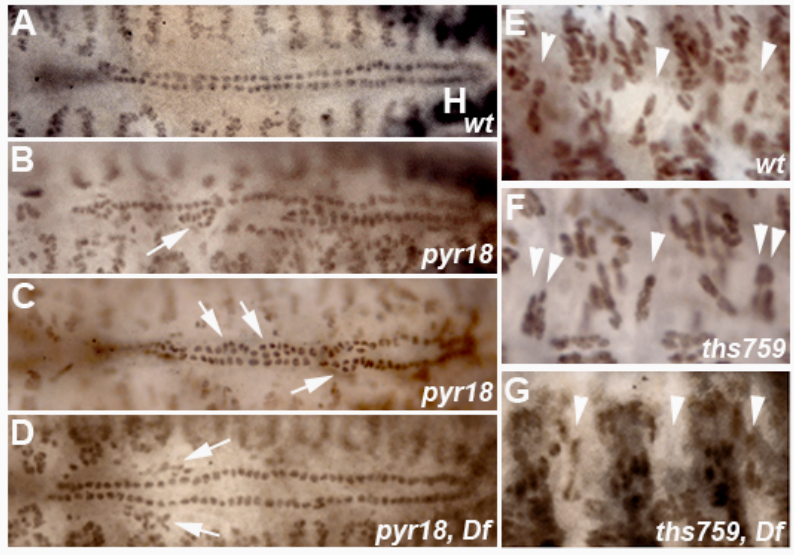

Fig. 47. Additional cardioblast formation and defects in formation of segment border muscle (SBM) progenitor differentiation.
Dorsal (A-D) and lateral (E-G) sections of embryos stained for Mef-2 displaying cardioblasts (A-D), and SBM progenitors in three consecutive segments. Defects in heart formation are highlighted for pyr^{18} mutants and defects in SBM progenitor formation are highlighted for ths^{759} mutants, because the respective phenotypes were most expressive and penetrant in absence of *pyr* or *ths*, respectively. **(A)** wild-type alignment of cardioblasts. **(B-D)** in absence of *pyr*, also additional cardioblasts (arrows) are discernible and misalignment (B) of the normal parallel rows. Cardioblasts are found within (C) or outside (D) of the normal structure representing the prospective vessel. **(E)** wild-type progenitor pattern of SBM at the border of each segment (arrowheads). **(F, G)** in absence of *ths*, SBM formation is disturbed. Several segments show duplication of SBM progenitors (F), but the progenitors are also lost (G).

Dorsal, lateral and ventral muscle cell fates were also affected in pyr^{18}, Df^{2238} hemizygotes and progenitors and the corresponding muscles failed to differentiate in some segments (Fig. 45W, Y and Fig. 46F, F', M, P). The analysis of pyr^{18}, Df^{2238} hemizygotes shows that one copy of *ths* in absence of *pyr* is not sufficient for normal differentiation of heart and somatic muscles and defects are more severe than in pyr^{18} embryos, which carry two copies of *ths* in absence of *pyr*. The increase in expressivity as well as in penetrance of differentiation defects thus is the result of altered *ths* dosage

and further supports the idea that *ths*^{759}, *Df*^{2238} hemizygotes show a phenotype related to reduced *pyr* dosage, as opposed to a second unidentified mutation.

In summary, *ths* and *pyr* both are required for heart and somatic muscle differentiation, but are not involved in formation of specific muscle groups. Imperfect mesoderm migration in *ths*^{759} and *pyr*^{18} single mutants suggests defects in rather dorsal somatic muscle and heart differentiation. Defects occur but as well in lateral and ventral positions independent of dorsal cell fates (Fig. 45M, Q, Y, Fig. 47G). Further more, loss of *ths* or *pyr* function not only results in failure of differentiation of cardioblasts or muscles, and their progenitors. *pyr*^{18} mutants characteristically also showed increased numbers of heart precursors (Fig. 47C, D). Disorders of the tubular pattern further suggest defects in positioning of the heart precursors subsequent to normal differentiation of cardioblasts (Fig. 45P, 47B). SBM formation defects as well include both loss and duplication of the SBM, with the exception of *ths*^{759} single mutants where only a duplication of SBM was observed (Fig. 6 and Table1, Klingseisen et al., 2009, appendix 1). Whereas *ths*^{759}, *Df*^{2238} hemizygotes showed less defects in dorsal and ventral muscle differentiation, defects in SBM formation occurred at highest penetrance in these embryos compared to *ths*^{759} and *pyr*^{18} single mutants and *pyr*^{18}, *Df*^{2238} hemizygotes. Thus, the results indicate that differentiation of heart and somatic muscles requires distinct levels of both Ths and Pyr mediated Htl signalling during progenitor formation in general rather than specific.

Conclusions of part III. 2

The gene expression pattern of the FGF ligands *Ths* and Pyr suggested redundant as well as individual functions during embryogenesis. Analysis of effects upon deletion of *ths* and *pyr* on mesoderm development shows confirming results and conclusions.

Mesoderm spreading, protrusive activity and differentiation of heart and somatic muscles require the combined function of both *ths* and *pyr* and indicate supporting functions rather than substitutable roles in regulation of dynamic processes. The experiments also showed that expressivity and penetrance of defects alter with gene dosage of one FGF in absence of the other. Embryos heterozygous as well as hemizygous for ths^{759} and pyr^{18} showed defects in respective processes at low, only slightly increased percentages as wild-type embryos (2%-5% compared to 0%- 2,4% in wild-type, on average). Thus, *Ths* and Pyr act redundantly in Htl mediated signalling, as phenotypes of single mutants were always less severe than the *ths, pyr* deficient condition, and in presence of both FGF ligands, the ratio of gene dosage is not vital. However, single mutant analysis of mesoderm development also revealed a stronger dependence on *pyr* function in general, as defects in *pyr* single mutants were of higher penetrance and expressivity.

Early protrusive activity of migrating dorsal edge cells depends on *pyr* function, whereas *ths* is sufficient in absence of *pyr*, but not essential for the formation of radial protrusions. Moreover, *pyr* individually is required for initial and later robust MAPK activation and the presumably related formation of initial ectodermal contacts during mesoderm migration. Further, the differentiation of pericardial cells depends on activation of Htl mediated Ras/MAPK signalling exclusively by Pyr. Conclusively, both *ths* and *pyr* are required for normal mesoderm development, and despite a larger dependence on *pyr* function, both Htl ligands Ths and Pyr are essential for *Drosophila* development beyond the larval stage.

III. 3 Effects of ectopic over-expression on mesoderm development

Another powerful way of determining gene function is the expression in cells in which it is not normally active. In addition to loss-of-function experiments, effects upon gain-of-function were analyzed in overexpression studies of mesoderm migration and differentiation. Using the UAS-Gal4 system (Experimental Procedures, II. 4. 3, Fig. 28; Brand and Perrimon, 1993), overexpression of *ths* and *pyr* was performed ectopically in all mesodermal cells as well as in ectodermal domains.

The transcripts of both *ths* and *pyr* show a dynamic expression pattern that is dynamically modified during embryonic development. With emphasis on *pyr*, mesoderm spreading and differentiation are expected to be disturbed in consequence to ectopic expression of the Htl ligands, as temporal and positional information is no longer provided correctly.

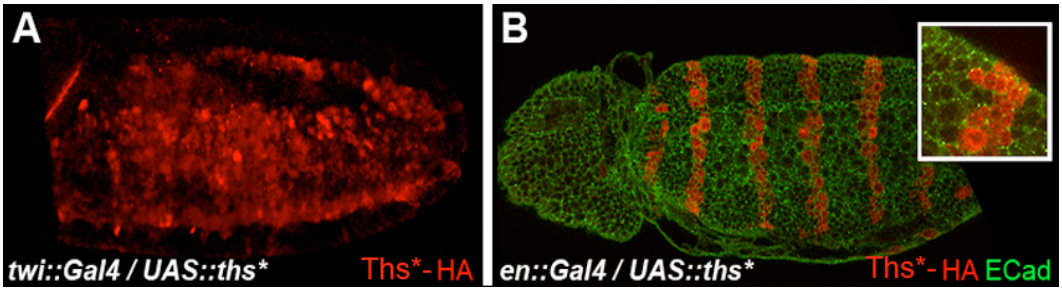

Fig. 48. Transgenic overexpression of ths* in all mesoderm cells (A) and in epidermal stripes (B).
Expression of the transgene *ths** under control of the *twi* promotor in the mesoderm **(A).** The staining is restricted to the expressing cells. **(B)** Expression of *ths*-HA* in ectodermal stripes. The stainings shows that the protein is only present in expressing cells. The localisation of Ths*-HA appears cytoplasmic as well as cortical (boxed magnification).

III. 3. 1 Htl activation of Ths is dependent on conserved amino acids of the FGF core domain

Ectopic overexpression of *ths** in all mesoderm cells (*twi >ths**) (Fig. 48A) caused only minor defects during mesoderm spreading. *twi >ths** expressing embryos showed

normal collapse of the mesodermal tube and subsequent ectodermal attachment, and dorso-lateral migration was even and symmetric (Fig. 49E1-3, F1, G1). However, during early stages of mesoderm spreading, the mesoderm showed no definition of ventral most positions aligned above the ventral midline. In wild-type, the mesoderm cells on the ventral midline are located in ventral-most positions within the mesoderm

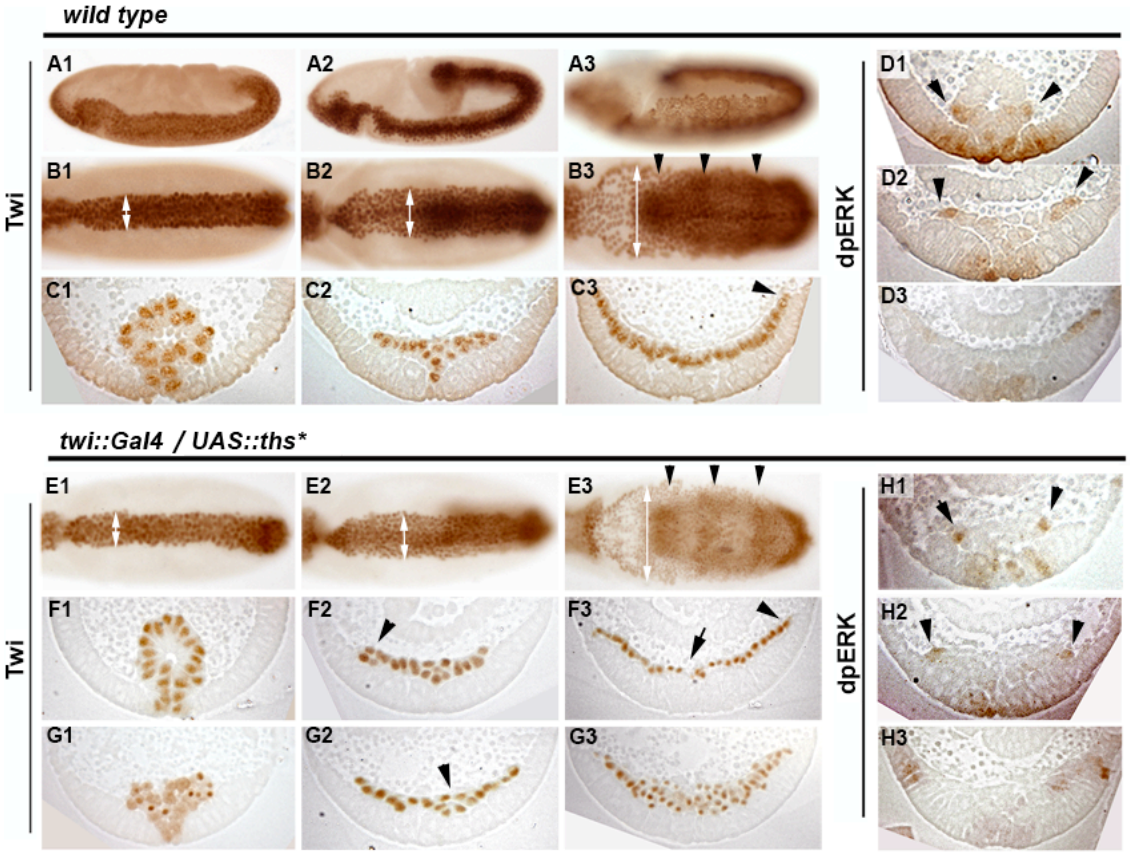

Fig. 49. Mesoderm spreading defects in embryos after uniform expression of *ths in all mesoderm cells.**
Embryos of the indicated phenotypes stained with anti-Twi (A-C and E-G, 1-3, respectively) and anti-dpERK (D1-3 and H1-3; detects activated MAPK) shown as whole mount (A1-3, B1-3, E1-3 from ventral view; anterior is to the left) or cross section (between 40% and 60% egg length). Stages 7, 8 and 10 are shown in panels 1-3 each, respectively. **(A-D)** Wild-type. White double arrows in B1-3 show the even extension of the mesoderm domain during spreading. The expression of Twi formss segmental crescents (arrowheads in B3). Mesoderm cells acquire dorsalmost positions relative to the ectodermal margin (arrowhead in (C3)). **(D1-3)** MAPK is activated at the leading edge (arrowheads). **(E-H)** expression of *ths** under control of the *twi* promotor. (E1-3) mesoderm spreading proceeds normal upon overexpression of *ths** (white double-arrows). The crescents of *twi* expression are enhanced (arrowheads). **(F1-3, G1-3)** The mesoderm tube collapses normal. Ectodermal attachment is disturbed during early migration and the ventralmost cells at the ventral midline are not positioned (F2, G2). Locally mesoderm cells form clusters (arrowheads). (F3, G3) Monolayer formation shows defects upon ths* overexpression. Respective to the position along the anterior-posterior axis as indicated in E3, the mesoderm is multilayerd (G3) or shows missing cells at ventral positions (arrow in F3). The cells acquire dorsal-most positions as in wild-type (arrowhead in F3). **(H1-3)** MAPK activation at the leading edge is unaltered, and dpERK is not displayed in mesoderm cells expressing *ths** in other positions.

collective after tube collapse, and reside above two mesectodermal cells within the ectodermal cells layer (Fig. 49C2). Dorsal-lateral mesoderm cells start to migrate away from the site of invagination, but ventral midline cells hardly change their positions during mesoderm spreading (Murray and Saint, 2007).

These ventral midline cells were not defined in *twi >ths** expressing embryos and early dorso-lateral spreading appeared regular but not related to a central position (Fig. 49F2, G2). In wild-type, *ths* is expressed during the early stage of mesoderm spreading in the lateral ectoderm, and the domain of expression shows a sharp and distinct border to the most ventral ectoderm cells (S4 in appendix 1). The positional information that might be generated by the distinct expression domains presumably is lost when not only lateral, but also ventral mesoderm cells are exposed to *Ths*.

Despite the ventral disturbed positional information in *twi >ths** embryos, dorsal spreading was normal during later phase and dorsal positions at the ectodermal edge were covered by mesoderm cells (Fig. 49E3, F3). However, embryos expressing *ths** in the mesoderm showed a more prominent segmental organization of mesoderm cells subsequent to complete spreading (Fig. 49B3, E3). Monolayer formation was disturbed, as the mesoderm was unevenly composed of cellular multi-layers in alteration with imperfect monolayered regions (Fig. 49F3, G3).

Overexpression of *ths**, strikingly, had no influence on MAPK activation because, as in wild-type, only cells at the dorsal front showed high levels of dpERK (Fig. 49H1-3, Fig. 50C). Conclusively, overexpression of *ths** does not fundamentally intervene in Htl signalling during mesoderm spreading, as occurring defects in *twi >ths** expressing embryos are only minor and *ths** is not able to trigger MAPK activation ectopically. *twi >ths** overexpression was also not affecting later mesoderm pericardial cell differentiation from dorsal mesoderm cells. The domain of MAPK activation in prospective pericardial cell clusters was defined as in wild-type embryos (Fig. 50B,D)

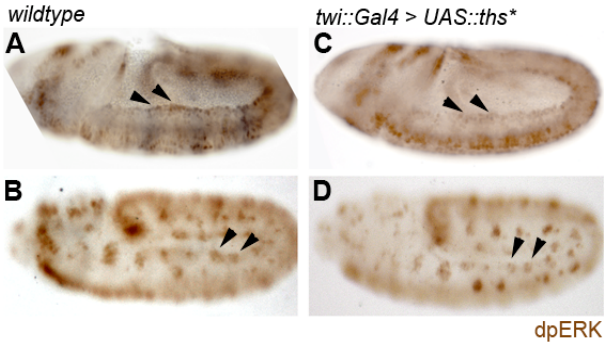

Fig. 50. Early and late MAPK activation in mesoderm cells is unaltered in embryos upon transgenic expression of *ths in the mesoderm**
Embryos at stage 8 (A, C) and stage 10 (B, D) stained for dpERK; lateral views. Genotypes are indicated. **(A, B)** wild-type embryos display dpERK in leading edge cells (arrowheads). (B) At stage 10, MAPK is activated in prospective pericardial cell clusters at the dorsal margin**. (C)** The exclusive activation of MAPK at the leading edge is unaltered upon pan-mesodermal expression of *ths**. **(D)** dpERK is displayed as in wild-type in segmental clusters of prospective pericardial cells in embryos over-expressing *ths**.

and consequently, the differentiation marker Eve was expressed in 2-5 cells per cluster as in wild-type embryos (Fig. 51A, B). Pericardial cell fates are also not affected by ectodermal overexpression under control of the *dpp* or *en* promotor (data not shown), or by overexpression of *ths** in combination of mesodermal and ectodermal expression domains using *prd::Gal4* (Fig. 51C, D). Segmental expression in the ectoderm using *en::Gal4* further showed that transgenic Ths* localization was sharply restricted to the cells of the *en* expression domain (Fig. 48B), suggesting that its signalling range only includes the cells expressing the allele *ths**.

Despite normal pericardial cell differentiation, single pericardial cell fates could be rescued upon additional ectopic *ths** expression in a *ths, pyr* deficient background (Fig. 51D, F). The single mutant analysis of ths^{759} showed that *ths* is dispensable for Htl dependent MAPK activation and pericardial cell differentiation, thus the results from *ths** overexpression experiments were not considered being controversial.

Data from others contradict these results. Mesodermal overexpression of *ths* was able to trigger MAPK activation in all mesoderm cells (Stathopoulos et al, 2004). It was also shown that mesodermal as well as ectodermal ectopic expression results in increased numbers of pericardial cells, even in absence of both *ths* and *pyr* (Kadam et al., 2009). For this reason, the transgenic allele *ths** was in doubt to represent a perfectly functional allele of *ths*.

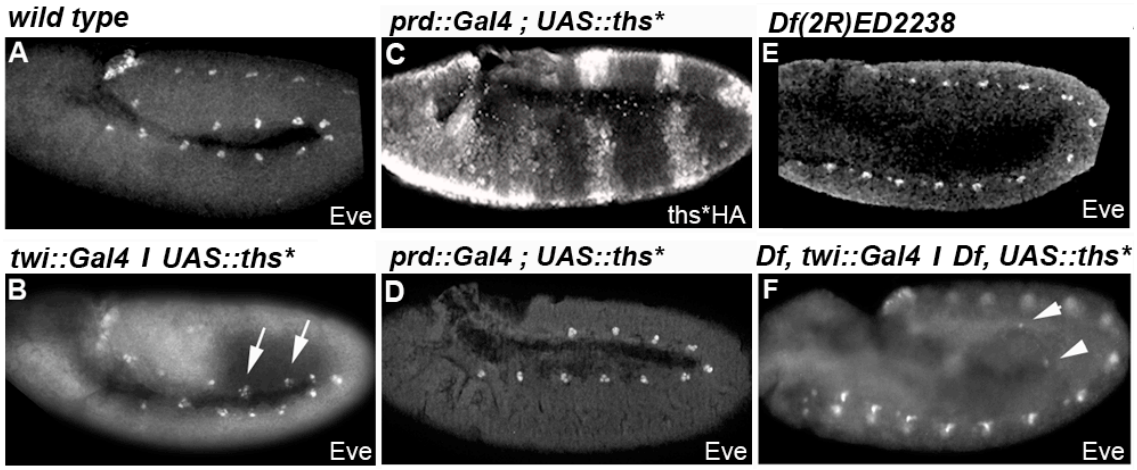

Fig. 51. The differentiation of dorsal mesoderm derivatives is unaltered upon over-expression of *ths*.*
Embryos stained for Eve (A, B, D-F) at stage 10. Staining for HA of an embryo ectopically expressing ths* in stripes under control of the *paired* (*prd*) promotor. Lateral views, genotypes are indicated. **(A)** 11 Eve positive clusters are segmentally formed in wild-type. **(B)** The expression of *eve* and the number of Eve positive mesoderm cells remains unaltered despite pan-mesodermal expression of *ths**. **(C, D)** Ectopic expression of ths* in ectodermal domains (C) has no effect on pericardial cell specification (D). In a *ths, pyr* deficient background, mesodermal over-expression of *ths** results in a rescue of only single mesoderm cells expressing *eve* **(F).** Ths* is not able to rescue the loss of pericardial cell fates in absence of endogenous *pyr* **(E, F).**

The sequence of *ths** was obtained by sequencing of cDNA cloned from RT PCR on RNA probes for the predicted gene *CG12443* (Gryzik and Müller, 2004). The annotation of *CG12443* in *flybase* at this point was substantially different from the newly discovered sequence of *FGF8-like1* (*ths*), therefore a revision of the *ths** coding sequence was not considered. Comparative sequence alignment of *ths** and the present *flybase* annotation, which was changed twice since discovery of the FGF gene, revealed 4 point mutations which all result in amino acid exchanges within the FGF core domain of Ths (Fig. 52). One of these point mutations leads to an exchange of a conserved amino acid that was found to be identical in all FGFs (Gryzik and Müller 2004). Consequently, the transgenic allele analyzed presumably provides a template for a mutated protein Ths* that might not able to normally activate Htl signalling. The defects upon *ths** overexpression in monolayer formation during mesoderm spreading and the ability to rescue single pericardial cell fates probably results from a residual function of Ths* to activate the receptor Htl, and remains to be discussed.

The failure of Ths* to activate Htl mediated Ras/MAPK activation suggests that exchange of the highly conserved amino acid Cysteine (C) to Arginine (R) within the FGF core domain of Ths results in a reduced function. According to this assumption, the amino acid C^{100} of the FGF peptide sequence is vital for Ths function in activation of the receptor Htl.

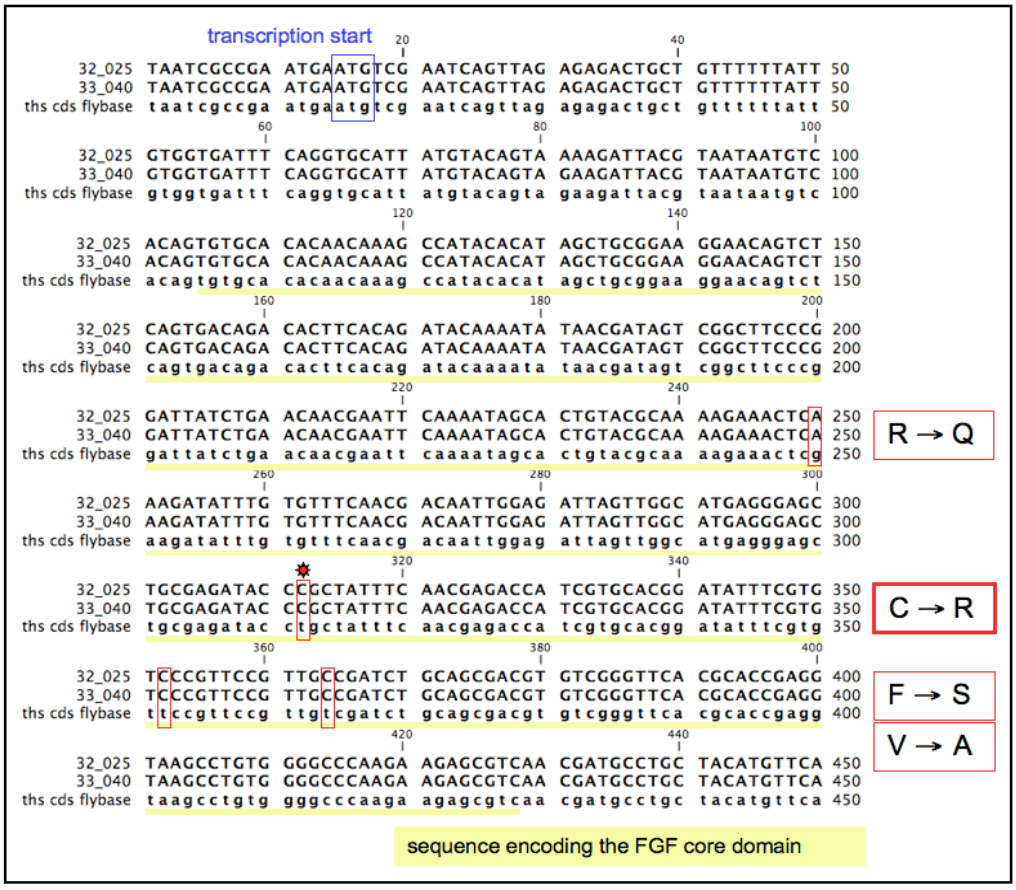

Fig. 52. The ability of Ths to activate Htl-mediated ERK phosphorylation upon ectopic expression is dependent on conserved amino acids of the FGF core domain.
Sequence of ths* encoding the FGF core domain (yellow). Sequencing of *ths** revealed that the transgenic *ths** gene contains point mutations within the sequence coding for the FGF core domain of Ths. 4 point mutations result in exchanges of amino acids; the positions are indicated. Arginine (R) is change to Glutamine (Q), Cysteine (C) is change to Arginine (R), Phenylalanine (F) is change to Serine (S) and Valine is change to Alanine (A). The point mutation at position 312 of the sequence displayed (marked with an asterisk) affects a conserved residue at position 100 of the amino acid sequence of Ths.

III. 3. 2 Spatiotemporal control of Pyr mediated Htl signalling is required for normal mesoderm spreading and differentiation

III. 3. 2. 1 Overexpression of *pyr* in mesoderm cells

Mesoderm migration requires a restricted domain of Pyr mediated MAPK activation

Mesodermal overexpression of *pyr* in a wild-type background (*twi >pyr*) (Fig. 53) resulted in obvious defects in mesoderm migration and monolayer formation.

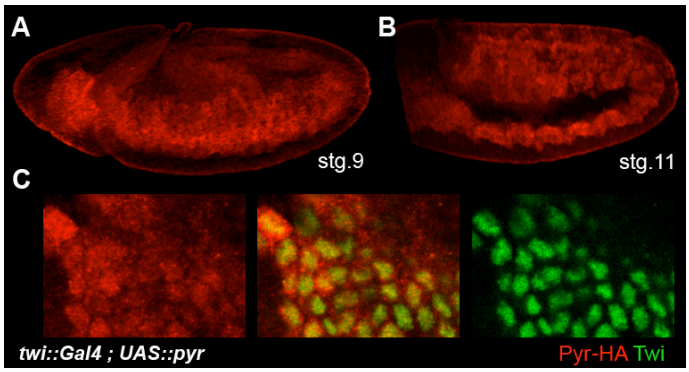

Fig. 53. Transgenic expression of *pyr* in mesoderm cells. Ectopic mesodermal expression of the transgenic pyr-HA under control of the twi promotor. Embryos stained for HA from ventral-lateral (A) and lateral (B) view. (C) shows a magnification of mesoderm cells expressing pyr-HA, stained for HA and Twi as indicated. (A, B) Pyr-HA is restricted to the mesoderm. (C) Pyr-HA shows cytoplasmic and cortical intracellular localisation.

In 80% of all embryos examined, invagination and tube collapse of the mesoderm was normal and symmetric (Fig. 54H1, 4). However 20% of all *twi >pyr* expressing embryos also exhibited slight defects during invagination (Fig. 54G1). The lateral dispersal of the cells was symmetric, but dorso-lateral migration was irregular (Fig. 54F2, G2). In later phases of mesoderm spreading, *twi >pyr* expressing embryos showed defects in the organization of the mesoderm. Spreading in anterior regions was restricted compared to posterior regions of the embryo, and the distribution of mesoderm cells in hemisegments was more prominent than in wild-type embryos (Fig. 54A3, B3, F3, G3). The migration of *pyr* over-expressing mesoderm cells also appeared to involve the formation of transverse cell rows rather than a collective movement of single motile cells (Fig. 54G2, H2, H5). The dorsal positioning of mesoderm cells was highly irregular, but phenotypes were varying in expressivity. Monolayer formation

was severely impaired and cells were remaining in ventral positions as spreading failed to complete (Fig. 54G3, H3). At some anterior-posterior positions however, embryos expressing *twi >pyr* contained a cell layer, albeit uneven, and showed cells in positions at the dorsal margin of the ectoderm (Fig. 54H6).

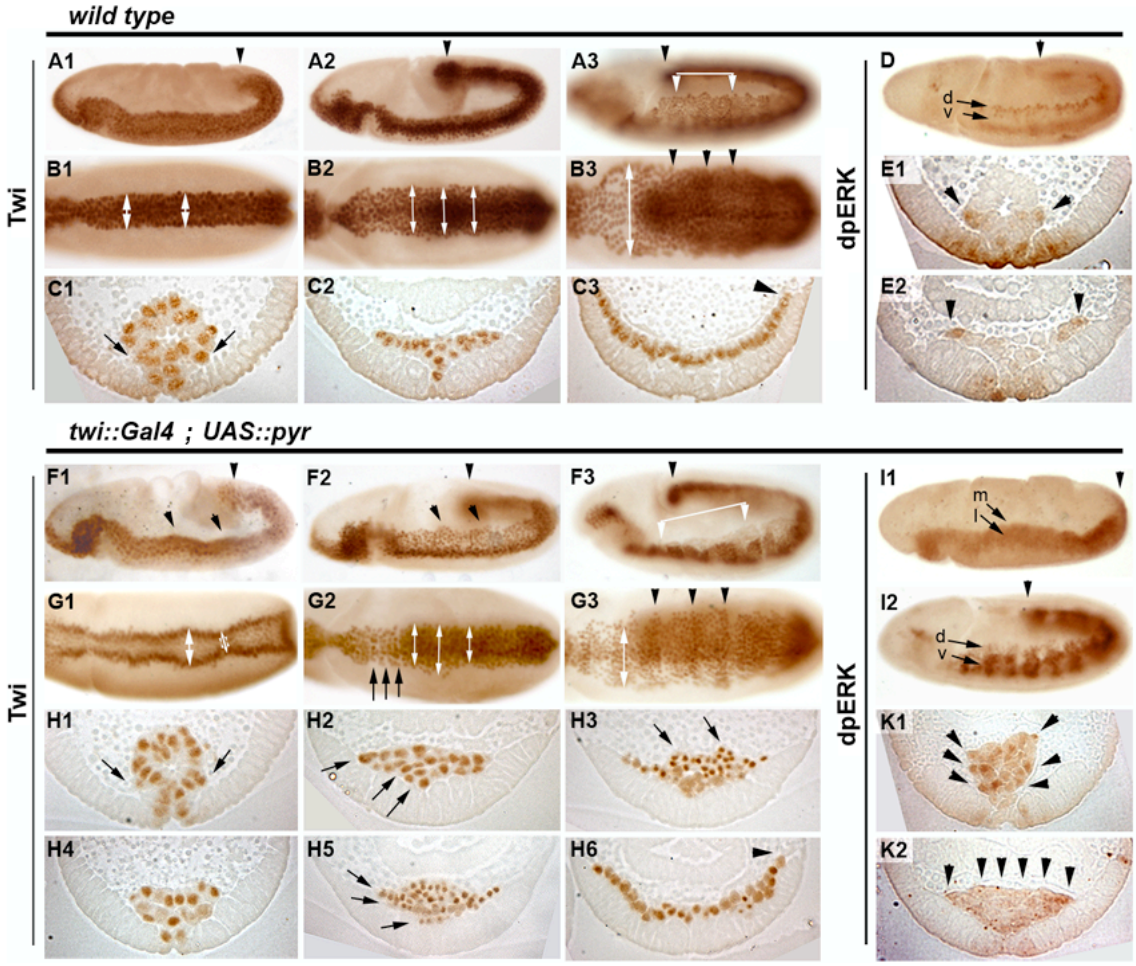

Fig. 54. Mesoderm spreading after uniform activation of Htl by Pyr in all mesoderm cells. Embryos of the indicated phenotypes stained with anti-Twi and anti-dpERK (detects activated MAPK) as indicated shown as whole mount (A1-3 , D, F1-3, G1-3 from ventral view; anterior is to the left) or cross section (between 40% and 60% egg length). **(A-E)** Wild-type. White double arrows in **B1-3** show the even lateral extension of the mesoderm domain during spreading. (A3) The white arrow indicates the even position of dorsal-most mesoderm cells at stage 9/10. (B3) The expression of Twi forms segmental crescents (arrowheads). Mesoderm cells make contact to the ectoderm **(C1)** and acquire dorsal-most positions relative to the ectodermal margin (arrowhead in (**C3**)). **(D, E1-2)** MAPK is activated at the leading edge in dorsal mesoderm cells (arrow d) but not ventrally (arrow v); most-lateral cells of the mesoderm display dpERK (arrowheads). **(F-K)** pan-mesodermal expression of *pyr*. **(F1-F3)** Mesoderm migration is disturbed upon pyr overexpression. The white arrow indicates uneven positions of dorsal-nost mesoderm cells after spreading. **(G1)** Over-expression of *pyr* interferes with invagination; double-arrows indicate uneven positions of mesoderm cells. **(G2, G3)** lateral spreading is asymmetric (white double-arrows) and mesoderm cells build rows of lined up cells (arrows). The formation of segmental crescents is enhanced **(H1-6)** cross sections show that tube collapse is normal (H1, H4). The formation of cell rows is discernible (arrows). (H3, H6) monolayer formation is disturbed and alters at different positions along the anterior-posterior axis. Mitotic activity (fuzzy Twi stainings indicate cells in mitosis) is disturbed in relation to stage of development. **(I1, 2; K1, 2)** expression of *pyr* results in MAPK activation in each mesoderm cell not only at the leading edge (d) but also in ventral (v) positions, obvious in cross sections (K1, 2). **(I2)** The mesoderm forms an early and unusual segmental pattern.

In addition to spreading defects, the timing of mesodermal mitosis intervals was disturbed in *twi >pyr* expressing embryos, and the mesoderm showed a untypical high simultaneity of mitotic activity (Fig. 54H6).

Expression of *twi >pyr* resulted in ectopic MAPK activation in mesodermal cells, and embryos displayed high levels of dpERK not only in dorsal edge cells but also in ventral and medial positions (Fig. 54I1-2, K1-2). Moreover, MAPK was activated uniformly in all mesoderm cells from as early as the initial phase before tube collapse (Fig. 54I2), confirming that Pyr mediated Htl signalling is responsible for initial MAPK activation prior to ectodermal attachment.

The formation of dorsal filopodia is dependent on ectodermal expression of *pyr*

Endogenous expression of *pyr* at early stages is restricted dynamically to further dorsal domains of the ectoderm according to dorsal progression of migration (Fig. 39P, Q, R and S4, appendix 1). Wild-type embryos exhibit cellular protrusions at the dorsal edge of migration mesoderm cells, and these are strongly reduced in absence of *pyr* (see above). Thus, Pyr presumably provides positional information for cells to protrude and migrate dorsally.

Embryos expressing *twi >pyr* are deprived of Pyr mediated dorsal positional information, as localisation of Htl activation at the dorsal edge is lost. *twi >pyr* overexpression resulted in formation of only very few and short protrusions during initial and early phase of migration (Fig. 55D, E). Consistent with the observed defects in early and later migration of *twi >pyr* expressing embryos, mesoderm cells appeared disorganised and the cell collective showed defects in inter-mesodermal cell adhesion (Fig. 55D). The short protrusions of dorsal edge cells were undirected in early stages and the cells only showed a consistent dorsal direction of protrusion formation in late phase of mesoderm spreading. Compared to mesoderm cells during late phase of wild-

type embryos, cells were stretched towards dorsal regions, but filopodia were obviously shorter and lamellipodia were not discernable (Fig. 55C, F).

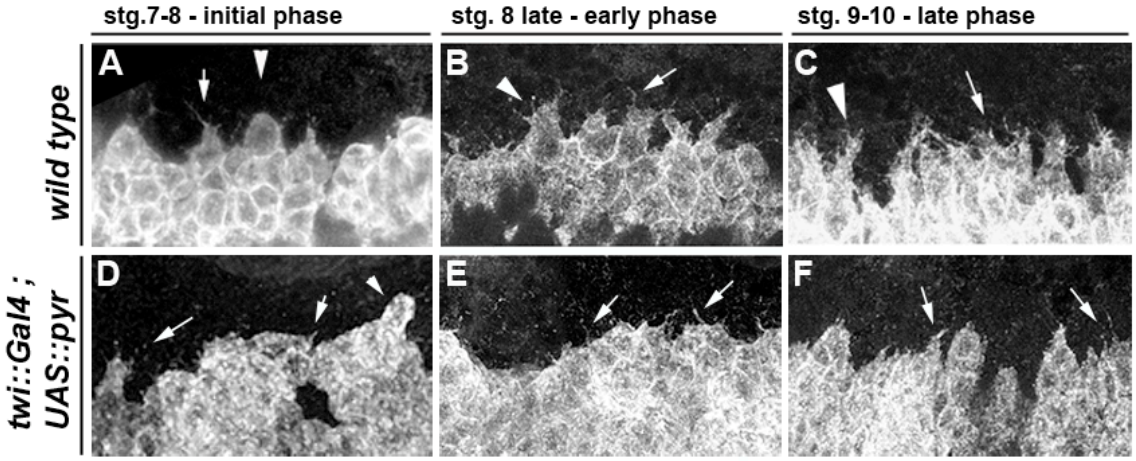

Fig. 55. Morphology of dorsal edge cells during mesoderm migration in response to over-activation of Pyr mediated Htl signalling in all mesoderm cells.
Magnification of leading edge cells stained for the membrane marker twi::CD2. Dorsal is up. Phases of mesoderm migration and genotypes are indicated. Arrows indicate filopodial protrusions, arrowheads indicate lamellipodial structures. (A-C) wild-type. **(A)** During initial ectoderm attachment, the cells exhibit hairy filopodia and are of round shape. **(B)** Many long filopodia are discernible during early lateral migration. **(C)** In late phase of mesoderm spreading, mesoderm leading edge cells show a stretched shape and more lamellipodia are formed. (D-F) pan-mesodermal expression of *pyr* results in change of mesoderm morphology. Only short, hairy protrusions are exhibited in initial phases and some cells exhibit round shape in most dorso-lateral position (arrows and arrowhead in **D**). **(E)** During the early phase of migration, the cells are not polarised into dorsal direction but exhibit few, short and thin filopodial protrusions (arrows) **(F)** At later phases of mesoderm spreading, the cells eventually gain dorsal directionality and begin to stretch towards the dorsal ectoderm. The formation of protrusions however is still impaired and lamellipodial structures are not discernible.

Conclusively, overexpression of *pyr* in the mesoderm results in severe defects in mesoderm spreading. Mesoderm cells appear disorganized and the formation of dorsal edge protrusions is highly disturbed, in resemblance to impaired protrusive activity upon *pyr* loss of function and thus loss of positional information. Hence, Pyr provides spatial regulation of Htl signalling to guide filopodia extension towards dorsal ectoderm domains and is not simply required for general protrusive activity. The dorsal restriction of MAPK activation in the mesoderm is important for normal mesoderm migration. Uniform MAPK activation by *pyr* overexpression in the mesoderm is reconfirming that Htl signalling upon activation by Pyr characteristically strongly triggers MAPK signalling.

The differentiation of cardiac and muscle progenitors is dependent on site-specific Htl activation by Pyr

Pericardial cell fates are dependent on activation of MAPK upon Pyr induced Htl signalling (see above). The differentiation of pericardial cells was strongly affected in embryos expressing *pyr* in all mesoderm cells. Mesoderm cells expressing the differentiation marker Eve were highly increased in number (Fig. 56 A, B). During later embryogenesis, the domain of pericardial cell clusters also extended laterally, and the segmental pattern was lost in consequence of segmental fusion of these enlarged cell clusters (Fig. 56 E, F).

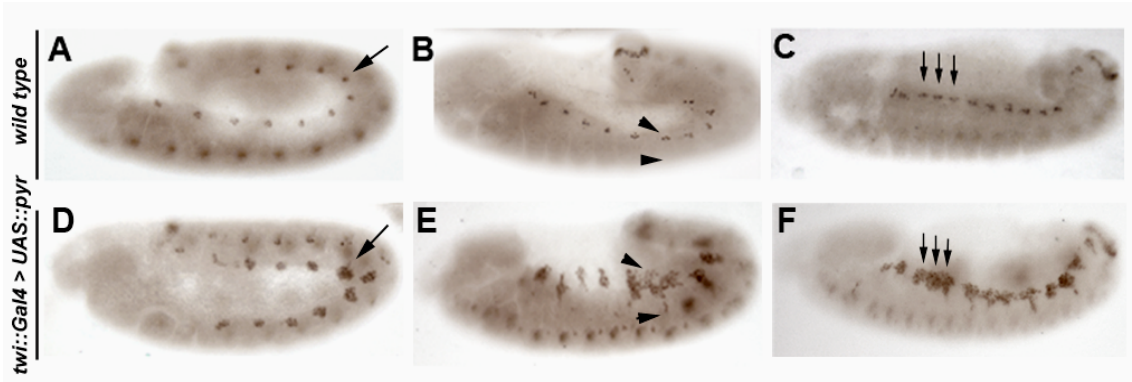

Fig. 56. Over-expression of pyr in mesoderm cells results in supernumerary fusing cell clusters containing Eve positive nuclei.
Embryos at stage 10- 13/14 were stained for the transcription factor Eve expressed in pericardial cell clusters. Anterior is left, dorsal is up. Genotypes are indicated. **(A-C)** In wild-type, Eve positive cell clusters are specified in each segment of dorsal mesoderm cells. **(D-F)** Overexpression of pyr in all mesoderm cells results in clusters of increased numbers of Eve positive cells (arrow in D). At later stages, these clusters extend towards ventral regions (arrowheads in E, compare to B in wild-type) and fuse with Eve positive cell clusters of neighbouring segments (arrows in F indicate three consecutive segments, the borders of which are no longer discernible with regard to segmental clusters as in wild-type (C)).

Pericardial cell numbers also appeared to increase further after initial formation of Eve positive progenitors in contrast to wild-type. In wild-type embryos, pericardial cells once differentiated maintain cell clusters of 2-4 cells per segment (Fig. 56A-C). Thus, ectopic expression in all mesoderm cells is able to induce pericardial cell fates not only from dorsal mesoderm domains, indicating that Pyr mediated Htl signalling is required

for early specification of mesoderm cells to become competent to respond to further differentiation signals. The increase of pericardial cell numbers thus possibly is in consequence to more mesoderm cells being specified and differentiated. Another possibility would involve further mitotic cell divisions of already specified progenitor cells during later stages. *twi >pyr* expressing embryos also showed effects on intervals of mitotic activity in the mesoderm (see above). The enlargement of pericardial cell clusters might depend on general disturbed mitotic activity in the mesoderm. A third explanation might involve that high levels of Pyr mediated, Htl dependent MAPK signalling generate pericardial cell fates before muscle cell fates become specified.

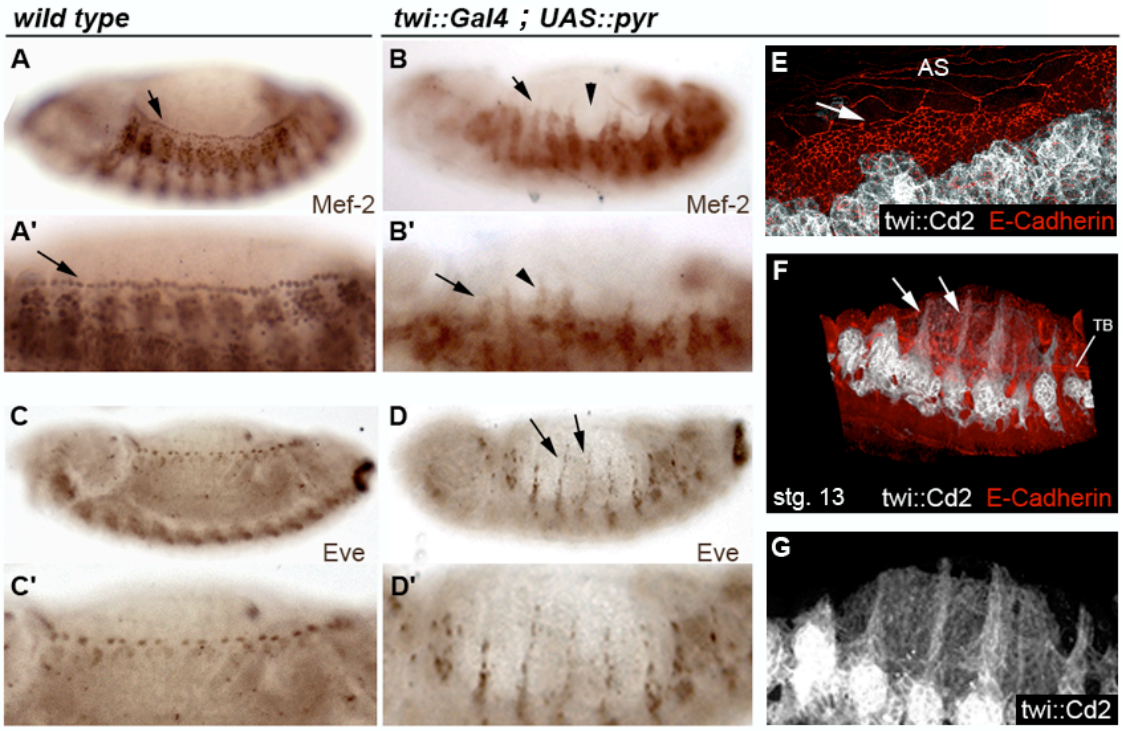

Fig. 57 Over-expression of pyr in mesoderm cells disrupts the pattern of somatic muscle progenitors and results in formation of unusual syncytia-like structures.
Embryos stained for Mef-2 (A, A', B, B'), Eve (C, C', D, D') or twi::CD2 and E-cadherin (E-G). Genotypes are indicated. Anterior is left, dorsal is up. **(A)** wild-type pattern of dorsally aligned cardioblasts, **A'** shows a magnification. **(B, B')** Over-expression of pyr results in loss of cardioblasts and pattern of Mef-2 positve mesoderm cells. A dorsal mesoderm edge is not formed (arrow) but cells form segmentally rows of ventral-dorsal extension (arrowhead). **(C, C')** Staining foe Eve in wild-type embryos show the alignment of pericardial cells at the dorsal mesoderm margin. **(D, D')** In embryos over-expressing pyr, the ventral-dorsal extensions observed in Mef-2 stainings are also discernible in stainings for Eve. Co-stainings for E-cadherin and twi..CD2 show that the mesoderm does not reach the ectodermal margin (**E**, arrow) but syncytia-like structures form in later stages **(F, G)** that extend over the border of ectoderm and Amnioserosa (AS). TB, tracheal branch.

For example, it is shown that pericardial cell progenitors are specified before the DA1 muscle progenitor is determined from the same mesodermal cell cluster (Buff et al. 1998). Other progenitor cells then would be lost in favour of more pericardial cells upon consisting high levels of activated MAPK.

Dorsal mesoderm derivatives were differentiated despite the defects in dorsal mesoderm spreading in *twi >pyr* expressing embryos. Thus, dorsal cell fates were specified although mesoderm cells failed to cover dorsal domains of inductive ectoderm cells (Fig. 57E). In contrast to an enhancement of Eve positive cells, other dorsal derivatives such as cardioblasts were not differentiated in consequence to *pyr* gain-of-function (Fig. 57A', B'). Additionally, the pattern of Mef-2 expressing somatic muscle progenitors was entirely irregular (Fig. 57B) and showed similarity to phenotypes of *ths, pyr* deficient or *htl* mutant embryos, or embryos expressing *ths* in all mesodermal cells (Stathopoulos, 2004). These similarities again show that over-activation and uniformity of Htl signalling in mesoderm cells results in defects upon loss of signals distinct for migration and differentiation. However, in contrast to loss of function phenotypes of Htl and its ligands, overexpression of *pyr* in mesoderm cells resulted not only in defects of muscle progenitor development, but in segmental, dorso-ventral aligned cell formations, which showed expression of the differentiation markers Mef-2 and Eve (Fig. 57B, B', D, D'). These syncytia-like structures are also observed in embryos expressing active forms of Ras, and were identified to derive from the differentiation of supernumerary muscle founders (Carmena et al., 1998).

As the transgenic, mesodermal cell surface marker twi::CD2 pertains longer expression than endogenous *twi* (Dunin-Borkowski et al., 1995), mesodermally derived cells can be followed in later stages. Stainings for twi::CD2 in late stage 13 showed that a regular dorsal edge was not formed in embryos expressing *twi >pyr* but rather a network of

mesodermally derived cells which also form large syncytia-like structures elongating in dorsal direction (Fig. 57 F, G).

Ectopic *pyr* expression rescues pericardial cell fates in *ths, pyr* deficient embryos

Uniform mesodermal expression of *pyr* rescued pericardial cell fates in *ths, pyr* deficient embryos (Fig. 58B, C). The numbers of Eve positive cells per cluster were extended compared to wild-type (Fig. 58A, C). Increased size of pericardial cell clusters was further observed upon *twi >ths* overexpression in embryos lacking endogenous *ths* and *pyr* (Stathopuolos, 2004). *twi >pyr* overexpression led as well in *ths, pyr* deficient embryos to differentiation of supernumerary syncytia-like structures of Eve expressing muscle founders (Fig. 58D). These structures were not observed upon *ths* overexpression (Stathopuolos et al., 2004).

Fig. 58. Ectopic expression of *pyr* in all mesoderm cells rescues the missing expression of *eve* in prospective pericardial cells of *ths, pyr* deficient embryos.
Embryos stained for Eve at stage 10; anterior is left, dorsal is up. The arrowheads indicate neural *eve* expression (A) which is not affected by Htl signalling (B, C). **(A)** wild-type specification of Eve positive pericardial cell clusters. **(B)** Eve positive cell clusters in the mesoderm are missing in *ths, pyr* deficient embryos (arrows). **(C)** Pan-mesodermal expression of *pyr* rescues the expression of Eve in dorsal mesoderm cells. The segmental clusters tend to fuse (arrows).

Both *ths* and *pyr* function in mesoderm cells result in induction of pericardial cells fates in absence of endogenous expression. However, only *pyr* expression in mesoderm cells resulted in formation of ectopic supernumerary syncytia-like structures of muscle founders. Conclusively, mesoderm spreading as well as differentiation of mesodermal derivatives is inducible and regulated by *ths* and *pyr*, respectively. *pyr* however provides a function more prominent in differentiation of mesoderm cells, as pericardial

cells are not only inducible but dependent on *pyr* function to differentiate, and muscle cell fates are additionally affected by ectopic expression of *pyr* but not of *ths*.

III. 3. 2. 2 Ectopic over-expression of *pyr* in ectoderm cells

pyr gain-of-function affects early, but not later phases of mesoderm spreading

As described above, spatiotemporal uniform Htl activation by Pyr in mesoderm cells resulted in severe defects of mesoderm migration and differentiation. Uniform expression of *pyr* in the ectoderm from stage 9 (*69B >pyr*; Staehling-Hampton et al., 1994) resulted in uniform MAPK activation including lateral and ventral regions, but mesoderm spreading was not affected in these embryos (Fig. 59 D-F).

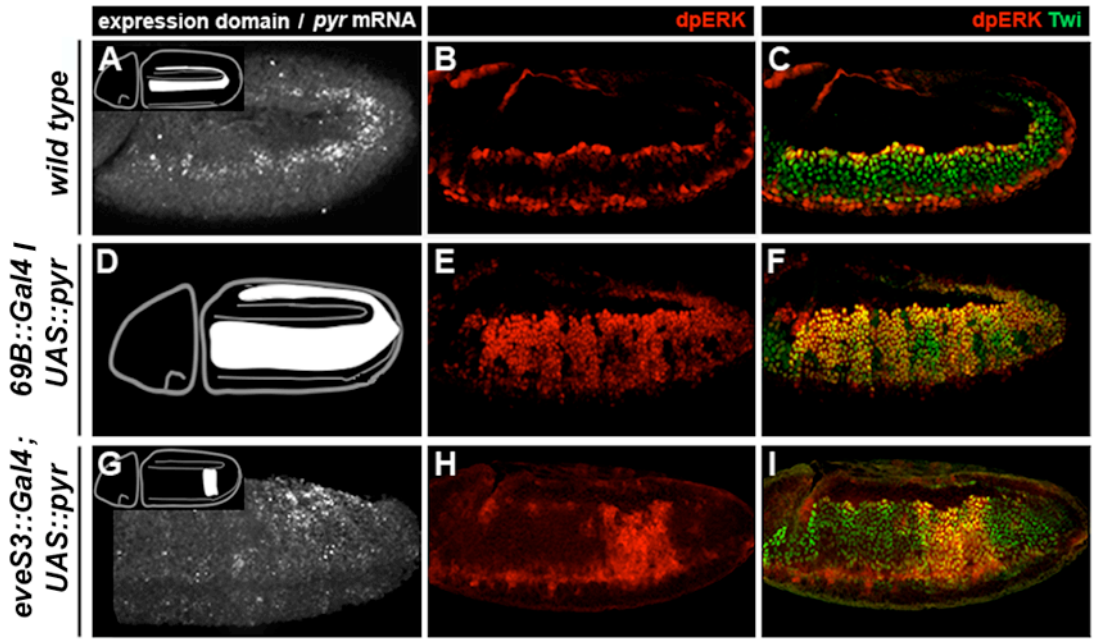

Fig. 59. Pyr mediated Htl signalling results in activation of MAPK within the domain of pyr expression.
In situ hybridisation of pyr transcripts (A, G) demonstrate the expression of *pyr* in wild-type (A) and using the *eveS3::Gal4* driver (G); see also Fig. 63A for expression domain. Expression domains of *pyr* in wild-type, within the ectoderm using the *69B::Gal4* driver (D) and the *eveS3::Gal4* driver are indicated by cartoons. Embryos were stained for dpERK and Twi as indicated; anterior is left, dorsal is up. **(A)** In wild-type, the expression domain of *pyr* restructs to the dorsal ectoderm. **(B, C)** MAPK is activated in leading edge cells. **(D-F)** Ectopic expression of *pyr* in the ectoderm from stage 9 results in additional activation of MAPK in lateral and ventral mesoderm cells. **(G)** Expression of *pyr* under control of the promotor region responsible for expression in eveS3 (eve stripe 3) pattern. **(H, I)** Local expression of *pyr* results in local activation of MAPK. Mesoderm cells within the ectopic domain of pyr expression did not acquire the dorsal positions reached by cells in neighbouring segments where MAPK is not activated in all mesoderm cells.

To distinguish from uniform ectodermal but also early pan-mesodermal over-expression, *pyr* was expressed using *eve-stripe3::Gal4* in a defined region of the ectoderm onwards from stage 5/6 prior to gastrulation (*eveS3 >pyr*; Sharma et al., 2002). *eveS3 >pyr* expressing embryos showed enhanced MAPK activation within the expression domain and dorsal migration appeared retarded compared to neighbouring, unaffected regions (Fig. 59G-I). These results indicate that non-localised MAPK activation only causes defects during early phases of mesoderm migration, but uniform mesodermal activation of MAPK has no influence on late phase of mesoderm spreading, including terminal dorsal positioning of mesoderm cells.

Pyr mediated Htl signalling is strictly site-specific

The range of the Pyr signal could not be investigated by localisation of the transgenic FGF protein as a reliable antibody is currently not available for Pyr. Stainings for the tagged peptide were unsatisfying during the period of these experiments. Detection of HA in *twi >pyr-HA* expressing embryos detected the protein in the cytoplasm of mesoderm cells (Fig. 53C). Transcripts of the transgenic *pyr* allele were detected in respective domains of Gal4-induced expression (Fig. 59G, C, Fig. 60C). The observed effects in consequence to local overexpression of *pyr* were confined to the domain of expression and showed no influence on adjacent mesodermal cell fates.

The *eve-stripe3::Gal4* expression domain shows sharp borders within two hemisegments, involving Eve positive cell clusters of two neighbouring hemisegments (Fig. 60A, B). Expression of *pyr* within this domain resulted in mesodermal MAPK activation even more sharply confined as the expression domain itself (Fig. 60C-F). This strict ectopic MAPK activation pattern indicates that the signalling range of Pyr is very limited. Also, activation of Htl could depend on certain levels of Pyr, or the signal transduction to MAPK activation in mesoderm cells could involve certain thresholds of

Pyr mediated Htl signalling. The results indicate that Pyr dependent Htl activation might function as an on/off switch of Htl dependent MAPK activation and consecutive differentiation of muscle and pericardial cell progenitors.

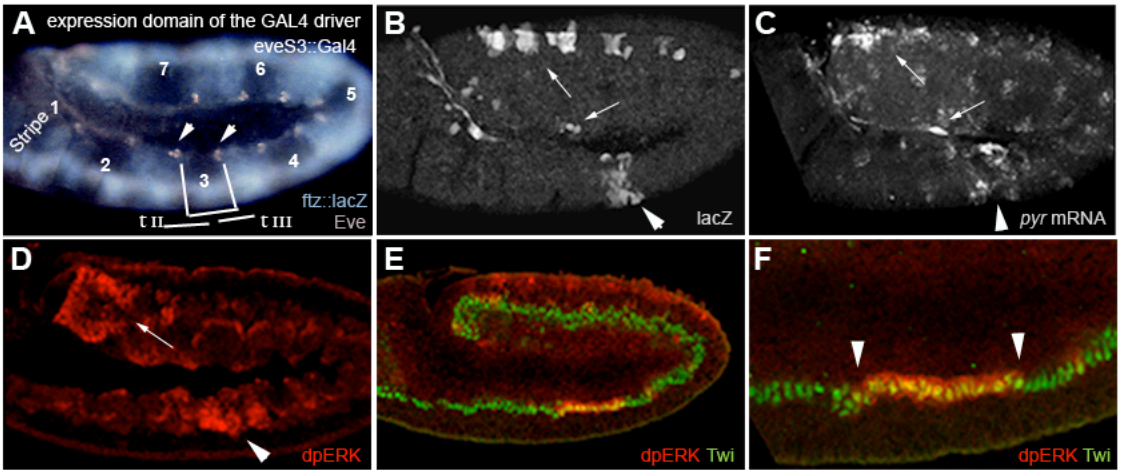

Fig. 60. Expression of *pyr* induces activation of ERK in sharp borders.
Embryos at stage 10 in lateral view; anterior is left, dorsal is up. **(A)** wild-type embryo. Expression domains of *fushi tarazu (ftz)* (blue) alter with expression domains of *eve* (without staining). Stripe 3 of the *eve* expression pattern is indicated between segment t II and t III; the domain affects two clusters of Eve positive mesoderm cells (arrowheads). **(B)** *eveS3::Gal4-UAS::lacZ* expression illustrates the expression pattern of the *eveS3::Gal4* driver that is reflected in pyr expression under control of *eveS3::Gal4* (**C**). **(D)** MAPK is activated in the expression pattern of eveS3::Gal4. (E) Within the expression domain affecting mesoderm cells, dpERK is displayed within sharp borders. The magnification in **(F)** shows that direct neighbouring cells display only Twi and MAPK is not activated. The signal of *pyr* is locally specific.

Localized *pyr* expression in the ectoderm provides the limiting factor of Pyr function in regulation of progenitor selection and differentiation

In contrast to normal mesoderm spreading, late ectopic expression in ectoderm cells using the *69B:Gal4* promotor caused defects in differentiation of mesoderm cells.

Activation of MAPK in all mesoderm cells during specification of pericardial and muscle progenitor cells resulted in supernumerary clusters of cells expressing the differentiation marker Eve in every segment (Fig. 61D, E). In later stages of embryogenesis, these clusters were extending in ventral areas (Fig. 61 F), as also observed in embryos expressing *twi >pyr*.

The ectodermal source of the Htl ligand hence was not limiting in the extent of differentiation defects, indicating that Pyr levels and thus Htl activation are not fundamentally regulated by other, extra-cellular factors. Eve positive cell clusters rather were enlarged in embryos over-expressing *pyr* in the ectoderm compared to over-expressing *pyr* in the mesoderm (Fig. 56D, 61E).

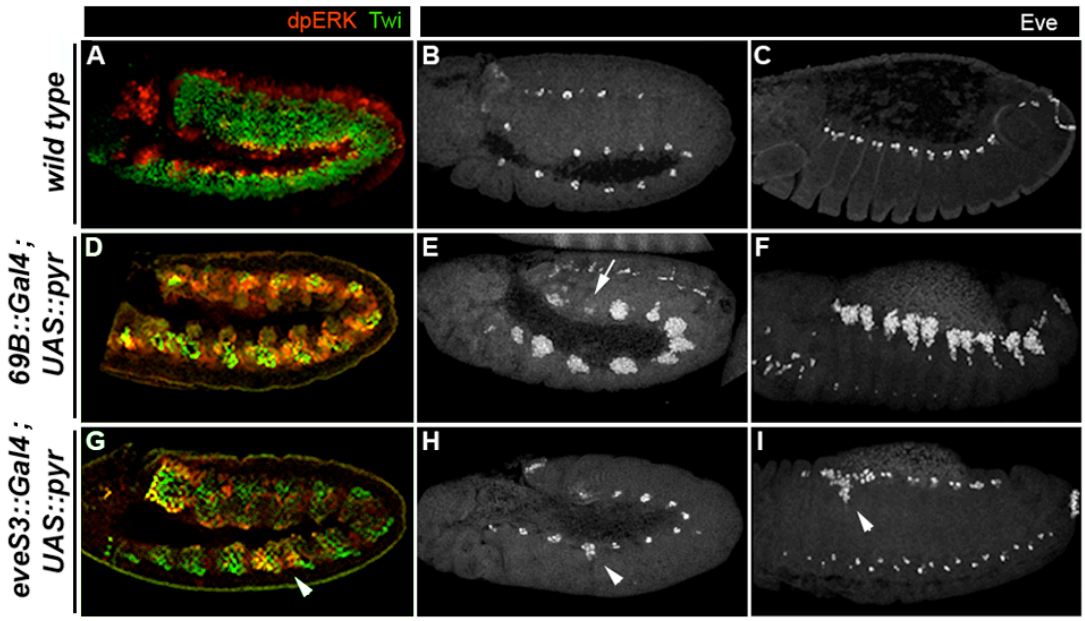

Fig. 61. Ectopic expression of pyr specifically induces the expression of the transcription factor Eve in unusual large cell clusters.
Embryos at stage 10 and stage 13 (C, F, I) stained for dpERK or Eve as indicated. Lateral views, anterior is to the left, dorsal is up. (A-C) wild-type embryos display dpERK in cell clusters of the dorsal mesoderm which correspond to the specification of Eve positive pericardial cell clusters in each segment. The size of the clusters is unaltered after specification. (D) Expression of *pyr* in all ectoderm cells from stage 9 results in MAPK activation in mesoderm cells of the outer group of somatic muscle progenitors. The mesoderm cells in more medial position giving rise to visceral muscle progenitors and fat body are not affected. (E) pan-ectodermal *pyr* expression from stage 9 under control of the 69B::Gal4 promotor results in formation of supernumerary Eve positive cell clusters, but clusters 1 and 11 are not affected (arrow indicates cluster 11). (F) The Eve positive cell clusters extend ventrally but fusion as observed for mesodermal over-expression of *pyr* does not occur. (G) Localized over-expression of *pyr* activates MAPK ectopically in a hemisegment (arrowhead). (H) Within the expression domain of *pyr,* expression of *eve* is locally induced in a higher number of mesoderm cells compared to unaffected neighbouring segments. (I) The cluster extends ventrally and fuses with neighbouring pericardial cell clusters (arrowhead).

The difference in cluster size confirms that spreading is not affected in embryos over-expressing *pyr* in the ectoderm, because more cells acquired dorsal positions relative to the normally, and thus additionally, inductive ectoderm domains.

Embryos expressing *eveS3 >pyr* showed local differentiation defects, in accordance with local uniform MAPK activation (Fig. 61G). Stainings for Eve showed more progenitor cells specified in segments 2 and especially 3 compared to the other segments, and cell numbers were increased in later embryogenesis as observed upon mesodermal uniform overexpression of *pyr* (Fig. 61H, I). Quantification of differentiated cells in these clusters showed that overexpression of *pyr* on average led to a threefold increased number of specified cells (Fig. 62D). Embryos at later stage 13 showed tenfold more Eve expressing cells within the ectopic *pyr* expression domain, confirming previous observations that Eve positive cell clusters were enlarged with progressed development.

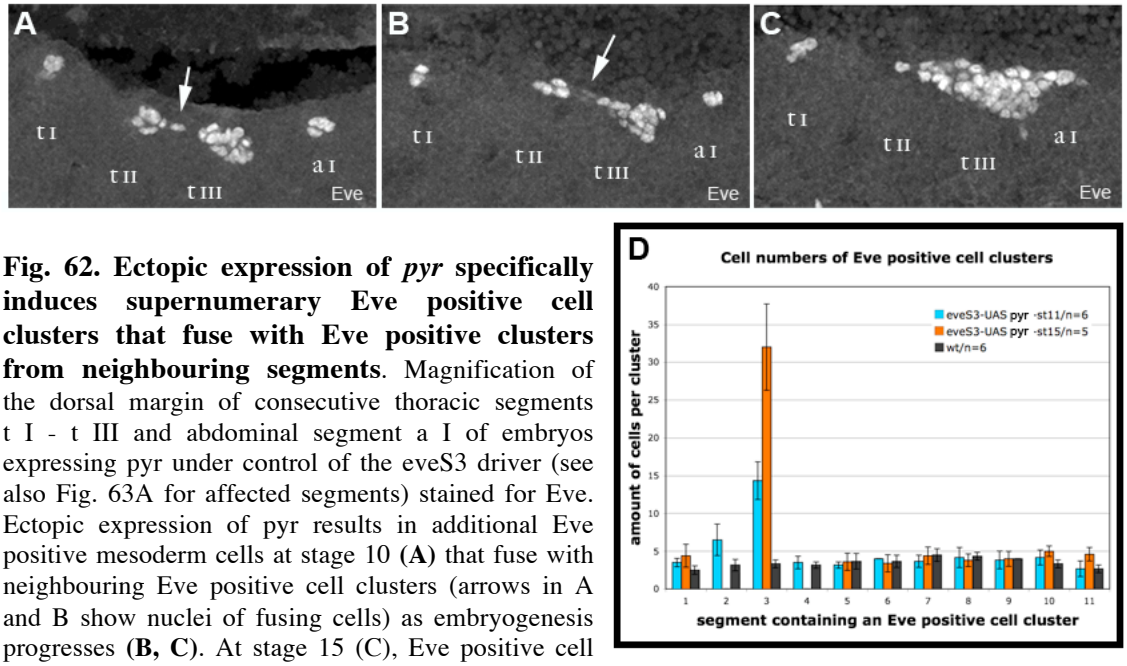

Fig. 62. Ectopic expression of *pyr* specifically induces supernumerary Eve positive cell clusters that fuse with Eve positive clusters from neighbouring segments. Magnification of the dorsal margin of consecutive thoracic segments t I - t III and abdominal segment a I of embryos expressing pyr under control of the eveS3 driver (see also Fig. 63A for affected segments) stained for Eve. Ectopic expression of pyr results in additional Eve positive mesoderm cells at stage 10 **(A)** that fuse with neighbouring Eve positive cell clusters (arrows in A and B show nuclei of fusing cells) as embryogenesis progresses **(B, C)**. At stage 15 (C), Eve positive cell clusters from t II, t III and s I are fused to one supernumerary cell cluster. **(D)** Quantification of Eve positive nuclei in each cluster of embryos expressing *eveS3::Gal4-UAS::pyr*. The clusters 2, 3 and 4 are spatially not distinguishable any more at stage 15 and therefore are shown as one cluster in position of cluster 3.

The local restriction of *pyr* over-expression in these embryos allowed to better follow the process of enlargement of these clusters, as neighbouring segments were unaffected. The changing morphology of these single clusters indicates a recruitment of Eve expressing nuclei rather than proliferating progenitor cells (Fig. 62 A-C).

Dorsal-ventral extending syncytia-like structures as observed upon mesodermal over-expression were not exhibited in *eveS3 >pyr* expressing embryos, but the supernumerary cluster in segment 3 similarly appeared to fuse with Eve positive cell clusters of neighbour segments (Fig. 62B). Thus, Pyr mediated Htl signalling presumably over-activates Ras/MAPK signalling, leading to maintained Eve expression in mesoderm cells during differentiation involving other signals. As a result, fusion-competent founder cells incorporate Eve positive progenitors in formation of large syncytia (Carmena et al., 1998), and the clusters do not represent increased numbers of pericardial cells.

A similar effect was also observed for the formation of lateral progenitors. The SBM founders derive from lateral mesodermal cells expressing the differentiation marker Lbe (Jagla et al., 1998; Fig. 63A). *eveS3 >pyr* expressing embryos showed increased numbers of *lbe* expressing cells in this domain upon ectopic activation of Htl signalling by Pyr.

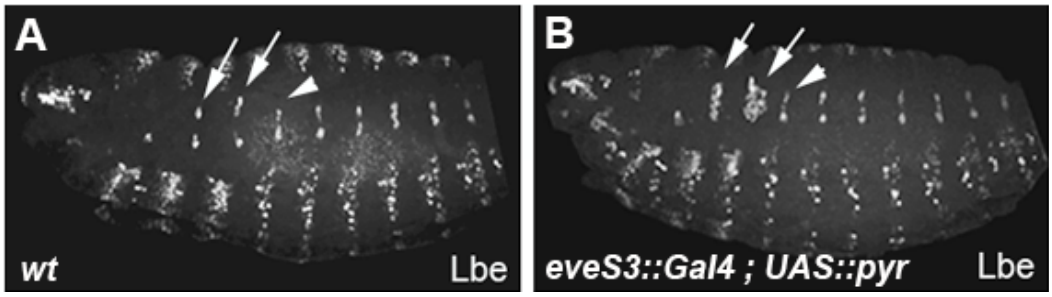

Fig. 63. Ectopic expression of *pyr* induces *lbe* expression in large clusters of SBM progenitors.
Embryos at stage 16 stained for Lbe. Lateral views, anterior is left, dorsal is up. **(A)** wild-type embryo showing *lbe* expressing SBM muscle progenitors (arrows, arrowhead; arrows indicate slightly affected and main affected progenitors). **(B)** *pyr* induces ectopic expression of *lbe* in mesoderm cells resulting in increased numbers of progenitors and formation of Lbe positive cell clusters (arrows). Neighbouring segments unaffected show no increase in numbers of Lbe positive nuclei.

Strikingly, only the cluster generating the SBM progenitor was affected, and dorsal as well as ventral Lbe expressing cells showed no differentiation defects (Fig. 63). The results indicate that Pyr mediated Htl signalling is specific for SBM progenitors,

confirming results from single mutant analysis showing defects in SBM development (see above).

Conclusions from III. 3

The analysis from ectopic overexpression experiments showed that mesoderm development is controlled by spatiotemporal regulation of the Htl signalling cascade by Ths and Pyr. The activation of the receptor is dependent on the conserved amino acid sequence of the FGF core domain, as mutation of C^{100} in Ths resulted in the inability to activate MAPK signalling or additional Eve positive progenitors. Pyr mediated MAPK activation is required restrictedly in early phases of mesoderm migration, and is fundamentally involved in specification of mesoderm cells to differentiate into pericardial cells and muscle progenitors. The signal range of both Htl ligands appears very limited and confined to the site of expression. Especially during differentiation of progenitor cells involving lateral inhibition by single progenitors specified (Carmena et al., 2002), Pyr mediated Htl signalling presumably acts through thresholds of Ras/MAPK activation rather than gradient dependent signal transduction. Thus, increased progenitor cells despite imperfect mesoderm spreading upon ectopic overexpression would be confirming with an interference of other RTK signals involving Ras/MAPK activation.

In summary, analysis from loss-of-function and gain-of-function studies indicates multiple functions of *ths* and *pyr* during mesoderm development. Both mesoderm spreading and differentiation is orchestrated by the combined function of the FGF ligands in spatiotemporal regulation of Htl signalling. Pyr thereby inhabits a more distinct and individual role in comparison to Ths, the function of which was observed to more generally ensure the robustness of the processes dependent on Htl signalling.

IV. Discussion

FGF signalling via the receptor Htl is essential in mesoderm migration and differentiation during embryogenesis. *ths* and *pyr*, encoding the ligands for Htl, show dynamic expression patterns according to the different phases of mesoderm development and suggesting overlapping as well as individual functions in the activation of the mesoderm specific FGF signalling pathway. However, how Ths and Pyr control the process of mesoderm spreading, the cell shape changes involved and the later specification of cardiac and somatic muscle progenitors is unclear. The present study presents an approach of functional characterization of *ths* and *pyr* and provides evidence for requirement of combinatorial as well as individual function of both Htl ligands. As a conclusion of the results presented here a hypothesis is proposed and it will be discussed how Ths and Pyr orchestrate mesoderm migration and regulate specification of mesodermal derivatives.

IV. I Generation of single mutant alleles for *ths* and *pyr*

The individual analysis of *ths* and *pyr* function required the generation of single mutant alleles that only disrupt the function of either *ths* or *pyr* without affecting other neighbouring genes.

A single mutant allele of *ths* was generated by imprecise P-element excision of the transposon *EP(2)G18816* (Experimental procedures, II. 4. 4.). The insertion of a transposable element may disrupt the function of a gene producing visible or lethal phenotypes (Ryder and Russell, 2003). *EP(2)G18816* was inserted into the *ths* coding sequence of the last exon upstream of the 5' UTR The insertion of the 8 kb large transposon did not disrupt the function of *ths*, as homozygous flies were viable and

fertile and did not exhibit any defects in mesoderm development, in contrast to the mutant allele *ths*^{759} which was obtained by imprecise excision of *EP(2)G18816*. Flies homozygous for the P-element insertion also complemented the mutant allele *ths*^{759} and the deficiency *Df(2R)ED2238 (Df*^{2238}*)*, lacking both *ths* and *pyr* genes. These findings suggest that the 5' region downstream of the FGF core domain coding sequence is not essentially required to generate a functional Ths FGF protein. The C-terminal region thus would not contain any functionality and the induced truncation of the transcript without effect on mRNA translation.

Another possibility would suggest the presence of a splicing site within this C-terminal region, resulting in removal of the transposon together with the long C-terminal region of the gene. Ths comprises 748 amino acids, 611 of which belong to a large C-terminal tail, which was found to bear no homology to known protein domains (Gryzik and Müller, 2004). However, it also has been found that the *Drosophila* FGF genes additionally encode a second region with weaker similarity to the FGF core encoding sequence, suggesting the possibility that *Drosophila* FGFs act as functional FGF dimers (Itoh and Ornitz, 2004,). Furthermore, BLAST analysis with Uniprot (www.uniprot.org) for protein domain prediction shows possible cleavage sites for both ths and *pyr*, which would produce shorter peptides of 97 – 435 amino acids. Thus, a spliceform of *ths* containing 97 amino acids would cleave off the region containing the P-element inserted at position 158 of the peptide chain. Cleavage of the FGF peptides during maturation of the FGF proteins Ths and Pyr may also be obvious, as vertebrate FGF proteins in comparison are much smaller in size, compromising 150-250 amino acid residues (Ornitz and Itoh, 2001; Itoh and Ornitz, 2004). Also other invertebrate FGFs, such as EGL-17 and LET-756 in the nematode *C.elegans,* or the FGF proteins of the cnidarian *Nematostella vectensis* contain only between 216 - 425 amino acid residues and 174 -301 amino residues, respectively (Matus et al., 2007; Rentzsch et al., 2008;

Ornitz and Itoh, 2001). Furthermore, the single FGF gene in the mosquito (*Anopheles gambiae*) showing relation to *ths* and *pyr* encodes 330 amino acid residues (www.agambiae.vectorbase.org), indicating that the large FGF genes are characteristic for *Drosophilidae* and might be modified on a post-transcriptional level.

The excision of a P-element from a chromosome creates double-strand breaks in the DNA and can result in a partial or complete removal of the transposon (Engels et al., 1990; Ryder and Russell, 2003). If the ends of the double strand breaks are degraded before repair, a deletion of the genetic material will occur, an event known as imprecise excision. To identify a deletion allele of *ths* by imprecise excision of *EP(2)G18816*, 800 lines were scored and two of only 24 lethal lines showed a proximal deletion of flanking genomic sequence of *ths* extending into the region encoding the FGF core domain. The low efficiency imprecise excision events and the generation of only small deletions of maximal 2,5 kb however is not surprising. Imprecise excision events of transposable elements in general amount approximately 1% of all excision events, and deletion sizes can range from a few base pairs to several kilo bases (Daniels et al., 1985; Ryder and Russell, 2003). Moreover, the P-element insertion line *EP(2)G18816* utilized for generation of a mutant allele was generated in an EP screen that served as a test bed for developing high-throughput methods for sequencing transposon flanks (Rorth, 1996; Rorth et al., 1998; Liao et al. 2000). Other P elements show higher efficiency in generating a chromosomal deletion like in the case of the imprecise excision of *P(2)5-SZ-3066* which resulted in complete deletion of the *pyr* locus and which was identified in the first 20 lines scored (see below). Two single mutant alleles of *ths* were obtained by imprecise excision of *EP(2)G18816*, ths^{141} and ths^{759}, which show a deletion of 330bp and >2500bp, respectively.

IV. I. 1 The allele *ths* ^{141}

The allele *ths*^{141} was homozygous viable and fertile and showed no obvious defects in mesoderm development, and therefore was not included in further analysis. Nevertheless, *ths*^{141} homozygous flies showed 30% less progeny compared to wild-type, which was caused by degeneration of follicles in the ovary. This phenotype by comparison is similar to egg chambers undergoing programmed cell death (McCall, 2004; Baum et al., 2007). Cell-death in mid-oogenesis occurs in response to a checkpoint where the status of the egg chamber is monitored before maturing egg production (Drummond-Barbosa and Spradling, 2001). Diverse stimuli can impair normal oocyte growth such as lack of nutrients, steroids and influence of day length and temperature. Both ambient nutrients such as amino acids and insulin growth factors stimulate growth via the TOR (target of rapamycin) pathway (Avruch et al., 2006). The TOR pathway regulates growth primarily through regulation of ribosome biogenesis and protein translation (Sarbassov et al., 2005). The growth factor signalling pathway resulting in TOR activation has been demonstrated to involve the PI3K (phosphoinositide 3-kinase) or MAPK (mitogen-activated protein kinase) signalling cascades.

A screen for pathways mediating signalling by nutrients identified the serine/threonine kinase MOS (DMOS) as an essential positive regulator of MAPK activation within the TOR pathway (Findlay et al., 2007). Ivanovska et al., 2004, had also found the requirement of *mos* for MAPK activation in *Drosophila* ovaries by identifying the *Drosophila* homolog of vertebrate MOS. MOS kinase dependent MAPK activation is essential for the meiosis I to meiose II transition during oocyte maturation and prevents DNA replication between meiotic divisions. Thus, MOS function coordinates the completion of meiosis with fertilisation, (Tachibana et al, 2000; Tang et al., 2008) and its role seems to be highly conserved phylogenetically (Extavour, 2009). Accordingly to

the findings from other phyla, MAPK activation in *Drosophila* ovaries during prophase I (stages 1-13), and metaphase I (stage14) is dependent on DMOS signalling (Ivanovska et al., 2004). High levels of *mos* transcript were observed from stages 10-14 of oogenesis, and MAPK phosphorylation was most affected during metaphase I -arrested oocytes.

The phenotype of ths^{141} homozygotes shows a striking similarity to the $mos^{-/-}$ homozygous mutant phenotype, and a possible interaction of MOS and Ths is supported by *ths* being strongly expressed by nurse cells in stage 10 to 14 egg chambers. $dmos^{-/-}$ homozygotes are also viable and fertile as observed for ths^{141} homozygous mutant flies. In accordance with the 30% reduction of progeny of ths^{141} homozygous females due to the increased degeneration of follicles of comparable percentage, $dmos^{-/-}$ mutant females had 28%-55% fewer progeny than heterozygous siblings, caused by ovarioles contain increased numbers of degenerating egg chambers to 36% (Ivanovska et al., 2004).

RT-PCR showed that ths^{141} is still expressed, and sequencing of the cDNA showed that in ths^{141} single mutant embryos, a shorter transcript of *ths* was expressed that carried an internal deletion of 330 bp, which encodes a protein that contains a deletion within the C-terminus. But this mutation did not cause a frame shift of the open reading frame. The phenotype suggested that either the function of the FGF ligand was not compromised by the removal of 11 amino residues of the C-terminal end of the FGF core domain, or that the function of *ths* was either not essential for development or redundant with *pyr*. Taking into account that the prediction of the mRNA splicing sites would result into two different splice forms, the shorter splicing variant would remain unaltered by the small deletion in ths^{141} and thus explain the normal development of ths^{141} homozygous single mutants. A function of Ths during oogenesis thus is possible which might not be affected in ths^{141}. Further investigation of a possible interaction with

Mos, for example, will be required to reveal a functionality of Ths in addition to the requirement of an intact FGF core domain.

IV. I. 2 The allele *ths*^{759}

The single mutant allele *ths*^{759} represents the allele of the largest chromosomal deletion obtained from all P-element excision events tested and created a lesion within the gene of approximately 2,5kb.. In *ths*^{759}, all of the conserved amino acids of the FGF core domain are removed. Because at present, a specific antibody against Ths is not available, the expression of a mutant protein could not be tested by immunohistological or biochemical methods. The possibility of a rudimental activity of the protein via the remaining N-terminal 23 amino acids of the FGF core domain to bind to the receptor, to heparin proteoglycans and for glycosylation is rather unlikely, and *ths*^{759} was therefore identified as a functional null allele of *ths* (Klingseisen et al., 2009).

IV. I. 3 The allele *pyr* ^{18}

In case of *pyr*, imprecise excision of a P-element inserted proximal to the transcription start resulted in a complete deletion of the gene (Gryzik, 2005). In situ hybridisation using a probe against *pyr* mRNA furthermore showed that no transcript is present in *pyr*^{18} single mutants (data not shown). Thus, the allele *pyr*^{18} represents a null allele of *pyr* (Gryzik and Müller, 2004). In situ hybridisations with *ths* and *pyr* antisense probes on either *pyr*^{18} or *ths*^{759} homozygous mutant embryos confirmed that the expression of *ths* and *pyr* is not mutually influenced but shows the same strength and pattern of expression as observed in wild-type (Kadam et al., 2009; Klingseisen et al., 2009: S1 appendix 1). The expression of the Htl ligands thus is regulated independently in distinct expression patterns (Gryzik et al., 2004; Stathopoulos et al., 2004; Klingseisen,

2005; Kadam et al., 2009), which indicates a first hint that despite having a common ancestor and early overlapping expression domains, *ths* and *pyr* are assigned to different functional activity. On the other hand, if functional redundancy is addressed, for instance to gain robustness for providing an essential signal, independent regulation of expression could ensure that loss of either *ths* or *pyr* function does not cause deleterious consequences.

IV. I. 4 Comparison of currently available ths^{759} and pyr^{18} alleles

In a previous, recent study two other mutant alleles of *ths* and *pyr* carrying transposon insertions were identified, ths^{02026} and pyr^{02915}, and two chromosomal deletions uncovering either *ths* or *pyr*, *Df(2R)ths238* and *Df(2R)pyr36* (Kadam et al., 2009). The *ths* allele ths^{02026} was reported to have a reduced expression of the gene, but was otherwise normal with respect to expression of mesoderm markers. Genetic complementation analysis with ths^{759} and pyr^{18} of the transposon associated alleles ths^{02026} and pyr^{02915} (S2, S3 appendix 1) supports the view that ths^{02026} and pyr^{02915} represent hypomorphic alleles. Both ths^{02026} and ths^{759} exhibit no defects in pericardial cell specification indicating normal mesoderm spreading into dorsal regions (Shishido et al., 1997), but the viability of homozygous mutant flies is clearly decreased in ths^{759} compared to ths^{02026} (3,5% to 17%).

Strikingly, flies that are trans-heterozygous for ths^{02026} and ths^{759} are to 72,7 % viable. This suggests, that both alleles lack sequences important for a fully functional FGF protein, but maintain a rudimental function different from each other. This might indicate that both alleles of *ths* result in partially functional FGF proteins, that in combination are able to restore most of Ths functions during development, and thus act in a way as two different isoforms of the protein. Moreover, this supports the idea that *ths* might actually occur in different splice-forms, and that the C-terminal domain,

which is mostly retained in *ths*^{759} in contrast to the FGF core, may encode domains not identified so far. As viable *ths*^{759} homozygous mutants only occur at 3,5% of the homozygous fraction from a heterozygous cross, the lack of a functional FGF core domain hence seems to be of higher influence to a loss of Ths function than putative C-terminal domains. Because *ths*^{02026} nevertheless exhibits a higher viability in homozygousity and complements the high lethality of *ths*^{759} homozygous flies, *ths*^{02026} is assumed to be a hypomorphic allele, whereas *ths*^{759} represents a loss of function allele. Furthermore, *ths*^{759} was generated by deletion of coding sequence. *ths*^{02026} by contrast carries a transposon insertion, the exact influence of which on *ths* transcription and Ths function is less clear.

It is unlikely that the transposon associated allele *pyr*^{02915} represents a null allele, because the loss of dorsal mesoderm derivatives indicate defects in mesoderm development in *pyr*^{18} single mutants, which are partially rescued in *pyr*^{18} / *pyr*^{02915} trans-heterozygous embryos. The viability of these flies is increased to 34% compared to >1% of viable *pyr*^{18} homozygotes, thus partially complementing the *pyr*^{18} null phenotype. This is also supported by analysis of *pyr* mutant phenotypes in glial development by Franzdottir et al., 2009. Here the mutant phenotype caused by *pyr*^{02915} is enhanced in embryos trans-heterozygous for *pyr*^{02915} and a deficiency removing both FGF genes, which was also seen for the transposon associated allele of *ths*, *ths*^{02026}.

The chromosomal deletions *Df(2R)ths238* and *Df(2R)pyr36* uncover the loci of *ths* and *pyr*, respectively, but do not represent clean single mutant alleles as they also delete neighboring genes within their ~100kb extended lesions (Kadam et al., 2009). Observed effects thus might be also the result of uncharacterized interfering phenotypes of these additional gene deletions, and cannot account for a clean single mutation of either *ths* or *pyr*. Comparison of the reported phenotype of embryos homozygous for the deficiency

Df(2R)ths238 and ths^{759} homozygous mutants however reveals no drastic differences in expressivity. Conversely, the *Df(2R)ths238* causes no defects in mesoderm differentiation as all pericardial cell clusters are specified as in wild-type (Kadam et al., 2009). Later defects in muscle development or neuronal cell fate were not reportedly tested for *Df(2R)ths238*, and thus cannot be compared to ths^{759}. Conclusively, with regard to mesoderm spreading and pericardial cell fate differentiation, the single mutant allele ths^{759} shows the same phenotype as the deficiency *Df(2R)ths238* which deletes the complete *ths* locus. Thus, the allele ths^{759} represents a loss-of-function allele, and the defects observed in ths^{759} single mutants are specific for loss of *ths* function.

The comparison of pyr^{18} to the deficiency *Df(2R)pyr36* indicates that *pyr* expression might not be completely deleted in *Df(2R)pyr36* as it was suggested by Kadam et al., 2009. At some level, *pyr* transcript still seems to be present, and the phenotype in pericardial cell specification (8 out of 11 clusters are missing) is weaker than in pyr^{18} single mutants lacking all 11 pericardial cell clusters.

Conclusively, the alleles analyzed in this study are clean single mutants of *ths* and *pyr*. pyr^{18} represents a mutant null allele. ths^{759} is a functional null allele and to 96,5% homozygous lethal, but the complementation cross to the transposon associated line ths^{02026} indicates that in ths^{759}, some function of *ths* may be retained which has to be noted. A complementation cross of ths^{759} and *Df(2R)ths238* would be required to test this hypothesis. The 100% lethality of the deficiency containing *ths* should be rescued to some extent, if ths^{759} remains certain functionality.

IV. II Regulation of mesoderm spreading by *ths* and *pyr*

IV. II. 1 Initial formation of adhesion contacts are connected to MAPK activation

htl as well as *ths* and *pyr* mRNAs are expressed zygotically from stage 5 of embryogenesis as the mesoderm is specified, prior to mesoderm invagination (Gryzik and Müller, 2004; Stathopoulos et al., 2004; Klingseisen et al., 2009; S1, appendix 1). However, mesoderm invagination is not dependent on Htl signalling, and *htl* mutant embryos or Df^{2238} homozygotes lacking both Htl ligands exhibit no defects in invagination (Beimann et al., 1996; Gryzik and Müller, 2004; this study). The first defects in mesoderm morphogenesis in FGF pathway mutants are seen in flattening of the mesodermal epithelial tube against the underlying ectoderm and the initial establishment of cell contact (Schumacher et al., 2004). Cells at the ventral-most positions actively seek contact with the ectoderm by exhibiting cellular extensions. Upon contact formation, these cells display MAPK activation (Wilson et al., 2005). The current model places the initiation of an epithelial-to-mesenchymal transition (EMT) subsequent to this initial event of contact formation (Wilson et al., 2005).

During EMT, epithelial cell–cell junctions are disassembled and the actin cytoskeleton is reorganised to be accessible for dynamic changes in response to external stimuli. Consequently, adhesion to neighbouring cells becomes more dynamic while focal adhesions with the extracellular matrix are established to allow movement of the mesenchymal cells. In the absence of Htl signalling, the formation of an initial ectodermal contact is not established, and MAPK is not activated (Schumacher et al., 2004; Gryzik et al., 2004). Similarly to embryos lacking the FGF receptor, embryos deficient for *ths* and *pyr* exhibit defects in establishing a mesenchymal cell shape and dynamic cell-cell connections. Consequently, the mesoderm cells fail to disaggregate

properly and fail to attach symmetrically to the basal surface of the ectoderm cells. Thus, the formation of these initial contacts to the ectodermal cell layer appears to be a crucial event marking the 'start-point' of mesoderm migration. However, the transition from an epithelial cell shape to a motile mesenchymal state is not inhibited in absence of Htl per se (Schumacher et al., 2004). Apical adherens junctions (AJs), a hallmark of epithelial integrity, are lost from mesoderm cells and immunolabelling of E-Cadherin and β-catenin confirmed that their typical epithelial polarized distributions were rearranged. It was therefore concluded that the htl^{AB42} mutant phenotype was associated with a disability of the mesoderm cells to acquire a mesenchymal cell shape, e.g. to remodel the cytoskeleton subsequently and establish new contacts of adhesion (Schumacher et al., 2004: Smallhorn et al., 2004).

Analysis of ths^{759} or pyr^{18} single mutants revealed that deletion of one ligand alone does not result in similarly severe defects. Only the deletion of both Htl FGF ligands resembles the defects in mesoderm spreading as observed in embryos lacking the receptor. Thus, Ths and Pyr act in concert during this early phase to provide the essential signals. Both *ths* and *pyr* are expressed in an overlapping lateral domain in the ectoderm at this stage, which might indicate a redundant function during this process. This expression pattern might indicate that both ligands accomplish a sufficient activation of the FGF pathway in absence of the other FGF, in order to ensure the proper disintegration of the internalised epithelial mesoderm and the formation of ectodermal contacts. A second possibility would imply individual functions of Ths and Pyr, but the mutual ability to substitute for each other. Third, Ths and Pyr might induce different cellular responses each essential for mesodermal tube collapse and acquirement of mesenchymal characteristics. In either case, the collapse of the mesoderm onto the ectoderm appears to be regulated by both Ths and Pyr.

Strikingly, the single mutant analysis revealed that the activation of MAPK in the cells establishing the initial contact to the surface of migration is exclusively dependent on Pyr mediated Htl signalling. MAPK activation in mesoderm cells was strongly reduced in pyr^{18} homozygotes while loss of *ths* function had no effect on MAPK activation throughout embryogenesis,. This specific activation of MAPK however has no effect on mesoderm migration per se, as the collapse of the tube and cell spreading occurred in ths^{759} mutants nevertheless. In addition, the activation of MAPK upon initial cell contact appears to be regulated differently to MAPK activation in leading edge cells during later phases of mesoderm spreading. A first evidence for this idea is provided by analysis of embryos mutant for the RhoGEF encoding gene pebble *(pbl)*. *pbl* mutants show a phenotype resembling the defects observed in htl^{AB42} mutant embryos during the initial phase of ectoderm attachment (Schumacher et al., 2004). Distinct from its function to activate Rho during cytokinesis, Pbl is required for acquiring mesenchymal characteristics and spreading (Schumacher et al., 2004). As observed in pyr^{18} mutants, MAPK is not activated during the initial phase in *pbl* mutants, indicating that contact establishment and MAPK activation in the mesoderm is connected (Wilson et al., 2005). Moreover, cells that were able to make contacts in later phase spread out in directed movement and cells at the leading edge of the mesoderm showed activation of MAPK and hence the FGF signalling pathway as in wild-type (Smallhorn et al., 2004; Schumacher et al., 2004). Recent findings show that Pbl is required for activation of the small GTPase Rac during mesoderm migration and that a C-terminal domain may be involved in localising Pbl to the membrane and shift its activity from Rho to Rac activation (van Impel et al., 2009). These data are consistent with the major role for Rac in leading cytoskeleton modulation at the leading edge of migrating cells (Raftopoulou and Hall, 2004).

The mutant phenotype of *pbl* in comparison to *ths, pyr* deficient mesodermal defects shows that Htl signalling may act upstream or in parallel to Pbl, as Htl mediated MAPK activation occurs in absence of *pbl*. Importantly however with regard to Ths and Pyr function, these findings show that the initial activation of MAPK in the mesoderm is dependent on Pyr-mediated cell contact formation, and that later ectoderm attachment restores Htl activation resulting in activation of the MAPK signalling cascade. These findings are confirmed by the result that some mesoderm cells in pyr^{18} single mutants that managed to establish contact to the ectoderm showed activated MAPK. However, this also demonstrates that Pyr function is not entirely essential for contact formation, but might be required to regulate or facilitate proper initiation of cell adhesion. If MAPK activation is required for mesoderm migration hence remains elusive, as mesoderm cells are capable to spread out in pyr^{18} single mutants. Although early migration is compromised by uneven attachment to the ectoderm and imperfect formation of a monolayer in later stages, these defects are only minor compared to the deranged appearance of the mesoderm collective in embryos lacking both FGFs.

Thus, both *ths* and *pyr* seem to provide a signal for mesoderm cells to attach to the basal ectodermal surface and spread out laterally. These signals rather are not redundant as loss of Pyr mediated MAPK activation cannot be compensated by Ths, subsequent attachment by contrast is restored after the cells establish contacts after the initial phase following invagination. Mesenchymal properties are acquired in FGF single mutant embryos in contrast to embryos lacking *htl* or *pbl*, thus either Ths or Pyr are sufficient for the required cell shape changes to become motile.

In wild-type embryos, all mesoderm cells are observed to extent filopodia almost immediately after the mesoderm epithelium has been internalised, even prior to the collapse of the epithelial tube (Wilson et al., 2005; this study). These protrusions are lost in absence of *pyr*, but not in ths^{759} single mutants. Pyr-mediated FGF signalling thus

activates protrusive behaviour of mesoderm cells, which is a first event in the process of acquaintance of a mesenchymal state. Pyr function hence is required to initiate active cellular behaviour to establish new adhesion contacts to further proceed in the process of transition from epithelial cell-cell contacts to more dynamic cell-substratum adhesiveness essential for migration. Activation of Htl initially might not result in activation of the MAPK signalling cascade, but in membrane remodelling and cytoskeletal changes which lead to the formation of cell protrusions. This would support the model of Wilson et al. (2005), who propose that initial contact provides a signal to trigger cytoskeletal changes and releases the inhibition of MAPK activation by further activation of the FGF receptor. Pyr-mediated adhesion thus is followed by further transition to a motile mesenchymal fate and a regulated, symmetric tube collapse as well as ectodermal attachment in early lateral movement. Contact to the substrate of migration and activation of MAPK thus appears to provide the required signals for the mesoderm to complete the transition from a specified group of epithelial cells to a motile mesenchymal cell collective.

Further, all components of the Htl/FGF signalling pathway are expressed prior to mesoderm invagination (Gryzik and Müller, 2004; Stathopoulos et al., 2004; Klingseisen et al., S1 appendix 1; Klingseisen, 2005, diploma thesis). Conversely, mesoderm invagination is impaired upon over-expression of a truncated form of Pbl lacking its protein-protein interaction domains (van Impel et al., 2009). Over-expression of *pyr* causes invagination defects at lower penetrance. With regard to the Htl receptor, no published data can be found reporting defects in mesoderm invagination (NCBI/pubmed). However, in situ hybridisations clearly showed expression in the nurse cells in egg chambers from stage 10 (Klingseisen, 2005, diploma thesis). Nurse cells in the *Drosophila* ovary produce mRNAs and proteins that are sequestered in the oocyte (Gilbert, 2000). Data on the phenotype of *htl* mutant germline clones, which would lack

maternally provided *htl* mRNA, were not yet reported. It might therefore not be impossible that maternal Htl is present in zygotic mutants, which would then rescue early-required function.

The formation of cellular extensions requires polarisation and structural changes of the membrane, such as E-cadherin redistribution and polymerization of actin bundles at the newly formed leading edge of the cell (Webb et al., 2002; Friedl, 2004). The mesoderm tube invaginates by apical constriction of the ventral most cells (Leptin, 1999; Leptin, 2005) and thus, the cellular leading edge extending filopodia has to be established at the former basal side. The imaging data presented here show that the mesoderm cell initiates contact formation most likely.

Because short filopodia are already discernible before the epithelial tube collapses in wild-type, but not in pyr^{18}, *ths, pyr* deficient, *pbl* or *htl* mutant embryos, Htl signalling appears to be activated at this stage. Further, the presence of filopodia indicates that the basal membrane of the mesoderm cells already is being remodelled and the cells start to acquire mesenchymal characteristics. Thus, the Pyr-mediated Htl-signal first seems to initiate subtle cell shape changes, which lead to a mechanic weakening of the cell cortex and allow the extension of a protrusion, and further receptor activation and attachment to the ectoderm result in activation of MAPK. Additionally, this could involve a short-range signal, creating a decreasing gradient between the secreting ectoderm cells and the mesoderm tube from ventral-lateral to medial. In this case, the mesoderm cells would extend protrusions towards the source of the FGF ligand to sense the position of the substrate they have to attach to. Such behaviour reminds of the mechanism, where leader cells protrude into direction of the source of a chemo-attractive ligand. Examples for this mechanism are well-characterised during border cell migration or tracheal development, the process of dorsal closure where cells seek to contact the cells of the matching opposite segment, single cell migration towards a chemo-attractant in general

or axonal outgrowth of motor-neurons to muscles (Friedl, 2004; Cabernard and Affolter, 2005; Rorth, 2007; Prasad and Montell, 2007; Ng et al., 2004, 2008; Weijer, 2009).

IV. II. 2 Possible signalling mechanisms to induce cell shape changes in mesoderm cells

Htl signalling is important for contact establishment of mesoderm cells to the ectoderm. How the signalling pathway transmits signals to induce cell shape changes is unclear. After mesoderm invagination, Htl is activated by Ths and/or Pyr, which are expressed in overlapping lateral domains. Activation of Htl might induce a decrease in cell-cell contact and membrane cortical stability. These changes then might facilitate further reorganisation of the cytoskeleton resulting in formation of cellular protrusions and cell contacts. Possible mechanisms to mediate cytoskeletal reorganisation in response to Htl activation might be similar to mechanisms during axon outgrowth and glia development, where the Htl signalling pathway is involved in (Shishido et al., 1997; Garcia-Alonso, 2000; Klämbt et al., 2001; Franzdottir et al., 2009). The comparison to vertebrate models further provides a possible mechanism to interconnect Htl signalling with other pathways such as Wnt signalling (Tsai et al., 2007). Rho and Rac signalling, and engagement of the Ras related GTPase Rap1 are candidate mechanisms to function downstream of Htl/FGF signalling in these processes.

IV. II. 2. 1 The comparison to glial development reveals a possible engagement of the Ras related GTPase Rap1

ths and *pyr* are expressed in a subset of neuroblasts and *htl* is expressed in glial cells (Shishido et al., 1997; Klämbt et al., 2001; Gryzik and Müller, 2004; Stathopoulos et al., 2004; Franzdottir et al., 2009; Klingseisen et al., 2009, S1 appendix 1). The Htl/FGF

signalling pathway recently was analysed during glial cell migration in the eye imaginal disc (Franzdottir et al., 2009). The mechanism of signal transduction revealed during glial development might also be applicable to Htl signalling in mesoderm development. Glial cells have to migrate towards a neuronal axon, establish contact and differentiate in a process of wrapping around the neuronal axon. Htl is expressed in glial cells, and the process of migration was found to be dependent on Htl signalling mediated by Ths through the G protein Rap1 (Franzdottir et al., 2009). Activation of the Ras proteins present in *Drosophila* (Ras85D and Ras64B) in contrast were dispensable for this process, but required for differentiation of the glial cell upon contact formation with the respective axon.

Epithelial cell shape and migration during embryogenesis are mediated through Rap1 interaction, which acts both via integrin and cell-cell contacts (Boettner and van Aelst, 2007, 2009). Rap1 can function as a mechano-sensor and facilitate the turnabout between cadherins and intergrin, and was identified to recruit Rac GEF to the membrane to promote cell spreading (Arthur et al., 2004; Balzac et al., 2005; Retta et al., 2006). Mesoderm invagination in *Drosophila* was also shown to be dependent on Rap1 function, as invagination is severely impaired in Rap1 mutants (Asha et al., 1999). A differential regulation via Ths and Rap1 on one hand and Pyr and Ras on the other hand might be a hypothesis that suggests a very attractive model for mesoderm migration. Initial contact formation requires Pyr function, but if contact can be established, dpERK is displayed in mesoderm cells in absence of Pyr. The activation of MAPK in absence of Ths might be due the activation of Rap1 in parallel to Ths induction through contact formation, which is provided by Pyr/Htl signalling.

The requirement of Rap1 during gastrulation is also known from vertebrate models. In zebrafish, the pathway activating Rap1 during gastrulation is regulated by Wnt signalling and Casein kinase Iε (CKIε) (Tsai et al., 2007). Interestingly, Wnt D (the

Wnt8 homolog) is expressed in the *Drosophila* mesoderm regulated by the Dorsal (Dl) gradient (Ganguly et al., 2005; Hong et al., 2008), and CKIε *(discs overgrown, dco)* was identified to promote both Wnt-Fz/beta-catenin and Fz/PCP signaling in *Drosophila* (Klein et al., 2006). Interaction of WntD, Dco and Rap1 might thus also play a major role during gastrulation in *Drosophila*.

An important effector of Rap1 signalling is the Afadin-6 homolog Canoe (Cno) (Boettner et al., 2003). Cno regulates the linkage of the actin cytoskeleton to adherens junctions during apical constriction of epithelia in *Drosophila*, including the invaginating mesoderm (Sawyer et al., 2009). Cno was also found to link the pathways of Ras-MAPK, Notch and Wnt signalling by direct interaction with Ras, Notch and Dishevelled during later differentiation of mesodermal progenitors (Carmena et al., 2006). Thus, taken together, a possible involvement of FGF/Htl signalling in the mesoderm in regulation of Rap1 in mutual interference with Wnt signalling is tempting to speculate. Supporting this idea, the Rap PDZ-GEF is present in the mesoderm and maternally provided in large amount prior to zygotic onset of transcription (Boettner and van Aelst, 2007). Moreover, a regulation of cytoskeletal organization and membrane stability provides a possible function of Ths/Pyr-mediated Htl signalling for EMT- and potentially also in reverse to regain epithelial character, which might be important in differentiation of mesoderm cells after spreading is complete.

IV. II. 2. 2 Rho and Rac signalling in mesoderm cells might involve the regulation of LIMK via effector kinases

The formation of protrusions and adhesion contacts might be controlled via regulation of activity of the Rho associated kinase Rok (the homolog of vertebrate ROCK). Rho-Rok signalling is known to control epithelial cell polarity, cell-cell adhesion, cell-substratum adhesion and actin cytoskeleton organization (Jaffe and Hall, 2005; Ridley,

2006). The analysis of axon growth of motor-neurons to innervate somatic muscles shows that via Rho and Rac activation, the activity of LIM kinase (LIMK1 in *Drosophila*) is regulated to induce cytoskeletal changes resulting in formation of protrusions and focal adhesion contacts (Ng et al., 2004, 2008). LIMK phosphorylates Cofilin (the unique gene *twinstar (tsr)* in *Drosophila*) to inhibit its function. Tsr promotes the rapid turnover of actin filaments through severing filamentous actin (F-actin) and depolymerizing actin filaments from the pointed ends (Bamburg et al., 1999; Ng et al., 2004). The RhoGEF Pbl has been identified to interact genetically with LIMK activity (Ng et al., 2004). Inducing one mutant copy of *pbl* suppressed the LIMK1 overexpression phenotype, indicating that Pbl positively regulates LIMK activity. In regulation of LIMK1, Rho1 activity is dependent on RhoGEF2 activation, in similarity to Rho1 signalling during mesoderm invagination (Dawes-Hoang et al., 2005; Kölsch et al., 2007; Ng. et al., 2008). The regulation of RacGEFs involved in LIMK activity in contrast is unclear (Ng et al., 2008). Similarly, the regulation of Pbl's function in the context of FGF signalling is unclear in mesoderm cells.

It is shown that Pbl is essential for mesoderm migration apart from its role in cytokinesis (Schumacher et al., 2004). Structure function analysis showed that Pbl genetically as well as *in vitro* interacts with the small GTPase Rac in addition to its GEF activity for Rho during cytokinesis (van Impel et al., 2009). Rac is known to be essential for controlling actin dynamics and cell adhesion induced by chemoattractants such as growth factors (Etienne-Manneville and Hall, 2002; Raftopuoluo and Hall, 2004; Schiller, 2006). Pbl might thus be the important factor to transmit the signal of Htl/FGF via Rac into reorganisation of cell cortex and the formation of protrusions (van Impel et al., 2009). The regulation of actin-cytoskeletal dynamics by Pbl might be upstream of LIMK1, but in parallel to or antagonizing Rho-Rok signalling. In this context, studies from fibroblasts are interesting that showed a competition of the Pbl

homolog Ect2 and p190RhoGAP in regulation of RhoA activity (Lim et al., 2008). Conversely, the Rho-Rok dependent LIMK1 activation observed in neuronal development is antagonized by p190RhoGAP (Ng et al., 2004).

Conclusively, Pyr-mediated activation of Htl might activate Rho-Rok-signalling, which in turn activates LIMK1 to induce the formation of filopodia and adhesive contacts. In regulation of Rho activity, Pbl might be regulated to mediate the signal to activate Rac at the leading edge of mesoderm cells. In this model, the signal strength or duration of Htl/FGF signalling might indirectly influence Pbl activity towards Rac activation by mediating levels of activated Rho1 via other RhoGEFs such as RhoGEF2. The properties of Rap1 to recruit RacGEFs to the membrane and also activate RhoGAPs, as shown in vitro and neurite outgrowth (Arthur et al., 2004; Yamada et al., 2005), might be interesting to incorporate in a hypothetical model of regulation via Ths and Pyr. Pyr might induce activation of Rho-Rok-LIMK1 activation, which results in extension of initial protrusions. Upon contact formation promoted by Ths, Rap1 activity then might lead to a switch from predominant Rho- to Rac signalling, resulting in formation of leading edge protrusions. Thus, adhesion and Rap1-signalling might be facilitated by Ths, thereby regulating Rho and Rac activity in the cell dependent on Htl-activation by Pyr.

IV. II. 2. 3 Dof and Cdep as possible regulators of Rho / Rac and Rap1 signalling of the Htl/FGF signalling pathway

In response to activation of Htl, possible candidates to mediate the signal to activate Rho and Rac signalling is the adaptor protein Dof, which is essential for FGF signal transduction in *Drosophila* (Imam et al., Vincent et al., 1999; Petit et al.,2004, Wilson et al., 2004; Sandmann et al., 2006). Dof is phosphorylated by Htl upon activation and auto-phosphorylation and directly binds to the FGF receptor (Battersby et al., 2003;

Wilson et al., 2004). Cdep was identified in a yeast-two-hybrid screen as a putative binding partner of Dof and represents an excellent downstream effector of the Htl pathway (Battersby et al., 2003).

Cdep is a protein containing a FERM (band 4.1, ezrin, radixin, moesin (FERM) protein family) domain and an additional RhoGEF domain, and can be activated by PKA or PKC (Protein kinase A or C, respectively) (Koyano et al., 1997; Baines, 2006). Proteins from the band 4.1 family are known to regulate interactions between integral plasma membrane proteins and the cytoskeleton (Sun et al., 2002), and among other functions are also involved in regulating cell cycle progression and proliferation, establishment of cell polarity, cell motility, and/or cell-to-cell communication (Nakamura et al., 2000; Diakowski et al., 2006). Cdep however is not well characterised with regard to its binding affinities and function in a developmental background of embryogenesis. Thus far it was best characterised by in vitro analysis and studies of cell cultures of chondrocytes (hence the name, chrondrocyte-derived ezrin-like protein) (Koyano et al., 1997). Cdep was identified to catalyse the GDP-to-GTP exchange of RhoA and to induce cell differentiation when the GEF was removed (Koyano et al., 2001). This implicates that Cdep might be involved in transducing signals from growth factors in regulation of cell fate. The expression of *Cdep* in mesoderm cells in *Drosophila* is only low in early stages and becomes enhanced during later phases of development (BDGP, *flybase*). This does not exclude a potential function of Cdep in establishment of initial contact and protrusion formation might because it be restricted only in leading edge cells of the mesoderm. Cdep might also be involved in later differentiation processes of mesoderm cells.

Another binding partner of Dof identified in the screen is β-spectrin (Battersby et al., 2003; NCBI/pubmed). This might provide a direct link of Htl/FGF signalling to regulate the mechanical properties of the cell cortex. As proteins from the 4.1 band family such

as Cdep are known to build ternary complexes with spectrin, actin and adducin (*Drosophila huli-tai-shao, hts*), a possible mechanism emerges to regulate the spectrin-actin network in direct response to FGF/Htl signals (Manno et al., 2005; Diakowski et al., 2006). Apart from LIMK1, another target of Rho-Rok signalling in regulation of cytoskeletal reorganization is adducin/Hts (Burridge and Wennerberg, 2004). Roles for Rok in tissue morphogenesis during *Drosophila* development were reported (Verdier et al., 2006). In response to activation through Htl, Dof might be able to form a membrane-associated complex of proteins, which might control the regulation of membrane mechanics and cytoskeletal organisation. With regard to the activation and regulation of Rho-Rok signalling, a balance of signalling via Ths and Pyr might control pathways, which might induce the coordinated cell shape changes of mesoderm cells during spreading.

The regulatory mechanism proposed here might also provide a possible function of Ths/Pyr-mediated Htl signalling for EMT- and potentially also in reverse to regain epithelial character, which might be important in differentiation of mesoderm cells after spreading is complete.

IV. II. 3 Mesoderm migration

IV. II. 3. 1 Adhesion of mesoderm cells to the ectoderm is important for mesodermal cell fates and regulated by Ths and Pyr mediated Htl signalling

Differential adhesion between neighbouring cells of similar or different commitment or between cells and the extracellular matrix is a major mechanism in morphogenetic processes during embryogenesis. Cell behaviour during cell migration can be regulated through adhesive properties of the cells and their environment. Moreover, adhesion to ECM proteins such as integrins is a crucial characteristic for many cell types for survival (Worth and Parsons, 2008; Lim et al., 2008). Recent findings revealed a direct

connection between integrin signalling and apoptotic consequences when integrin contacts are lost, which is mediated by focal adhesion kinase (Fak) and p53 (Foley, 2008; Cance and Golubovskaya, 2008).

Mesoderm cells in *Drosophila* were also observed to require adhesion for survival (Müller and Hay, unpublished). Attachment to the ectoderm as substrate for mesoderm migration therefore could be a crucial aspect for each mesoderm cell. The formation of a cellular monolayer hence would be a prerequisite for further as well as maintained development of each mesoderm cell and provide the possibility to differentiate in response to signals emitted from the ectoderm. A functional model of contact formation towards locally restricted FGF ligands thus is attractive. Functional divergence between Ths and Pyr might provide the promotion of different cell responses even in overlapping expression domains. Ths might be an attractive signal for the mesoderm cells and provide the information where to adhere to, that is to the ectoderm and not to endodermal tissues as the midgut for instance. The broad, ventral-lateral expression pattern of *ths* within the ectoderm distinctly excludes the most ventral region. FGF signalling via Ths might thus determine the migratory zone for mesoderm cells. Pyr function in turn might be required for polarization of the cells into dorsal direction. In addition, Pyr-mediated Htl signalling might control the differentiation status of the mesoderm cell receiving the signal.

Ths might be involved in regulation of adhesive conditions during mesoderm migration

In line with a role for Ths to promote ectodermal adhesion, a recent study from Kadam et al. (2009) showed that mesoderm cells stick to ventral regions upon ectopic expression of *ths* in the most ventral ectoderm cells. Adhesion in addition providing a pro-survival feedback signal might lead to inhibition of apoptotic regulators within the displaced mesoderm cell. Another possibility would Ths assign to stimulate the

secretion of components of the ECM by mesoderm cells. This might be important for symmetric and proper adhesion of the mesoderm to the ectodermal cell layer. FGF2 for instance was identified to stimulate fibronectin expression in osteoblasts (Tang et al., 2007). The modulation of cell adhesion was also shown as a regulator of migration by establishing migratory zones of different adhesive properties via modulation of cadherin-mediated cell adhesion (von der Hardt et al., 2007). Interestingly, studies on cultured human cancer cells showed that TGF-β signalling involving Rho and the FERM-RhoGEF FARP, could switch the cells from cohesive to single cell motility (Giampieri et al., 2009). A similar mechanism might be possible in mesoderm cells. Ths mediated Htl signalling through Rho and the FERM-RhoGEF Cdep might be modulated by TGF-β/Dpp (the *Drosophila* TGF-β homolog) signalling. Dpp is expressed in dorsal ectoderm domains, and reportedly forms gradients throughout the region of signal receiving cells (Frasch, 1995; Fujise et al., 2003; Belenkaya et al., 2004; Affolter and Basler, 2007; Akiyama et al., 2008). The Dpp gradient in addition is very precise with regard to induction of cellular response (Bollenbach et al., 2008). Such modulation by Ths and Dpp signalling might provide instructive cues for the migration of the mesoderm collective. Ectodermal attachment, cohesion and motility might be regulated in a fine tuned balance of Ths and Dpp signalling to ensure optimal conditions for mesoderm spreading.

ths^{759} single mutants controversially show no defects in formation of initial contacts, but only slightly later in even attachment during early migration. This phenotype contradicts an essential chemo-attractive function of Ths for ectodermal adhesion of mesoderm cells. On the other hand, the slight defects observed in symmetric alignment and lateral distribution related to the ventral midline support the idea of a balanced interaction of Ths/Htl and Dpp signalling. In absence of Ths, the presence of Dpp might be sufficient for mesoderm attachment, but even spreading is not robust.

Pyr controls dorsal polarisation of mesoderm cells and might be required in regulation of early mesoderm fate commitment

The early function of Pyr might be to provide directional guidance cues for mesoderm cells into dorsal direction. The initiation of lateral migration is disturbed in pyr^{18} single mutants, as outlined above. Additionally, Pyr is required for the differentiation of dorsal mesoderm cells to pericardial cells later in embryogenesis (Gryzik and Müller, 2004; Stathopoulos et al., 2004; Kadam et al., 2009; Klingseisen et al., 2009). For this reason, Pyr might additionally regulate the cellular response to signals determining the differentiation status of the cell. Mesoderm cellular fate commitments possibly are controlled onwards from very early phases of mesoderm spreading. Misexpression of *pyr* in the ventral midline in embryos lacking endogenous *ths* and *pyr* expression caused a strong migration phenotype as reported by Kadam et al. (2009). The mesoderm cells pile up along the ventral midline and fail to form a monolayer. The authors suggest a chemo-attractive role of Pyr to explain this phenotype. Contradictory to this suggestion, the mesoderm migrates in directed movement into dorsal direction in absence of *pyr*, indicating that *pyr* is not essential for directed migration. The influence of Pyr-mediated Htl signalling on cell migration additionally was found to be of short range during glial cell migration on the eye imaginal disc (Franzdottir et al., 2009). Cells not in direct contact to the ectoderm or not in immediate proximity thus might not receive levels of Pyr high enough to stimulate a cellular response. Last, ectopic expression of *pyr* in a single segment did not influence the direction of migration of mesoderm cells in neighbouring segments *pyr* was not expressed in ectopically. A classic chemo-attractive role therefore is rather unlikely. The phenotype caused by ventral misexpression of *pyr* in a *ths, pyr* deficient background as shown by Kadam et al. (2009) therefore could be the result of an inherent pool of mesoderm cells. Only the cells not in contact to the ectodermal substrate remain in ventral positions and fail to migrate, strongly suggesting

that other factors are involved to direct the migrating mesoderm dorsally. By contrast, activation of Htl and ectodermal expression of the Htl ligands is required for mesoderm cells to seek ectodermal contact. Additionally, missing Htl activation by Pyr might keep these cells in an intermediate state of differentiation in resemblance of the *pyr*^{18} mutant condition. Mesoderm differentiation is severely impaired in absence of *ths* and *pyr* and progenitors fail to be specified (Gryzik and Müller, 2004; Stathopoulos et al., 2004; Klingseisen et al., 2009). Equally, mesoderm migration is impaired in absence of Htl signalling and the defects observed resemble the phenotype described for ectopic ventral expression of *pyr*. Thus, mesoderm cells that lack Pyr-mediated Htl signalling do not initiate the formation of substrate contacts and additionally fail to differentiate to give rise to mesodermal derivatives.

Previous studies consistently suggested that lack of the expression of differentiation markers such as Eve in embryos lacking components of the Htl/FGF pathway occur as a result of imperfect dorsal migration towards dorsal-most regions of the ectodermal margin (Beimann et al., 1996; Gisselbrecht et al., 1996; Shishido et al., 1997). Differentiation signals such as Dpp thus cannot be received and dorsal derivatives failed to be specified. To support this model, ectopic expression of *dpp* in all mesoderm cells of *htl* homozygous mutant embryos restored the expression of differentiation markers (Gisselbrecht et al., 1996; Michelson et al., 1998). The expression of transcription factors at the top of the hierarchy that pattern the mesoderm such as Myocyte enhancing factor-2 (Mef-2) and Tinman (Tin) is directly induced by Twist independent of FGF signalling (Sandmann et al., 2006, 2007). Therefore, the cells may already be committed to a general progenitor fate and competent to respond to further differentiation signals. Ectopic expression of Dpp under the control of the *twi* promotor, thus, would induce the normal response of otherwise dorsally positioned cells. That is, the specification of cell fates of cardiac, pericardial or dorsal somatic muscle progenitors. The expression of Eve

in mesoderm cells of those embryos however was not reportedly tested, which leaves room to speculate, that further differentiation may still require FGF signalling. Additionally, all cells within the ectopic expression domain expressed the induced differentiation markers not the response intended in wild-type embryos. This supports the hypothesis of a general "pre-progenitor" state of all mesoderm cells, which would further imply that later commitment to differentiate into a specific lineage is mediated by Pyr/Htl signalling.

In conclusion, a model can be proposed where Ths establishes the zone of migration for mesoderm cells, e.g. the ectoderm and stimulates the adhesion to the substrate. Pyr induces the initiation of active contact formation of mesoderm cells to the ectodermal substrate and further regulates the differentiation of derivative mesoderm lineages. The concerted function of Ths and Pyr thus might render mesoderm spreading robust and Ths and Pyr individually are sufficient to ensure mesoderm spreading per se.

IV. II. 3. 2 Influence of Htl signalling in response to Ths and Pyr on the phasing of migration and proliferation intervals during mesoderm spreading

Mitotic activity of mesoderm cells has to be tightly regulated, as uncontrolled cell divisions would be incompatible with directed collective movement. Inhibition of mitoses has no influence on mesoderm migration (Schumacher et al., 2004), but deletion of inhibitive regulators such as the RNA binding protein How or the putative serine/threonine kinase Tribbles cause severe defects during invagination and migration (Seher and Leptin, 2000; Toledano-Katchalski et al., 2007). Proliferation thus is regulated by the release of mitotic inhibitors at particular time points of mesoderm development. In the absence of both *ths* and *pyr*, the timing of mesodermal mitoses was disturbed. Furthermore, it is difficult to dissect a possible role of Htl/FGF signalling in regulation of mesodermal proliferation in these embryos, because the spreading of

mesoderm cells is severely impaired. However, the migration of the mesoderm can be described in three different phases with which mesodermal cell divisions correlate. First, the cells form initial contacts and align symmetrically along the anterior-posterior axis. During the second phase of early migration, the mesoderm spreads out in lateral-dorsal direction, and in the terminal phase of late migration, the cells acquire dorsal-most positions relative to the ectodermal margin. The intervals of proliferation occur just between these phases. That is, immediately after the cells established initial contacts to the ectoderm, between the early and late phase of migration and after mesoderm spreading is complete (Seher and Leptin, 2000; Nabel-Rosen et al., 2005; Murray and Saint, 2007). Live imaging data tracking single cells confirmed that the divisions in the mesoderm are ordered in space and time. These divisions are also synchronous with cell intercalations thus forming a monolayer (McMahon et al., 2008).

A mutual regulation of pathways controlling mesoderm migration and proliferation is therefore both possible and important for mesoderm development. A possible function of Ths to specify the substrate for mesodermal cell adhesion and stimulation of contact formation, as well as fate commitment induced by Pyr/Htl signalling, might play a role in this context. A model for such regulation might further imply that mesoderm cells proliferate to cover each region fully along the ventral-dorsal distance on which they migrate. The cells that arise in the first division in this model would form the ventral portion of mesoderm progenitor cells; the second round of mitosis will give rise to the lateral progenitor population; and the third division of cells in dorsal-most positions will build the dorsal progenitor group. A phasing of the intervals during which the mesoderm proliferates and migrates, thus, might not influence mesoderm migration but be of importance for progenitor differentiation. Indeed, in embryos mutant for string/Cdc25 where mesodermal cell divisions are blocked, the overall mesodermal segmentation is significantly affected (Han and Bodmer, 2003). The *Mef-2, tin* and *eve*

expressing progenitor cells that normally give rise to somatic muscle, heart and pericardial cells are reduced dramatically (Carmena et al., 1998; Han and Bodmer, 2003). Loss of these progenitors similarly was observed in *ths*^{759} and *pyr*^{18} single mutants in in varying degrees of expressivity and penetrance, obviously the most in *ths, pyr* deficient embryos (Gryzik and Müller, 2004; Stathopoulos et al., 2004; Kadam et al., 2009; Klingseisen et al., 2009).

Thus, Ths/Pyr-mediated FGF signalling may act together with another pathway in mutual regulation to control spreading and intermediate phases of cell proliferation. The Dpp signalling pathway represents a good candidate for such a signal. The Dpp pathway is well studied and identified as regulator of proliferation during wing development (Rogulja and Irvine, 2005; Affolter and Basler, 2007; Rogulja et al., 2008). Dpp forms a gradient throughout the tissue and thus establishes "routes" of cell proliferative regulators. Migrating cells receive inductive signals to proliferate when distinct positions are achieved. The formation of a gradient of Dpp molecules mediated by the HSPG Dally might provide the necessary dynamic regulation of such "routes" for mesoderm cells (Fujise et al., 2003; Belenkaya et al., 2004; Affolter and Basler, 2007; Akiyama et al., 2008). In support of this model, recent studies have shown that the establishment of the Dpp activity gradient crucial for dorsal embryonic patterning is regulated by stage-specific regulation of HSPG expression (Bornemann et al., 2008). *dpp* shows a very dynamic expression pattern during gastrulation, which, similar to the *pyr* expression domains, is restricted to the dorsal ectoderm region. As Dpp also regulates the differentiation of mesoderm cells that later contribute to the cardiac tissues, intersection of Htl/FGF and Dpp signalling pathways would present an effective mechanism to couple proliferation, migration and differentiation events in the mesoderm.

IV. II 3. 3 The role of MAPK activation in migration and differentiation of mesoderm cells

Questions that remain unanswered in analysis of mesoderm development are both the function and regulation of the domain of MAPK activation that is restricted to the cells of the leading edge during mesoderm migration. MAPK activation in the mesoderm is dependent on Pyr-mediated Htl signalling (Michelson et al., 1998b; Gryzik and Müller, 2004; Stathopoulos et al., 2004; Wilson et al, 2005; Klingseisen et al., 2009). Analysis from vertebrate models might provide a mechanism that can be applied to the function and regulation of MAPK in response to FGF signalling.

Studies from mouse and chick embryos showed that FGF-mediated ERK activation results in the differentiation of developing structures such as the somites, the spinal cord and the sclerotome. FGF mediated MAPK signalling induces also the expression of MAPK inhibitors or retinoid synthesis and Notch-mediated inhibitory function to prevent pre-maturation of committed cell lineages (Brent and Tabin, 2004; Akai et al., 2005; Olivera-Martinez et al., 2007; Wahl et al., 2007; Ekerot et al., 2008; Urness et al., 2008). In cyclic changes of regulative balance control and progressing expression domains of the regulative signals, FGF-mediated repression is attenuated and cells differentiate. Lack of MAPK antagonists such as MKP-3 results in elevated ERK phosphorylation in limb bud mesenchyme (Li et al., 2007). The loss of inhibitors or over-activation of ERK activity similarly results in premature differentiation of skeletal structures, cranial sutures and deafness, all of which are phenotypes associated with increased levels of FGF signalling. Thus, FGF signalling in these systems maintains undifferentiated cell fates in order to precisely regulate morphogenetic development. This regulation of differentiation occurs concurrent to cell migration as, for example, during development of the paraxial mesoderm of the chick embryo (Iimura et al., 2007).

The function of MAPK signalling during migration

MAPK activation in the *Drosophila* mesoderm in response to Pyr/Htl signalling might have a similar function as in vertebrate somitogenesis. In contrast to anterior-posterior axis specification in vertebrate models, the fly embryo is patterned and segmentally structured by an early transcriptional cascade of a network of transcriptional regulation and signalling pathways (Stathopoulos and Levine, 2002; Sandmann et al., 2006. 2007; Chopra and Levine, 2009). Dorso-ventral axis specification is set up already during oogenesis (Poulton and Deng, 2007). The mesoderm nevertheless has to migrate from ventral to dorsal positions of the embryo to give rise to progenitor cells relative to the axis that has been established previously. Hence, a model is attractive that involves the FGF signalling pathway to ensure the correct distribution of progenitor cells along the established pattern of the dorso-ventral axis. The progenitors further have to be competent to respond to the framework of differentiation signals. MAPK activation through Pyr/Htl signalling might inhibit downstream targets, which antagonize other signalling pathways. These pathways for example might be instructive for the mesoderm cells to stop their migration and undergo MET to initiate a particular differentiation program. When MAPK activation fades, the inhibition of such inhibitors might be released. Pyr-mediated MAPK signalling thus might regulate the timing and position of cell differentiation along the dorso-ventral axis. In this model, MAPK signalling prevents a premature stop of migration and differentiation of cells at the leading edge.

The *Drosophila* Notch as well as MKP-3 proteins are expressed in the developing mesoderm (*flybase*). Notch and MKP-3 might hence be possible candidates as antagonists of FGF-induced MAPK activation. Inhibitor activation by MAPK signalling would imply that the mesoderm leading edge comprises "tip cells" which remain unspecified during mesoderm migration. In addition, MAPK activation is dependent on

ectodermal contact, as outlined above. Both ectodermal contact and MAPK activation might thus regulate the initiation of differentiation in mesoderm cells. In this model, differentiation is inhibited in leading edge cells, which are in contact to the ectoderm. This inhibition is regulated by Pyr-mediated MAPK signalling. "Follower cells" in contact to the ectoderm, in which levels of dpERK have been reduced, are released from the inhibition of differentiation pathways. In consequence, these cells might discontinue their dorsal movement and initiate a differentiation program in response to signals from the ectoderm. A second group of "follower cells" comprises cells that do not display dpERK but also have not established ectodermal contacts. These cells might receive varying degrees of Pyr levels to polarise and continue their migration dorsally, and to seek adhesion to the ectoderm. Thus, they might migrate over other mesoderm cells already in stable adhesion to the ectoderm, Indeed, such "over-taking" of mesoderm cells was observed by live imaging analysis of mesoderm movement (Murray and Saint, 2007; I. Clark and H.A-J, Müller, unpublished). A monolayer is established during the late phase of mesoderm migration, when MAPK activation normally fades (Gabay et al., 1997). In support of this model, embryos lacking Pyr function, and thus MAPK signalling in mesoderm cells, show defects in formation of a monolayer. The function of Pyr/MAPK signalling during migration in leading edge cells, conclusively, might hence be to ensure the gradual positioning of the cells along the dorso-ventral axis. This mechanism further might prevent the premature differentiation of the cells subsequent to discontinued migration.

Possible candidates of antagonistic effectors of MAPK signalling might be represented by Notch or MKP-3, following the vertebrate model of regulation. Another antagonist might be the protein Sprouty (Sty). Sty acts antagonistically downstream of Htl in regulation of glial cell development, and downstream of the second FGF pathway in *Drosophila*, the Bnl/Btl signalling pathway (Haconen et al., 1998; Casci et al., 1999;

Horowitz and Simons, 2008; Franzdottir et al., 2009). Analysis from tracheal development further confirms a combinatorial function of Notch and Sty to antagonize FGF mediated MAPK activation (Horowitz and Simons, 2008). In the mesoderm, *sty* over-expression was able to inhibit MAPK activation, indicating that Sty might also be a possible antagonist of Htl-mediated MAPK activation in mesoderm cells (Reich et al., 1999). Last, *sty* mutants show reduced numbers of Eve positive pericardial cells (J. Gehlen and H.A.-J. Müller, unpublished). The reduction of pericardial precursors supports the idea that Sty might be involved to prevent a premature stop of dorsal migration and consequent differentiation in more ventral domains. A possible connection of the reduction of pericardial cell fates and elevated dpERK levels during migration in *sty* mutants, however, remains to be analyzed. In contrast, activation of MAPK signalling by over-expression of Htl, Ths and Pyr or Ras induces increased numbers of Eve positive progenitors (Michelson et al., 1998a; Kadam et al., 2009; Klingseisen et al., 2009). How MAPK signalling induces both inhibition of premature differentiation and later is required for differentiation of pericardial cells, in this model, is an issue that remains to be solved. A very attractive explanation comes again from the analysis of Htl-signalling during glia development. The MAPK pathway is differentially regulated by Rap1 and activation of ERK (the *Drosophila* Rolled MAPK). Rap1 activity is required for migration of the cells. Ras-mediated activation by contrast induced the differentiation of glial cells (Franzdottir et al., 2009). Applied to the mesoderm, this model might explain how overexpression of Ras results in supernumerary pericardial cell clusters, but shows no effect on mesoderm migration (Michelson et al., 1998a). Overexpression of active Ras further does not fully rescue the loss of pericardial cells in absence of *htl*. Conversely, Rap1 mutants show defects in mesoderm migration, but differentiation of the cells is not disturbed when the cells receive differentiation signals from the ectoderm (Asha et al., 1999). Parallel pathways

of Rap1 and Ras in stimulation of MAPK signalling have been reported in *Drosophila* and show that Rap1 and Ras act in concert (Ishimaru et al., 1999; Mishra et al., 2005). Thus, MAPK signalling in mesoderm cells might as well involve a regulation of Ras and Rap1 activity to trigger different biological response to FGF-mediated MAPK signalling.

Regulation of MAPK signalling during differentiation of mesoderm cells

Embryos over-expressing *pyr* in all mesoderm cells show rather the same phenotype as *ths, pyr* deficient embryos with regard to mesoderm spreading and adhesion between mesoderm cells. In comparison with the vertebrate model mentioned above, this phenotype might be related to the skeletal dwarfism described in mice as a consequence of elevated levels of activated MAPK (Li et al., 2007). In consequence of enhanced MAPK signalling, in mesenchymal mesoderm cells, the differentiation of the mesenchyme occurs prematurely and the cells undergo MET. Indeed, *ths, pyr* deficient embryos show a phenotype of cells closely adhering to each other which seem not be able to dissociate, thus forming the typical observed "snake-like" pattern (Gryzik and Müller, 2004; Klingseisen et al., 2009). The phenotype might be caused by cells trying to spread out in response to signalling pathways working in parallel to FGF signalling or adhesive cues as mentioned above. The mesoderm cells may have differentiated prematurely in consequence to lack of FGF signals that normally would have inhibited their differentiation. The pre-programmed mesoderm cells thus might have acquired a more epithelial character that is expected much later in development during muscle or cardiac progenitor differentiation. To support this model, mesoderm cells over-expressing *pyr* show the expression of *Mef-2*, *eve* and *lbe* that are characteristic for somatic muscle and pericardial cell progenitors. The clusters of Eve positive mesoderm cells in these embryos are formed in regions more ventral than in wild-type. This result might support the idea that Pyr/Htl signalling regulates both the competence of

mesoderm cells to respond to differentiation signals and the position in which the cells will initiate their differentiation.

Regulation of MAPK signalling by cytoplasmic and nuclear localization of dpERK

The intracellular regulation of dpERK levels further might be important for differential cellular response to FGF/Htl signalling during mesoderm migration and differentiation. dpERK levels in the cytoplasm in contrast to a nuclear localization of dpERK might be regulated to address signalling pathways involved in cell migration and transcriptional activity, respectively. The control of cell response to MAPK activity during migration of tracheal cells forming the air sac represents an example for this mechanism (Cabernard and Affolter, 2005). dpERK levels form a gradient from the tip cells to stalk cells behind. High levels of dpERK were found in nuclei of tip cells. Lower levels of dpERK were identified to reflect dpERK in the cytoplasm. The tip cells respond to Bnl/Btl signalling with directed migration. Cell proliferation and survival of the stalk cells in contrast are dependent on Egfr signalling (Sato and Kornberg, 2002; Cabernard and Affolter, 2005; Affolter and Caussius, 2008). The localization of dpERK in the nucleus or the cytoplasm thus reflects the response to FGF and EGF signalling, respectively.

During migration, the mesoderm only shows activated MAPK in response to Htl activation in specific response to Pyr (Wilson et al., 2005; Klingseisen et al., 2009). Egfr signalling therefore can be excluded to regulate cytoplasmic localization of dpERK in mesoderm cells, or might be dependent on Pyr signalling. However, MAPK activation in the mesoderm also shows declining levels from the leading edge to more ventral cells, which could indicate nuclear versus cytoplasmic ERK activation. Low levels of ERK might represent the switch from transcriptional inhibition of differentiation markers towards their activation. If actually Dpp gradients determine a course for the mesoderm cells of morphogen concentration thresholds indicating certain

checkpoints, the combination of dpERK levels in the cytoplasm and modulating Dpp inputs could present an attractive model how FGF signalling synchronizes directional guidance of mesoderm spreading and further development.

The role of Csw/Shp-2 in integration of FGF/Htl signalling and other signalling pathways

The function of Ths and Pyr mediated Htl-signalling might involve the regulation of MAPK activity and interfering signalling pathways, that is Dpp and Egfr for example. This mechanism is very likely because the phosphatase Csw/Shp2 has been identified to have a pivotal role in regulation of Dpp, EGF and FGF mediated ERK activation pathways (Jarvis et al., 2006; Ding et al., 2007). Csw/Shp-2 mediates the activatin of MAPK in response to growth factor signalling by controlling the antagonistic activity of Sprouty. Csw/Shp-2 was further identified to bind to activated Dof upon Btl or Htl activation, and to mediate Ras activity (Petit et al., 2004). Cell culture studies found that Csw/Shp2 regulates the response to RTK activation between activation of ERK and Src by recruiting Csk, which implies phosphorylation of paxillin and Src through the focal adhesion kinase Fak (Manes et al., 1999; Ren et al., 2004; Zhang et al., 2004). Cells containing dominant active Csw/Shp-2 showed enhanced focal adhesion contacts and filopodia. Directing the FGF signal towards activation of Src thus might be a mechanism to promote mesoderm migration in contrast to differentiation induced by ERK activity. Recent studies showed further, that nuclear localisation of phosphorylated ERK depends on integrin signalling and importin-7 *(Drosophila moleskin)*, a nuclear importer protein (James et al., 2007). Csw/Shp-2 recruits importin-7 to the membrane and mediates the complex formation of importin-7 and dpERK, which allows nuclear transport. Thus, Csw/Shp-2 functions in parallel to the Ras-Raf-MEK cascade. In accordance with esults from cell culture studies, Petit et al. (2004) found that Ras activation alone is not sufficient for tracheal cell migration, which depends on Csw/Shp-

2 activation. Furthermore, Src42A, which accumulates as well at mesoderm-ectoderm interfaces, was identified in migrating tracheal cells to fulfil a role in redistribution of E-cadherin (Shindo et al., 2008). In contrast, the other Src present in *Drosophila*, Src64B, is required for Raf activation (Xia et al., 2008). Thus, recruitment of Csw/Shp-2 by Dof upon activation by Htl might result in different cellular responses via a switch in Src activation, which promotes either cell migration or MAPK dependent differentiation. In this context, different levels of ERK appear to be regulated upon FGF signal -mediated activation as well as integrin/Src42A signalling via cell attachment. Such parallel regulation of cell responses supports again a model in which Ths might activate signalling pathways involved in adhesion to the ectoderm via Src activity, whereas Pyr might in parallel instruct the cells to migrate dorsally and induce Ras-mediated activation of ERK required for differentiation of mesoderm cells

Here again live imaging data could contribute the most to detect dynamic changes in ERK activation. To circumvent the obstructive auto-fluorescence of the yolk, which is in close proximity to the migrating mesoderm, cultures of S2 cells (*Drosophila* Schneider cells) or myoblast development in leg and wing imaginal discs, could be exploited to investigate subcellular localisation of dpERK upon Pyr-mediated Htl signalling. Measurement of ERK activation could be achieved by a FRET (fluorescence resonance energy transfer) assay as described by Fujioka et al. (2006). Results obtained from these experiments might allow drawing conclusions of dpERK localisation and hence possible differential function in mesoderm cells during migration.

IV. II. 3. 4 Pyr is required for polarised dorsal protrusions whereas Ths promotes radial filopodia

To migrate into a specific direction cells need not only to adhere to the substrate but also must polarize along the direction of their migration. However, the formation of

polarised protrusions is not essential for directed migration. In *pyr*^{18} single mutant embryos, protrusive activity was strongly reduced at the leading edge, and filopodia were shorter and very thin. Although early migration showed slight defects in symmetric mesoderm-ectoderm attachment, and mesoderm spreading appeared delayed in comparison to wild-type cell migration proceeded and mesoderm cells acquired dorsal most positions at the ectodermal margin. A lack of polarised filopodia was also found not to be crucial for mesoderm migration in *Xenopus* and zebrafish gastrulation. Mesoderm cells lacking protrusions migrated slightly slower but in coordinated and directed fashion (Lin et al., 2002; Montero et al., 2003; Nagel et al., 2004). Here, the cellular response was caused by lack of PI3 kinase activity, which suggests a similar involvement in *Drosophila* mesoderm migration in striking similarity to the phenotype. Although PI3 kinase signalling is difficult to address in early embryos genetically, it is interesting to note that Dof contains putative phosphorylation sites for PI3 kinase (Battersby et al., 2003; Wilson et al., 2004; Petit et al., 2004).

The data presented in this thesis indicate that Pyr is required for polarised cell protrusions, because *ths*^{759} homozygotes show normal filopodia and lamellipodia in fixed embryos. Similar to the filopodia at the leading edge of epithelial cells during dorsal closure (Jacinto et al., 2000, 2002; Millard and Martin, 2008) cell protrusions in the mesoderm might not be essential for cell migration as such, but might be required to sense the signal gradient and transmit positional information. Cell culture experiments of collective migration across a flat two-dimensional substratum showed that cells behind the front row of cells contain continuous lamellipodia that extend underneath of cells migrating in front, and these cells drive the leading edge forward (Farooqui and Fenteany, 2005; Trepat et al., 2009). Thus, mesoderm migration might not only be driven by leading edge cells that pull the aggregate into dorsal direction, but also by

lateral and ventral cells which interdigitate the underlying ectoderm and promote a force that pushes the leading cells dorso-laterally.

Protrusions in radial direction towards ectoderm cells were unaffected in pyr^{18} homozygotes, further indicating that adhesion and directed cell migration are differentially regulated and not both dependent on *pyr* function. In contrast to pyr^{18} mutants, mesoderm cells in ths^{759} mutants exhibit fewer and shorter filopodia in radial direction towards the surface of migration. The measurement and imaging of radial protrusions however is technically difficult, because the section of the embryo that is imaged is very large. The scanning process to obtain the imaging data for radial protrusions measurement takes much longer than to obtain the data for dorsal protrusion measurement. During the scanning process, the staining of the tissue can be reduced by a so-called 'bleaching-effect'. This alters the actual pattern of the protein visualised and thus results in analysis of imaging data, which do not reflect the actual distribution of the visualised protein. Nevertheless, despite an allowed tolerance of 1μm, the measurement of filopodia length showed obvious differences in ths^{759} and pyr^{18} single mutant embryos. Independent measurements of filopodia in pyr^{18} and ths^{759} embryos also confirmed the findings presented here (Clark and Muller, unpublished). *ths, pyr* deficient embryos contained almost no cellular protrusions and the attachment to the ectoderm was highly impaired. This suggests that both Htl ligands are required to render dorsal migration robust and may act in concerted fashion rather than in an overlapping or redundant fashion. This idea is supported by the phenotype of hemizygous embryos, which showed additional reduction in radial filopodia in a pyr^{18}, Df^{2238} mutant background, or additionally less and shorter leading edge protrusions in ths^{759}, Df^{2238}.

Overexpression of *pyr* in all mesoderm cells or in a single hemisegment during early migration resulted in short and non-polarised filopodia and decreased motility similar to a pyr^{18}, or *ths, pyr* deficient genetic background. This phenotype supports a function of

pyr for polarized protrusive activity as well as maintenance of mesenchymal characteristics at low levels of MAPK in contrast to enhanced MAPK activity required for increased contact formation and subsequent differentiation. On the other hand, as only leader cells display elevated levels of phosphorylated ERK, expression of Pyr in all mesoderm cells could turn every cell into a leader cell and thus inhibit directional movement. If cells behind the leading edge of the mesoderm create a pushing force for dorsal migration, a collective lacking 'followers' might also be less able to move.

IV. III Differentiation of mesoderm derivatives

A large transcriptional network regulates the specification and differentiation of heart, pericardial cell and muscle progenitors, with the pan-mesodermally expressed transcriptions factors Tin and Mef-2 at the top of this cascade (Lilly et al., 1994; Bour et al., 1995; Gajewski et al., 1997; Furlong et al., 2001; Han et al., 2002, 2006; Sandmann et al., 2006, 2007; Zaffran et al., 2006; Medioni et al., 2008). Another important role is assigned to the two isoforms of Ladybird (Lbe, including both Lb short and long isoforms). During progenitor specification of the segment boundary muscle (SBM), Lbe antagonizes the role of Krüppel (Kr) expression specifying the neighbouring lateral transverse muscle progenitors LT1-3 (Jagla et al., 1998, 2001). Further, *lbe* is expressed in a subset of heart precursors and specifies the progenitors of the ventral acute (VA) muscles. Recent muscle and heart-targeted genome-wide transcriptional profiling and chromatin immuno-precipitation (ChIP)-on-chip search revealed a wide range of target genes regulated by Lbe (Junion et al., 2007). Among other identity genes controlling progenitor and muscle diversification, Lbe target genes included several components of cell adhesion, signalling and motility, including several components of the Rho, Ras

and PI3K pathways. Lbe, either negatively or positively regulates transcription factor expression of heart, pericardial and somatic muscle progenitors.

The distinction between neighbouring developing tissues of heart and dorsal somatic muscles requires cell lineage commitment and is accompanied by the expression of one or several specific cell identity factors like Lbe, Eve, Muscle homeodomain factor (Msh) or Kr (Ruiz-Gómez and Bate, 1997; Jagla et al., 1997; Fujioka et al., 2005; Sellin et al., 2008).

Lateral inhibition mediated by Notch activity integrates influence of Wg/Wnt-, Hh- and Dpp pathways, which are prerequisite to further differentiation signals from FGF/Htl and Egfr signalling (Baylies et al., 1998; Buff et al., 1998; Frasch, 1999; Carmena et al., 1995, 1998, 2002; Jagla et al., 1998; Halfon et al., 2000; Lee and Frasch, 2000; Liu et al., 2006; Sellin et al., 2008).

FGF signalling mediated by Ths and Pyr, which are dynamically expressed in the ectoderm interferes with this large network of progenitor regulation.

IV. III. 1 Differentiation of pericardial cells is dependent on Pyr

In addition to its segmental specification, the mesoderm is subdivided into a dorsal Tin domain and lateral-ventral Twi domain (Sellin et al., 2008). Maintenance of Tin expression within the cardiogenic mesoderm requires the Dpp and Htl-signalling pathways (Zaffran et al., 2006), and as mentioned above, embryos mutant for *htl*, or lacking both *ths* and *pyr* show strong reduction in Tin expression (Gisselbrecht et al., 1996; Shishido, 1997). Tin is required for expression of Mef-2, thus Mef-2 expression and regulation of target genes are affected in absence of FGF/Htl-signalling (Gajewski et al., 1997). The analysis of progenitor specification and differentiation of the heart and somatic musculature showed that both Htl ligands Ths and Pyr contribute to these processes, but are not essential individually. Only simultaneous deletion of both FGF

genes leads to severe defects resembling the mutant phenotype of a null mutation of the receptor and causing the loss of distinct structures of all somatic muscle groups, including the heart. Thus, Ths and Pyr together ensure proper formation of precursors and subsequent differentiation.

In both single mutant conditions, progenitors of somatic muscles and cardioblasts failed to be specified or were duplicated, but a stereotypic pattern of regional, specific requirement of FGF/Htl-signalling was not discernible. The presence of specified cardioblasts and dorsal muscles in segments where lateral or ventral muscles failed to be specified indicates that these defects are not resulting from defects in dorsal migration of the mesoderm. pyr^{18} mutant embryos fail to specify pericardial cells, but defects in neighbouring dorsal muscle progenitors or heart precursors are random and less penetrant. Pyr thus is specifically required to regulate the commitment to a pericardial cell fate, but not to the fate of a particular muscle progenitor. Ths function is dispensable for pericardial cell differentiation, indicating that the required Htl-dependent activation of MAPK in the pericardial cell progenitor solely depends on Pyr (Carmena et al., 1998, 2002). ths^{759} mutant embryos however showed defects during muscle progenitor differentiation of the same progenitor groups as observed in pyr^{18} single mutants, which indicates that the specification of somatic muscle progenitors is regulated by other factors and the defects observed in FGF mutants might result from irregularities of mesoderm migration and monolayer formation.

Carmena et al. (2006) showed that fine tuned balance of activated Ras levels is an important determinant of cell fate by a mechanism that integrates Wg/Wnt, Htl and Egfr signals. The specification of the pericardial founder cell in each segment, which subsequently divides to generate a cluster of 2-5 segmental pericardial cells, is dependent on Htl-signalling (Carmena et al., 1998; Tao and Schulz 2007). The neighbouring progenitor cell of the dorsal acute muscle DA1 in contrast requires both

Htl- and Egfr-dependent Ras activation (Frasch et al., 1987; Baylies et al. 1998; Buff et al., 1998). Thus, in the absence of Pyr and Htl-dependent Ras activation, both progenitors fail to express the differentiation marker Eve specific for both pericardial and DA1 progenitors. The number of PCs is also influenced by the size of the dorsal Tin domain (Sellin et al., 2008), which indicates that Ths is dispensable for Htl-dependent maintenance of *tin* expression, as all pericardial cells are specified in all samples examined.

The defects in *tin* and *lbe* expression in pyr^{18} mutants might be related to mutations in *lame duck* (*lmd*). *lmd* encodes a Gli-like transcription factor, which functionally antagonizes the zinc finger homeodomain factor Zfh1 (Duan et al., 2001). The interaction of Lmd and Zfh1 is dependent on Dpp and is not mutual as Zfh1 opposes Lmd function indirectly (Sellin et al., 2008). In wild-type embryos, expression of *tin* is restricted to the dorsal domain of the mesoderm as result of early Dpp function while subsequent Dpp signalling provides pro-myogenic input to modulate the pericardial field in favour of the specification of fusion competent myoblasts (FCM) (Frasch, 1995, Johnson et al., 2007). In embryos mutant for *lmd*, *tin* expression persists and as a result, FCM's adopt the fate of pericardial cells (Sellin et al., 2008). The combination of pericardial cell identity and fusion competence leads to a pericardial hyperplasia phenotype (Johnson et al., 2007). Furthermore, *lmd* mutant embryos show increased Twi expression and ectopic AMP's, which normally express both Twi and Lbe, but in the absence of *lmd,* they express only Twi. The hyperplasia phenotype in addition is very similar to the pericardial phenotype observed in embryos over-expressing *pyr* in all mesoderm cells. Proliferation is not involved in the hyperplasia phenotype, which is caused by recruitment of nuclei to enlarged syncytia by the fusion-stimulative function of the FCM's pericardial fate commitment (Johnson et al., 2007; Sellin et al., 2008). The pericardial cell clusters of increased size in response to Htl-mediated Ras activation

were also identified as large syncytia containing multiple numbers of Eve positive nuclei (Buff et al., 1998; Carmena et al., 1998). Thus, loss of Lmd function or over-expression of its antagonist Zfh1 show phenotypic outcomes similar to over-activation of the Htl/FGF pathway in response to Pyr.

FCM's need active Notch signalling to be properly specified, and Lmd was identified as a downstream target of Notch to induce the FCM differentiation program (Duan et al., 2001; Estrada et al., 2006). This is also restricted to individual mesodermal lineages, as a subset of pericardial cells asymmetrically derived is not affected by the loss of Lmd function. As mentioned above, Pyr-dependent Ras activation by Htl signalling mediates the Notch induced selection of pericardial cell fates (Simon, 2000; Carmena et al., 2002, 2006) and thus induces the pericardial differentiation program. As *lmd* was identified as a downstream target of Notch signalling and Pyr/Htl-mediated Ras activation influenced regulation by Notch, Pyr could regulate the balance between Lmd and Zfh1 function, possibly in cross talk with Dpp signals.

IV. III. 2 Differentiation of somatic muscles requires both Ths and Pyr

The defects during muscle development revealed no defined segmental pattern or specific requirement for Ths or Pyr function. That is, muscle progenitors from ventral, lateral and dorsal groups showed loss of progenitors, as well as heart precursors were missing in single segments. A particular group of progenitors was not identified as dependent on Htl/FGF signalling. However, the defects were not observed in specification of muscle progenitors in general. The defects occurred predominantly in specification of the lateral transverse muscles LT1-3, the segment border muscles and the ventral oblique muscles VO4-6. Two isoforms of the homeobox gene Lbe are expressed in the progenitors of the segment border muscles, which derive from the same precursor cell as the lateral transverse muscles LT1-3, which express the transcription

factor Kr (Jagla et al., 1998). Overexpression of *lbe* in all mesoderm cells leads to a cell fate change in Kr-positive cells, resulting in duplication of the SBM progenitor and loss of LT1-3. In addition, more lateral adult muscle precursors (LaP), which do not normally express Mef-2, are formed at the expense of ventral adult muscle precursors (VaP) (Sellin et al., 2008). Conversely, loss of *lbe* expression results in supernumerary Kr-positive cells and duplication of VaP at the expense of LaP.

pyr^{18} single mutants showed a loss of *lbe* expression in some hemisegments (Klingseisen et al., 2009), which might be the result of low levels of Tin in response to lack of transcriptional maintenance in response to Htl activation. Thus, loss or duplication of SBM in pyr^{18} single mutants might occur as a result of an imbalance between Lbe and Kr mediated progenitor specification. Over-expression of *pyr* might also induce expression of *lbe* specifically in these progenitors, supporting the idea that Pyr-mediated Htl/FGF signalling influences specific muscle development. With respect to the wide range of Lbe target genes revealed (Junion et al., 2007), Htl signalling might thus have a general function in regulation of the signals required for mesoderm differentiation.

The function of Ths in SBM development might not be involved in progenitor specification but subsequently influence the progenitor cell fate. ths^{759} single mutants only contained duplicated SBM's but no loss of these muscles. As both Htl ligands appear to be required in combination, the phenotype in ths^{759} indicates a function to support inhibitory events as precursors divide to give rise to different progenitors or to promote asymmetric cell divisions the result of which are different daughter cells. A division of a progenitor that gives rise to two different muscle founders occurs for example during formation of the LT1-3 and the SBM founder cells (Jagla et al., 1998; Sellin et al., 2008). In contrary to SBM formation, loss of lateral transverse muscles occurred in ths^{759} homozygotes. This might indicate that the fate of Lbe positive SBM

founders is the "default fate" acquired in contrast to further specified LTs, as in case of pericardial cell fate versus DA1 via Notch, which renders cell fates always non-myogenic if not overruled by other signals (Sellin et al., 2008).

Loss of the lateral transverse muscles LT1, 2 or 3 was observed in both ths^{759} and pyr^{18} single mutants, although a loss of the progenitors for these muscles was never discovered. This is in contrast to the defects in SBM or ventral oblique VO4-6 muscles observed, where also Mef-2 positive progenitors were missing from some segments. This phenotype might be caused subsequent to progenitor specification and represents muscle-specific requirements of Ths and Pyr function. Indeed the mutation of the putative E3 ubiquitin ligase Mind bomb2 (Mib2), which is specifically expressed in founder myoblasts (FM's) shows similar phenotypes as both ths^{759} and pyr^{18} homozygotes (Carrasco-Rando and Ruiz-Gómez, 2008). Loss of Mib-2 function compromises myoblast fusion and FMs undergo a reduced number of rounds of fusion with FCMs. Further, many muscles degrade with onset of muscle contraction, display aberrant sarcomeric structure and detach from tendons at muscle attachment sites of the body wall. Among the muscles most affected by impaired Mib-2 function are muscles that were aberrant in ths^{759} and pyr^{18} single mutants, namely VO5 and 6, LT3 and LT 1 and 2, in order of severity. Ths^{759} homozygotes showed a slightly enhanced phenotype regarding LT muscles. In other genetic backgrounds of pyr^{18} homozygous and hemizygous conditions, only the LT3 muscle fibre was missing from some segments, which is affect first upon impaired Mib-2 function. In ths^{759} mutants, often two of the three LT fibres were absent at later stages. This might suggest a role for Ths in mediating adhesion and attachment of mesoderm cells and their derivatives.

During the fusion process of FM and FCM, Mib-2 is suggested to be required for elimination of the FCM-specific activator Lmd from nascent myotubes (Carrasco-Rando and Ruiz-Gómez, 2008). Mib2 also accumulates in sarcomeres and interacts

physically with non-muscle myosin, which lead to the idea of a secondary structural role of Mib-2 in maintaining sarcomeric stability. Lmd acts antagonistically to Htl dependent FGF signalling, judged by phenotypic comparison, and as shown may be downstream of the signalling network Htl/FGF function is involved. Consistent with a model involving Htl signalling in sarcomeric stability, *mib-2* was identified as a target gene positively regulated of the Htl/FGF pathway (Leatherbarrow and Halfon, 2009). Thus, activation of Htl appears to influence also both muscle fusion and later stability in addition to specification of progenitors.

IV. III. 3 Heart formation depends on both differentiation and migration signals

The number of cardioblasts was also altered in absence of either *ths* or *pyr* and no cardioblasts were differentiated in embryos lacking both Htl ligands; this phenotype is similar to over-expression of *pyr* or *tin* in the mesoderm (Wang et al., 2005). Both increased and reduced numbers of cardioblasts were caused by removal of either *ths* or *pyr* function. Additionally, cardioblasts seemed misaligned and were increased in numbers in one segment, but missing from the neighbouring segment. In contrast to pericardial cells, the cardioblasts have to migrate to their destined positions, to align themselves and to polarize (Tao and Schulz, 2007). In embryos mutant for the FGF target gene *pointed (pnt)*, Mef-2 positive cardioblasts were increased in numbers and showed additional heart precursors between and next to the two rows of the wild-type cardioblast pattern (Alvarez et al., 2003). Thus, Pnt was identified to repress cardioblast differentiation in favour of pericardial cell fates, and loss of *pnt* resulted in additional differentiation of cardioblasts. The authors further showed that Ras activity is not involved in cardioblast specification and migration, as over-expression of dominant negative Egf and FGF receptors abolished earlier events dependent on Ras activity in

the mesoderm but showed no influence on cardioblast formation. As a consequence, it is suggested that Pnt acts in a pathway parallel to Ras-ERK dependent signalling (Alvarez et al., 2003).. Similarly, FGF dependent heart cell migration of the ascidian *Ciona intestinalis* requires the FGF target FoxF, which acts downstream to the FGF/MAPK/Ets (Pnt) cascade, but does not interfere with differentiation (Beh et al, 2007). Inhibition of FoxF resulted in a striking phenotype of a beating heart in ectopic position. The *Drosophila* homolog of FoxF is Biniou, which is identified so far as a universal regulator of the network regulating visceral muscle development (Jakobsen et al., 2007). In summary, these results nicely demonstrate that activation of Htl might engage two different pathways downstream of Dof to activate MAPK to induce or repress differential expression of target genes involved in differentiation, and a signal via Rap-mediated ERK activation in parallel to Ras to control the regulation of cytoskeletal organization during migration.

IV. IV. Differential and overlapping functions of Ths and Pyr

Mesoderm migration and differentiation in *Drosophila* requires the function of both Htl ligands Ths and Pyr. Either single mutant condition exhibits defects much less severe than observed in embryos lacking both *ths* and *pyr* FGF genes or the FGF receptor (Gryzik and Müller, 2004; Schumacher et al., 2004; Klingseisen et al., 2009). Analysis of trans-heterozygous embryos, containing only one gene of *ths* and *pyr* each, showed that the equal reduction of Ths and Pyr levels is not crucial for Htl signalling. Hemizygous embryos in contrast showed an enhancement of the mutant phenotype of the respective single mutant condition. The importance of a balance between *ths* and *pyr* dosage supports that Ths and Pyr act in concert to regulate the response to Htl/FGF signalling. Another possibility involves, that both Ths and Pyr need to bind in a

heterodimeric conformation to generate the optimal signalling strength, duration or recruitment of intracellular adaptor and effector proteins.

two different models might explain the fact that embryos homozygous for *ths*^{759} or *pyr*^{18} show only mild defects compared to *ths, pyr* deficient embryos

(1) Ths and Pyr have similar signalling properties and are able to substitute for one another in the activation of Htl to induce the same or similar cellular responses. In support of this model, over-expression of either *ths* or *pyr* in all mesoderm cells results in MAPK activation and causes supernumerary clusters of Eve positive dorsal mesoderm cells (Kadam et al., 2009; Klingseisen et al., 2009). Ectopic over-expression of *ths* and *pyr* induces further the same biological response in glial development, that is, a hyper-wrapping of axons (Franzdottir et al., 2009). Expression of either *ths* or *pyr* in embryos lacking both Htl ligands also rescues the defects in Eve positive pericardial cell specification (Kadam et al., 2009; this study).

However, *ths*^{759} single mutants contain normal differentiated pericardial cell clusters, which indicates that *ths* is dispensable for this process. By contrast, specification of muscle progenitor cells shows defects in both single mutants, suggesting that both the function of *ths* and *pyr* are required for proper differentiation of mesoderm derivatives. Loss-of-function of either *ths* or *pyr* is larval lethal to > 96% of all homozygotes each, which indicates that Ths and Pyr do not act in redundant fashion during development. These partial discrepancies allow the consideration of a second model of function of Ths and Pyr during mesoderm migration and differentiation.

(2) Ths and Pyr individually promote the same developmental process by activating differential signalling pathways each required for mesoderm development. For example, during mesoderm migration, the polarisation of the cells to move in dorsal direction is equally essential as proper attachment to the ectoderm. Both modulation of cellular attachment and polarisation contribute to robust cell migration (van der Hardt et al.,

2007; Affolter and Caussius, 2008; Iilina and Friedl, 2009), thus, providing one essential requirement in absence of the other could stabilize the process sufficiently to cause only minor defects as observed in ths^{759} or pyr^{18} single mutant embryos. Furthermore, Ths and Pyr might induce MAPK signalling in response to Htl activation via Rap versus via Ras as reported by Franzdottir et al. (2009). Over-expression in the mesoderm thus would have the same phenotypic outcome. The over-activation of one pathway might trigger the activation of the other, as a balance between the differential pathways is lost. In support of this model, expression of a constitutively activated form of Htl or active Ras leads to supernumerary Eve positive cell clusters, but is not able to fully rescue the *htl* null mutant phenotype in contrast to the wild-type receptor (Michelson et al., 1998a, 1998b; Imam et al., 1999; Schumacher et al., 2004). Thus, activation of Ras alone appears not to be sufficient for mesoderm development.

Different results to the data published by Kadam et al. (2009) were obtained by overexpression of *ths* in mesoderm cells. The *ths* over-expression construct utilized in this study, *ths**, contained amino acid exchanges within the FGF core domain affecting amino acid residues conserved in all FGFs. Ths over-expression as shown by Kadam et al. (2009) resulted in ectopic activation of ERK resembling the phenotype of *pyr* over-expression. This phenotypic difference suggests that the amino acids exchanged in *ths** are essential for the signalling properties of Ths in activation of the MAPK pathway in response to Htl activation. Effects in response to *ths* over-expression during migration, in contrast to the phenotype describes for ths* in this study, was not reported by Stathoupoulos et al. (2004) or Kadam et al. (2009). The analysis of a transgene of *ths* containing the exact sequence as notated at present (Pubmed/NCBI) will be required to further investigate the effects on mesoderm development upon overexpression of *ths* in comparison to *pyr*.

The clusters of dorsal mesoderm cells generated by over-activation through Ths or Pyr exhibit a different morphology, which is also discernible in the data presented by Kadam et al. (2009). The analysis from ectopic expression of *pyr* further showed that the influence of Pyr/Htl-signalling is dependent on the site of expression as well as the developmental timing. Expression of *pyr* in the mesoderm under control of the *twi* promotor or a specific ectodermal domain under control of the *eveS3* promotor, during early development, caused defects in formation of protrusions and migration. The early over-activation of MAPK signalling further induced the formation of supernumerary Eve positive clusters, which fused with cell clusters from neighbouring segments. By contrast, expression in lateral ectoderm cells during the late phase of mesoderm spreading under control of the 69B promotor did as well induce ectopic activation of MAPK in mesoderm cells, but mesoderm migration was not affected. Supernumerary Eve positive cell clusters were formed as well, but these clusters remained within the segmental boundaries. Thus, late/ectodermal *pyr* expression in contrast to early/mesodermal enhanced Pyr-dependent MAPK activation does not result in the syncytial structures observed upon constitutive activation of Ras in the mesoderm (Buff et al., 1998; Carmena et al., 1998). Conclusively, early responses to ectopic Pyr-mediated Htl activation differ from late responses. In addition, such differences were not observed upon *ths* ectopic expression (Kadam et al., 2009), indicating that Pyr-mediated MAPK activation interferes with processes different from those that Ths does. A possible interference with the specification of fusion competent muscle founders is consistent with an individual function of Pyr-MAPK signalling during progenitor differentiation. The lack of Eve positive cells in pyr^{18} single mutants that is not observed in absence of *ths* emphasizes this individual function.

The differential response to Pyr/Htl signalling in context of and with regard to mesoderm spreading and differentiation further supports the model that MAPK

activation via Pyr/Htl signalling in mesoderm cells might be inhibited during migration to prohibit premature differentiation. Pyr additionally provides a polarisation signal for the cells, as filopodia formation at the leading edge of the mesoderm collective is dependent on localized *pyr* expression leading to Pyr-mediated MAPK activation. Ths in contrast appears to promote the formation or stabilisation of radial protrusions, which are shorter in fixed samples of ths^{759} mutant embryos. The induction of active radial-lateral contact establishment by Ths with lateral-dorsal polarisation of the cells by Pyr thus might act together to achieve orchestrated mesoderm migration. Activation of MAPK in leading edge cells might activate the inhibitory function of Sty to prevent premature differentiation. This signal would be overridden by forced activation of MAPK via ectopic *pyr* or *ths* over-expression, resulting in Eve positive cell clusters despite impaired migration of mesoderm cells. Supporting an involvement of Sty in the Htl-signalling pathway, *sty* expression was induced in glial cells upon Htl/FGF signalling in the eye imaginal disc (Franzdottir et al, 2009). Further experiments would be required to test a possible function of Sty in mesoderm development, such as spatiotemporally dependent over-expression as described above for *pyr*, for example.
Finally, a switch in FGF signalling upon differential expression of the two Htl ligands as reported by Franzdottir et al. (2009) would fit in with the data presented so far on Ths/Pyr-mediated regulation of mesoderm development (Gryzik et al., 2004 Stathopoulos et al., 2004; Kadam et al., 2009; in this study). The event of a switch might define a developmental time point that determines the completion of mesoderm spreading and the beginning of mesoderm differentiation, which may however intertwine.

Both Ths and Pyr do not appear to generate long-range signals. Expression of the tagged *ths** construct showed expression only in the respective expression domain and no signs of diffusion throughout the tissue. Assuming that the point mutation within the

coding sequence of the FGF core domain has no influence on the secretion, processing and diffusion of the protein, the signal range of Ths thus is likely not extending further than the neighbouring cell. To make a clear statement however, double-staining experiments with cell surface markers would be required. The same experiments are required to determine Pyr localisation. Nevertheless, expression of *pyr* in ectopic ectodermal domains resulted in MAPK activation in mesoderm cells. Expression in only a single, specific hemisegment showed sharp borders between cells that displayed activated MAPK and neighbouring cells that did not, indicating that (1) Pyr signals as well are of short range and (2) MAPK activation seems to require a certain threshold of FGF signal. The regulation of pericardial cell specification by different levels of active Ras as described by Carmena et al. (2002, 2006) supports this model. In addition, differentiation of Eve-positive or Lbe-positive mesoderm derivatives was only disturbed within the respective segment.

In summary, the results presented in this thesis are in conjunction with the reported function of Ths and Pyr function in glial cell development by Franzdottir et al. (2009), suggesting a model as depicted in Fig. 64.

Mesoderm migration and differentiation are regulated differentially, involving probably Rap1 and Ras to activate ERK in mesoderm cells respective to migration and differentiation. Pyr is required for activation of Ras to induce different transcriptional response, whereas Ths might be required for activation of Rap1 for proper attachment during migration and adhesion of differentiated cells at the determined positions. In absence of both *ths* and *pyr*, Mef-2 expression indicated that specific dorsal, lateral or ventral muscle progenitor groups/domains, are no longer discernible, and the random formation of muscle fibres is no longer connected to a specific position or muscle attachment site. Thus, Ths and Pyr are required for proper distribution, positioning and differentiation of mesoderm cells along the ventral-dorsal axis, which is segmentally

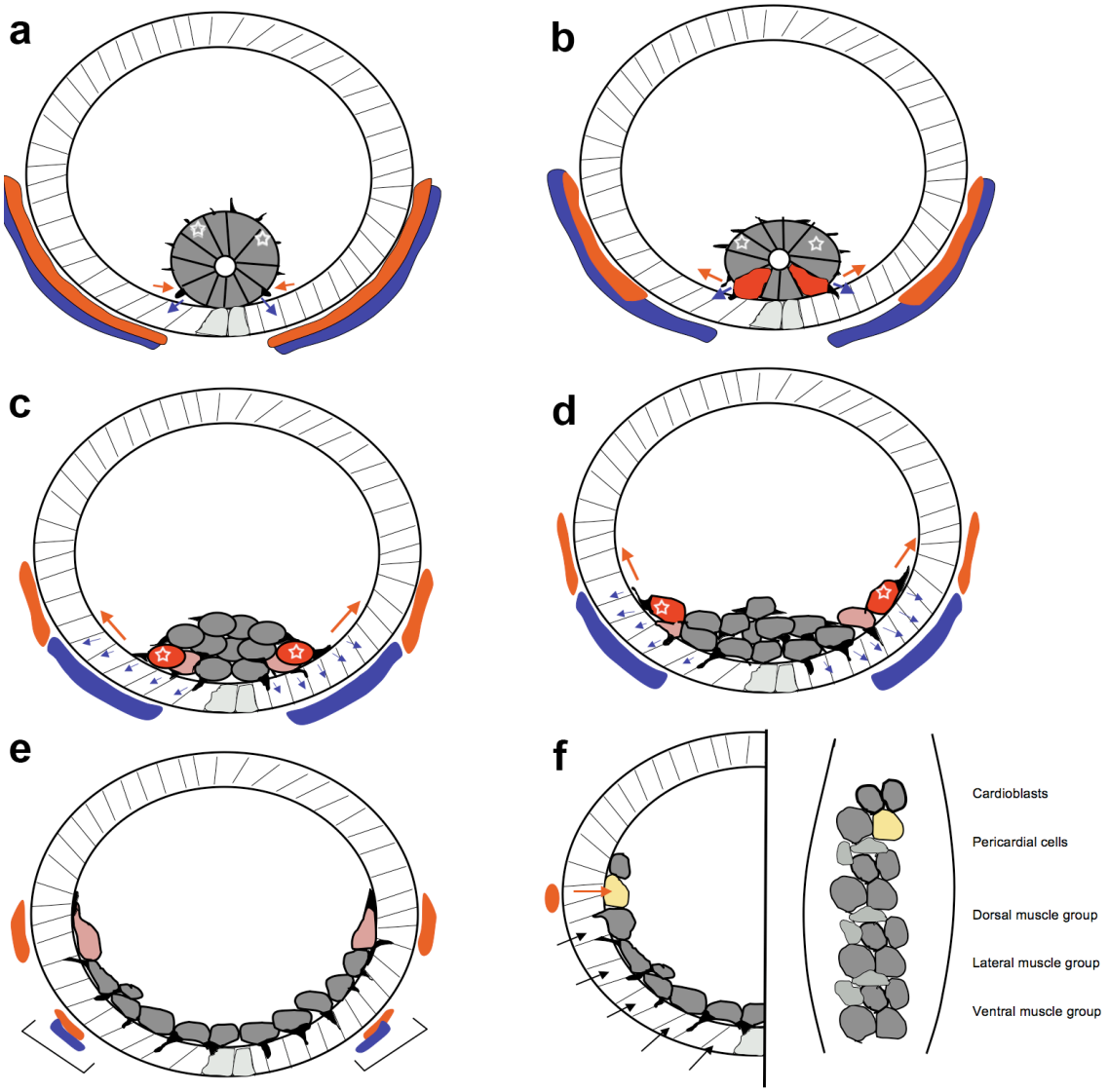

Fig. 64: Proposed model for mesoderm spreading in *Drosophila*.
Expression domains of ths are indicated in blue, pyr expression domains are indicated in orange. Arrows in related colours demonstrate the direction of cellular protrusive activity in response to Ths and Pyr mediating ectodermal attachment and dorsal polarisation of the cells, respectively. The stars indicate cells that likely contribute to the leading edge, MAPK activation (red) does highlight the same cells in initial phase (b) and later migration (c-f) **(a)** After invagination, the mesoderm cells exhibit short filopodia to sense high concentrations of Pyr or Ths. **(b)** Before EMT, the tube flattens to protrusions are extended towards the ectoderm. These are initiated by cytoskeletal rearrangements in response to activation and signalling via Htl. Establishment of contact results in phosphorylation of ERK. This event stabilizes the symmetric tube collapse and even alignment of the mesoderm along the anterior-posterior axis after EMT. **(c)** The combination of signals via Ths and Pyr provides guidance for even mesoderm migration. Signalling via Ths mediates ectodermal attachment and formation of radial protrusions, whereas Pyr is required for polarisation of cells in dorsal direction and formation of filopodia at the leading edge. **(d)** Activation of Htl by Pyr results in phosphorylation of ERK in leading edge cells, which migrate further into dorsal direction and do not differentiate until dorsal-most positions are acquired **(e).** At this stage, lateral cells acquire epithelial characteristics in response to specific sites of lateral ths and pyr expression (exemplified by lateral expression in brackets; the actual expression domains are dynamic and partially overlapping). The most dorsal mesoderm cells are still not committed and exhibit elongated cell shape and protrusions**. (f)** Finally, the mesoderm cells are distributed equally along the ventral-dorsal axis and form a monolayer. Black arrows indicate differentiation signals from the ectoderm such as Dpp. Dorsally, Pyr is required to induce expression of eve (yellow). The right panel shows a single segment with groups of specified mesoderm cells from ventral (bottom) to dorsal (top), committed to the indicated somatic muscle groups. Different shades of grey colour should indicate the patterning along the ventral-dorsal axis, which takes place gradually in this model. Cells in ventral positions thus are specified first, and most dorsal cell fates are specified last, which depends on Pyr-induced Htl signalling.

pre-patterned by Wg/Wnt and Dpp signalling. The process of gradual MET might involve combinatorial signals from both Ths and Pyr inducing the transition from mesenchymal to epithelial cell behaviour, maintained adhesion in this region and thus making cells competent to respond to further differentiation signals. The segmental and dynamically changing expression pattern of both genes, according to the stage of mesoderm development, account for such function.

Subsequent differentiation of heart and somatic muscles requires a network of transcription initiation and inhibition regulated by interaction of signalling pathways involving Dpp, Wg/Wnt and Notch which might act downstream of FGF signals, in accordance with the proposed predominant role of FGF signalling during mouse somitogenesis (Wahl et al., 2007). Mesoderm differentiation essentially requires FGF signalling to influence the expression of essential genes such as *tin* and *lbe,* which in turn are required for further induction of specific determinants.

A last issue unanswered remains the role of an attractive function to direct mesoderm migration into dorsal positions. Kadam et al. (2009) proposed that Ths and Pyr both would be able to direct mesoderm cells dorsally, the crucial requirement for such function being the restricted expression domain of the ligand. However, even in absence of *htl* or both *ths* and *pyr*, a small proportion of cells still spread in dorsal direction, and this phenomenon appears to be connected with establishment of attachment to the ectoderm (Shishido et al., 1997; Michelson et al., 1998a; Gryzik and Müller, 2004; Schumacher et al., 2004; Murray and Saint, 2007 McMahon et al, 2008). Striped over-expression of *pyr* in ectodermal domains did also not alter protrusive activity at the leading edge supporting a functional requirement for polarisation per se than attracting the cells towards the source of Pyr secretion. Thus, an obvious attractive role could not be verified for one of the Htl ligands. A possible candidate might be Dpp, which acts also together with Bnl/Btl signalling during tracheal development, but an involvement

in mesoderm migration still remains to be demonstrated (Sato and Kornberg, 2002; Ribeiro et al., 2002; Cabernard and Affolter, 2005).

IV. V. Outlook

The comparison to vertebrate FGF8 function was not stressed for the discussion on purpose. The comparison of the allele *ths*^{141} to the *C.elegans* FGF LET-756 suggests functions of Ths and Pyr that are distinct from activation of Htl. LET-756 contains a glutamine rich (Q-rich) stretch in its C-terminus, which is abolished by a mutation causing a stop codon in the allele *s2613* (Birnbaum et al., 2005). *s2613* showed a similar phenotype in comparison with *ths*^{141} with regard to reduced fertility (Popovici et al., 2004; Birnbaum et al., 2005). LET-756 has been studied extensively in structure function analyses, revealing several nuclear localisation sequences (NLS) and intracellular binding partners, assigning the *C.elegans* FGF to functions in ribosomal biogenesis, protein degradation, folding secretion and traffic, extracellular matrix remodelling, cellular physiology and transcriptional regulation, in addition to signalling (Popovici et al., 2006a, 2006b). Comparison of the C-terminal region of LET-746 and Ths revealed that a Q-rich stretch is present in the C-terminal peptide sequence of Ths as well, which similarly is deleted in Ths^{141}. The Q-stretch in LET-756 was found to be required to direct LET-756 to the speckles, sub-nuclear compartments involved in RNA metabolism and export, suggesting a role in regulation of splicing activity (Lamond and Spector, 2003; Politz et al., 2006; Popovici et al., 2004, 2006a, 2006b; Xie et al., 2006; Ishihama et al., 2008). Thus, if the loss of the Q-rich region would be associated with the phenotype observed in *ths*^{141} homozygous ovaries, Ths could also be involved in similar processes. Furthermore, analysis of both Ths and Pyr using the protein domain prediction program PSORT II (http://psort.nibb.ac.jp/psort/) revealed several putative NLS sequences for both FGFs.

Analysis of Ths and Pyr for conserved domains and comparison to known protein domains at NCBI (http://www.ncbi.nlm.nih.gov/pubmed/protein) additionally indicated now a newly assignment of both Ths and Pyr to the acidic and basic growth factor family, and also structural similarity to fibroblast homologous factor FGF13 in case of Ths and FGF7 concerning Pyr. Several domains in both the C-termini are predicted which would lead to many new intracellular functions of the Htl ligands and reveal functional requirements for the long C-terminal domains.

Itoh and Ornitz (2004) concluded that *bnl* is most similar to the FGF genes from *C.intestinalis* and vertebrate FGFs. *ths* and *pyr* by contrast are thought to be ancestral FGF genes not to have been derived from an ancestor of chordate FGF genes, and similar to *let-756* might have been lost during early metazoan evolution. Unlike LET-756, which contains an alternative secretion signal (Popovici et al., 2006a, 2006b), Ths and Pyr both contain predicted N-terminal signal peptides, although the related sequence in Ths also contains a predicted mitochondrial localisation sequence. In reference to Itoh and Ornitz (2004), *ths* and *pyr* evolved later than the *C.elegans* FGF genes, but earlier than *C.intestinalis* or vertebrate FGF genes and are not assigned to a specific FGF subfamily directly. In consequence, it might thus be possible that the loss-of function allele ths^{759}, which contains an internal deletion removing almost the coding sequence for the FGF core domain could still maintain some within its C-terminal domain. The defects observed in ths^{759} single mutants might therefore reflect the functional loss of the receptor-binding activity of Ths, but other functions might be not compromised. Structure-function analysis of Ths and Pyr by generating different constructs of partially deleted predicted amino acid sequence domains would be required and also binding assays as in case of LET-756 could reveal a lot of new requirements of both Ths and Pyr. It will be very interesting to analyse these new

possible intracellular activities and to further dissect the roles of Ths and Pyr during mesoderm development in *Drosophila*.

Appendix 1:

Anna Klingseisen, Ivan B. N. Clark, Tanja Gryzik* and H.-Arno J. Müller (2009) Differential and overlapping functions of two closely related *Drosophila* FGF8-like growth factors in mesoderm development, *Development* **136**, 2393-2402

Development ePress online publication date 10 June 2009

Development 136, 2393-2402 (2009) doi:10.1242/dev.035451

Differential and overlapping functions of two closely related *Drosophila* FGF8-like growth factors in mesoderm development

Anna Klingseisen[1], Ivan B. N. Clark[1], Tanja Gryzik[2,*] and H.-Arno J. Müller[1,†]

Thisbe (Ths) and Pyramus (Pyr), two closely related *Drosophila* homologues of the vertebrate fibroblast growth factor (FGF) 8/17/18 subfamily, are ligands for the FGF receptor Heartless (Htl). Both ligands are required for mesoderm development, but their differential expression patterns suggest distinct functions during development. We generated single mutants and found that *ths* or *pyr* loss-of-function mutations are semi-lethal and mutants exhibit much weaker phenotypes as compared with loss of both ligands or *htl*. Thus, *pyr* and *ths* display partial redundancy in their requirement in embryogenesis and viability. Nevertheless, we find that *pyr* and *ths* single mutants display defects in gastrulation and mesoderm differentiation. We show that localised expression of *pyr* is required for normal cell protrusions and high levels of MAPK activation in migrating mesoderm cells. The results support the model that Pyr acts as an instructive cue for mesoderm migration during gastrulation. Consistent with this function, mutations in *pyr* affect the normal segmental number of cardioblasts. Furthermore, Pyr is essential for the specification of *even-skipped*-positive mesodermal precursors and Pyr and Ths are both required for the specification of a subset of somatic muscles. The results demonstrate both independent and overlapping functions of two FGF8 homologues in mesoderm morphogenesis and differentiation. We propose that the integration of Pyr and Ths function is required for robustness of Htl-dependent mesoderm spreading and differentiation, but that the functions of Pyr have become more specific, possibly representing an early stage of functional divergence after gene duplication of a common ancestor.

KEY WORDS: Gastrulation, Mesoderm migration, Heart development, Fibroblast growth factor

INTRODUCTION

Growth factors provide extracellular signals that promote distinctive cell responses such as cell division, survival and migration, as well as cell fate decisions. Fibroblast growth factors (FGFs) play important roles in development in organisms ranging from simple metazoans to mammals (Szebenyi and Fallon, 1999). Among the various functions of FGF signalling, FGFs have been implicated in orchestrating complex developmentally controlled cell rearrangements (Ghabrial et al., 2003; Böttcher and Niehrs, 2005). In vertebrates, up to 22 different family members are known to interact with four different FGF receptors in a complex combinatorial fashion (Ornitz and Itoh, 2001; Itoh and Ornitz, 2004). Several different FGFs often act together in a non-overlapping way to promote morphogenetic events in vertebrate mesoderm development (Yang et al., 2002; Fletcher et al., 2006; Guo and Li, 2007). The complexity of FGFs and their receptors is much lower in invertebrate models such as *Caenorhabditis elegans* and *Drosophila melanogaster*, making them particularly amenable for functional analysis of FGF signalling (Huang and Stern, 2005). *Drosophila* contains three FGF-encoding genes, namely *branchless* (*bnl*), *thisbe* (*ths*; *FGF8-like1*) and *pyramus* (*pyr*; *FGF8-like2*), and two FGF receptors encoded by *breathless* (*btl*) and *heartless* (*htl*) (Itoh and Ornitz, 2004). Their interactions are mutually exclusive, with Ths and Pyr acting as ligands for Htl, and Bnl acting as ligand for Btl (Wilson et al., 2005; Kadam et al., 2009). The functions of Bnl and Btl are particularly well established and present a classic example of FGF signalling providing instructive signals during organ formation (Sutherland et al., 1996; Sato and Kornberg, 2002). The Htl ligands Ths and Pyr are important for mesoderm formation, but their individual roles in this process are not well understood (Gryzik and Müller, 2004; Stathopoulos et al., 2004; Kadam et al., 2009).

FGF signalling plays an important role in the specification and morphogenesis of mesodermal tissues (Slack et al., 1996; Lewandoski et al., 1997; Leptin and Affolter, 2004; Schier and Talbot, 2005; Dormann and Weijer, 2006). Members of the FGF8/17/18 subfamily in vertebrates are directly involved in gastrulation. FGF8 is required for migration of mesoderm cells away from the primitive streak in the mouse embryo (Sun et al., 1999; Guo and Li, 2007). It has been suggested that in the chick embryo, FGF8 might exert this function by repelling post-ingression mesoderm cells away from the primitive streak, whereas FGF4 acts as an attractive cue (Yang et al., 2002). Interestingly, in mouse and *Xenopus* it has been shown that FGF8 is produced as different isoforms through differential splicing and that these isoforms exhibit different functions (Fletcher et al., 2006).

Signalling of the FGF8-like growth factors Pyr and Ths through Htl is essential for proper mesoderm spreading during gastrulation and for the differentiation of mesodermal lineages (Beiman et al., 1996; Gisselbrecht et al., 1996; Shishido et al., 1997; Gryzik and Müller, 2004; Stathopoulos et al., 2004). In *Drosophila*, the ventral part of the blastoderm epithelium invaginates, resulting in the internalisation of the mesoderm primordium (Costa et al., 1993; Leptin, 1999). Once internalised, the mesoderm cells establish contact with the basal surfaces of the ectoderm cells and undergo an epithelial-mesenchymal transition. The cells then spread out dorsolaterally to establish a monolayer by the end of gastrulation

[1]Division of Cell and Developmental Biology, College of Life Sciences, University of Dundee, Dundee DD1 5EH, UK. [2]Institut für Genetik, Heinrich Heine Universität Düsseldorf, 40225 Düsseldorf, Germany.

*Present address: Medtronic GmbH, Cardiac Rhythm Disease Management, 40670 Meerbusch, Germany
†Author for correspondence (e-mail: h.j.muller@dundee.ac.uk)

Accepted 14 May 2009

(Schumacher et al., 2004; Murray and Saint, 2007; McMahon et al., 2008). Although it is known that Ths and Pyr together are essential for this process, it has yet to be established whether they act redundantly or exhibit distinct functional requirements in mesoderm spreading.

The Ths and Pyr proteins exhibit 39% amino acid identity in their FGF core domains and share the highest degree of similarity with the core domains of the chordate FGF8/17/18 subfamily (Itoh and Ornitz, 2004). Previous studies suggested that Ths and Pyr might exert different functions in gastrulation simply because they are differentially expressed from late gastrulation onwards (Gryzik and Müller, 2004; Stathopoulos et al., 2004). In the present study, we report the individual functional characterisation of Ths and Pyr in mesoderm development using loss- and gain-of-function approaches. Our data support a model in which both FGF ligands play both overlapping and distinct roles in mesoderm morphogenesis and differentiation. Neither of the single mutations affects mesoderm spreading as severely as a deletion that eliminates both ligands, suggesting redundancy of *pyr* and *ths* function in the process of mesoderm spreading. Pyr is required for formation of cellular protrusions during dorsolateral migration of the mesoderm and for differentiation of pericardial and cardioblast lineages. Other mesodermal lineages, however, require both ligands for their consistent specification. Despite these distinct requirements of *pyr* and *ths* for mesoderm development, single mutant homozygotes survive at a low rate. We therefore conclude that the gene pair *pyr ths* confers robustness to Htl signalling during mesoderm development. The subtle specialisation of *pyr* can be considered as an early stage of functional divergence after gene duplication in a *Drosophila* ancestor.

MATERIALS AND METHODS

Genetics

Fly stocks were maintained under standard conditions. The chromosomes utilised in this study are described in FlyBase (www.flybase.org) unless otherwise indicated. The P-element insertion *EP(2)G18816* is located in the fourth exon of *ths*; this allele is predicted to produce a transcript encoding a C-terminally truncated protein with an intact N-terminus that includes the entire FGF core domain. Flies homozygous for ths^{G18816} are viable and fertile and do not exhibit any gross morphological defects (T.G. and H.-A.J.M., unpublished). We generated imprecise excisions of *EP(2)G18816* and obtained two alleles containing internal deletions within the *ths* locus. ths^{141} deletes sequences corresponding to the C-terminal 12 amino acids of the highly conserved 107 amino acid FGF core domain, whereas in ths^{759} 84 amino acids of the FGF core domain are deleted (see Fig. 1). In the case of *pyr*, we mobilised the transposon insertion *P(2R)5-SZ-3066* and obtained an imprecise excision named pyr^{18}, which eliminates the entire *pyr* gene without affecting neighbouring transcription units (Fig. 1). These data indicate that ths^{759} and pyr^{18} represent loss-of-function alleles. The generation of *Df(2R)2238*, removing both *ths* and *pyr*, is described by Gryzik and Müller (Gryzik and Müller, 2004). Homozygous embryos were selected with the help of balancer chromosomes marked with *ftz::lacZ* transgenes. w^{1118} flies were used as wild-type control.

Molecular biology

Molecular cloning was performed following standard procedures. For *pyr* overexpression, a *pyr* cDNA was cloned into the pUAST vector, which was then employed for germ line transformation using standard procedures. Antisense RNA probes were produced with *ths* and *pyr* full-length cDNAs as templates using the DIG Labeling Kit (Roche, Germany).

Immunohistology and in situ hybridisation

Embryos were fixed and stained as described (Müller, 2008). For genotyping, embryos were stained with anti-β-galactosidase antibodies to detect the marked balancer chromosome, and homozygous embryos were staged and selected under the dissecting microscope. Staging was by morphological criteria, including cephalic furrow, anterior and posterior midgut invagination and extent of germ band elongation (Campos-Ortega and Hartenstein, 1997). Selected embryos were embedded in Araldite (Durcupan, Sigma) and sectioned at 5 μm. In situ hybridisation was conducted with digoxygenin-labelled antisense RNA probes following standard protocols. The following antibodies were used: rabbit anti-Twist, mouse anti-rat CD2 (Serotec), rabbit anti-β-galactosidase (β-Gal) (Cappel), mouse anti-β-Gal (Promega), mouse anti-Eve (DSHB), rabbit anti-Mef2 (gift from K. Jagla, Clermont-Ferrand, France), mouse anti-Mhc (gift from B. Patterson, Bethesda, USA), mouse anti-Lb (Jagla et al., 1997b), mouse anti-dpERK (Sigma), and mouse anti-digoxygenin conjugated with alkaline phosphatase (Roche). For detection of horseradish peroxidase, the Vectastain ABC Kit (Vector Labs) was used. Fluorescence-conjugated secondary antibodies and antibodies conjugated with alkaline phosphatase were from Jackson ImmunoResearch (Stratech). Brightfield micrographs were taken on an Olympus Axiophot. Fluorescent imaging was performed on a widefield Deltavision Spectris (Applied Precision) or on a Leica SP2 confocal laser microscope. Images were processed with Volocity software (Improvision), ImageJ (NIH) and Photoshop CS (Adobe) on an Apple computer.

RESULTS

ths and *pyr* are both required for early events in mesoderm spreading

The *ths* and *pyr* genes are located in tandem within 100 kb on the right arm of the second chromosome at cytological position 48C3-4. To determine whether *pyr* and *ths* act in redundant or independent genetic pathways, we generated mutant alleles that specifically disrupt either *pyr* or *ths* gene function without affecting any neighbouring genes (Fig. 1; see Materials and methods). Expression of *ths* was unaffected in pyr^{18} mutant embryos and expression of *pyr* was unaffected in ths^{759} embryos (see Fig. S1 in the supplementary material). Genetic complementation with two transposon-induced mutations, ths^{02026} and pyr^{02915}, indicate that these mutations are allelic to ths^{759} and pyr^{18}, respectively, but represent weaker alleles (Kadam et al., 2009) (see Figs S2 and S3 in the supplementary material). Each of the single mutations was semi-lethal, with adult homozygotes hatching at 3.4% (n=4148 total offspring of heterozygous cross of ths^{759}) and 0.71% (n=565 total offspring of heterozygous cross of pyr^{18}) (see Fig. S3 in the supplementary material). Since mutations in the Htl FGF receptor are embryonic lethal, these results indicated that the presence of either FGF8-like gene can partially compensate for the loss of the other and we therefore conclude that *pyr* and *ths* have overlapping functions during embryonic development.

We first analysed the distribution of mesoderm cells in single mutants to assess whether *ths* and *pyr* play any separable roles during mesoderm spreading. Spreading occurs in several phases that can be identified in fixed embryos by immunolocalisation of Twist (Twi). After invagination, the epithelial mesoderm primordium first contacts the ectoderm cells and then undergoes an epithelial-to-mesenchymal transition (Schumacher et al., 2004; Wilson et al., 2005). Subsequently, the cells spread out to form a monolayer.

In the wild type, the mesoderm is precisely aligned along the ventral midline and spreading occurs evenly away from the midline in a highly symmetric fashion (Fig. 2A). In embryos homozygous for *Df(2R)2238* (deleting both ligands), the mesoderm was not aligned along the midline, and ectoderm-mesoderm adhesion was severely disturbed. Subsequently, the cells failed to spread out dorsally (Fig. 2B). ths^{759} homozygotes exhibited only subtle defects in equal lateral spreading of the mesoderm (Fig. 2C). In ths^{759} mutants, mesoderm-ectoderm attachment was occasionally uneven along the anterior-posterior axis. This phenotype was more severe

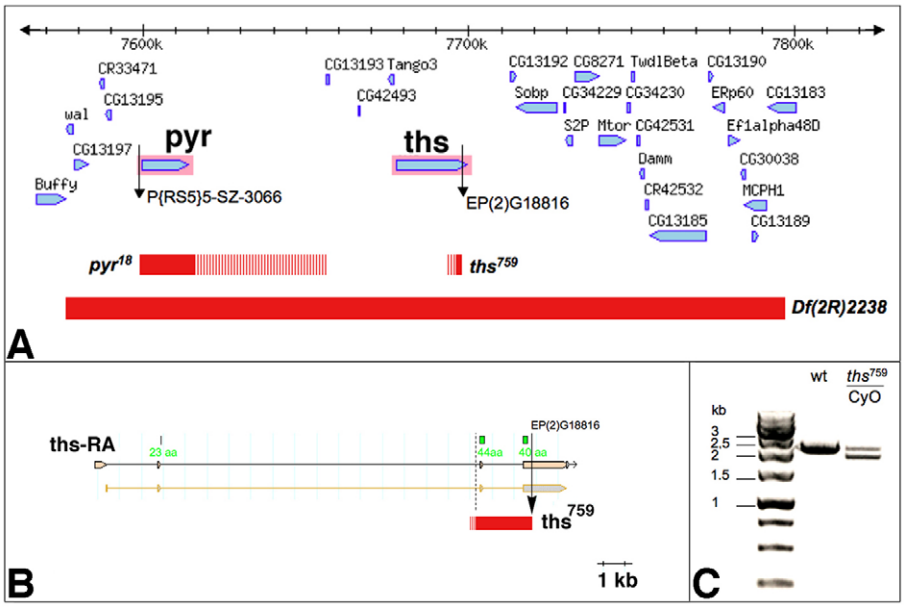

Fig. 1. Genomic characterisation of single mutant alleles for *ths* and *pyr*. (**A**) Region of the *Drosophila* genome corresponding to cytological bands 48C1-48C4. Red bars indicate the extent of deletions in *Df(2R)ED2238*, pyr^{18} and ths^{759}, as determined by PCR and RT-PCR mapping (striped bars mark regions containing breakpoints that have not been confirmed by sequencing). The pyr^{18} deletion extends to the insertion site of *P[RS5]5-SZ-3066* proximally and excludes *CG13193* distally. (**B**) ths^{759} deletes exon 3, the third intron and part of exon 4 of *ths*. This deletes 84 amino acids of the FGF core domain (regions that encode amino acids of the core domain are indicated in green). The distal breakpoint represents the insertion site of *EP(2)G18816* and the proximal breakpoint is ~300 bp 5′ of exon 3. (**C**) RT-PCR on polyA$^+$ RNA from wild-type (wt) and ths^{759} heterozygous embryos showing a 2.4 kb band corresponding to the wild-type *ths* mRNA and an additional 1.9 kb band in ths^{759} heterozygotes. The 1.9 kb product was sequenced and corresponds to the deletion depicted in B.

in pyr^{18} homozygous mutant embryos (Fig. 2C-F). At slightly later stages we observed defects in mesoderm monolayer formation in pyr^{18}, which, however, were never observed in the wild type or in ths^{759} homozygotes (Fig. 2A,C-F). We conclude that *ths* and *pyr* are both required for normal cell rearrangements during early events in mesoderm spreading. The equal mesoderm collapse onto the ectoderm requires the function of both ligands, whereas proper monolayer formation depends on *pyr* (see below). Strikingly, in the absence of *ths* function, a single copy of *pyr* is sufficient for normal monolayer formation (Fig. 2D). Nevertheless, neither of the single mutants recapitulated the strong defects in monolayer formation that were seen in the absence of both ligands, suggesting that Pyr and Ths together promote robust spreading of the mesoderm.

One response of mesoderm cells to the Htl signal is the activation of the Ras-Raf-MAPK pathway, resulting in phosphorylation of MAPK (Rolled – FlyBase) that can be measured with an antibody against double-phosphorylated ERK (dpERK) (Gabay et al., 1997). In embryos lacking FGF8-like ligands, no MAPK activation is observed in mesoderm cells at any stage during spreading (Gryzik and Müller, 2004) (Fig. 2B). In early stages during collapse and initial dorsolateral spreading, pyr^{18} mutants exhibited strongly reduced activation of MAPK, whereas activation appeared normal in ths^{759} mutants (Fig. 2C,E). Embryos with only one copy of *pyr* or one copy of *ths* exhibited reduced MAPK activation in early spreading, consistent with a requirement for each of the ligands in Htl activation. However, during monolayer formation, activation of MAPK in the dorsal-most mesodermal cells was strictly dependent on Pyr activity. In ths^{759} homozygous embryos, MAPK was activated in dorsal mesoderm cells as in the wild type (Fig. 2C,E). Thus, *pyr* is involved in normal mesoderm monolayer formation and is required for normal levels of MAPK activation. Interestingly, *pyr* expression at this stage was mainly localised in the dorsal ectoderm (Fig. 2G-I). These results indicate that the dorsal expression domain of *pyr* is required for high levels of MAPK activation during dorsolateral migration of the mesoderm.

Pyr is involved in protrusion formation during dorsolateral mesoderm migration

After ectoderm-mesoderm attachment, mesoderm cells migrate dorsolaterally. This dorsolateral migration is associated with the formation of cellular protrusions at the dorsal edge of the mesoderm aggregate (Schumacher et al., 2004) (Fig. 3A). Protrusive activity of mesoderm cells coincides with dynamic changes of *pyr* expression towards an accumulation at the dorsal edge of the ectoderm (Fig. 2G-I). Thus, an attractive model suggests that localised expression of *pyr* provides a directional cue for the mesoderm cells, instructing them to migrate in a dorsolateral direction. To assess whether loss of either FGF8-like ligand affects the formation of dorsal edge protrusions, we used the *twi::CD2* transgene as a marker for cellular protrusions (Dunin-Borkowski and Brown, 1995). In homozygous *Df(2R)ED2238* embryos, mesoderm cells did not spread out dorsally and the cells failed to form dorsal edge protrusions (Fig. 3B). In ths^{759} homozygous or hemizygous mutants, dorsal edge cells formed leading edge protrusions similar to those of the wild type (Fig. 3C,D). By contrast, in pyr^{18} homozygous and hemizygous embryos, cellular protrusions at the dorsolateral edge of the mesoderm were strongly reduced (Fig. 3E,F). Interestingly, short filopodial protrusions were still present, even in embryos lacking both ligands (Fig. 3B,E,F). Thus, mesoderm cells possess a capacity to form filopodia even in the absence of FGF signalling. This might enable the cells to sense the environment for positional cues or substrates upon which they can extend and change their shape. The phenotype

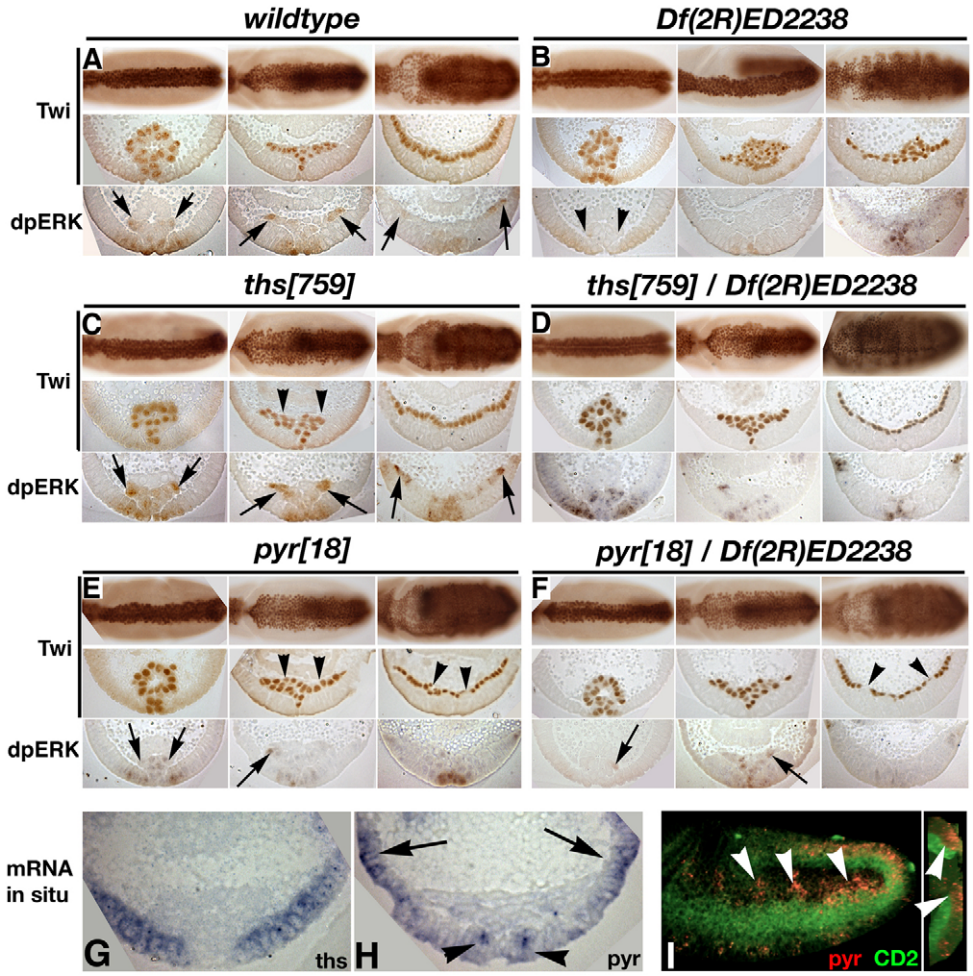

Fig. 2. Mesoderm spreading defects in *ths* and *pyr* single mutants. (**A-F**) *Drosophila* embryos of the indicated genotypes stained with anti-Twi (top two rows of each panel) or anti-dpERK (bottom row, detects MAPK) shown as whole-mount (top row) or in cross-section (between 40% and 60% egg length). Stages 7 (left column of each panel), 8 (middle) and 9 (right) are shown. (A) Wild type. Note activation of MAPK at mesoderm-ectoderm contacts and at the mesoderm leading edge (arrows). (B) In embryos lacking both *pyr* and *ths* function, mesoderm cells fail to establish initial contact, activate MAPK (arrowheads) or spread to a monolayer. (C) In ths^{759} homozygotes initial contact is normal, but unequal spreading can be observed at stage 8 (arrowheads). No major changes in monolayer formation were observed and MAPK activation was normal (arrows). (D) Embryos lacking *ths* function and one copy of *pyr* [ths^{759}/*Df(2R)ED2238*] exhibit similar defects to ths^{759} homozygotes. (E) Pyramus is required for equal dorsal spreading and monolayer formation (arrowheads). MAPK activation is strongly reduced in the absence of *pyr* function (arrows). (F) Similar defects are observed in pyr^{18}/*Df(2R)ED2238* embryos. Note the strong reduction of dpERK staining in leading edge cells (arrows). (**G-I**) *pyr* and *ths* are expressed in distinct domains during mesoderm spreading. In situ hybridisation of stage 8 embryos with antisense probes against *ths* (G) and *pyr* (H,I). (G,H) Cross-sections. (I) Fluorescent detection of *pyr* RNA (red) in an embryo expressing *twi::CD2* (green). The right-hand panel shows a reconstructed cross-section. *pyr* expression is restricted to dorsal ectoderm (arrows in H, arrowheads in I) and ventral ectodermal patches (arrowheads in H).

in *pyr*, but not *ths*, single mutant embryos strongly suggests that Pyr provides a signal that allows dorsal mesoderm cells to form long directional cell protrusions, which might reflect their migration in a dorsolateral direction.

pyr is required for dorsal mesoderm differentiation

Despite defects in equal collapse of the mesoderm to the ectoderm in embryos lacking a single ligand, monolayer formation was not affected in ths^{759} homozygotes and only subtly affected in pyr^{18} homozygotes (Fig. 2D,F). We therefore asked whether the defects in mesoderm spreading in pyr^{18} homozygotes translate into mesoderm differentiation defects in any way. To assess various mesoderm lineages, we analysed expression of *Myocyte enhancing factor 2* (*Mef2*) as a marker for somatic, visceral and cardiac muscle precursors, *Myosin heavy chain* (*Mhc*) for somatic muscles and *eve* and Ladybird genes (*lbe* and *lbl*, referred to collectively as *lb* because the antibody recognises both gene products) as markers for specific cardiac and somatic muscle lineages (Frasch et al., 1987; Jagla et al., 1997a; Jagla et al., 1998).

As mesoderm spreading is a prerequisite for dorsal mesoderm differentiation, we first looked at derivatives of the dorsal mesoderm. Late embryos lacking the Htl receptor or both ligands show a total lack of Mef2-positive muscle cells in this region (Fig. 4A-F) (Michelson et al., 1998). Embryos lacking *pyr* also showed disrupted dorsal vessel and dorsal somatic muscle development, even though these defects were less severe than in embryos lacking both ligands (Fig. 4J-L). In some cases, both cardioblasts and dorsal muscles were lacking in the

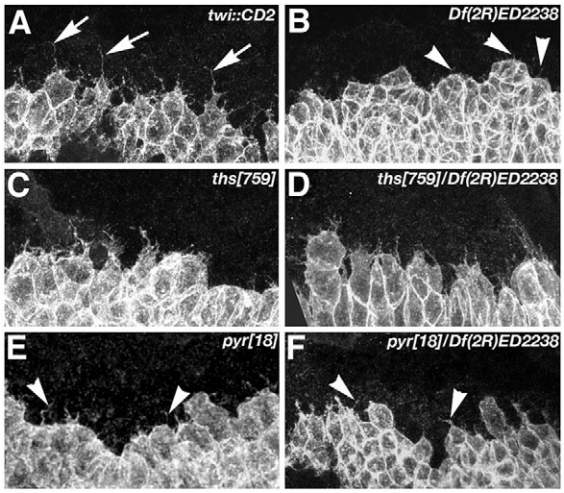

Fig. 3. Morphology of dorsal edge cells during mesoderm migration in FGF8-like ligand mutants. Cell shape at the dorsal edge of the mesoderm during dorsolateral migration visualised using *twi::CD2*. In wild type (*twi::CD2*), dorsal edge cells form thin and long protrusions (**A**, arrows). Only short, filopodial protrusions (arrowheads) are present in embryos lacking *pyr* gene function (**B**,**E**,**F**). In ths^{759} homozygous (**C**) or hemizygous (**D**) embryos, long protrusions are present similar to those in the wild type. Note that cells at the dorsal edge in E,F fail to extend along the dorsal ventral axis (dorsal is up and ventral is down).

same hemisegment (Fig. 4K,M), whereas in other cases a lack of cardioblasts did not correlate with a corresponding lack of dorsal muscles in the same hemisegment (Fig. 4L,N,O). These differences in the expressivity of the phenotype might originate from defects in dorsolateral migration during gastrulation or reflect requirements for *pyr* for the specification of specific muscle lineages (see below).

In wild-type embryos, Eve is expressed in segmental clusters in the dorsal mesoderm from stage 10; these Eve-expressing cells will form a subset of pericardial cells and the founder cell for muscle DA1 (Fig. 5A). This expression was always absent in pyr^{18} homozygous mutants (Fig. 5E,F), suggesting that the development of these cell types is disrupted at an early stage. Consistent with a lack of major defects in mesoderm spreading, *ths* was found to be largely dispensable for dorsal mesoderm development including the specification of Eve-expressing dorsal mesoderm cells (Fig. 4G-I; Fig. 5C,D). Strikingly, a single copy of the *pyr* gene was able to support all of the functions of FGF signalling during specification of cardioblasts, dorsal muscles and dorsal Eve-positive clusters in the mesoderm (Fig. 4G-I; Fig. 5D).

Formation of all dorsal mesodermal derivatives requires Dpp signalling from the dorsal ectoderm, which maintains *tinman* (*tin*) expression and regulates several other factors important in determining cell fates (Frasch, 1995). As mesoderm spreading is abnormal in pyr^{18} homozygotes, it is possible that a delay in cells reaching dorsal positions might prevent them from receiving inductive signals required for Eve expression. If this were the case, we would expect that neighbouring cell populations, which also require inductive signals, should be affected to a similar degree when FGF signalling is compromised. Indeed, we found that the induction of another marker of dorsal mesoderm derivatives, Lb, is affected in dorsal mesoderm cells adjacent to the Eve-positive clusters (Fig. 5G,H). However, in contrast to the lack of mesodermal Eve expression, the majority of hemisegments in pyr^{18} homozygotes expressed Lb (7/8 embryos have at least one cluster missing; Fig. 5G,H). Because Lb expression requires Tin, which in turn is dependent on Dpp from the dorsal ectoderm, this result implies that any delay in migration in the absence of *pyr* might indeed have an effect on patterning downstream of Dpp (Jagla et al., 1997a). With the exception of the requirement for Eve expression, mutations in *pyr* impinge on all dorsal mesodermal lineages in a random manner, consistent with variable and subtle defects in mesoderm spreading in *pyr* mutants.

ths and *pyr* are required for ventral and lateral muscle differentiation

The complete loss of Eve-positive dorsal mesoderm lineages in pyr^{18} homozygotes suggests that FGF signalling has specific functions in the early specification of certain mesoderm derivatives. This is supported by the occurrence of defects in tissues arising

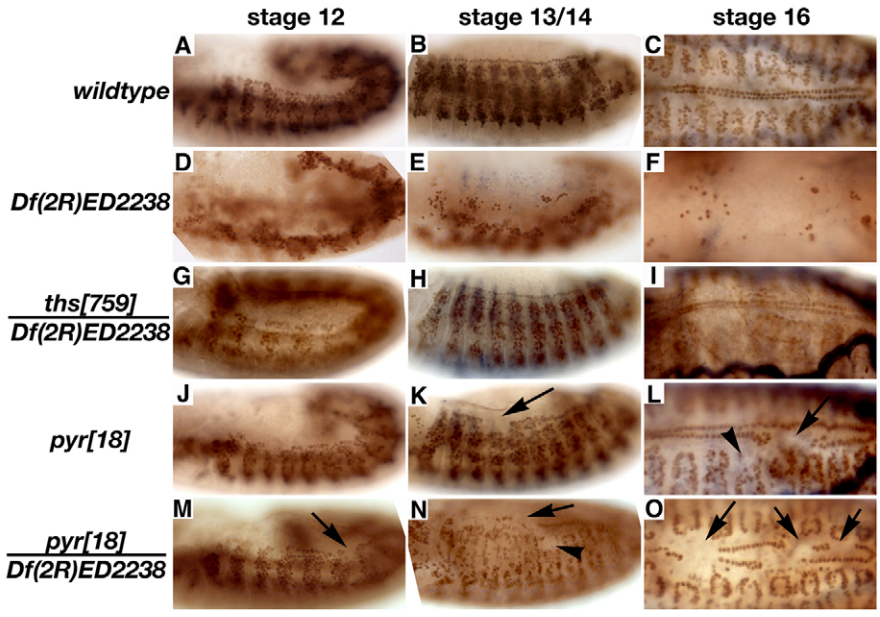

Fig. 4. Defects in somatic and cardiac muscles in FGF8-like mutant *Drosophila* embryos. Embryos at stage 12 (left column), stage 13 or 14 (middle) and stage 16 (right) were fixed and stained for Mef2. (**A-C**) Wild-type pattern of cardiac and somatic muscle cell nuclei. (**D-F**) The pattern is severely disrupted in *Df(2R)ED2238* homozygotes. Mef2-positive nuclei cluster in the ventral region (D) and the number of cardiac precursors is strongly reduced (E,F). (**G-I**) ths^{759} hemizygous embryos exhibit normal Mef2 expression. (**J-O**) pyr^{18} homozygous (J-L) and hemizygous (M-O) embryos exhibit missing nuclei in the cardiac (arrows) and somatic (arrowheads) muscle domains. The cardioblast defect is more severe in hemizygous embryos than in *pyr* homozygotes (compare O with L). Defects in dorsal somatic muscles and cardioblasts often occurred at the same anterior-posterior positions (M,K,L,O, arrows).

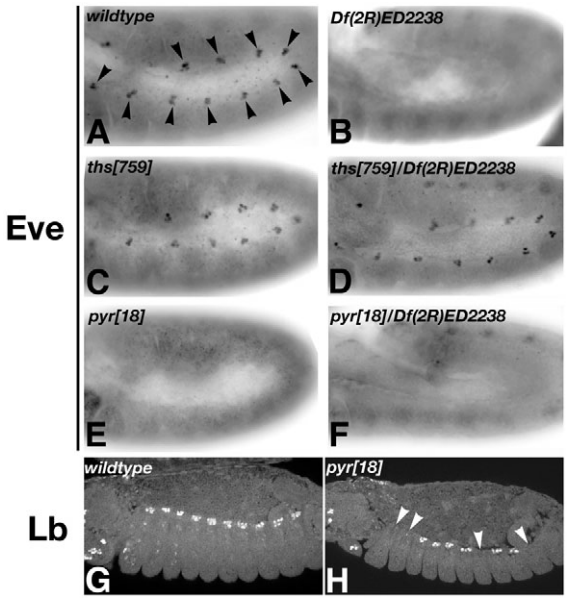

Fig. 5. Requirement of FGF8-like ligands for dorsal mesoderm differentiation. *Drosophila* embryos at stage 10 (A-F) or stage 13/14 (G,H) were fixed and stained with antibodies against Eve (A-F) or Lb (G,H). (**A**) Wild-type expression of Eve in 11 hemisegmental cell clusters (arrowheads). (**B**) In *Df(2R)ED2238* homozygotes, Eve expression is absent. (**C**,**D**) ths^{759} homozygous (C) or hemizygous (D) embryos show normal Eve expression. (**E**,**F**) pyr^{18} homozygous (E) and hemizygous (F) embryos lack Eve-positive dorsal mesodermal precursors. (**G**) Wild-type cardiac Lb expression. (**H**) Several, but not all, cardiac Lb clusters are missing in pyr^{18} homozygous embryos (arrowheads).

from the ventral and lateral mesoderm, which might not require dorsolateral migration to receive patterning signals from the ectoderm. In late embryos, we observed a range of somatic muscle defects consistent with the participation of FGF signalling in specific cell fate decisions (Fig. 6). Wild-type embryos develop a stereotyped arrangement of ~30 body wall muscles in each hemisegment, with variations in the anterior and posterior regions of the embryo (Bate, 1990). Each muscle arises from a single founder myoblast, specified at a defined segmental position through the influence of ectodermal signals on the expression of mesodermal factors (Baylies et al., 1998). It was noted previously that expression of dominant-negative Htl blocks formation of ventral oblique (VO) muscles and that an intact ventral nerve chord is required for their formation (Beiman et al., 1996; Michelson et al., 1998; Schulz and Gajewski, 1999). This implied that FGF ligands expressed in the ventral neuroblasts might be required for founder specification for these muscles. Pyr and Ths are both expressed in a subset of neuroblasts (see Fig. S4 in the supplementary material) and we found that ventral oblique muscles VO4, VO5 and VO6 are affected in pyr^{18} and ths^{759} homozygous mutants (Fig. 6A-G). Defects in pyr^{18} were more frequent when the gene dosage of *ths* was also reduced (Fig. 6C,D; Table 1).

In addition to loss of specific muscles, we also observed muscle duplications in embryos lacking the ligands of Htl. The most frequent duplication involved the segment border muscle (SBM) (Fig. 6H-K). *ths* and *pyr* single mutants exhibited duplications at a similar penetrance. In addition, only *pyr* mutants also showed occasional loss of this muscle (Table 1). The lineage of the SBM founder is also marked by expression of Lb (Jagla et al., 1998). Indeed, Lb staining in *pyr* mutant embryos revealed the absence of SBM founder cells in some segments (Fig. 6L,M; 5/10 embryos had at least one cluster missing). These results demonstrate that the formation of the SBM is affected at an early stage. More rarely, we also observed loss or duplications of other muscles (e.g. VA3 duplication; I.B.N.C. and H.-A.J.M., unpublished), suggesting that FGF signalling plays a supportive role in other cell fate decisions as well.

In summary, specific somatic muscle lineages are affected by the absence of the FGF ligands Pyr and Ths. These defects are not confined to the dorsal mesoderm, implying that the phenotypes are not simply consequences of defects in dorsolateral spreading of the mesoderm. Rather, our results indicate that muscle development in multiple lineages depends on activation by FGF signalling during mesoderm differentiation. Some *pyr* mutant phenotypes appear more severe, such as the loss of VO4-6 and SBM, suggesting that *pyr* function is more limiting than that of *ths* for the development of certain muscles. However, the robust, correct specification of these lineages requires both of the FGF8-like ligands.

Localised activation of Htl by Pyr is important for mesoderm spreading and differentiation

The data suggest that Pyr plays multiple roles: during gastrulation it is required for normal mesoderm spreading, and later it is required for mesoderm differentiation. If these functions rely upon a spatially restricted expression pattern of *pyr*, its ectopic expression in the mesoderm should abolish localised information and affect mesoderm development. Such gain-of-function analyses also have the potential to reveal whether Pyr is able to induce certain cellular behaviours, such as migration, division and differentiation.

Ectopic expression of Pyr in mesoderm cells resulted in defects in both spreading and mesoderm differentiation (Fig. 7A-L). In contrast to pyr^{18} homozygous mutant embryos, monolayer formation was severely affected upon overexpression of Pyr. Unlike expression of constitutively active forms of Htl, overexpression of Pyr resulted in a massive activation of MAPK in all mesoderm cells (Fig. 7E,F) (Wilson et al., 2005). The defects in generation of the mesoderm monolayer correlated with a defect in the formation of cellular protrusions at the dorsal edge during migration (Fig. 7M,N). Together, these data demonstrate that non-localised overactivation of the Htl pathway by Pyr results in severe migration defects and supports the idea that Pyr provides spatially restricted cues for dorsolateral migration of mesoderm cells.

Pyr is required for the formation of Eve-positive mesodermal precursor cells (see above). Differentiation of dorsal mesoderm derivatives was also strongly affected in embryos overexpressing Pyr. Cell numbers of Eve-positive mesoderm cells were strongly increased and Eve-positive cells were present at more ventral positions in embryos at later stages (during germ band retraction, stages 12 and 13) (Fig. 7G-J). Thus, although the enlargement of Eve-positive cell clusters suggests a shift in favour of dorsal mesoderm cell fates, these Eve-positive cells were not localised dorsally. This result demonstrates that Pyr can induce more ventral-lateral mesoderm to express *eve*, consistent with the idea that Pyr is a limiting factor in the induction of *eve* in mesodermal precursors. Since overexpression of Pyr also resulted in a defect in mesoderm cells reaching the dorsal ectoderm margin, we expected to see a lack of dorsal mesoderm in these embryos. Indeed, Pyr overexpression led to a complete lack of cardioblasts, indicating that the defects in mesoderm spreading translate into a dramatic loss of dorsal mesodermal cell fates (Fig. 7K,L). The overexpression phenotypes support the view that spatiotemporal control of Htl activation by Pyr

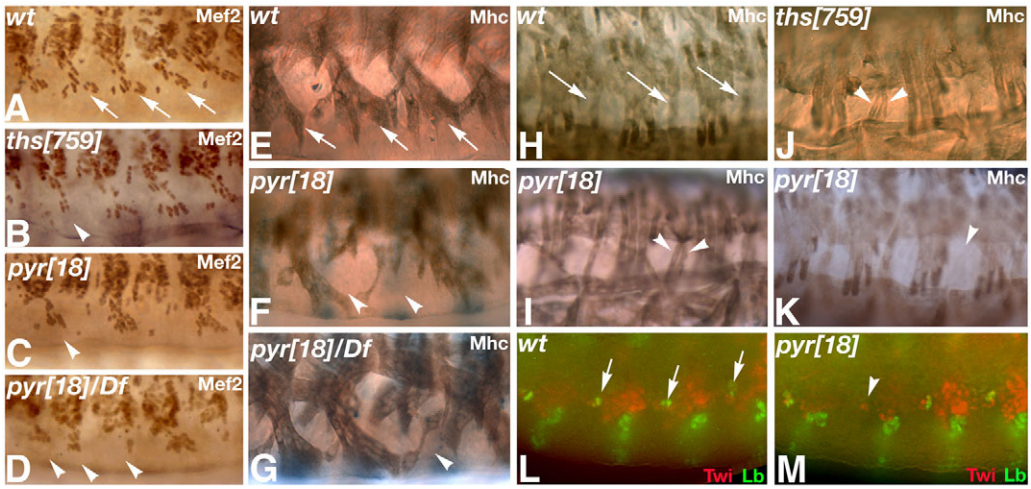

Fig. 6. Requirement of FGF8-like ligands for the differentiation of specific subgroups of somatic muscles. (**A-D**) Ventral somatic muscle nuclei (stained for Mef2) in late stage *Drosophila* embryos. (A) Wild type (wt). Nuclei of ventral oblique (VO) muscles 4-6 are indicated by arrows. VO muscle nuclei are missing in a few hemisegments of ths^{759} homozygotes (B) and in several hemisegments of pyr^{18} homozygous (C) and hemizygous (D) embryos (arrowheads) (see also Table 1). (**E-K**) Myosin heavy chain (Mhc) staining showing somatic muscles in stage 17 embryos. (E-G) Ventrolateral views showing ventral muscles. One or more of VO muscles 4-6 (arrows in E, wild type) are missing in several hemisegments of pyr^{18} homozygous (F) or hemizygous (G) embryos (arrowheads). (H-K) Lateral views. Segment border muscles (SBMs) are indicated by arrows in the wild type (H). SBM duplications are observed in both pyr^{18} (I) and ths^{759} (J) homozygous mutants (arrowheads), and hemisegments lacking an SBM are also observed in pyr^{18} homozygotes (arrowhead in K). (**L**) Wild-type stage 10 embryo showing Lb expression (green) in the ectoderm and mesoderm. Arrows indicate segmental expression of Lb in the lateral mesoderm. (**M**) Lb expression in a pyr^{18} embryo showing absence of Lb-positive mesoderm cells in one hemisegment (arrowhead).

is required for normal dorsal spreading and mesoderm differentiation, and provide evidence for an essential role of Pyr in the specification of Eve-positive mesoderm progenitor cells.

DISCUSSION

Signalling via the FGF receptor Htl is essential for mesoderm development from gastrulation onwards, but how its two ligands, Ths and Pyr, control these events is unclear. Here we present an analysis of *ths* and *pyr* single mutants and provide evidence that Pyr and Ths exhibit individual and overlapping functions in gastrulation and mesoderm differentiation.

Genetics of FGF8-like single mutants

Previously, the identification of two transposon-associated alleles, ths^{02026} and pyr^{02915}, and two chromosomal deletions, *Df(2R)ths238* and *Df(2R)pyr36*, was reported (Kadam et al., 2009). Genetic complementation analysis with pyr^{18} and ths^{759} supports the view that pyr^{02915} represents a loss-of-function allele, whereas ths^{02026} is a hypomorphic allele. However, the weaker Eve phenotype of pyr^{02915} compared with pyr^{18} indicates that pyr^{02915} is unlikely to be a null allele (see Figs S2 and S3 in the supplementary material). The alleles presented in this study represent loss-of-function alleles: in pyr^{18} the entire *pyr* gene is deleted, and in ths^{759} most of the conserved FGF core domain is deleted. In both cases, neighbouring genes remain unaffected. *Df(2R)ths238* and *Df(2R)pyr36* uncover *ths* and *pyr*, respectively, but also delete neighbouring genes (Kadam et al., 2009). In summary, whereas a null allele for *pyr* exists (pyr^{18}), there is currently no null allele of *ths* available that does not simultaneously delete other genes. In ths^{759}, 84 of the apparent 107 amino acids of the Ths FGF core domain are deleted. The FGF core domain is conserved in all FGFs, with 28 highly conserved and six identical amino acids (Ornitz and Itoh, 2001). The core domain contains amino acids important for heparin proteoglycan binding, glycosylation and FGF receptor activation (Eswarakumar et al., 2005). We previously identified nine conserved amino acids in Ths that are identical within the FGF8 subfamily, four of which are identical in all FGFs (Gryzik and Müller, 2004). In the ths^{759} allele, all of these nine identical amino acids are deleted. Therefore, if we exclude the formal possibility that the ths^{759} gene product retains activity independent of the FGF core domain, ths^{759} represents a functional null allele.

Functions of FGF8-like ligands in mesoderm differentiation

The complex expression patterns of *htl* and its two ligands, *pyr* and *ths*, in post-gastrulation stages suggested that Htl signalling functions directly in cell fate decisions during mesoderm differentiation (Shishido et al., 1993; Beiman et al., 1996;

Table 1. Defects in somatic muscles (VO and SBM) in FGF mutants

	Percentage of embryos showing muscle defects in each genotype			
Muscle affected	ths^{759}/CyO	ths^{759}/CyO × Df/CyO	pyr^{18}/CyO	pyr^{18}/CyO × Df/CyO
VO	7.8 (28)	15 (26)	16 (19)	21.4 (42)
SBM (duplication)	34.8 (23)	24 (25)	29.6 (37)	3.6 (28)
SBM (absence)	0 (23)	16 (25)	22.2 (37)	14.3 (28)

Quantification of muscle defects in stage 16/17 embryos stained with antibodies to Mhc (as depicted in Fig. 6). Because selection of homozygous embryos using a marked balancer was not possible at this stage, muscle defects were scored in all embryos from a heterozygous cross as indicated. *n*, number of embryos analysed. *Df*, *Df(2R)ED2238*; VO, ventral oblique muscles 4-6; SBM, segmental border muscle.

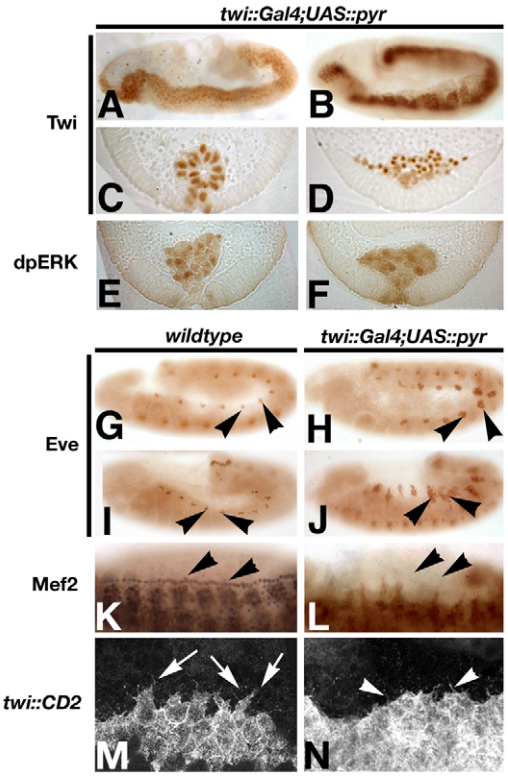

Fig. 7. Mesoderm defects after uniform activation of Htl by Pyr in mesoderm cells. (**A-F**,**H**,**J**,**L**,**N**) Pyr was overexpressed in the mesoderm using a *twi::Gal4* driver and *UAS::Pyr-HA* embryos were fixed and stained with the antibodies indicated. (**G**,**I**,**K**,**M**) Wild-type embryos for comparison. Mesoderm spreading defects in stage 7 (A,C) and stage 9 (B,D) embryos. All mesoderm cells exhibit high levels of MAPK activation at stages 7 (E) and 9 (F). Overexpression of Pyr results in large ectopic Eve-positive clusters at stages 10 and 12 (H and J, respectively, arrowheads; compare with G and I). Cardiac precursors are absent at stage 13/14 (compare K with L, arrowheads). Protrusions at the dorsal edge of the migrating mesoderm (stage 8, arrows in M) are strongly reduced (N). Note that only short filopodia-like protrusions are present (N, arrowheads).

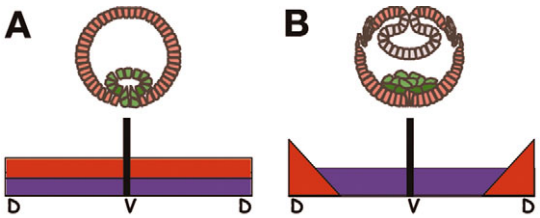

Fig. 8. Model for Ths and Pyr function in mesoderm spreading. Model for permissive and instructive functions of FGF8-like factors in *Drosophila* gastrulation. (**A**) During stages 6 and 7, both *ths* (blue) and *pyr* (red) are expressed in the ectoderm from the ventral midline (V) to the dorsal edge (D) of the neuroectoderm. We propose that both FGF8-like factors provide a permissive cue during collapse of the mesoderm (green) and attachment to the ectoderm (pink). (**B**) During dorsolateral migration of the mesoderm, expression of *ths* remains broad, whereas expression of *pyr* becomes restricted to the dorsal aspect of the neuroectodermal and ectodermal cells. We propose that at this stage, *pyr* generates an instructive cue and might act as a long-range signal.

Gisselbrecht et al., 1996; Stathopoulos et al., 2004). *pyr* is required for Eve expression in dorsal mesoderm derivates, whereas *ths* is dispensable (Kadam et al., 2009) (this study). In addition, overexpression of Pyr leads to an expansion of mesodermal Eve-positive clusters in a similar fashion to experimental overactivation of the Ras1 (Ras85D) pathway (Carmena et al., 1998; Michelson et al., 1998; Liu et al., 2006). Ths exhibits similar gain-of-function effects to Pyr with respect to expansion of Eve-positive clusters in dorsal mesoderm, suggesting that Ths and Pyr have similar signalling properties (Kadam et al., 2009) (A.K. and H.-A.J.M., unpublished). However, as Eve expression is unaffected in *ths* single mutants, it is unlikely that Ths contributes to the expression of Eve in these cells (Kadam et al., 2009) (this work).

Expression of Eve in the precursors of the pericardial cells and DA1 muscle founders depends on the activation of several signalling pathways in a group of mesodermal pre-clusters expressing *lethal of scute* (Carmena et al., 1998). Wingless (Wg) and Dpp signalling define a dorsal domain of mesoderm cells that are competent to activate transcription of *eve* in response to localised activation of Ras1. This localised Ras1 activation is largely dependent on Htl signalling (Carmena et al., 1998). During this specification process, Pyr is expressed in segmental dorsal ectodermal patches in close proximity to the sites in the mesoderm where the dorsal Eve-positive clusters form. Whereas the effect on Eve expression is fully penetrant, the generation of other dorsal mesodermal precursors, e.g. those expressing Lb, is only mildly affected in *pyr* mutant embryos. Interestingly, we observed that overexpression of Pyr results in strong activation of MAPK and ectopic Eve expression in the absence of normal dorsolateral migration. These results indicate that Pyr expression causes cells to become more sensitive to Dpp and Wg signalling and thus represents a limiting factor of the signalling network that triggers specification of Eve-positive dorsal mesoderm.

With the exception of the lack of Eve-expressing mesodermal precursors, none of the other mesoderm differentiation defects in *pyr* single mutants occurred with similar expressivity; for instance, the defects in formation of specific somatic muscles (SBM, VO4, VO5 and VO6) were penetrant at a low expressivity as they did not occur in each segment. In addition, the defects in SBM and VO muscles were also evident in *ths* homozygotes and became even more severe when one copy of the *ths* gene was removed in a *pyr* homozygous background. These observations suggest overlapping functions of *pyr* and *ths* in the specification of these muscles. In summary, we conclude that both ligands are involved in the differentiation of specific subsets of muscles.

Regulation of mesoderm spreading by Pyr and Ths

Whereas *htl* mutants exhibit severe defects, *ths* and *pyr* single mutants exhibit weak defects in mesoderm spreading (Kadam et al., 2009) (this work). Nevertheless, we found that both ligands are required for equal attachment of the mesoderm cells on to the ectoderm after invagination. As this phenotype occurs in both single mutants, either the overall level of FGF ligand at this stage is crucial, or both of the ligands need to bind to Htl-expressing cells, or each of the FGFs exerts independent functions in this process. When the gene dosage of both of the ligands is reduced by half, early mesoderm morphogenesis was normal, excluding the possibility that the overall level of FGF plays a major role (A.K. and H.-A.J.M., unpublished). Furthermore, it was recently shown that each ligand is able to signal in the absence of the other, suggesting that Ths and Pyr do not directly cooperate in Htl activation (Kadam et al., 2009)

(A.K. and H.-A.J.M., unpublished). It will be interesting to determine how each of the ligands might independently support particular aspects of early mesoderm movements.

Although both ligands are required for the early stages, only *pyr* mutants exhibited defects in dorsolateral migration and mesoderm monolayer formation (Kadam et al., 2009) (this work). The defects in monolayer formation observed in our mutants were only subtle, in contrast to the defects reported by Kadam et al. (Kadam et al., 2009). These discrepancies might reflect differences in the alleles used in the two studies. We did not observe monolayer defects in ths^{759} mutant alleles, whereas a deletion uncovering *ths* exhibits defects in monolayer formation (Kadam et al., 2009). This raises the possibility that domains other than the FGF core domain present in the protein encoded by the ths^{759} allele might exert some function in monolayer formation. We think that this is unlikely as the non-conserved C-terminal tail is dispensable for activation of Htl (A.K. and H.-A.J.M., unpublished). The deletion that was used to eliminate *ths* function, *Df(2R)ths238*, eliminates *ths* and ten proximal genes raising the alternative possibility that deletion of a gene (or genes) within *Df(2R)ths238* contributes to the rather severe mesoderm spreading defect presented by Kadam et al. (Kadam et al., 2009). Rescue experiments using full-length genomic constructs will be informative to further characterise these *ths* deletion alleles.

The presently available data are consistent with a role of the localised expression of Pyr at the dorsal edge of the ectoderm in providing an instructive cue for the cells to migrate in a dorsal direction (Fig. 8). For example, Pyr expression might produce an instructive cue that promotes dorsolateral movement of the mesoderm. It has been shown previously that FGFs can exhibit characteristics of chemoattractants in other systems (Ribeiro et al., 2002; Yang et al., 2002). Although loss- and gain-of-function analyses demonstrate that *pyr* is required for normal protrusive activity during dorsolateral migration, monolayer formation is much less affected than in *htl* mutants or ligand double mutants (Kadam et al., 2009) (this work). Therefore, although Pyr might provide a directional cue, non-polarised expression of Ths alone can compensate to some extent for the absence of this putative directional cue. In this sense, the two ligands differ slightly in their requirements for mesoderm spreading, but it is the directional movement through localised expression of *pyr* that causes this to be a robust morphogenetic process.

Overlapping and distinct functions of Pyr and Ths

The FGF8-like ligands exhibit overlapping functions except for the induction of mesodermal Eve expression, the formation of the SBM and dorsolateral migration. They cooperate to provide robustness of Htl-dependent mesoderm morphogenesis and differentiation. These imperfect redundancies become obvious in the single mutant phenotypes and might reflect the fact that *pyr* and *ths* are likely to be derived from a gene duplication event in the Drosophilids (Stathopolous et al., 2004). In more basic insects, such as *Anopheles gambia* and *Tribolium castaneum*, only one FGF8-like gene exists, and this is more similar to *ths* and might represent a common ancestor (Beermann and Schröder, 2008). It has therefore been suggested that *ths* might have retained some of the ancestral functions of the *Fgf8* homologue in *Drosophila melanogaster*. This would imply that the establishment of a localised dorsal expression domain and the hypothesised instructive role of Pyr are derived qualities. The data presented here indicate that localised expression of *pyr* renders mesoderm spreading more robust than in the absence of *pyr* expression. It would be of interest to analyse the expression and function of FGF8-like signalling in more basic insects that exhibit long germ band development and contain only one FGF8 homologue. Gene duplication has been proposed as a general mechanism in vertebrates to explain the expansion of FGF genes. Studies in dipteran species might provide insights into the evolution of the requirements for localised expression of a growth factor in directional cell movement during gastrulation.

Acknowledgements

We thank Kystrof Jagla, Bruce Patterson and the Developmental Studies Hybridoma Bank (University of Iowa, Iowa City, IA, USA) for antibodies; John James and Ryan Webster for expert technical assistance; Kate Storey and Reinhard Schröder for comments on the manuscript; and the members of the Müller laboratory for discussions. This work was funded by grants from the Deutsche Forschungsgemeinschaft (SFB590-TPB1) and a Senior Non-Clinical Research Fellowship from the Medical Research Council (MRC G0501679) to H.-A.J.M. Deposited in PMC for release after 6 months.

Supplementary material

Supplementary material for this article is available at
http://dev.biologists.org/cgi/content/full/136/14/2393/DC1

References

Bate, M. (1990). The embryonic development of larval muscles in Drosophila. *Development* **110**, 791-804.
Baylies, M. K., Bate, M. and Ruiz Gomez, M. (1998). Myogenesis: a view from Drosophila. *Cell* **93**, 921-927.
Beermann, A. and Schröder, R. (2008). Sites of Fgf signalling and perception during embryogenesis of the beetle Tribolium castaneum. *Dev. Genes Evol.* **218**, 153-167.
Beiman, M., Shilo, B. Z. and Volk, T. (1996). Heartless, a Drosophila FGF receptor homolog, is essential for cell migration and establishment of several mesodermal lineages. *Genes Dev.* **10**, 2993-3002.
Böttcher, R. T. and Niehrs, C. (2005). Fibroblast growth factor signaling during early vertebrate development. *Endocr. Rev.* **26**, 63-77.
Campos-Ortega, J. A. and Hartenstein, V. (1997). *The Embryonic Development of Drosophila melanogaster*, pp. 9-102. Berlin, Germany: Springer Verlag.
Carmena, A., Gisselbrecht, S., Harrison, J., Jimenez, F. and Michelson, A. M. (1998). Combinatorial signaling codes for the progressive determination of cell fates in the Drosophila embryonic mesoderm. *Genes Dev.* **12**, 3910-3922.
Costa, M., Sweeton, D. and Wieschaus, E. (1993). Gastrulation in Drosophila: cellular mechanisms of morphogenetic movements. In *The Development of Drosophila melanogaster* (ed. M. Bate and A. Martinez Arias), pp. 425-465. Cold Spring Harbor, NY: Cold Spring Harbor Laboratory Press.
Dormann, D. and Weijer, C. J. (2006). Chemotactic cell movement during Dictyostelium development and gastrulation. *Curr. Opin. Genet. Dev.* **16**, 367-373.
Dunin-Borkowski, O. M. and Brown, N. H. (1995). Mammalian CD2 is an effective heterologous marker of the cell surface in Drosophila. *Dev. Biol.* **168**, 689-693.
Eswarakumar, V. P., Lax, I. and Schlessinger, J. (2005). Cellular signaling by fibroblast growth factor receptors. *Cytokine Growth Factor Rev.* **16**, 139-149.
Fletcher, R. B., Baker, J. C. and Harland, R. M. (2006). FGF8 spliceforms mediate early mesoderm and posterior neural tissue formation in Xenopus. *Development* **133**, 1703-1714.
Frasch, M. (1995). Induction of visceral and cardiac mesoderm by ectodermal Dpp in the early Drosophila embryo. *Nature* **374**, 464-467.
Frasch, M., Hoey, T., Rushlow, C., Doyle, H. and Levine, M. (1987). Characterization and localization of the even-skipped protein of Drosophila. *EMBO J.* **6**, 749-759.
Gabay, L., Seger, R. and Shilo, B. Z. (1997). MAP kinase in situ activation atlas during Drosophila embryogenesis. *Development* **124**, 3535-3541.
Ghabrial, A., Luschnig, S., Metzstein, M. M. and Krasnow, M. A. (2003). Branching morphogenesis of the Drosophila tracheal system. *Annu. Rev. Cell Dev. Biol.* **19**, 623-647.
Gisselbrecht, S., Skeath, J. B., Doe, C. Q. and Michelson, A. M. (1996). heartless encodes a fibroblast growth factor receptor (DFR1/DFGF-R2) involved in the directional migration of early mesodermal cells in the Drosophila embryo. *Genes Dev.* **10**, 3003-3017.
Gryzik, T. and Müller, H. A. (2004). FGF8-like1 and FGF8-like2 encode putative ligands of the FGF receptor Htl and are required for mesoderm migration in the Drosophila gastrula. *Curr. Biol.* **14**, 659-667.
Guo, Q. and Li, J. Y. (2007). Distinct functions of the major Fgf8 spliceform, Fgf8b, before and during mouse gastrulation. *Development* **134**, 2251-2260.
Huang, P. and Stern, M. J. (2005). FGF signaling in flies and worms: more and more relevant to vertebrate biology. *Cytokine Growth Factor Rev.* **16**, 151-158.
Itoh, N. and Ornitz, D. M. (2004). Evolution of the Fgf and Fgfr gene families. *Trends Genet.* **20**, 563-569.

Jagla, K., Frasch, M., Jagla, T., Dretzen, G., Bellard, F. and Bellard, M. (1997a). ladybird, a new component of the cardiogenic pathway in Drosophila required for diversification of heart precursors. *Development* **124**, 3471-3479.
Jagla, K., Jagla, T., Heitzler, P., Dretzen, G., Bellard, F. and Bellard, M. (1997b). ladybird, a tandem of homeobox genes that maintain late wingless expression in terminal and dorsal epidermis of the Drosophila embryo. *Development* **124**, 91-100.
Jagla, T., Bellard, F., Lutz, Y., Dretzen, G., Bellard, M. and Jagla, K. (1998). ladybird determines cell fate decisions during diversification of Drosophila somatic muscles. *Development* **125**, 3699-3708.
Kadam, S., McMahon, A., Tzou, P. and Stathopoulos, A. (2009). FGF ligands in Drosophila have distinct activities required to support cell migration and differentiation. *Development* **136**, 739-747.
Leptin, M. (1999). Gastrulation in Drosophila: the logic and the cellular mechanisms. *EMBO J.* **18**, 3187-3192.
Leptin, M. and Affolter, M. (2004). Drosophila gastrulation: identification of a missing link. *Curr. Biol.* **14**, R480-R482.
Lewandoski, M., Meyers, E. N. and Martin, G. R. (1997). Analysis of Fgf8 gene function in vertebrate development. *Cold Spring Harb. Symp. Quant. Biol.* **62**, 159-168.
Liu, J., Qian, L., Wessells, R. J., Bidet, Y., Jagla, K. and Bodmer, R. (2006). Hedgehog and RAS pathways cooperate in the anterior-posterior specification and positioning of cardiac progenitor cells. *Dev. Biol.* **290**, 373-385.
McMahon, A., Supatto, W., Fraser, S. E. and Stathopoulos, A. (2008). Dynamic analyses of Drosophila gastrulation provide insights into collective cell migration. *Science* **322**, 1546-1550.
Michelson, A. M., Gisselbrecht, S., Zhou, Y., Baek, K. H. and Buff, E. M. (1998). Dual functions of the heartless fibroblast growth factor receptor in development of the Drosophila embryonic mesoderm. *Dev. Genet.* **22**, 212-229.
Müller, H. A. (2008). Immunolabeling of embryos. *Methods Mol. Biol.* **420**, 207-218.
Murray, M. J. and Saint, R. (2007). Photoactivatable GFP resolves Drosophila mesoderm migration behaviour. *Development* **134**, 3975-3983.
Ornitz, D. M. and Itoh, N. (2001). Fibroblast growth factors. *Genome Biol.* **2**, 3005.3001-3012.
Ribeiro, C., Ebner, A. and Affolter, M. (2002). In vivo imaging reveals different cellular functions for FGF and Dpp signaling in tracheal branching morphogenesis. *Dev. Cell* **2**, 677-683.
Sato, M. and Kornberg, T. B. (2002). FGF is an essential mitogen and chemoattractant for the air sacs of the drosophila tracheal system. *Dev. Cell* **3**, 195-207.
Schier, A. F. and Talbot, W. S. (2005). Molecular genetics of axis formation in zebrafish. *Annu. Rev. Genet.* **39**, 561-613.
Schulz, R. A. and Gajewski, K. (1999). Ventral neuroblasts and the heartless FGF receptor are required for muscle founder cell specification in Drosophila. *Oncogene* **18**, 6818-6823.
Schumacher, S., Gryzik, T., Tannebaum, S. and Müller, H. A. (2004). The RhoGEF Pebble is required for cell shape changes during cell migration triggered by the Drosophila FGF receptor Heartless. *Development* **131**, 2631-2640.
Shishido, E., Higashijima, S., Emori, Y. and Saigo, K. (1993). Two FGF-receptor homologues of Drosophila: one is expressed in mesodermal primordium in early embryos. *Development* **117**, 751-761.
Shishido, E., Ono, N., Kojima, T. and Saigo, K. (1997). Requirements of DFR1/Heartless, a mesoderm-specific Drosophila FGF-receptor, for the formation of heart, visceral and somatic muscles, and ensheathing of longitudinal axon tracts in CNS. *Development* **124**, 2119-2128.
Slack, J. M., Isaacs, H. V., Song, J., Durbin, L. and Pownall, M. E. (1996). The role of fibroblast growth factors in early Xenopus development. *Biochem. Soc. Symp.* **62**, 1-12.
Stathopoulos, A., Tam, B., Ronshaugen, M., Frasch, M. and Levine, M. (2004). pyramus and thisbe: FGF genes that pattern the mesoderm of Drosophila embryos. *Genes Dev.* **18**, 687-699.
Sun, X., Meyers, E. N., Lewandoski, M. and Martin, G. R. (1999). Targeted disruption of Fgf8 causes failure of cell migration in the gastrulating mouse embryo. *Genes Dev.* **13**, 1834-1846.
Sutherland, D., Samakovlis, C. and Krasnow, M. A. (1996). branchless encodes a Drosophila FGF homolog that controls tracheal cell migration and the pattern of branching. *Cell* **87**, 1091-1101.
Szebenyi, G. and Fallon, J. F. (1999). Fibroblast growth factors as multifunctional signaling factors. *Int. Rev. Cytol.* **185**, 45-106.
Wilson, R., Vogelsang, E. and Leptin, M. (2005). FGF signalling and the mechanism of mesoderm spreading in Drosophila embryos. *Development* **132**, 491-501.
Yang, X., Dormann, D., Munsterberg, A. E. and Weijer, C. J. (2002). Cell movement patterns during gastrulation in the chick are controlled by positive and negative chemotaxis mediated by FGF4 and FGF8. *Dev. Cell* **3**, 425-437.

Supplemental figure S1

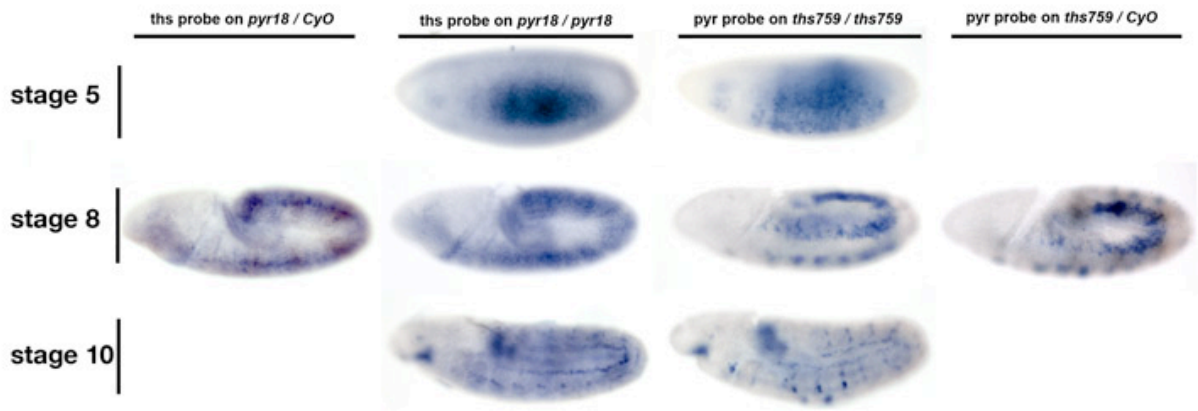

Fig. S1. Expression of *ths* and *pyr* in pyr^{18} and ths^{759} homozygous embryos.
In situ hybridisation with antisense RNA probes against *pyr* and *ths* of embryos from pyr^{18} and ths^{759} heterozygous (pyr^{18}/CyO and ths^{759}/CyO) and homozygous (ths^{759}/ths^{759} and pyr^{18}/pyr^{18}) embryos, respectively. Note that the expression pattern remained unimpaired in the mutants.

Supplemental figure S2

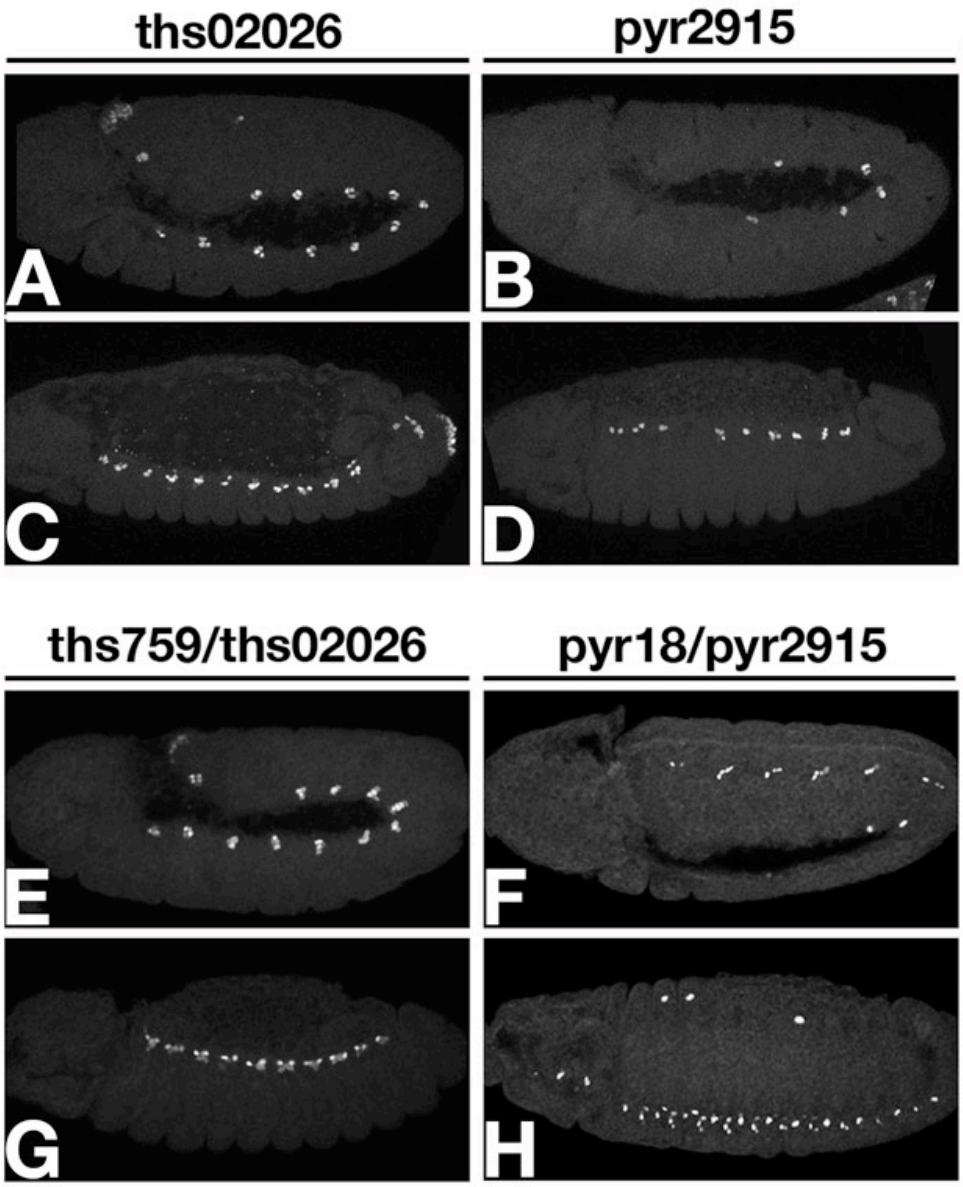

Fig. S2. Mesoderm phenotype in ths02026 and pyr02915 mutants. Embryos were fixed and stained for Eve.
(A,B,E,F) Embryonic stage 10; (C,D,G,H) embryonic stage 14. Normal numbers of Eve-positive cells were observed in *ths02026* homozygotes (A,C). The number of Eve clusters was reduced, but they were never completely absent, in homozygous *pyr02915* embryos (B,D). In transheterozygous combinations with ths^{759} and pyr^{18}, ths mutants did not exhibit any defects (E,G), whereas the number of Eve-positive hemisegments was further reduced in pyr transheterozygotes (F,H). For quantification, see Fig. S3

Supplemental figure S3

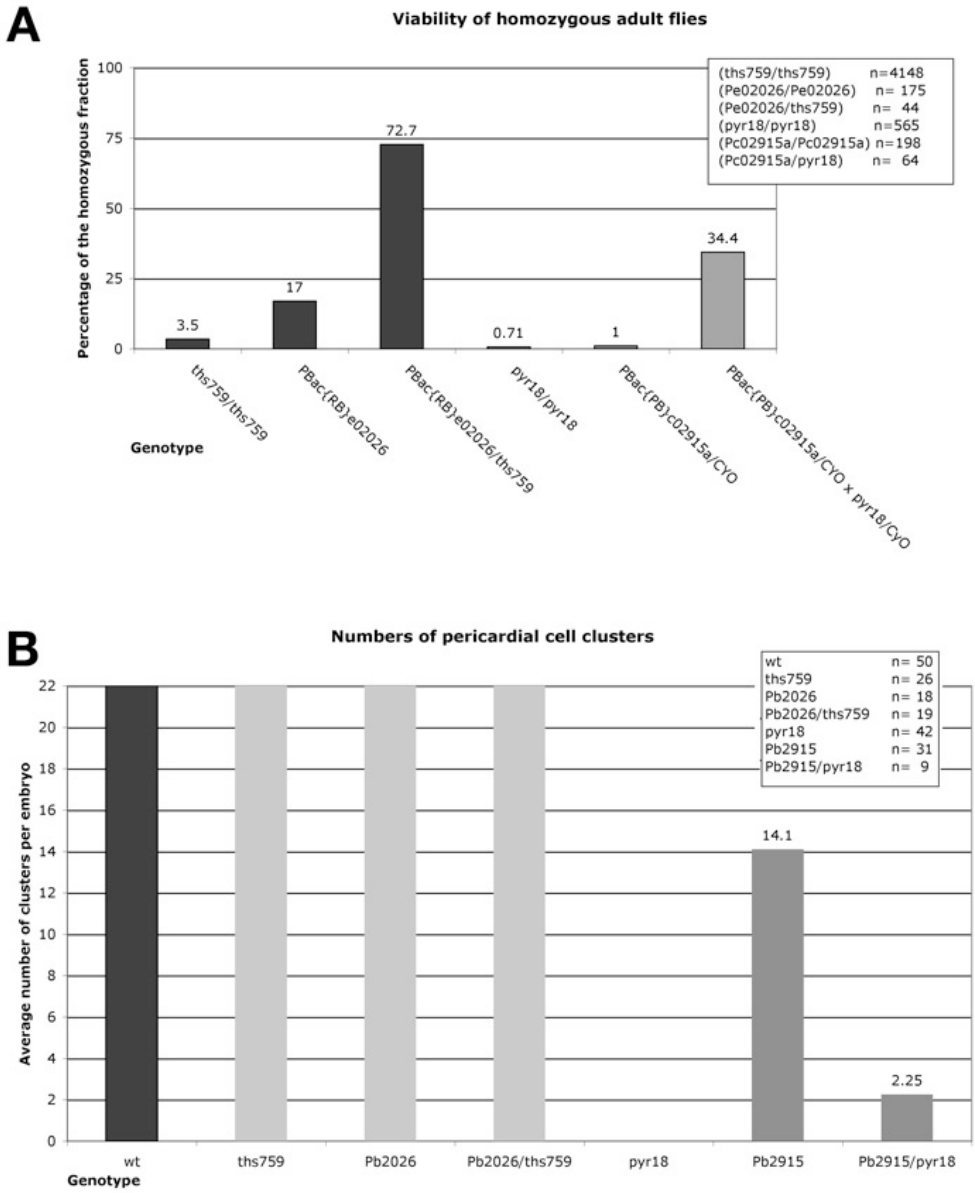

Fig. S3. Quantitative analysis of complementation of ths and pyr single mutant alleles.
(A) Hatching adult homozygous escaper flies from *ths* and *pyr* mutant alleles. The number of surviving adult homozygotes (Cy+) was determined and is presented as a percentage of the expected Mendelian number of homozygotes. All crosses were incubated at 25°C. (B) Eve-positive pericardial cell clusters were determined from fixed embryos (stage 10-13) of the phenotypes indicated. Note that the Eve phenotype of *pyr2915* is strongly enhanced in trans to pyr^{18}.

Supplemental figure S4

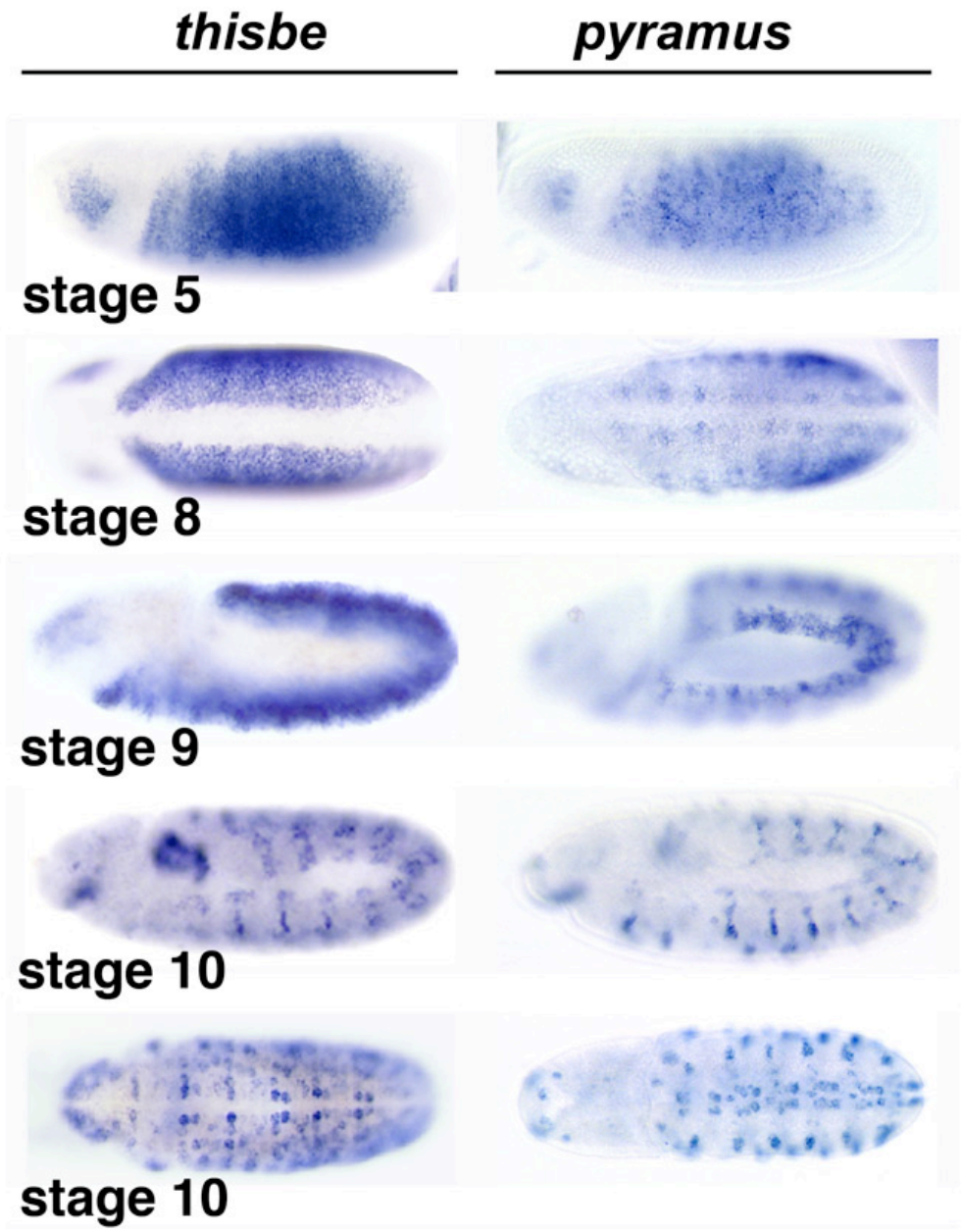

Fig. S4. Localisation of ths and pyr transcripts as determined by in situ hybridisation.
Stage 5 (lateral view) showing expression of ths and pyr in an overlapping domain in the neuroectoderm. Stage 8 (ventral view) showing that during dorsal-lateral migration of the mesoderm, expression of ths remains throughout the entire neuroectoderm (ventral view). Expression of pyr becomes restricted to ventral segmental patches and a strong expression along the dorsal edge of the ectoderm. At stage 9 (lateral view), ths remains expressed in the neuroectoderm. In addition, expression in the delaminating neuroblast becomes obvious. pyr expression is confined to the dorsal edge in the ectoderm. Neuroblast expression begins as neuroblasts delaminate from the neuroectoderm. Stage 10 (lateral view), showing overlapping segmental expression of ths and pyr. The expression domains are strongly overlapping. Stage 10 (ventral view), showing that both ths and pyr are expressed in the neuroblasts.

Appendix 2

Internal lesions in Ths^{141} and Ths^{759} protein sequence

MSNQLERLLFFIVVISGALCTVEDYVIMSQCAHNKA [759 IHIAAEGTVSVTDTSQ
IQNITIVGFPDYLNNEFKIALYAKETRRYLCFNDNWRLVGMRELRDTCYFN
ETIVHGYFVFRSVVDLQRRVGFTHR [141 GKPVGPKK SVNDACYMF NKIEAEQF
FRHHHNNGNSGNNNGNGSGNDNGNGSNNSRKPPRNNKNNRHKSNNQNQKL
QQQQEHHGHNNNNNNVILNNSNTSLSSTNKKQL [141 A] [759 INRQRQQQQQHQVRHHH
NDPSLLLRRQQHEKKQKRRKQQKQQQHQQRVSASPTNPMPATPTAAPAATPT
VAATSPATATRSTTAAMSSKRKGRRRKAKVRPKAQQQQQLQLLATAATSPYT
DDTLYGSSSSSSSTGFEDLDIYNSSSSSGSSSSLDPWSTWSTIDSFSGSSTTATSDD
SISSSSSSNYDAWATYITEMEAEASAMTPEMGGNDTELMQYEAELVDDPEAES
TATIETKATSVTSTIAATAATTTSTAGSQLVIEQTPLARSNISNKSSSSTKATPTAT
SQTETAQSTQQPSRHRSNSREDHLDNSDMLLAGENEVKPQQPRKLLWTVQPPL
ATRGSTLATLVATPEQQHTSTTATAATTPEQHVAPSLFSVDKNINSNLNNTLTE
ASPTATSTSSITSATTMKRPIRKFTKKLMATPYHQLTYVRNAGGDIDIDNLDNIS
VYPVLYDGDLEGNGGGNSSDGGFSGFLPTSTTSHLTEPIRIGMNRIRPNKTLHW
FTHQRFA

Amino sequence of Ths.

The sequence of the signal peptide is indicated in green and the FGF core domain in red.

The brackets indicate the extent of the lesions in *ths*^{141} (141) and *ths*^{759} (759), respectively, e.g. the sequence within the brackets is missing in the respective alleles. The lesion in Ths^{759} removes most of the amino acid residues the FGF core domain comprises

In blue, a Q-stretch within the sequence is indicated which is removed in *ths*^{141}. Following the function in LET-756 (Popovici et al., 2006a, 2006b), this region could possess possible function in intracellular localisation of Ths.

Acknowledgements

I want to thank Arno Müller for the opportunity to carry out a research project in an interesting field of developmental biology, and further to do the PhD at the university of Dundee. I thank Arno for his support, interesting discussions, and also for having a laugh every now and then. I did learn a lot during the time of my PhD.

I thank Kate Storey and Eli Knust for reading the thesis and to take on the roles of the examiners for my PhD.

Further I want to thank all the stuff members from the university and the division for advice and support, and for help and support with all the media, washing and paperwork; and the facilities available that help to make everything easier to deal with.

Thank you to all the former members of the Düsseldorf genetic institute; we had a really good time together. Especially, I want to mention the members of our "A-team lab", Andreas, Eva Ines, Kathrin, Soya, Thorsten, Tanja (*x*), Sabine and Walther (when he was in). Thanks to the A-team, the worms (especially Tobi, Robin and Mic) and the other fly-guys, Carmen, Thomas, Mirjana, Manuel and all the members of the "Fliegen-lädchen" (including André and Ferdi), work was just easier and more fun, and I always felt we were having a good time together. I really miss all the barbecues on the roof!
And Carmen, what would I have done without all our "secret talks" in the box room..;-)

Nana, I don't have words either. You were always there even when you actually where not, and you'll be with me, always. Der Rapdt! wird immer bleiben.

Thank you sincerely to the members from the HAM-lab, Allister, Andreas, Daniel H, Daniel M, Ivan, Maggy and Ryan. I'll miss the "warm office" –lunch times, the fly-

room talk, and in general, I felt we were just really good as a group! And I hope we will stay in contact, and maybe I can join the "badminton-club" from time to time..

Thank you Andreas, for our good time together sharing a flat, all the talks in the hallway (even when spiders fell from the ceiling and you had to let them out), and for sharing the late work hours in the lab. I know, "*schön, ist es auf der welt zu sein, sagt die biene…*"..that song will stick in my head forever…

Maggy, I found a true good friend in you, thank you for being there all the time. HDSL

Special thanks also to Agata (*), Michelle and Daniel, dear friends and flatmates. Thank you for all the support, especially during the last months. The time in the house together was just really good. Nobody actually cared about water coming and going in the kitchen, having an antz-score or things like that, or make me buy the 10th bottle of oil..
:-) I hope you will all come visit me in Edinburgh and we won't lose contact to each other.

I further want to thank K. McMillan for her support.

A special thank you to Fiona G., I don't know how I would have come so far without her support.

Last, but not least, I am grateful for all the support and love I got from my parents and my sister Laura. I owe you a great deal of what I could accomplish and tackle.

It was a really hard time, but it was a really good time as well. I will definitely miss Dundee and everything connected. Fortunately, I don't have to move that far away and will come for a visit, 'more every now than then' :-)

References

Acloque, H., Thiery, J.P. and Nieto, M.A. (2008) The physiology and pathology of the EMT. Meeting on the epithelial-mesenchymal transition. *EMBO Rep*, **9**(4), 322–6.

Adams, M.D. et al. (2000) The genome sequence of *Drosophila melanogaster*. *Science*, **287**(5461), 2185–95.

Affolter, M. and Basler, K. (2007) The Decapentaplegic morphogen gradient: from pattern formation to growth regulation. *Nature Reviews Genetics*, **8**(9), 663–74.

Affolter, M. and Caussinus, E. (2008) Tracheal branching morphogenesis in *Drosophila*: new insights into cell behaviour and organ architecture. *Development (Cambridge, England)*, **135**(12), 2055–64.

Affolter, M. and Weijer, C.J. (2005) Signaling to cytoskeletal dynamics during chemotaxis. *Dev Cell*, **9**(1), 19–34.

Akai, J., Halley, P.A. and Storey, K.G. (2005) FGF-dependent Notch signaling maintains the spinal cord stem zone. *Genes and Development*, **19**(23), 2877–87.

Akiyama T, Kamimura K, Firkus C, Takeo S, Shimmi O, Nakato H. (2008) Dally regulates Dpp morphogen gradient formation by stabilizing Dpp on the cell surface. *Dev Biol*, **313**(1), 408–19.

Allen, B.L. and Rapraeger, A.C. (2003) Spatial and temporal expression of heparan sulfate in mouse development regulates FGF and FGF receptor assembly. *J Cell Biol*, **163**(3), 637–48.

Alvarez AD, Shi W, Wilson BA, Skeath JB. (2003) Pannier and pointedP2 act sequentially to regulate *Drosophila* heart development. *Development (Cambridge, England)*, **130**(13), 3015–26.

Amarasinghe AK, MacDiarmid R, Adams MD, Rio DC. (2001) An in vitro-selected RNA-binding site for the KH domain protein PSI acts as a splicing inhibitor element. *RNA*, **7**(9), 1239–53.

Artero R, Furlong EE, Beckett K, Scott MP, Baylies M, (2003) Notch and Ras signaling pathway effector genes expressed in fusion competent and founder cells during *Drosophila* myogenesis. *Development*, **130**(25), 6257–72.

Arthur, W.T., Quilliam, L.A. and Cooper, J.A. (2004) Rap1 promotes cell spreading by localizing Rac guanine nucleotide exchange factors. *J Cell Biol*, 167(1), 111–22.

Asha H, de Ruiter ND, Wang MG, Hariharan IK (1999) The Rap1 GTPase functions as a regulator of morphogenesis in vivo. *EMBO J*, **18**(3), 605–15.

Avruch J, Hara K, Lin Y, Liu M, Long X, Ortiz-Vega S, Yonezawa K. (2006) Insulin and amino-acid regulation of mTOR signaling and kinase activity through the Rheb GTPase. *Oncogene*, **25**(48), 6361–72.

Azpiazu, N. and Frasch, M. (1993) Tinman and bagpipe: two homeo box genes that determine cell fates in the dorsal mesoderm of *Drosophila*. *Genes and Development*, 7(7B), 1325–40.

Azpiazu N, Lawrence P, Vincent J, Frasch M. (1996) Segmentation and specification of the *Drosophila* mesoderm. *Genes and Development*, **10(**24), 3183–94.

Bachmann, A. and Knust, E.,(2008) The use of P-element transposons to generate transgenic flies. *Methods Mol Biol*, 420, 61–77.

Bailly, M., Condeelis, J.S., Segall, J.E. (1998) Chemoattractant-induced lamellipod extension. *Microsc Res Tech*, 43(5), 433–43.

Bailly M, Wyckoff J, Bouzahzah B, Hammerman R, Sylvestre V, Cammer M, Pestell R, Segall JE. (2000) Epidermal growth factor receptor distribution during chemotactic responses. *Mol Biol Cell*, **11**(11), 3873–83.

Baines, A.J. (2006) A FERM-adjacent (FA) region defines a subset of the 4.1 superfamily and is a potential regulator of FERM domain function. *BMC Genomics*, 7, 85.

Balzac F, Avolio M, Degani S, Kaverina I, Torti M, Silengo L, Small JV, Retta SF. (2005) E-cadherin endocytosis regulates the activity of Rap1: a traffic light GTPase at the crossroads between cadherin and integrin function. *Journal of Cell Science*, **118**(Pt 20), 4765–83.

Bamburg, J.R., McGough, A. and Ono, S. (1999) Putting a new twist on actin: ADF/cofilins modulate actin dynamics. *Trends Cell Biol*, **9**(9), 364–70.

Bate, M. and Rushton, E. (1993) Myogenesis and muscle patterning in *Drosophila*. *C R Acad Sci III, Sci Vie*, **316**(9), 1047–61.

Battersby, A. (2001) Identification of molecules that interact with the adaptor protein Dof - phd thesis. Available at: http://deposit.ddb.de/cgi-bin/dokserv?idn=962733261anddok_var=d1anddok_ext=pdfandfilename=962733261.pdf.

Battersby A, Csiszár A, Leptin M, Wilson R. (2003) Isolation of Proteins that Interact with the Signal Transduction Molecule Dof and Identification of a Functional Domain Conserved between Dof and Vertebrate BCAP. *Journal of Molecular Biology*, **329**(3), 479–493.

Baum, J.S. et al. (2007) The *Drosophila* caspases Strica and Dronc function redundantly in programmed cell death during oogenesis. *Cell Death Differ*, **14**(8), 1508–17.

Baylies, M.K., Bate, M. and Gomez, M.R. (1998) Myogenesis: a view from *Drosophila*. *Cell*, **93**(6), 921–7.

Beh J, Shi W, Levine M, Davidson B, Christiaen L. (2007) FoxF is essential for FGF-induced migration of heart progenitor cells in the ascidian *Ciona intestinalis*. *Development*, **134**(18), 3297–305.

Beiman, M., Shilo, B.Z. and Volk, T (1996) Heartless, a *Drosophila* FGF receptor homolog, is essential for cell migration and establishment of several mesodermal lineages. *Genes and Development*, **10**(23), 2993–3002.

Belenkaya TY, Han C, Yan D, Opoka RJ, Khodoun M, Liu H, Lin X (2004). *Drosophila* Dpp morphogen movement is independent of dynamin-mediated endocytosis but regulated by the glypican members of heparan sulfate proteoglycans. *Cell*, **119**(2), 231–44.

Bernfield M, Götte M, Park PW, Reizes O, Fitzgerald ML, Lincecum J, Zako M (1999) Functions of cell surface heparan sulfate proteoglycans. *Annu. Rev. Biochem.*, **68**, 729–77.

Bianco A, Poukkula M, Cliffe A, Mathieu J, Luque CM, Fulga TA, Rørth P (2007). Two distinct modes of guidance signalling during collective migration of border cells. *Nature*, **448**(7151), 362–5.

Birnbaum, D., Popovici, C. and Roubin, R (2005). A pair as a minimum: the two fibroblast growth factors of the nematode Caenorhabditis elegans. *Dev Dyn*, **232**(2), 247–55.

Blackwell, T.K. (2004) Germ cells: finding programs of mass repression. *Curr Biol*, **14**(6), R229–30.

Boettner, B. and van Aelst, L. (2009). Control of cell adhesion dynamics by Rap1 signaling. *Current Opinion in Cell Biology*, **21**(5), 684–93.

Boettner, B. and van Aelst, L. (2007a) The Rap GTPase Activator *Drosophila* PDZ-GEF Regulates Cell Shape in Epithelial Migration and Morphogenesis. *Molecular and Cellular Biology*, 27(22), 7966.

Boettner, B. and van Aelst, L. (2007b) The Rap GTPase activator *Drosophila* PDZ-GEF regulates cell shape in epithelial migration and morphogenesis. *Molecular and Cellular Biology*, **27**(22), 7966–80.

Boettner B, Harjes P, Ishimaru S, Heke M, Fan HQ, Qin Y, Van Aelst L, Gaul U (2003) The AF-6 homolog canoe acts as a Rap1 effector during dorsal closure of the *Drosophila* embryo. *Genetics*, **165**(1), 159–69.

Bollenbach T, Pantazis P, Kicheva A, Bökel C, González-Gaitán M, Jülicher F (2008) Precision of the Dpp gradient. *Development (Cambridge, England)*, **135**(6), 1137–46.

Borkowski, O.M., Brown, N.H. and Bate, M. (1995). Anterior-posterior subdivision and the diversification of the mesoderm in *Drosophila*. *Development*, **121**(12), 4183–93.

Boucaut JC, Johnson KE, Darribère T, Shi DL, Riou JF, Bache HB, Delarue M (1990) Fibronectin-rich fibrillar extracellular matrix controls cell migration during amphibian gastrulation. *Int J Dev Biol*, **34**(1), 139–47.

Bour BA, O'Brien MA, Lockwood WL, Goldstein ES, Bodmer R, Taghert PH, Abmayr SM, Nguyen HT (1995) *Drosophila* MEF2, a transcription factor that is essential for myogenesis. *Genes and Development*, **9**(6), 730–41.

Böttcher, R.T. and Niehrs, C. (2005) Fibroblast growth factor signaling during early vertebrate development. *Endocr Rev*, **26**(1), 63–77.

Brand, A.H. and Perrimon, N. (1993) Targeted gene expression as a means of altering cell fates and generating dominant phenotypes. *Development*, **118**(2), 401–15.

Branford, W.W. and Yost, H.J. (2002) Lefty-dependent inhibition of Nodal- and Wnt-responsive organizer gene expression is essential for normal gastrulation. *Curr Biol*, **12**(24), 2136–41.

Brent, A.E. and Tabin, C.J. (2004) FGF acts directly on the somitic tendon progenitors through the Ets transcription factors Pea3 and Erm to regulate scleraxis expression. *Development (Cambridge, England)*, **131**(16), 3885–96.

Buff E, Carmena A, Gisselbrecht S, Jiménez F, Michelson A (1998). Signalling by the *Drosophila* epidermal growth factor receptor is required for the specification and diversification of embryonic muscle progenitors. *Development*, **125**(11), 2075–86.

Bui, Y.K. and Sternberg, P.W. (2002) *Caenorhabditis elegans* inositol 5-phosphatase homolog negatively regulates inositol 1,4,5-triphosphate signaling in ovulation. *Mol Biol Cell*, **13**(5), 1641–51.

Burridge, K. and Wennerberg, K. (2004) Rho and Rac take center stage. *Cell*, **116**(2), 167–79.

Cabernard, C. and Affolter, M. (2005) Distinct roles for two receptor tyrosine kinases in epithelial branching morphogenesis in *Drosophila*. *Dev Cell*, **9**(6), 831–42.

Cabernard, C., Neumann, M. and Affolter, M. (2004) Cellular and molecular mechanisms involved in branching morphogenesis of the *Drosophila* tracheal system. *J Appl Physiol*, **97**(6), 2347–53.

Cance, W.G. and Golubovskaya, V.M. (2008) Focal Adhesion Kinase Versus p53: Apoptosis or Survival *Science Signaling*, **1**(20), pe22–pe22.

Carballada, R., Yasuo, H. and Lemaire, P. (2001) Phosphatidylinositol-3 kinase acts in parallel to the ERK MAP kinase in the FGF pathway during *Xenopus* mesoderm induction. *Development*, **128**(1), 35–44.

Carmena, A., Bate, M. and Jiménez, F. (1995) Lethal of scute, a proneural gene, participates in the specification of muscle progenitors during *Drosophila* embryogenesis. *Genes and Development*, **9**(19), 2373–83.

Carmena A, Gisselbrecht S, Harrison J, Jiménez F, Michelson A (1998) Combinatorial signaling codes for the progressive determination of cell fates in the *Drosophila* embryonic mesoderm. *Genes and Development*, **12**(24), 3910–22.

Carmena A, Buff E, Halfon MS, Gisselbrecht S, Jiménez F, Baylies MK, Michelson AM (2002) Reciprocal regulatory interactions between the Notch and Ras signaling pathways in the *Drosophila* embryonic mesoderm. *Dev Biol*, **244**(2), 226–42.

Carmena, A., Speicher, S. and Baylies, M. (2006) The PDZ protein Canoe/AF-6 links Ras-MAPK, Notch and Wingless/Wnt signaling pathways by directly interacting with Ras, Notch and Dishevelled. *PLoS ONE*, **1**, e66.

Carrasco-Rando, M. and Ruiz-Gómez, M. (2008) Mind bomb 2, a founder myoblast-specific protein, regulates myoblast fusion and muscle stability. *Development (Cambridge, England)*, **135**(5), 849–57.

Casci, T., Vinós, J. and Freeman, M. (1999) Sprouty, an intracellular inhibitor of Ras signaling. *Cell*, **96**(5), 655–65.

Cayuso, O. and Martı, E. (2005) Morphogens in motion: Growth control of the neural tube. *Journal of Neurobiology*, **64(**4), 376–387.

Cela, C. and Llimargas, M. (2006) Egfr is essential for maintaining epithelial integrity during tracheal remodelling in *Drosophila*. *Development*, **133**(16), 3115.

Chen Y, Li X, Eswarakumar VP, Seger R, Lonai P (2000) Fibroblast growth factor (FGF) signaling through PI 3-kinase and Akt/PKB is required for embryoid body differentiation. *Oncogene*, 19(33), 3750–6.

Chopra, V.S. and Levine, M. (2009) Combinatorial patterning mechanisms in the *Drosophila* embryo. *Briefings in Functional Genomics and Proteomics*, **8**(4), 243–9.

Chuai, M. and Weijer, C.J. (2009) Regulation of cell migration during chick gastrulation. *Curr Opin Genet Dev*, **19**(4), 343–9.

Ciruna, B. and Rossant, J. (2001) FGF signaling regulates mesoderm cell fate specification and morphogenetic movement at the primitive streak. *Dev Cell*, **1**(1), 37–49.

Cooley, L. and Theurkauf, W.E. (1994) Cytoskeletal functions during *Drosophila* oogenesis. *Science*, **266**(5185), 590–6.

Coumoul, X. and Deng, C. (2003). Roles of FGF receptors in mammalian development and congenital diseases. *Birth Defects Res C Embryo Today*, **69(**4), 286–304.

Dammai V, Adryan B, Lavenburg KR, Hsu T (2003) *Drosophila awd*, the homolog of human nm23, regulates FGF receptor levels and functions synergistically with shi/dynamin during tracheal development. *Genes and Development*, **17**(22), 2812–24.

Daniels, S.B., Strausbaugh, L.D. and Armstrong, R.A. (1985) Molecular analysis of P-element behavior in *Drosophila* simulans transformants. *Mol Gen Genet*, **200**(2), 258–65.

Dawes-Hoang RE, Parmar KM, Christiansen AE, Phelps CB, Brand AH, Wieschaus EF (2005) Folded gastrulation, cell shape change and the control of myosin localization. *Development (Cambridge, England)*, **132**(18), 4165–78.

Déjardin, J. and Cavalli, G. (2004). Transgenesis in *Drosophila*. *Protocol*. Available at: http://www.igh.cnrs.fr/equip/cavalli/Lab%2520Protocols/Transgenesis in *Drosophila*.pdf.

Diakowski, W., Grzybek, M. ad Sikorski, A.F. (2006) Protein 4.1, a component of the erythrocyte membrane skeleton and its related homologue proteins forming the protein 4.1/FERM superfamily. *Folia Histochem Cytobiol*, **44(**4), 231–48.

Ding W, Shi W, Bellusci S, Groffen J, Heisterkamp N, Minoo P, Warburton D (2007) Sprouty2 downregulation plays a pivotal role in mediating crosstalk between TGF-1 signaling and EGF as well as FGF receptor tyrosine kinase-ERK pathways in mesenchymal cells. *J Cell Physiol*, 212(3), 796–806.

Dormann, D. and Weijer, C.J. (2006) Chemotactic cell movement during *Dictyostelium* development and gastrulation. *Curr Opin Genet Dev*, **16**(4), 367–73.

Dossenbach, C., Röck, S. and Affolter, M.(2001) Specificity of FGF signaling in cell migration in *Drosophila*. *Development*, **128**(22), 4563–72.

Draper, B.W., Stock, D.W. and Kimmel, C.B. (2003) Zebrafish fgf24 functions with fgf8 to promote posterior mesodermal development. *Development (Cambridge, England)*, **130**(19), 4639–54.

Drummond-Barbosa, D. and Spradling, A.C. (2001) Stem cells and their progeny respond to nutritional changes during *Drosophila* oogenesis. *Dev Biol*, **231**(1), 265–78.

Duan, H., Skeath, J.B. and Nguyen, H.T. (2001) *Drosophila* Lame duck, a novel member of the Gli superfamily, acts as a key regulator of myogenesis by controlling fusion-competent myoblast development. *Development (Cambridge, England)*, **128**(22), 4489–500.

Dubrulle, J. and Pourquié, O. (2004) Fgf8 mRNA decay establishes a gradient that couples axial elongation to patterning in the vertebrate embryo. *Nature*, **427**(6973), 419–22.

Dunin-Borkowski, O.M. and Brown, N.H. (1995) Mammalian CD2 is an effective heterologous marker of the cell surface in *Drosophila*. *Dev Biol*, **168**(2), 689–93.

Dutta D, Shaw S, Maqbool T, Pandya H, Vijayraghavan K (2005) *Drosophila* Heartless acts with Heartbroken/Dof in muscle founder differentiation. *PLoS Biol*, **3**(10), e337.

Eblaghie MC, Lunn JS, Dickinson RJ, Münsterberg AE, Sanz-Ezquerro JJ, Farrell ER, Mathers J, Keyse SM, Storey K, Tickle C (2003) Negative feedback regulation of FGF signaling levels by Pyst1/MKP3 in chick embryos. *Curr Biol*, **13**(12), 1009–18.

Ekerot M, Stavridis MP, Delavaine L, Mitchell MP, Staples C, Owens DM, Keenan ID, Dickinson RJ, Storey KG, Keyse SM (2008) Negative-feedback regulation of FGF signalling by DUSP6/MKP-3 is driven by ERK1/2 and mediated by Ets factor binding to a conserved site within the DUSP6/MKP-3 gene promoter. *Biochem J*, 412(2), 287–98.

Elliott, D.A. and Brand, A.H. (2008). The GAL4 System: A Versatile System for the Expression of Genes . *Drosophila: Methods in Molecular Biology*, 978-1-58829-817-1 (Print) 978-1-59745-583-1 (Online). Available at: http://www.ncbi.nlm.nih.gov/pubmed/18641942.

Engelman, J.A. (2009) Targeting PI3K signalling in cancer: opportunities, challenges and limitations. *Nature Reviews Cancer*, **9**(8), 550.

Engels WR, Johnson-Schlitz DM, Eggleston WB, Sved J (1990) High-frequency P element loss in *Drosophila* is homolog dependent. *Cell*, **62**(3), 515–25.

Estrada B, Choe SE, Gisselbrecht SS, Michaud S, Raj L, Busser BW, Halfon MS, Church GM, Michelson AM (2006) An integrated strategy for analyzing the unique developmental programs of different myoblast subtypes. *PLoS Genet*, **2**(2), e16.

Eswarakumar, V.P., Lax, I. and Schlessinger, J. (2005) Cellular signaling by fibroblast growth factor receptors. *Cytokine Growth Factor Rev*, **16(**2), 139–49.

Etienne-Manneville, S. and Hall, A. (2002) Rho GTPases in cell biology. *Nature*, **420**(6916), 629–35.

Extavour, C. (2009) Oogenesis: making the mos of meiosis. *Curr Biol*, **19**(12), R489–91.

Farooqui, R. and Fenteany, G. (2005) Multiple rows of cells behind an epithelial wound edge extend cryptic lamellipodia to collectively drive cell-sheet movement. *J Cell Sci*, **118**(Pt 1), 51–63.

Fernández, B.G., Arias, A.M. and Jacinto, A. (2007) Dpp signalling orchestrates dorsal closure by regulating cell shape changes both in the amnioserosa and in the epidermis. *Mech Dev*, 124(11-12), 884–97.

Findlay G, Yan L, Procter J, Mieulet V, Lamb R (2007) A MAP4 kinase related to Ste20 is a nutrient-sensitive regulator of mTOR signalling. *Biochemical Journal*, **403**(Pt 1), 13.

Firth L, Manchester J, Lorenzen JA, Perkins MBLA (2000) Identification of Genomic Regions That Interact With a Viable Allele of the *Drosophila* Protein Tyrosine Phosphatase Corkscrew . *Genetics*, **156,** 733–748.

Fischer, A., Viebahn, C. and Blum, M. (2002) FGF8 acts as a right determinant during establishment of the left-right axis in the rabbit. *Curr Biol*, **12**(21), 1807–16.

Flaumenhaft, R., Moscatelli, D. and Rifkin, D.B. (1990) Heparin and heparan sulfate increase the radius of diffusion and action of basic fibroblast growth factor. *J Cell Biol*, **111**(4), 1651–9.

Fletcher, R.B., Baker, J.C. and Harland, R.M. (2006) FGF8 spliceforms mediate early mesoderm and posterior neural tissue formation in Xenopus. *Development*, **133**(9), 1703–14.

Foley, J. (2008) FAK Goes Nuclear. *Science Signaling*, **1**(4), ec33.

Forni JJ, Romani S, Doherty P, Tear G (2004) Neuroglian and FasciclinII can promote neurite outgrowth via the FGF receptor Heartless. *Mol Cell Neurosci*, **26**(2), 282–91.

Franzdóttir SR, Engelen D, Yuva-Aydemir Y, Schmidt I, Aho A, Klämbt C (2009) Switch in FGF signalling initiates glial differentiation in the *Drosophila* eye. *Nature*, **460**(7256), 758–61.

Frasch, M. (1995) Induction of visceral and cardiac mesoderm by ectodermal Dpp in the early *Drosophila* embryo. *Nature*, **374**(6521), 464–7.

Frasch, M. (1999) Intersecting signalling and transcriptional pathways in *Drosophila* heart specification. *Semin Cell Dev Biol*, **10**(1), 61–71.

Frasch M, Hoey T, Rushlow C, Doyle H, Levine M (1987) Characterization and localization of the even-skipped protein of *Drosophila*. *EMBO J*, **6**(3), 749–59.

Friedl, P. (2004) Prespecification and plasticity: shifting mechanisms of cell migration. *Current Opinion in Cell Biology*, **16**(1), 14–23.

Friedl, P. and Gilmour, D. (2009) Collective cell migration in morphogenesis, regeneration and cancer. *Nat Rev Mol Cell Biol*, **10**(7), 445–57.

Fujioka A, Terai K, Itoh RE, Aoki K, Nakamura T, Kuroda S, Nishida E, Matsuda M (2006) Dynamics of the Ras/ERK MAPK cascade as monitored by fluorescent probes. *J Biol Chem*, **281**(13), 8917–26.

Fujise M, Takeo S, Kamimura K, Matsuo T, Aigaki T, Nakato SH (2003) Dally regulates Dpp morphogen gradient formation in the *Drosophila*wing . *Development*, **130**, 1515–1522.

Furlong EE, Andersen EC, Null B, White KP, Scott MP (2001) Patterns of gene expression during *Drosophila* mesoderm development. *Science*, **293**(5535), 1629–33.

Furlong EE, Andersen EC, Null B, White KP, Scott MP (2001) Sprouty4 acts in vivo as a feedback-induced antagonist of FGF signaling in zebrafish. *Development*, **128**(12), 2175–86.

Fürthauer M, Van Celst J, Thisse C, Thisse B (2004) Fgf signalling controls the dorsoventral patterning of the zebrafish embryo. *Development*, **131**(12), 2853–64.

Fürthauer M, Lin W, Ang SL, Thisse B, Thisse C (2002) Sef is a feedback-induced antagonist of Ras/MAPK-mediated FGF signalling. *Nat Cell Biol*, **4**(2), 170–4.

Gabay, L., Seger, R. and Shilo, B.Z. (1997) MAP kinase in situ activation atlas during *Drosophila* embryogenesis. *Development*, **124**(18), 3535–41.

Gajewski K, Kim Y, Lee YM, Olson EN, Schulz RA (1997) D-mef2 is a target for Tinman activation during *Drosophila* heart development. *EMBO J*, **16**(3), 515–22.

Ganguly, A., Jiang, J. and Ip, Y.T. (2005) *Drosophila* WntD is a target and an inhibitor of the Dorsal/Twist/Snail network in the gastrulating embryo. *Development (Cambridge, England)*, **132**(15), 3419–29.

Garcia-Alonso, L., Romani, S. and Jiménez, F. (2000) The EGF and FGF receptors mediate neuroglian function to control growth cone decisions during sensory axon guidance in *Drosophila*. *Neuron*, **28**(3), 741–52.

Ghabrial, A.S. and Krasnow, M.A. (2006) Social interactions among epithelial cells during tracheal branching morphogenesis. *Nature*, **441**(7094), 746–9.

Giampieri S, Manning C, Hooper S, Jones L, Hill CS, Sahai E (2009) Localized and reversible TGF|[beta]| signalling switches breast cancer cells from cohesive to single cell motility. *Nature Cell Biology* **11**, 1287–1296

Gilbert, S., F. (2000/ 2003) Developmental Biology, Sinauer Associates, ISBN-10: 0878932585; ISBN-13: 978-0878932580

Gisselbrecht S, Skeath J, Doe C, Michelson A (1996) Heartless encodes a fibroblast growth factor receptor (DFR1/DFGF-R2) involved in the directional migration of early mesodermal cells in the *Drosophila* embryo. *Genes and Development*, **10**(23), 3003-17.

Goldfarb, M. (1996) Functions of fibroblast growth factors in vertebrate development. *Cytokine Growth Factor Rev*, **7**(4), 311–25.

Goldfarb, M. (2001) Signaling by fibroblast growth factors: the inside story. *Sci STKE*, **2001**(106), PE37.

Gómez, M.R. and Bate, M. (1997) Segregation of myogenic lineages in *Drosophila* requires numb. *Development (Cambridge, England)*, **124**(23), 4857–66.

Greenspan, R., J. (2005) Fly Pushing: The Theory and Practice of *Drosophila*. Cold Spring Harbor Laboratory Press; 2nd edition; ISBN-10: 0879697113; ISBN-13: 978-0879697112

Grieshammer U, Cebrián C, Ilagan R, Meyers E, Herzlinger D, Martin GR (2005) FGF8 is required for cell survival at distinct stages of nephrogenesis and for

regulation of gene expression in nascent nephrons. *Development (Cambridge, England)*, **132**(17), 3847–57.

Grosshans, J. and Wieschaus, E. (2000) A genetic link between morphogenesis and cell division during formation of the ventral furrow in *Drosophila*. *Cell*, **101**(5), 523–31.

Gryzik, T. (2005) Identifikation und Funktion neuer Fibroblasten-Wachstumsfaktoren in der Mesodermwanderung von *Drosophila melanogaster*. ("Identification and function of new fibroblast growth factors during mesoderm migration of *Drosophila melanogaster*) **Inaugural-Dissertation;** available at: http://deposit.ddb.de/cgi-bin/dokserv?idn=975033778

Gryzik, T. and Müller, H.J. (2004) FGF8-like1 and FGF8-like2 encode putative ligands of the FGF receptor Htl and are required for mesoderm migration in the *Drosophila* gastrula. *Curr Biol*, **14**(8), 659–67.

Guo, Q. and Li, J.Y.H. (2007) Distinct functions of the major Fgf8 spliceform, Fgf8b, before and during mouse gastrulation. *Development*, **134**(12), 2251–60.

Haastert, P.J.M.V. and Devreotes, P.N. (2004) Chemotaxis: signalling the way forward. *Nat Rev Mol Cell Biol*, **5**(8), 626–34.

Hacohen N, Kramer S, Sutherland D, Hiromi Y, Krasnow MA (1998) Sprouty encodes a novel antagonist of FGF signaling that patterns apical branching of the *Drosophila* airways. *Cell*, **92**(2), 253–63.

Halfon MS, Carmena A, Gisselbrecht S, Sackerson CM, Jiménez F, Baylies MK, Michelson A (2000) Ras pathway specificity is determined by the integration of multiple signal-activated and tissue-restricted transcription factors. *Cell*, **103**(1), 63–74.

Hamlet, M.R.J. and Perkins, L.A. (2001) Analysis of corkscrew signaling in the *Drosophila* epidermal growth factor receptor pathway during myogenesis. *Genetics*, **159**(3), 1073–87.

Han, Z. and Bodmer, R. (2003) Myogenic cells fates are antagonized by Notch only in asymmetric lineages of the *Drosophila* heart, with or without cell division. *Development*, **130**(13), 3039.

Han Z, Fujioka M, Su M, Liu M, Jaynes JB, Bodmer R (2002) Transcriptional integration of competence modulated by mutual repression generates cell-type specificity within the cardiogenic mesoderm. *Dev Biol*, **252**(2), 225–40.

Han Z, Yi P, Li X, Olson EN (2006) Hand, an evolutionarily conserved bHLH transcription factor required for *Drosophila* cardiogenesis and hematopoiesis. *Development (Cambridge, England)*, **133**(6), 1175–82.

Harada M, Murakami H, Okawa A, Okimoto N, Hiraoka S, Nakahara T, Akasaka R, Shiraishi Y, Futatsugi N, Mizutani-Koseki Y, Kuroiwa A, Shirouzu M, Yokoyama S, Taiji M, Iseki S, Ornitz DM, Koseki H (2009) FGF9 monomer-dimer equilibrium regulates extracellular matrix affinity and tissue diffusion. *Nat Genet*, **41**(3), 289–98.

Harden, N. (2002) Signaling pathways directing the movement and fusion of epithelial sheets: lessons from dorsal closure in *Drosophila*. *Differentiation*, **70**(4-5), 181–203.

Hardt, von der, S., Bakkers J, Inbal A, Carvalho L, Solnica-Krezel L, Heisenberg CP, Hammerschmidt M (2007) The Bmp gradient of the zebrafish gastrula guides migrating lateral cells by regulating cell-cell adhesion. *Curr Biol*, **17**(6), 475–87.

Hartenstein, V. (1995) Atlas of *Drosophila* development Cold Spring Harbor Laboratory Press; 1 edition ISBN-10: 0879694726; ISBN-13: 978-0879694722

Hay, E.D. (2005) The mesenchymal cell, its role in the embryo, and the remarkable signaling mechanisms that create it. *Dev Dyn*, **233**(3), 706–20.

Hayashi H, Tsuchiya Y, Nakayama K, Satoh T, Nishida E (2008) Down-regulation of the PI3-kinase/Akt pathway by ERK MAP kinase in growth factor signaling. *Genes Cells*, **13**(9), 941–7.

Heisenberg, C. and Solnica-Krezel, L. (2008) Back and forth between cell fate specification and movement during vertebrate gastrulation. *Curr Opin Genet Dev*, **18**(4), 311–6.

Hong JW, Hendrix DA, Papatsenko D, Levine MS (2008) How the Dorsal gradient works: insights from postgenome technologies. *Proc Natl Acad Sci USA*, **105**(51), 20072–6.

Horowitz, A. and Simons, M. (2008) Branching Morphogenesis. *Circulation Research*, **103**(8), 784.

Horwitz, R. and Webb, D. (2003) Cell migration. *Curr Biol*, **13**(19), R756–9.

Hou, X.S., Goldstein, E.S. and Perrimon, N. (1997) *Drosophila* Jun relays the Jun amino-terminal kinase signal transduction pathway to the Decapentaplegic signal transduction pathway in regulating epithelial cell sheet movement. *Genes and Development*, **11**(13), 1728–37.

Huang, P. and Stern, M.J. (2005) FGF signaling in flies and worms: more and more relevant to vertebrate biology. *Cytokine Growth Factor Rev*, **16**(2), 151–8.

Iijima, M., Huang, Y.E. and Devreotes, P. (2002) Temporal and spatial regulation of chemotaxis. *Dev Cell*, **3**(4), 469–78.

Iimura T, Yang X, Weijer CJ, Pourquié O (2007) Dual mode of paraxial mesoderm formation during chick gastrulation. *Proc Natl Acad Sci USA*, **104**(8), 2744–9.

Ilina, O. and Friedl, P. (2009) Mechanisms of collective cell migration at a glance. *Journal of Cell Science*, **122**(18), 3203–8.

Imam F, Sutherland D, Huang W, Krasnow MA (1999) Stumps, a *Drosophila* gene required for fibroblast growth factor (FGF)-directed migrations of tracheal and mesodermal cells. *Genetics*, **152**(1), 307–18.

Impel van, A., Schumacher S, Draga M, Herz H, Grosshans J, Muller H (2009) Regulation of the Rac GTPase pathway by the multifunctional Rho GEF Pebble is essential for mesoderm migration in the *Drosophila* gastrula. *Development*, **136**(5), 813–822.

Ishihamaa Y, Tadakumaa H, Tanib T, Funatsuc T (2008) The dynamics of pre-mRNAs and poly(A)+ RNA at speckles in living cells revealed by iFRAP studies. *Experimental Cell Research*, **314**(4), 748–762.

Ishimaru S, Williams R, Clark E, Hanafusa H, Gaul U (1999) Activation of the *Drosophila* C3G leads to cell fate changes and overproliferation during development, mediated by the RAS-MAPK pathway and RAP1. *EMBO J*, **18**(1), 145–55.

Itoh, N. (2007) The Fgf families in humans, mice, and zebrafish: their evolutional processes and roles in development, metabolism, and disease. *Biol Pharm Bull*, **30**(10), 1819–25.

Itoh, N. and Ornitz, D.M. (2004) Evolution of the Fgf and Fgfr gene families. *Trends Genet*, **20**(11), 563–9.

Itoh, N. and Ornitz, D.M. (2008) Functional evolutionary history of the mouse Fgf gene family. *Dev Dyn*, **237**(1), 18–27.

Ivanovska I, Lee E, Kwan KM, Fenger DD, Orr-Weaver TL (2004) The *Drosophila* MOS ortholog is not essential for meiosis. *Curr Biol*, **14**(1), 75–80.

Jacinto A, Wood W, Balayo T, Turmaine M, Martinez-Arias A, Martin P (2000) Dynamic actin-based epithelial adhesion and cell matching during *Drosophila* dorsal closure. *Curr Biol*, 10(22), 1420–6.

Jacinto, A., Woolner, S. and Martin, P. (2002) Dynamic analysis of dorsal closure in *Drosophila*: from genetics to cell biology. *Dev Cell*, **3**(1), 9–19.

Jaffe, A.B. and Hall, A. (2005) Rho GTPases: biochemistry and biology. *Annu Rev Cell Dev Biol*, **21**, 247–69.

Jagla, K., Bellard, M. and Frasch, M. (2001) A cluster of *Drosophila* homeobox genes involved in mesoderm differentiation programs. *BioEssays*, **23**(2), 125–33.

Jagla T, Bellard F, Lutz Y, Dretzen G, Bellard M, Jagla K (1998) Ladybird determines cell fate decisions during diversification of *Drosophila* somatic muscles. *Development*, **125**(18), 3699–708.

Jagla T, Bidet Y, Da Ponte JP, Dastugue B, Jagla K (2002) Cross-repressive interactions of identity genes are essential for proper specification of cardiac and muscular fates in *Drosophila*. *Development (Cambridge, England)*, **129**(4), 1037–47.

Jakobsen JS, Braun M, Astorga J, Gustafson EH, Sandmann T, Karzynski M, Carlsson P, Furlong EE (2007) Temporal ChIP-on-chip reveals Biniou as a

universal regulator of the visceral muscle transcriptional network. *Genes and Development*, **21**(19), 2448–60.

James BP, Bunch TA, Krishnamoorthy S, Perkins LA, Brower DL (2007) Nuclear localization of the ERK MAP kinase mediated by *Drosophila* alphaPS2betaPS integrin and importin-7. *Mol Biol Cell*, **18**(10), 4190–9.

Jankovics, F. and Brunner, D. (2006) Transiently reorganized microtubules are essential for zippering during dorsal closure in *Drosophila* melanogaster. *Dev Cell*, **11**(3), 375–85.

Jarvis LA, Toering SJ, Simon MA, Krasnow MA, Smith-Bolton RK (2006) Sprouty proteins are in vivo targets of Corkscrew/SHP-2 tyrosine phosphatases. *Development (Cambridge, England)*, **133**(6), 1133–42.

Johnson AN, Burnett LA, Sellin J, Paululat A, Newfeld SJ (2007) Defective decapentaplegic signaling results in heart overgrowth and reduced cardiac output in *Drosophila*. *Genetics*, **176**(3), 1609–24.

Johnson Hamlet MR, Perkins LA (2001) Analysis of corkscrew signaling in the Drosophila epidermal growth factor receptor pathway during myogenesis. *Genetics*,**159** (3)1073-87

Junion G, Bataillé L, Jagla T, Da Ponte JP, Tapin R, Jagla K (2007) Genome-wide view of cell fate specification: ladybird acts at multiple levels during diversification of muscle and heart precursors. *Genes and Development*, **21**(23), 3163–80.

Kadam S, McMahon A, Tzou P, Stathopoulos A (2009) FGF ligands in *Drosophila* have distinct activities required to support cell migration and differentiation. *Development (Cambridge, England)*, 136(5), 739–47.

Kamimura K, Fujise M, Villa F, Izumi S, Habuchi H, Kimata K, Nakato H (2001) *Drosophila* heparan sulfate 6-O-sulfotransferase (dHS6ST) gene. Structure, expression, and function in the formation of the tracheal system. *J Biol Chem*, **276**(20), 17014–21.

Kamimura K, Koyama T, Habuchi H, Ueda R, Masu M, Kimata K, Nakato H (2006) Specific and flexible roles of heparan sulfate modifications in *Drosophila* FGF signaling. *J Cell Biol*, **174**(6), 773–8.

Keenan, I.D., Sharrard, R.M. and Isaacs, H.V., 2006. FGF signal transduction and the regulation of Cdx gene expression. *Dev Biol*, **299**(2), 478–88.

Kiehart DP, Galbraith CG, Edwards KA, Rickoll WL, Montague RA (2000) Multiple forces contribute to cell sheet morphogenesis for dorsal closure in *Drosophila*. *J Cell Biol*, **149**(2), 471–90.

Kim, H.J. and Bar-Sagi, D., 2004. Modulation of signalling by Sprouty: a developing story. *Nat Rev Mol Cell Biol*, **5**(6), 441–50.

Kim, H.J., Taylor, L.J. and Bar-Sagi, D., 2007. Spatial regulation of EGFR signaling by Sprouty2. *Curr Biol*, 17(5), 455–61.

Kim M, Cha G, Kim S, Lee JH, Park J, Koh H, Choi K, Chung J (2004) MKP-3 Has Essential Roles as a Negative Regulator of the Ras/Mitogen-Activated Protein Kinase Pathway during *Drosophila* Development. *Molecular and Cellular Biology*, **24**(2), 573.

Kirilly, D. and Xie, T. (2007) The *Drosophila* ovary: an active stem cell community. *Cell Res*, **17**(1), 15–25.

Kiselyov, V. (2008) NCAM and the FGF-Receptor. *© Springer Science+Business Media, LLC 2009*

Klämbt, C., Glazer, L. and Shilo, B.Z. (1992) Breathless, a *Drosophila* FGF receptor homolog, is essential for migration of tracheal and specific midline glial cells. *Genes and Development*, **6**(9), 1668–78.

Klämbt C, Hummel T, Granderath S, Schimmelpfeng K (2001) Glial cell development in *Drosophila*. *International Journal of Developmental Neuroscience*, **19**(4), 373–378.

Klämbt, C. (1993) The *Drosophila* gene pointed encodes two ETS-like proteins which are involved in the development of the midline glial cells . *Development*, **117**, 163–176.

Klein OD, Minowada G, Peterkova R, Kangas A, Yu BD, Lesot H, Peterka M, Jernvall J, Martin GR (2006) Sprouty genes control diastema tooth development via bidirectional antagonism of epithelial-mesenchymal FGF signaling. *Dev Cell*, 11(2), 181–90.

Klein OD, Lyons DB, Balooch G, Marshall GW, Basson MA, Peterka M, Boran T, Peterkova R, Martin GR (2008) An FGF signaling loop sustains the generation of differentiated progeny from stem cells in mouse incisors. *Development (Cambridge, England)*, **135**(2), 377–85.

Klein TJ, Jenny A, Djiane A, Mlodzik M (2006) CKIepsilon/discs overgrown promotes both Wnt-Fz/beta-catenin and Fz/PCP signaling in *Drosophila*. *Curr Biol*, **16**(13), 1337–43.

Klingseisen A, Clark I, Gryzik T, Muller H (2009) Differential and overlapping functions of two closely related *Drosophila* FGF8-like growth factors in mesoderm development. *Development*, **136**(14), 2393–2402.

Knust, E. and Müller, H.J. (1998) *Drosophila* morphogenesis: orchestrating cell rearrangements. *Curr Biol*, 8(23), R853–5.

Kooistra, M.R.H., Dubé, N. and Bos, J.L. (2007) Rap1: a key regulator in cell-cell junction formation. *Journal of Cell Science*, **120**(Pt 1), 17–22.

Kouhara H, Hadari YR, Spivak-Kroizman T, Schilling J, Bar-Sagi D, Lax I, Schlessinger J (1997) A lipid-anchored Grb2-binding protein that links FGF-receptor activation to the Ras/MAPK signaling pathway. *Cell*, **89**(5), 693–702.

Koyano Y, Kawamoto T, Shen M, Yan W, Noshiro M, Fujii K, Kato Y (1997) Molecular cloning and characterization of CDEP, a novel human protein

containing the ezrin-like domain of the band 4.1 superfamily and the Dbl homology domain of Rho guanine nucleotide exchange factors. *Biochem Biophys Res Commun*, **241**(2), 369–75.

Koyanoa Y, Kawamotoa T, Kikuchia A, Shena M, Kurutaa Y, Tsutsumia S, Fujimotoa K, Noshiroa M, Fujiia K, Katof Y (2001) Chondrocyte-derived ezrin-like domain containing protein (CDEP), a rho guanine nucleotide exchange factor, is inducible in chondrocytes by parathyroid hormone and cyclic AMP and has transforming activity in NIH3T3 Cells. *Osteoarthritis and Cartilage*, **9**(1), S64–S68.

Kölsch V, Seher T, Fernandez-Ballester GJ, Serrano L, Leptin M (2007) Control of *Drosophila* gastrulation by apical localization of adherens junctions and RhoGEF2. *Science*, **315**(5810), 384–6.

Kramer S, Okabe M, Hacohen N, Krasnow MA, Hiromi Y (1999) Sprouty: a common antagonist of FGF and EGF signaling pathways in *Drosophila*. *Development*, **126**(11), 2515–25.

Kunath T, Saba-El-Leil MK, Almousailleakh M, Wray J, Meloche S, Smith A (2007) FGF stimulation of the Erk1/2 signalling cascade triggers transition of pluripotent embryonic stem cells from self-renewal to lineage commitment. *Development*, **134**(16), 2895.

Kunwar PS, Starz-Gaiano M, Bainton RJ, Heberlein U, Lehmann R (2003) Tre1, a G protein-coupled receptor, directs transepithelial migration of *Drosophila* germ cells. *PLoS Biol*, 1(3), E80.

Kunwar PS, Sano H, Renault AD, Barbosa V, Fuse N, Lehmann R (2008) Tre1 GPCR initiates germ cell transepithelial migration by regulating *Drosophila* melanogaster E-cadherin. *J Cell Biol*, **183**(1), 157.

Kwan CP, Venkataraman G, Shriver Z, Raman R, Liu D, Qi Y, Varticovski L, Sasisekharan R (2001) Probing fibroblast growth factor dimerization and role of heparin-like glycosaminoglycans in modulating dimerization and signaling. *J Biol Chem*, **276**(26), 23421–9.

L. Lindsley D, Zimm G (1992) The genome of *Drosophila melanogaster*, 1st edition Academic Press ISBN-10: 0124509908; ISBN-13: 978-0124509900

Lamond, A.I. and Spector, D.L. (2003) Nuclear speckles: a model for nuclear organelles. *Nat Rev Mol Cell Biol*, **4**(8), 605.

Lauffenburger, D.A. and Horwitz, A.F. (1996) Cell migration: a physically integrated molecular process. *Cell*, **84**(3), 359–69.

Leatherbarrow, J.R. and Halfon, M.S. (2009) Identification of receptor-tyrosine-kinase-signaling target genes reveals receptor-specific activities and pathway branchpoints during *Drosophila* development. *Genetics*, **181**(4), 1335–45.

Lee, H.H. and Frasch, M. (2000) Wingless effects mesoderm patterning and ectoderm segmentation events via induction of its downstream target sloppy paired. *Development*, **127**(24), 5497–508.

Lee, H. and Frasch, M. (2005) Nuclear integration of positive Dpp signals, antagonistic Wg inputs and mesodermal competence factors during *Drosophila* visceral mesoderm induction. *Development (Cambridge, England)*, **132**(6), 1429–42.

Lee JM, Dedhar S, Kalluri R, Thompson EW (2006) The epithelial-mesenchymal transition: new insights in signaling, development, and disease. *J Cell Biol*, **172**(7), 973–81.

Lee J, Cho KS, Lee J, Kim D, Lee S, Yoo J, Cha G, Chung J (2002.)*Drosophila* PDZ-GEF, a guanine nucleotide exchange factor for Rap1 GTPase, reveals a novel upstream regulatory mechanism in the mitogen-activated protein kinase signaling pathway. *Molecular and Cellular Biology*, **22**(21), 7658–66.

Lee T, Hacohen N, Krasnow M, Montell DJ (1996) Regulated Breathless receptor tyrosine kinase activity required to pattern cell migration and branching in the *Drosophila* tracheal system. *Genes and Development*, **10**(22), 2912–21.

Leptin, M. (1999) Gastrulation in *Drosophila*: the logic and the cellular mechanisms. *EMBO J*, **18**(12), 3187–92.

Leptin, M. and Grunewald, B. (1990) Cell shape changes during gastrulation in *Drosophila*. *Development*, 110(1), 73–84.

Leptin, M. (2005) Gastrulation movements: the logic and the nuts and bolts. *Dev Cell*, **8**(3), 305–20.

Leptin, M. and Affolter, M. (2004) *Drosophila* gastrulation: identification of a missing link. *Curr Biol*, **14**(12), R480–2.

Li C, Scott DA, Hatch E, Tian X, Mansour SL (2007) Dusp6 (Mkp3) is a negative feedback regulator of FGF-stimulated ERK signaling during mouse development. *Development (Cambridge, England)*, **134**(1), 167–76.

Liao, G.C., Rehm, E.J. and Rubin, G.M. (2000) Insertion site preferences of the P transposable element in *Drosophila* melanogaster. *Proc Natl Acad Sci USA*, **97**(7), 3347–51.

Lilly B, Galewsky S, Firulli AB, Schulz RA, Olson EN (1994) D-MEF2: a MADS box transcription factor expressed in differentiating mesoderm and muscle cell lineages during *Drosophila* embryogenesis. *Proc Natl Acad Sci USA*, **91**(12), 5662–6.

Lim S, Chen XL, Lim Y, Hanson DA, Vo T, Howerton K, Larocque N, Fisher SJ, Schlaepfer DD, Ilic D (2008) Nuclear FAK promotes cell proliferation and survival through FERM-enhanced p53 degradation. *Mol Cell*, 29(1), 9–22.

Lim Y, Lim S, Tomar A, Gardel M, Bernard-Trifilo JA, Chen XL, Uryu SA, Canete-Soler R, Zhai J, Lin H, Schlaepfer WW, Nalbant P, Bokoch G, Ilic D, Waterman-Storer C, Schlaepfer DD (2008) PyK2 and FAK connections to p190Rho guanine nucleotide exchange factor regulate RhoA activity, focal adhesion formation, and cell motility. *J Cell Biol*, **180**(1), 187–203.

Lin W, Fürthauer M, Thisse B, Thisse C, Jing N, Ang SL (2002) Cloning of the mouse Sef gene and comparative analysis of its expression with Fgf8 and Spry2 during embryogenesis. *Mech Dev*, **113**(2), 163–8.

Lin X, Buff EM, Perrimon N, Michelson A (1999) Heparan sulfate proteoglycans are essential for FGF receptor signaling during *Drosophila* embryonic development. *Development*, **126**(17), 3715–23.

Lin, X. (2004) Functions of heparan sulfate proteoglycans in cell signaling during development. *Development*, **131**(24), 6009.

Liu J, Qian L, Wessells RJ, Bidet Y, Jagla K, Bodmer R (2006) Hedgehog and RAS pathways cooperate in the anterior-posterior specification and positioning of cardiac progenitor cells. *Dev Biol*, **290**(2), 373–85.

Lorenzen JA, Baker SE, Denhez F, Melnick MB, Brower DL, Perkins LA (2001) Nuclear import of activated D-ERK by DIM-7, an importin family member encoded by the gene moleskin. *Development (Cambridge, England)*, **128**(8), 1403–14.

Mañes S, Mira E, Gómez-Mouton C, Zhao ZJ, Lacalle RA, Martínez-A C (1999) Concerted activity of tyrosine phosphatase SHP-2 and focal adhesion kinase in regulation of cell motility. *Molecular and Cellular Biology*, **19**(4), 3125–35.

Manno, S., Takakuwa, Y. and Mohandas, N. (2005) Modulation of erythrocyte membrane mechanical function by protein 4.1 phosphorylation. *J Biol Chem*, 280(9), 7581–7.

Martin, P. and Parkhurst, S.M. (2004) Parallels between tissue repair and embryo morphogenesis. *Development*, **131**(13), 3021–34.

Mason JM, Morrison DJ, Basson MA, Licht JD (2006) Sprouty proteins: multifaceted negative-feedback regulators of receptor tyrosine kinase signaling. *Trends Cell Biol*, **16**(1), 45–54.

Matsubayashi Y, Ebisuya M, Honjoh S, Nishida E (2004) ERK activation propagates in epithelial cell sheets and regulates their migration during wound healing. *Curr Biol*, **14**(8), 731–5.

Matus, D.Q., Thomsen, G.H. and Martindale, M.Q. (2007) FGF signaling in gastrulation and neural development in Nematostella vectensis, an anthozoan cnidarian. *Dev Genes Evol*, **217**(2), 137–48.

McCall, K. (2004) Eggs over easy: cell death in the *Drosophila* ovary. *Dev Biol*, **274**(1), 3–14.

McMahon A, Supatto W, Fraser SE, Stathopoulos A (2008) Dynamic analyses of *Drosophila* gastrulation provide insights into collective cell migration. *Science*, **322**(5907), 1546–50.

Medioni C, Astier M, Zmojdzian M, Jagla K, Sémériva M (2008) Genetic control of cell morphogenesis during *Drosophila* melanogaster cardiac tube formation. *J Cell Biol*, **182**(2), 249–61.

Michelson A, Gisselbrecht S, Zhou Y, Baek KH, Buff EM (1998a) Dual functions of the heartless fibroblast growth factor receptor in development of the *Drosophila* embryonic mesoderm. *Dev Genet*, **22**(3), 212–29.

Michelson A, Gisselbrecht S, Buff E, Skeath J (1998b) Heartbroken is a specific downstream mediator of FGF receptor signalling in *Drosophila*. *Development*, **125**(22), 4379–89.

Millard, T.H. and Martin, P. (2008) Dynamic analysis of filopodial interactions during the zippering phase of *Drosophila* dorsal closure. *Development*, **135**(4), 621–6.

Mills, R.P. and King, R.C. (1965) The pericardial cells of *Drosophila* melanogaster. *Journal of Cell Science*, **3**(75), 261.

Minowada G, Jarvis LA, Chi CL, Neubüser A, Sun X, Hacohen N, Krasnow MA, Martin GR (1999) Vertebrate Sprouty genes are induced by FGF signaling and can cause chondrodysplasia when overexpressed. *Development (Cambridge, England)*, **126**(20), 4465–75.

Mishra S, Smolik SM, Forte MA, Stork PJ (2005) Ras-independent activation of ERK signaling via the torso receptor tyrosine kinase is mediated by Rap1. *Curr Biol*, **15**(4), 366–70.

Miyamoto, T. and Fox, J.C. (2000) Autocrine signaling through Ras prevents apoptosis in vascular smooth muscle cells in vitro. *J Biol Chem*, 275(4), 2825–30.

Mizuno, T., Tsutsui, K. and Nishida, Y. (2002) *Drosophila* myosin phosphatase and its role in dorsal closure. *Development*, **129**(5), 1215–23.

Montell, D.J. (1999) The genetics of cell migration in *Drosophila* melanogaster and Caenorhabditis elegans development. *Development*, **126**(14), 3035.

Montell, D.J. (2003) Border-cell migration: the race is on. *Nat Rev Mol Cell Biol*, **4**(1), 13–24.

Montero JA, Kilian B, Chan J, Bayliss PE, Heisenberg CP (2003) Phosphoinositide 3-kinase is required for process outgrowth and cell polarization of gastrulating mesendodermal cells. *Curr Biol*, **13**(15), 1279–89.

Montero, J. and Heisenberg, C. (2004) Gastrulation dynamics: cells move into focus. *Trends Cell Biol*, **14**(11), 620–7.

Murakami, M., Elfenbein, A. and Simons, M. (2008) Non-canonical fibroblast growth factor signalling in angiogenesis. *Cardiovascular Research*, **78**(2), 223–31.

Murphy AM, Lee T, Andrews CM, Shilo BZ, Montell DJ (1995) The breathless FGF receptor homolog, a downstream target of *Drosophila* C/EBP in the developmental control of cell migration. *Development*, **121**(8), 2255–63.

Murray, M.J. and Saint, R. (2007) Photoactivatable GFP resolves *Drosophila* mesoderm migration behaviour. *Development (Cambridge, England)*, **134**(22), 3975–83.

Müller, H.J. (2008) Immunolabeling of embryos. *Methods Mol Biol*, **420**, 207–18.

Myat MM, Lightfoot H, Wang P, Andrew DJ (2005) A molecular link between FGF and Dpp signaling in branch-specific migration of the *Drosophila* trachea. *Dev Biol*, **281**(1), 38–52.

Myers, D. (2002) Bmp Activity Gradient Regulates Convergent Extension during Zebrafish Gastrulation. *Dev Biol*, **243**(1), 81–98.

Nabel-Rosen H, Toledano-Katchalski H, Volohonsky G, Volk T (2005) Cell divisions in the *Drosophila* embryonic mesoderm are repressed via posttranscriptional regulation of string/cdc25 by HOW. *Curr Biol*, **15**(4), 295–302.

Nagel M, Tahinci E, Symes K, Winklbauer R (2004) Guidance of mesoderm cell migration in the Xenopus gastrula requires PDGF signaling. *Development*, **131**(11), 2727–36.

Nakamura N, Oshiro N, Fukata Y, Amano M, Fukata M, Kuroda S, Matsuura Y, Leung T, Lim L, Kaibuchi K (2000) Phosphorylation of ERM proteins at filopodia induced by Cdc42. *Genes Cells*, **5**(7), 571–81.

Nakaya, Y. and Sheng, G. (2008) Epithelial to mesenchymal transition during gastrulation: an embryological view. *Dev Growth Differ*, **50**(9), 755–66.

Nechiporuk, A. and Raible, D.W. (2008) FGF-dependent mechanosensory organ patterning in zebrafish. *Science*, 320(5884), 1774–7.

Neugebauer JM, Amack JD, Peterson AG, Bisgrove BW, Yost HJ (2009) FGF signalling during embryo development regulates cilia length in diverse epithelia. *Nature*, **458**(7238), 651.

Ng, J. and Luo, L. (2004) Rho GTPases regulate axon growth through convergent and divergent signaling pathways. *Neuron*, **44** (5) pp. 779-93

Ng, J. (2008) TGF-beta signals regulate axonal development through distinct Smad-independent mechanisms. *Development (Cambridge, England)*, **135**(24), 4025–35.

Nguyen, H.T. and Xu, X., 1998. *Drosophila* mef2 expression during mesoderm development is controlled by a complex array of cis-acting regulatory modules. *Dev Biol*, **204**(2), 550–66.

Niethammer P, Delling M, Sytnyk V, Dityatev A, Fukami K, Schachner M (2002) Cosignaling of NCAM via lipid rafts and the FGF receptor is required for neuritogenesis. *The Journal of Cell Biology*, **157**(3), 521.

Ninov, N., Manjón, C. and Martin-Blanco, E. (2009) Dynamic Control of Cell Cycle and Growth Coupling by Ecdysone, EGFR, and PI3K Signaling in *Drosophila* Histoblasts. *PLoS Biol*, **7**(4).

Nutt SL, Dingwell KS, Holt CE, Amaya E (2001) Xenopus Sprouty2 inhibits FGF-mediated gastrulation movements but does not affect mesoderm induction and patterning. *Genes and Development*, **15**(9), 1152–66.

Oda, H. and Tsukita, S. (1999) Dynamic features of adherens junctions during *Drosophila* embryonic epithelial morphogenesis revealed by a Dalpha-catenin-GFP fusion protein. *Dev Genes Evol*, **209**(4), 218–25.

Oda, H., Tsukita, S. and Takeichi, M. (1998) Dynamic behavior of the cadherin-based cell-cell adhesion system during *Drosophila* gastrulation. *Dev Biol*, **203**(2), 435–50.

Olivera-Martinez, I. and Storey, K.G. (2007) Wnt signals provide a timing mechanism for the FGF-retinoid differentiation switch during vertebrate body axis extension. *Development (Cambridge, England)*, **134**(11), 2125–35.

Ong SH, Hadari YR, Gotoh N, Guy GR, Schlessinger J, Lax I (2001) Stimulation of phosphatidylinositol 3-kinase by fibroblast growth factor receptors is mediated by coordinated recruitment of multiple docking proteins. *Proc Natl Acad Sci USA*, **98**(11), 6074–9.

Ornitz, D.M. and Itoh, N. (2001) Fibroblast growth factors. *Genome Biol*, **2**(3), REVIEWS 3005.

Ornitz, D.M. (2000) FGFs, heparan sulfate and FGFRs: complex interactions essential for development. *BioEssays*, **22**(2), 108–112.

Park, P.W., Reizes, O. and Bernfield, M. (2000) Cell surface heparan sulfate proteoglycans: selective regulators of ligand-receptor encounters. *J Biol Chem*, **275**(39), 29923–6.

Pera EM, Ikeda A, Eivers E, De Robertis EM (2003) Integration of IGF, FGF, and anti-BMP signals via Smad1 phosphorylation in neural induction. *Genes and Development*, **17**(24), 3023–8.

Perkins LA, Johnson MR, Melnick MB, Perrimon N (1996) The nonreceptor protein tyrosine phosphatase corkscrew functions in multiple receptor tyrosine kinase pathways in *Drosophila*. *Dev Biol*, 180(1), 63–81.

Petit V, Ribeiro C, Ebner A, Affolter M (2002) Regulation of cell migration during tracheal development in *Drosophila* melanogaster. *Int J Dev Biol*, **46**(1), 125–32.

Petit V, Nussbaumer U, Dossenbach C, Affolter M (2004) Downstream-of-FGFR is a fibroblast growth factor-specific scaffolding protein and recruits Corkscrew upon receptor activation. *Molecular and Cellular Biology*, **24**(9), 3769–81.

Plotnikov AN, Schlessinger J, Hubbard SR, Mohammadi M (1999) Structural basis for FGF receptor dimerization and activation. *Cell*, **98**(5), 641–50.

Politz JCR, Tuft RA, Prasanth KV, Baudendistel N, Fogarty KE, Lifshitz LM, Langowski J, Spector DL, Pederson T (2006) Rapid, diffusional shuttling of poly(A) RNA between nuclear speckles and the nucleoplasm. *Mol Biol Cell*, **17**(3), 1239–49.

Popovici C, Conchonaud F, Birnbaum D, Roubin R (2004) Functional phylogeny relates LET-756 to fibroblast growth factor 9. *J Biol Chem*, **279**(38), 40146–52.

Popovici C, Roubin R, Coulier F, Birnbaum D (2005) An evolutionary history of the FGF superfamily. *BioEssays*, **27**(8), 849–57.

Popovici C, Berda Y, Conchonaud F, Harbis A, Birnbaum D, Roubin R (2006a) Direct and heterologous approaches to identify the LET-756/FGF interactome. *BMC Genomics*, **7**, 105.

Popovici C, Fallet M, Marguet D, Birnbaum D, Roubin R (2006b) Intracellular trafficking of LET-756, a fibroblast growth factor of C. elegans, is controlled by a balance of export and nuclear signals. *Experimental Cell Research*, **312**(9), 1484–95.

Poulton, J.S. and Deng, W. (2007) Cell-cell communication and axis specification in the *Drosophila* oocyte. *Dev Biol*, **311**(1), 1–10.

Powers, C.J., McLeskey, S.W. and Wellstein, A. (2000) Fibroblast growth factors, their receptors and signaling. *Endocr Relat Cancer*, **7**(3), 165–97.

Prasad, M. and Montell, D.J. (2007) Cellular and molecular mechanisms of border cell migration analyzed using time-lapse live-cell imaging. *Dev Cell*, **12**(6), 997–1005.

Qiao F, Harada B, Song H, Whitelegge J, Courey AJ, Bowie JU (2006) Mae inhibits Pointed-P2 transcriptional activity by blocking its MAPK docking site. *EMBO J*, **25**(1), 70–9.

Raftopoulou, M. and Hall, A. (2004) Cell migration: Rho GTPases lead the way. *Dev Biol*, **265**(1), 23–32.

Redd MJ, Cooper L, Wood W, Stramer B, Martin P (2004) Wound healing and inflammation: embryos reveal the way to perfect repair. *Philos Trans R Soc Lond, B, Biol Sci*, **359**(1445), 777–84.

Reich, A., Sapir, A. and Shilo, B. (1999) Sprouty is a general inhibitor of receptor tyrosine kinase signaling. *Development*, **126**(18), 4139–47.

Reichman-Fried M, Dickson B, Hafen E, Shilo BZ (1994) Elucidation of the role of breathless, a *Drosophila* FGF receptor homolog, in tracheal cell migration. *Genes and Development*, **8**(4), 428–39.

Reim, I. and Frasch, M. (2005) The Dorsocross T-box genes are key components of the regulatory network controlling early cardiogenesis in *Drosophila*. *Development (Cambridge, England)*, **132**(22), 4911–25.

Ren Y, Meng S, Mei L, Zhao ZJ, Jove R, Wu J (2004) Roles of Gab1 and SHP2 in paxillin tyrosine dephosphorylation and Src activation in response to epidermal growth factor. *J Biol Chem*, **279**(9), 8497–505.

Rentzsch F, Fritzenwanker JH, Scholz CB, Technau U (2008) FGF signalling controls formation of the apical sensory organ in the cnidarian Nematostella vectensis. *Development (Cambridge, England)*, **135**(10), 1761–9.

Retta, S.F., Balzac, F. and Avolio, M. (2006) Rap1: a turnabout for the crosstalk between cadherins and integrins. *Eur J Cell Biol*, **85**(3-4), 283–93.

Ribeiro, C., Ebner, A. and Affolter, M. (2002) In vivo imaging reveals different cellular functions for FGF and Dpp signaling in tracheal branching morphogenesis. *Dev Cell*, **2**(5), 677–83.

Ribeiro, C., Petit, V. and Affolter, M. (2003) Signaling systems, guided cell migration, and organogenesis: insights from genetic studies in *Drosophila*. *Dev Biol*, **260**(1), 1–8.

Ridley, A.J. (2006) Rho GTPases and actin dynamics in membrane protrusions and vesicle trafficking. *Trends Cell Biol*, **16**(10), 522–9.

Ridley AJ, Schwartz MA, Burridge K, Firtel RA, Ginsberg MH, Borisy G, Parsons JT, Horwitz AR (2003) Cell migration: integrating signals from front to back. *Science*, **302**(5651), 1704–9.

Rogulja, D. and Irvine, K.D. (2005) Regulation of cell proliferation by a morphogen gradient. *Cell*, **123**(3), 449–61.

Rogulja, D., Rauskolb, C. and Irvine, K.D. (2008) Morphogen control of wing growth through the Fat signaling pathway. *Dev Cell*, **15**(2), 309–21.

Röttinger E, Saudemont A, Duboc V, Besnardeau L, McClay D, Lepage T (2008) FGF signals guide migration of mesenchymal cells, control skeletal morphogenesis [corrected] and regulate gastrulation during sea urchin development. *Development (Cambridge, England)*, **135**(2), 353–65.

Ryder, E. and Russell, S. (2003) Transposable elements as tools for genomics and genetics in *Drosophila*. *Briefings in Functional Genomics and Proteomics*, **2**(1), 57–71.

R\orth, P. (1996) A modular misexpression screen in *Drosophila* detecting tissue-specific phenotypes. *Proc Natl Acad Sci USA*, **93**(22), 12418–22.

R\orth, P. (1998) Gal4 in the *Drosophila* female germline. *Mech Dev*, **78**(1-2), 113–8.

R\orth, P. (2007) Collective guidance of collective cell migration. *Trends Cell Biol*, **17**(12), 575–9.

Sandmann T, Girardot C, Brehme M, Tongprasit W, Stolc V, Furlong EE (2007) A core transcriptional network for early mesoderm development in *Drosophila* melanogaster. *Genes and Development*, **21**(4), 436–49.

Sandmann T, Jensen LJ, Jakobsen JS, Karzynski MM, Eichenlaub MP, Bork P, Furlong EE (2006) A temporal map of transcription factor activity: mef2 directly regulates target genes at all stages of muscle development. *Dev Cell*, **10**(6), 797–807.

Sano H, Sano H, Renault AD, Renault AD, Lehmann R, Lehmann R (2005) Control of lateral migration and germ cell elimination by the *Drosophila* melanogaster lipid phosphate phosphatases Wunen and Wunen 2. *J Cell Biol*, **171**(4), 675.

Santos, A.C. and Lehmann, R. (2004) Germ cell specification and migration in *Drosophila* and beyond. *Curr Biol*, **14**(14), R578–89.

Sarbassov, D.D., Ali, S.M. and Sabatini, D.M. (2005) Growing roles for the mTOR pathway. *Current Opinion in Cell Biology*, **17**(6), 596–603.

Sasson, I.E. and Stern, M.J. (2004) FGF and PI3 kinase signaling pathways antagonistically modulate sex muscle differentiation in C. elegans. *Development (Cambridge, England)*, **131**(21), 5381–92.

Sato, M. and Kornberg, T.B. (2002) FGF is an essential mitogen and chemoattractant for the air sacs of the *Drosophila* tracheal system. *Dev Cell*, **3**(2), 195–207.

Sawyer JK, Harris NJ, Slep KC, Gaul U, Peifer M (2009) The *Drosophila* afadin homologue Canoe regulates linkage of the actin cytoskeleton to adherens junctions during apical constriction. *J Cell Biol*, 1**86**(1), 57–73.

Schiller, M.R. (2006) Coupling receptor tyrosine kinases to Rho GTPases–GEFs what's the link. *Cell Signal*, **18**(11), 1834–43.

Schlessinger, J., 2000. Cell signaling by receptor tyrosine kinases. *Cell*, **103**(2), 211–25.

Schlessinger J, Plotnikov AN, Ibrahimi OA, Eliseenkova AV, Yeh BK, Yayon A, Linhardt RJ, Mohammadi M (2000) Crystal structure of a ternary FGF-FGFR-heparin complex reveals a dual role for heparin in FGFR binding and dimerization. *Mol Cell*, **6**(3), 743–50.

Schneider DS, Hudson KL, Lin TY, Anderson KV (1991) Dominant and recessive mutations define functional domains of Toll, a transmembrane protein required for dorsal-ventral polarity in the *Drosophila* embryo. *Genes and Development*, **5**(5), 797–807.

Schober, M., Rebay, I. and Perrimon, N. (2005) Function of the ETS transcription factor Yan in border cell migration. *Development (Cambridge, England)*, **132**(15), 3493–504.

Schulz, R.A. and Gajewski, K. (1999) Ventral neuroblasts and the heartless FGF receptor are required for muscle founder cell specification in *Drosophila*. *Oncogene*, **18**(48), 6818–23.

Schumacher S, Gryzik T, Tannebaum S, Müller HA (2004) The RhoGEF Pebble is required for cell shape changes during cell migration triggered by the

Drosophila FGF receptor Heartless. *Development (Cambridge, England)*, **131**(11), 2631–40.

Seher, T.C. and Leptin, M. (2000) Tribbles, a cell-cycle brake that coordinates proliferation and morphogenesis during *Drosophila* gastrulation. *Curr Biol*, **10**(11), 623–9.

Seher TC, Narasimha M, Vogelsang E, Leptin M (2007) Analysis and reconstitution of the genetic cascade controlling early mesoderm morphogenesis in the *Drosophila* embryo. *Mech Dev*, 124(3), 167–79.

Sellin J, Drechsler M, Nguyen HT, Paululat A (2008) Antagonistic function of Lmd and Zfh1 fine tunes cell fate decisions in the Twi and Tin positive mesoderm of *Drosophila* melanogaster. *Dev Biol*, **326**(2), 444–55.

Shaw, R.J. and Cantley, L.C. (2006) Ras, PI(3)K and mTOR signalling controls tumour cell growth. *Nature*, **441**(7092), 424.

Shi W, Peyrot SM, Munro E, Levine M (2009) FGF3 in the floor plate directs notochord convergent extension in the Ciona tadpole. *Development*, **136**(1), 23–8.

Shindo M, Wada H, Kaido M, Tateno M, Aigaki T, Tsuda L, Hayashi S (2008) Dual function of Src in the maintenance of adherens junctions during tracheal epithelial morphogenesis. *Development (Cambridge, England)*, **135**(7), 1355–64.

Shishido E, Higashijima S, Emori Y, Saigo K (1993) Two FGF-receptor homologues of *Drosophila*: one is expressed in mesodermal primordium in early embryos. *Development*, **117**(2), 751–61.

Shishido E, Ono N, Kojima T, Saigo K (1997) Requirements of DFR1/Heartless, a mesoderm-specific *Drosophila* FGF-receptor, for the formation of heart, visceral and somatic muscles, and ensheathing of longitudinal axon tracts in CNS. *Development*, **124**(11), 2119–28.

Simon, M.A. (2000) Receptor tyrosine kinases: specific outcomes from general signals. *Cell*, **103**(1), 13–5.

Smallhorn, M., Murray, M.J. and Saint, R. (2004) The epithelial-mesenchymal transition of the *Drosophila* mesoderm requires the Rho GTP exchange factor Pebble. *Development*, **131**(11), 2641–51.

Smith RK, Carroll PM, Allard JD, Simon MA (2002) MASK, a large ankyrin repeat and KH domain-containing protein involved in *Drosophila* receptor tyrosine kinase signaling. *Development (Cambridge, England)*, **129**(1), 71–82.

Solnica-Krezel, L. (2005) Conserved patterns of cell movements during vertebrate gastrulation. *Curr Biol*, **15**(6), R213–28.

Staehling-Hampton K, Hoffmann FM, Baylies MK, Rushton E, Bate M (1994) Dpp induces mesodermal gene expression in *Drosophila*. *Nature*, **372**(6508), 783–6.

Starz-Gaiano M, Cho NK, Forbes A, Lehmann R (2001) Spatially restricted activity of a *Drosophila* lipid phosphatase guides migrating germ cells. *Development*, **128**(6), 983–91.

Stathopoulos, A. and Levine, M. (2002) Dorsal gradient networks in the *Drosophila* embryo. *Dev Biol*, **246**(1), 57–67.

Stathopoulos, A. and Levine, M. (2004) Whole-genome analysis of *Drosophila* gastrulation. *Curr Opin Genet Dev*, **14**(5), 477–84.

Stathopoulos A, Tam B, Ronshaugen M, Frasch M, Levine M (2004) Pyramus and thisbe: FGF genes that pattern the mesoderm of *Drosophila* embryos. *Genes and Development*, **18(**6), 687–99.

Sun, C., Robb, V.A. and Gutmann, D.H. (2002) Protein 4.1 tumor suppressors: getting a FERM grip on growth regulation. *J Cell Sci*, **115**(Pt 21), 3991–4000.

Sutherland, D., Samakovlis, C. and Krasnow, M.A. (1996) Branchless encodes a *Drosophila* FGF homolog that controls tracheal cell migration and the pattern of branching. *Cell*, **87**(6), 1091–101.

Tachibana K, Tanaka D, Isobe T, Kishimoto T (2000) c-Mos forces the mitotic cell cycle to undergo meiosis II to produce haploid gametes. *Proc Natl Acad Sci USA*, **97**(26), 14301–6.

Tang C, Yang R, Chen Y, Fu W (2007) Basic fibroblast growth factor stimulates fibronectin expression through phospholipase C , protein kinase C , c-Src, NF-B, and p300 pathway in osteoblasts. *Journal of Cellular Physiology*, **211**(1), 45–55.

Tang W, Wu JQ, Guo Y, Hansen DV, Perry JA, Freel CD, Nutt L, Jackson PK, Kornbluth S (2008) Cdc2 and Mos regulate Emi2 stability to promote the meiosis I-meiosis II transition. *Mol Biol Cell*, **19(**8), 3536–43.

Tao, Y. and Schulz, R.A. (2007) Heart development in *Drosophila*. *Semin Cell Dev Biol*, **18(**1), 3–15.

Taylor MV, Beatty KE, Hunter HK, Baylies MK (1995) *Drosophila* MEF2 is regulated by twist and is expressed in both the primordia and differentiated cells of the embryonic somatic, visceral and heart musculature. *Mech Dev*, 50(1), 29–41.

Thisse, B. and Thisse, C. (2005) Functions and regulations of fibroblast growth factor signaling during embryonic development. *Dev Biol*, **287**(2), 390–402.

Tian, E. and Hagen, K.G.T. (2007a) A UDP-GalNAc:polypeptide N-acetylgalactosaminyltransferase is required for epithelial tube formation. *J Biol Chem*, **282**(1), 606–14.

Tian, E. and Hagen, K.G.T. (2007b) O-linked glycan expression during *Drosophila* development. *Glycobiology*, **17**(8), 820–7.

Toledano-Katchalski H, Nir R, Volohonsky G, Volk T (2007) Post-transcriptional repression of the *Drosophila* midkine and pleiotrophin homolog miple by HOW is essential for correct mesoderm spreading. *Development (Cambridge, England)*, **134**(19), 3473–81.

Trepat X, Wasserman MR, Angelini TE, Millet E, Weitz DA, Butler JP, Fredberg JJ (2009) Physical forces during collective cell migration. *nature physics*, **5**(6), 426.

Tsai I, Amack JD, Gao Z, Band V, Yost HJ, Virshupn DM (2007) A Wnt-CKI Îµ-Rap1 Pathway Regulates Gastrulation by Modulating SIPA1L1, a Rap GTPase Activating Protein . *Dev Cell*, **12**(3), 335–347.

Tsang, M. and Dawid, I.B. (2004) Promotion and attenuation of FGF signaling through the Ras-MAPK pathway. *Sci STKE*, 2004(**228**), pe17.

Tsubota, S., Ashburner, M. and Schedl, P., 1985. P-element-induced control mutations at the r gene of *Drosophila* melanogaster. *Molecular and Cellular Biology*, **5**(10), 2567–74.

Urness LD, Li C, Wang X, Mansour SL (2008) Expression of ERK signaling inhibitors Dusp6, Dusp7, and Dusp9 during mouse ear development. *Dev Dyn*, **237**(1), 163–9.

Verdier, V., Guang-Chao-Chen and Settleman, J. (2006) Rho-kinase regulates tissue morphogenesis via non-muscle myosin and LIM-kinase during *Drosophila* development. *BMC Developmental Biology*, **6**, 38.

Verheyen, E.M. (2007) Opposing effects of Wnt and MAPK on BMP/Smad signal duration. *Dev Cell*, **13**(6), 755–6.

Vincent S, Wilson R, Coelho C, Affolter M, Leptin M (1998) The *Drosophila* protein Dof is specifically required for FGF signaling. *Mol Cell*, **2**(4), 515–25.

Vitorino, P. and Meyer, T. (2008) Modular control of endothelial sheet migration. *Genes and Development*, **22**(23), 3268–81.

Wahl MB, Deng C, Lewandoski M, Pourquié O (2007) FGF signaling acts upstream of the NOTCH and WNT signaling pathways to control segmentation clock oscillations in mouse somitogenesis. *Development (Cambridge, England)*, **134**(22), 4033–41.

Walid S, Eisen R, Ratcliffe DR, Dai K, Hussain MM, Ojakian GK (2008) The PI 3-kinase and mTOR signaling pathways are important modulators of epithelial tubule formation. *J Cell Physiol*, **216**(2), 469–479.

Wang J, Tao Y, Reim I, Gajewski K, Frasch M, Schulz RA (2005) Expression, regulation, and requirement of the toll transmembrane protein during dorsal vessel formation in *Drosophila* melanogaster. *Molecular and Cellular Biology*, **25**(10), 4200–10.

Webb, D.J., Parsons, J.T. and Horwitz, A.F. (2002) Adhesion assembly, disassembly and turnover in migrating cells – over and over and over again. *Nat Cell Biol*, **4**(4), E97–100.

Weijer, C.J. (2009) Collective cell migration in development. *Journal of Cell Science*, **122**(Pt 18), 3215–23.

Weijer, C.J. (2004) *Dictyostelium* morphogenesis. *Curr Opin Genet Dev*, **14**(4), 392–8.

Williams, G., Williams, E. and Doherty, P. (2002) Dimeric versions of two short N-cadherin binding motifs (HAVDI and INPISG) function as N-cadherin agonists. *J Biol Chem*, **277**(6), 4361–7.

Wilson C, Vereshchagina N, Reynolds B, Meredith D, Boyd CA, Goberdhan DC (2007) Extracellular and subcellular regulation of the PI3K/Akt cassette: new mechanisms for controlling insulin and growth factor signalling. *Biochem Soc Trans*, **35**(Pt 2), 219–21.

Wilson, R. and Leptin, M. (2000) Fibroblast growth factor receptor-dependent morphogenesis of the *Drosophila* mesoderm. *Philosophical Transactions of the Royal Society B: Biological Sciences*, **355**(1399), 891.

Wilson R, Battersby A, Csiszar A, Vogelsang E, Leptin M (2004) A functional domain of Dof that is required for fibroblast growth factor signaling. *Molecular and Cellular Biology*, **24**(6), 2263–76.

Wilson, R., Vogelsang, E. and Leptin, M. (2005) FGF signalling and the mechanism of mesoderm spreading in *Drosophila* embryos. *Development (Cambridge, England)*, **132**(3), 491–501.

Wortha, D.C., Parsons, M. (2008) Adhesion dynamics: Mechanisms and measurements. *The International Journal of Biochemistry and Cell Biology*, **40**(11), 2397–2409.

Wright, C.V. (2001) Mechanisms of left-right asymmetry: what's right and what's left? *Dev Cell*, **1**(2), 179–86.

Xia F, Li J, Hickey GW, Tsurumi A, Larson K, Guo D, Yan S, Silver-Morse L, Li WX (2008) Raf activation is regulated by tyrosine 510 phosphorylation in *Drosophila*. *PLoS Biol*, **6**(5), e128.

Xie SQ, Martin S, Guillot PV, Bentley DL, Pombo A (2006) Splicing Speckles Are Not Reservoirs of RNA Polymerase II, but Contain an Inactive Form, Phosphorylated on Serine2 Residues of the C-Terminal Domain. *Mol Biol Cell*, **17**(4), 1723.

Xu, H., Lee, K.W. and Goldfarb, M. (1998) Novel recognition motif on fibroblast growth factor receptor mediates direct association and activation of SNT adapter proteins. *J Biol Chem*, **273**(29), 17987–90.

Xu X, Weinstein M, Li C, Deng C (1999) Fibroblast growth factor receptors (FGFRs) and their roles in limb development. *Cell Tissue Res*, **296**(1), 33–43.

Yamada T, Sakisaka T, Hisata S, Baba T, Takai Y (2005) RA-RhoGAP, Rap-activated Rho GTPase-activating protein implicated in neurite outgrowth through Rho. *J Biol Chem*, **280**(38), 33026–34.

Yan, D. and Lin, X. (2007) *Drosophila* glypican Dally-like acts in FGF-receiving cells to modulate FGF signaling during tracheal morphogenesis. *Dev Biol*, **312**(1), 203–16.

Yang X, Dormann D, Münsterberg AE, Weijer CJ (2002) Cell movement patterns during gastrulation in the chick are controlled by positive and negative chemotaxis mediated by FGF4 and FGF8. *Dev Cell*, **3**(3), 425–37.

Yokoyama, H., Ide, H. and Tamura, K. (2001) FGF-10 stimulates limb regeneration ability in Xenopus laevis. *Dev Biol*, **233**(1), 72–9.

Zaffran S, Reim I, Qian L, Lo PC, Bodmer R, Frasch M (2006) Cardioblast-intrinsic Tinman activity controls proper diversification and differentiation of myocardial cells in *Drosophila*. *Development (Cambridge, England)*, **133**(20), 4073–83.

Zallen, J.A. and Blankenship, J.T. (2008) Multicellular dynamics during epithelial elongation. *Semin Cell Dev Biol*, **19**(3), 263–70.

Zhang N, Zhang J, Purcell KJ, Cheng Y, Howard K (1997) The *Drosophila* protein Wunen repels migrating germ cells. *Nature*, **385**(6611), 64–7.

Zhang SQ, Yang W, Kontaridis MI, Bivona TG, Wen G, Araki T, Luo J, Thompson JA, Schraven BL, Philips MR, Neel BG (2004) Shp2 regulates SRC family kinase activity and Ras/Erk activation by controlling Csk recruitment. *Mol Cell*, **13**(3), 341–55.